August 2019

Synthetic Studies on Small Molecule Modulators of Src Homology 2 (SH2) Domain-Containing Inositol 5'-Phosphatase (SHIP)

Otto Milhous Dungan
Syracuse University

Abstract

Small molecule modulators of SH2-containing inositol 5'-phosphatase (SHIP) have recently become a hotly pursued area in medicinal chemistry. Pharmaceutical targeting of SHIP with small molecules has been identified as a new method to directly influence the phosphoinositide 3-kinase (PI3K) cell signaling pathway. Modulation of this pathway may be utilized in the development of interesting new therapeutics. A better understanding of the role that SHIP phosphatase activity plays in a number of disease states ranging from cancer to autoimmune disease to obesity may be ascertained by use of small molecule inhibitors. These investigations involved the synthesis of aminosteroid inhibitors and a variety of aminosteroid analogs to allow for further evaluation of structure-activity relationships in these systems for both potency and selectivity against both paralogs of SHIP, SHIP1 (primarily expressed in hematopoietic cells) and SHIP2 (expressed across all cell types).

SHIP1 has also been recognized to be an allosterically activated enzyme, with several small molecule agonists having been reported in the literature. These studies have culminated in the identification of AQX-1125, which is currently undergoing phase III clinical evaluation for interstitial cystitis / bladder pain syndrome. To facilitate our own studies on SHIP1 signaling, a new synthetic route to the SHIP1 agonist AQX-1125 has been developed. This route allows for more rapid access to AQX-1125 from dehydroepiandrosterone than the published synthetic pathway, saving time and resources. Key features of the new route include utilizing an allylic oxidation, ozonolysis, and lactonization for a more selective and controlled synthesis. In addition, this work has led to the synthesis of several new AQX-1125 analogs, providing information on structure activity relationships in this structural class of SHIP1 agonists.

Synthetic Studies on Small Molecule Modulators of Src Homology 2 (SH2) Domain-Containing Inositol 5'-Phosphatase (SHIP)

By

Otto M. Dungan

B.S. Chemistry, Florida State University, 2014

M. Phil. Chemistry, Syracuse University, 2016

Dissertation

Submitted in partial fulfillment of the requirements for the degree of Doctor of Philosophy in Chemistry

Syracuse University

August 2019

Acknowledgments

Thank you to my advisor Dr. John Chisholm for all the guidance, wisdom, and mentorship that helped develop who I am as a person, chemist, and researcher. Thank you, Dr. Nancy Totah, Dr. Yan-Yeung Luk, and Dr. James Kallmerten for all the great advice and counsel expressed kindly as I progressed through the years of my graduate career. To Dr. Rachel Steinhardt, Dr. Michael Sponsler, and Dr. Scott Erdman, thank you for serving on my Ph.D. committee as my time as a graduate student came to a close.

Thank you to my family. My parents, Gregory and Ilona Dungan, thank you for always showing nothing but love and support as I chase and achieve my dreams. To my older brothers, thank you Gregory and Rutger for sharing all the incredible knowledge that helped me prepare for life and my future. To my younger brother Milhous, thank you for always being there and being my best friend that I can always look up to. Thank you to my favorite sister Helmut for all the incredible love and inspiration (and of course being my best friend too). And to my very loving grandparents, thank you for always believing in me.

To my great friends and labmates I met throughout my time in graduate school. Shea Meyer, Alexandra Millimaci, Katelyn Leets, Shawn Dormann, Rowan Meador, Nilamber Mate, Jacob Moose, Angela Pacciarelli, and Daniel Effiong. All of you made working in lab a positive and enjoyable experience with great memories that I will always appreciate. Thank you to Dr. Kyle Howard, Dr. Arijit Adhikari, Dr. Brian Duffy, Dr. Dan Wallach, and Dr. Alex Dixon. I would not be where I am if it was not for all of your great insight that helped me evolve as I worked in the lab. Thank you for always being there Yahireliz Flores Alvarez. A true friend who showed nothing but support and encouragement. And finally, thank you to María Victoria Pons.

Table of Contents

List of Figures

List of Schemes

Symbols/Abbreviations

3AC 3α-aminocholestane

˚C ..... celsius

Ac_2O ..... acetic anhydride

AKT ..... protein kinase B

AKT2 ..... protein kinase B2

AML ..... acute myelogenous leukemia

anal. calcd ..... combustion elemental analysis

approx ..... approximately

aq ..... aqueous

atm ..... atmosphere

BMDM ..... bone marrow derived macrophages

calcd ..... calculated

cat ..... catalyst

^{13}CNMR ..... carbon nuclear magnetic resonance

COPD ..... chronic obstructive pulmonary disease

CSA ..... camphorsulfonic acid

DCM ..... dichloromethane

dec ..... decomposed

DIAD ..... diisopropyl azodicarboxylate

DMAP 4-dimethylaminopyridine

DMF ..... dimethylformamide

DMSO-*d*6 ..... deuterated dimethyl sulfoxide

DPM ..... diphenylmethyl

EDCI ..... 1-ethyl-3-(3-dimethylaminopropyl)carbodiimide

G-CSF ..... granulocyte colony-stimulating factor

GvHD ..... graft versus host disease

^{1}HNMR ..... proton nuclear magnetic resonance

IBD ..... inflammatory bowel disease

IC ..... interstitial cystitis

IC_{50} ..... half maximal inhibitor concentration

IR ..... infrared spectroscopy

kDa ..... kilodalton

LAH ..... lithium aluminum hydride

LPS ..... lipopolysaccharide

m-CPBA ..... meta-chloroperoxybenzoic acid

MHz ..... megahertz

MIR ..... myeloid immunoregulatory cells

MM ..... multiple myeloma

mTOR ..... mammalian target of rapamycin

NK ..... natural killer

NMR ..... nuclear magnetic resonance

PH ..... pleckstrin homology

PI3K ..... phosphoinositide 3-kinase

$PI(3,4)P_2$ phosphatidylinositol-3,4-bisphosphate

$PI(3,4,5)P_3$ phosphatidylinositol-3,4,5-trisphosphate

$PI(4,5)P_2$ phosphatidylinositol-4,5-bisphosphate

PTEN..... phosphatase and tensin homolog protein

R_f..... retention factor

RTK..... receptor tyrosine kinase

SCF ..... stem cell factor

SHIP ..... SH2-containing inositol-5'-phosphatase

TEA..... triethylamine

THF ..... tetrahydrofuran

TLC ..... thin-layer chromatography

TNFα..... tumor necrosis factor alpha

Chapter 1 - Potential Therapeutics through SHIP Modulation

1.1 The Phosphoinositide 3-Kinase Cell Signaling Pathway

Eukaryotic cell development, longevity, and behavior are influenced by the transfer of stimuli from the extracellular environment, through the plasma membrane, to the cell nucleus. Many of these responses result from signaling cascades initiated by the activation of receptors which span the cell membrane. Once initiated the signal is amplified and passed through a complex system of protein phosphatases and protein kinases until the reaching the nucleus, where the molecular events trigger an appropriate response. Such responses can include rearrangement of the cytoskeleton, stimulation of an enzyme, or activation of a gene to drive protein synthesis. These actions influence macroscopic processes like cell division, survival, differentiation, or apoptosis.[1,2] Phosphatidylinositols intercalated in the cell membrane play a critical role in this intricate signaling network, acting as second messengers to the initial response. These phosphoinositols are decorated with lipids that intercalate into the plasma membrane, with the phosphoinositol being present on the inside of the plasma membrane. The phosphorylation patterns observed on the inositol rings are key to signals being passed on to the nucleus, as these are recognized by other protein kinases which pass the signal further on in the pathway.[1,3,4] Changes to these phosphorylation patterns on these phosphatidylinositols often alter the cell's course of action and may allow for a potential therapeutic intervention in cases where aberrant signaling is injurious.

The phosphoinositide 3-kinase (PI3K) cell signaling pathway is one of the most heavily investigated cell signaling pathways, playing a key role in many cell functions.[5] This activity is partially attributed to the essential kinase PI3K, which once activated by a receptor tyrosine kinase (RTK), phosphorylates the 3' position of the inositol phospholipid phosphatidylinositol-4,5-bisphosphate ($PI(4,5)P_2$) to generate a higher concentration of phosphatidylinositol-3,4,5-triphosphate ($PI(3,4,5)P_3$) in the cell (Figure 1.1).[5-7] The phosphorylation at 3' position is believed

to amplify the cell signaling cascade primarily through its recruitment and activation of pleckstrin homology (PH) containing signaling proteins to the membrane, such as the serine-threonine kinase protein kinase B (AKT).[5]

Figure 1.1: Intrinsic Activation of Cellular Signaling Induced by SHIP

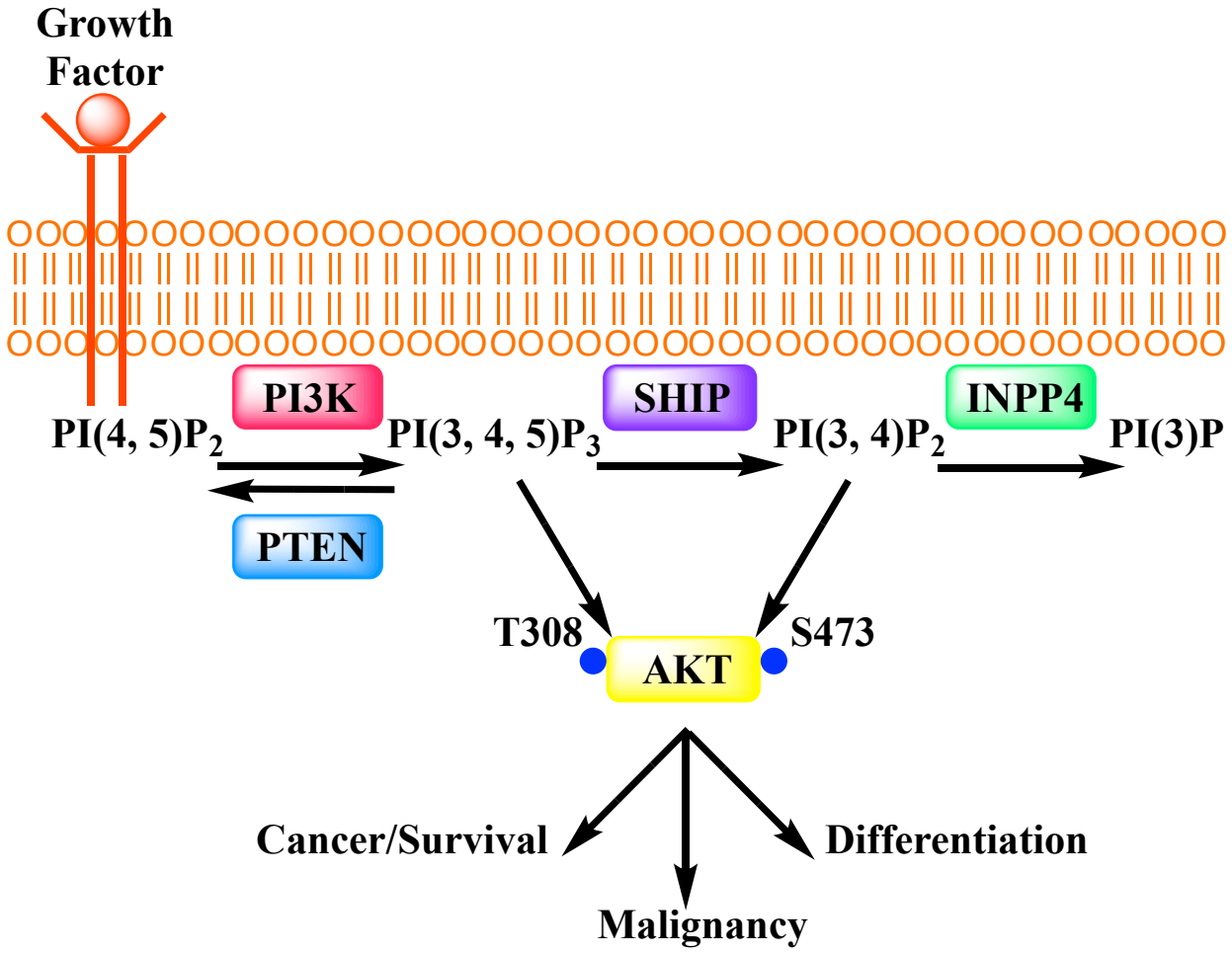

Once activated, AKT drives the continued phosphorylation and activation of other intracellular kinases until the signal is received by the cell nucleus prompting events such as migration, proliferation, differentiation, and apoptosis (Figure 1.2). To tightly regulate the concentration of the PI3K product $PI(3,4,5)P_3$ present in the cell, the key inositol phosphatases Phosphatase and tensin homolog protein (PTEN) and SH2-containing inositol-5'-phosphatase

(SHIP) are utilized.[5,8,9] PI3K's transduction of information can be negated through the reversal of the 3' phosphorylation by PTEN generating the initial $PI(4,5)P_2$.

However, PI3K's effect can also be modified by the hydrolysis of $PI(3,4,5)P_3$ to phosphatidylinositol-3,4-bisphosphate ($PI(3,4)P_2$) through the 5'-inositol phosphatase SHIP.[8] Reducing the amount of $PI(3,4,5)P_3$ in the system should lead to a decrease in AKT activation as SHIP activity increases. The system is more complex, however, as the product of SHIP, $PI(3,4)P_2$, has an increased affinity for the AKT PH domain and also activates AKT, with both $PI(3,4,5)P_3$ and $PI(3,4)P_2$ being required for full activation of AKT.[10] Therefore the activity of SHIP can also increase AKT activation in some instances. This complication demonstrates that SHIP plays a major role in the PI3K pathway due to its ability to both negate and promote cellular signaling.

Figure 1.2: PI3K Signaling Pathway

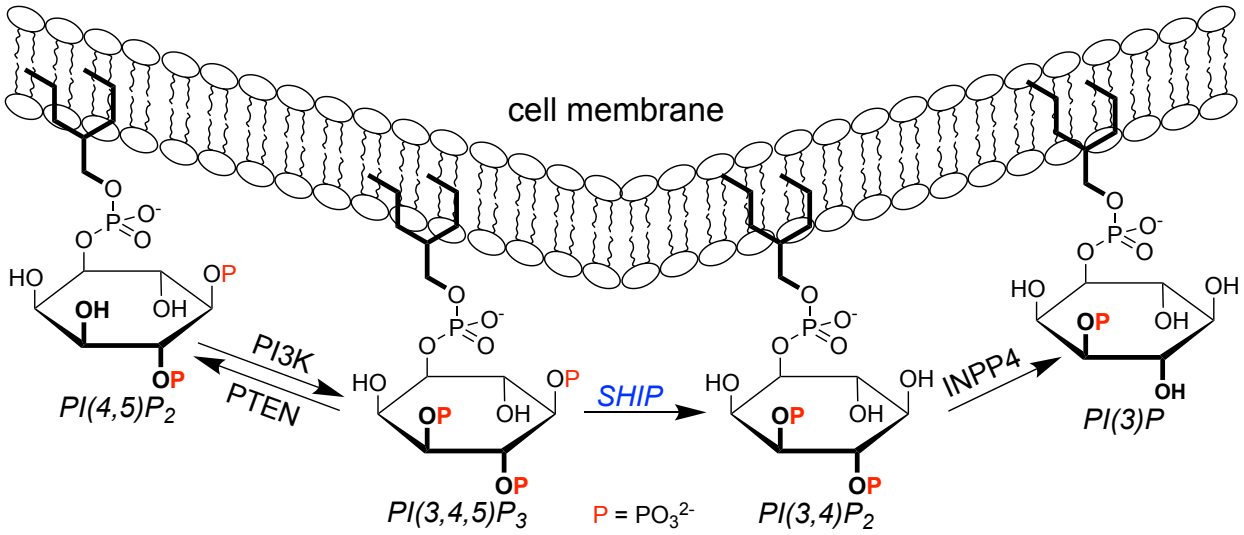

Regulation of this delicate balance between $PI(3,4,5)P_3$ and $PI(3,4)P_2$ has been found to influence the cellular physiology of blood and bone marrow (hematopoietic) cells,[11-13] endothelial cells,[14] and embryonic cells.[15] Modulation of SHIP and the effects it invokes on the PI3K signaling

pathway may allow for the development of interesting therapeutic treatments for cancer,[5,16,17] autoimmune diseases,[2] cardiovascular disease,[2] obesity,[18,19] and Crohn's disease.[20] Two major paralogs of SHIP have been found: SHIP1 (which is utilized primarily hematopoietic cells)[21] and SHIP2, which is expressed ubiquitously.[5] The two enzymes are very homologous, having an ~50% identical amino acid sequence in their structure. Interest in SHIP modulation as a potential therapeutic strategy has led to the discovery of selective SHIP1 inhibitors, selective SHIP2 inhibitors, pan-SHIP1/2 inhibitors, as well as SHIP1 agonists.

1.2 Targeting SHIP Modulation for Potential Therapeutics of Human Diseases

Positive and negative modulation of SHIP plays a critical role in cell physiology acting as a regulator to control cell concentrations of $PI(3,4,5)P_3$ and $PI(3,4)P_2$ present on the cell membrane, and therefore influencing downstream signaling. Perturbing this system alters the cells function as both of $PI(3,4,5)P_3$ and $PI(3,4)P_2$ are necessary to fully activate the signaling cascade through AKT (Figure 1.1). SHIP, PTEN and PI3K are the first soluble signaling proteins that take part in the PI3K signaling cascade, which avoids issues of working with membrane proteins as their expression, folding and isolation are not hampered by the need for a lipid bilayer. While SHIP is one of ten mammalian proteins with an inositol 5-phosphatase domain, it is the only one involved in cell signaling pathways.[22,23] Inhibition of SHIP using an antagonist would allow for an increase in $PI(3,4,5)P_3$ concentrations and a decrease in $PI(3,4)P_2$, while upregulation of SHIP activity by agonist would decrease the concentration of $PI(3,4,5)P_3$ and increase $PI(3,4)P_2$. The ability to control the balance of these secondary messengers has been shown to be a promising lead to the development of potential therapeutics in a number of areas.

1.3 SHIP Modulation in Cancer

Overstimulation of the PI3K-Akt-mTOR signaling pathway has often been implicated in facilitating both cell division and survival of cancerous cells, allowing a malignant state to be achieved through an overabundance of either $PI(3,4,5)P_3$ or $PI(3,4)P_2$ or both. Targeting SHIP1 in hematopoietic cells with the use of small-molecule inhibitors or agonists has been shown to kill human blood cancer cells, specifically in leukemia and multiple myeloma cell lines.[24,25] The targeting of SHIP1 is supported by the lack of activity against cell lines which only express SHIP2 and do not use SHIP1. For example, the leukemia cell line K562 (that express both PTEN and SHIP2, but lack expression of SHIP1) is unaffected by treatment with a selective SHIP1 inhibitor.[24] While SHIP1 inhibitors may be useful for the treatment of blood cancers, they will be limited to cancers which utilize SHIP1. Other types of cancer may also be treated with SHIP2 inhibitors. For example, breast cancer cells solely express the SHIP2 paralog and not SHIP1. Over activation of SHIP2 has been shown to lead to increased cell proliferation through EGF-induced signaling.[5,26-29] The over proliferation of breast cancer line MDA-MB-231 was greatly reduced and incurred apoptosis through SHIP2 inhibition[28] showing the potential for SHIP2 specific therapeutic targets. SHIP2 was also shown to be implicated in the pathogenesis of some types of colorectal cancer,[30] and treatment with a SHIP2 inhibitor was found to be useful in controlling cell growth in these cell lines. In some cases cancer cells may show resistance to selective SHIP1 or selective SHIP2 inhibitors by overexpressing the other SHIP paralog.[31] In these cases the use of pan-SHIP1/2 inhibitors may be employed, as these compounds should limit the development of resistance through the paralog compensation mechanism.

Another potential use for SHIP1 inhibitors in cancer treatment is to prime the immune system so that it is more sensitive to cancer immunotherapeutics. SHIP1 is expressed primarily in

hematopoietic cells, (mostly blood and bone marrow cells) which make up much of the human immune system. SHIP1 limits signaling from receptors that activate natural killer (NK) cells and T cells, therefore SHIP1 inhibitors usually are thought of as immunosuppressants. SHIP1 knockouts unexpectedly showed that the effector functions of SHIP1-deficient NK and T cells are compromised in vivo. Implicating that the immunosuppressant effects of SHIP1 inactivation is due to chronic activation of immune cells which renders them less responsive to activating signals. This effect is thought to be a host mechanism to avoid autoimmunity. Therefore reversible and pulsatile inhibition of SHIP1 with a small molecule inhibitor may increase the antitumor response of SHIP1 dependent immune cells. Recent experiments have shown that pulsatile inhibition of SHIP1 in myeloid cells can amplify the immune response by increasing the proinflammatory cytokine production.[32] Transient SHIP1 inhibition before challenge with cancer cells in mouse models of lymphoma and colon cancer improved the median and long-term tumor-free survival rates. These findings suggest that a pulsatile inhibition of SHIP1 prior to use of an immunotherapeutic might be more effective than the immunotherapeutic alone in some patients. Recently a similar dosing regimen was found to prevent bacterial infection in mice and human cells, likely through a similar mechanism of immune stimulation.[33]

1.4 SHIP Modulation in Diabetes and Obesity

SHIP2 has been shown to be an important negative regulator of the insulin-signaling pathway, and therefore its inhibition can lead to increased insulin sensitivity.[5,18,34] As diabetics often begin to develop resistance to insulin later in life, the ability to increase sensitivity to the protein could be useful as an adjuvant for people with diabetes. The specific role of SHIP2 in insulin signaling has been a controversial topic. Some studies have reported that SHIP2 knockout

mice have a reduced body weight despite increased food intake.[35] Placing these SHIP2 knockout mice on a high-fat diet showed that they were highly resistant to weight gain over a 12-week period. Over this time period the mice exhibited no increase in serum lipids and did not develop hyperglycemia or hyperinsulinemia. These results are attributed to enhanced insulin-stimulated AKT and p70S6K activation in the liver and skeletal glucose when compared to normal mice. Other SHIP2 knockout mice did not show this phenotype,[36] however this work did spur the design of new SHIP2 inhibitors as potential treatments for diabetes. Treatment of diabetic *db/db* mice with a selective SHIP2 inhibitor was found to lead to lowered the plasma glucose levels and improved glucose tolerance.[37] These *in vivo* effects were based in part on the activation of intracellular insulin signaling pathways in the liver, which were consistent with the inhibition of SHIP2.

Additional studies with a pan-SHIP1/2 inhibitor showed that these small molecules may also be an effective diabetes therapeutic regimen. In vivo studies showed that mice had a significant decrease in body weight and body fat, while maintaining a high fat diet, when administered the pan-SHIP1/2 inhibitor K118 compared to vehicle mice.[38] Treatment with the pan-SHIP1/2 inhibitor also maintained healthy blood sugar levels and improved insulin sensitivity. The use of a pan SHIP1/2 inhibitor may be superior to the use of a selective inhibitor as the increase in glucose sensitivity seen with SHIP2 can act synergistically with the SHIP1 inhibition leading to immunocalming in of adipose tissue stress associated with the consumption of a high caloric diet. As a key component in the insulin-signaling pathway, development of SHIP1/SHIP2 pan-inhibitors may be a potential therapeutic target for treatment of diabetes and obesity.

1.5 SHIP Modulation in Inflammatory Diseases

Continued investigation of the role of SHIP in the PI3K signaling pathway has established its ability to be a negative regulator in the cells inflammatory induced response as a controlling factor in cytokine secretion.[5,39] SHIP1 knockout mice showed inflammation through a myeloid cell response as the SHIP1 induced signal to AKT was removed.[40] An inflammatory disease phenotype was also observed in knockout mice with similarities to human Crohn's disease.[20]

The possibility of a SHIP1 agonist to upregulate the SHIP1 activation of AKT signaling could be a potential therapeutic for inflammatory diseases such as IBD and Crohn's disease. While the use of agonists is less precedented than antagonists in the realm of small molecule pharmaceuticals, SHIP1 has been shown to be an allosterically modulated enzyme. The product of the enzymatic reaction, $PI(3,4)P_2$, binds to SHIP1 at the C2-domain of the enzyme, increasing the rate of phosphate hydrolysis in a feed-forward manner.[41] SHIP1 agonists have therefore been explored as alternatives to PI3K inhibitors, as both mechanisms are effective in lowering $PI(3,4,5)P_3$ concentration.

1.6 SHIP Modulation in Alzheimer's Disease

Interestingly, SHIP2 expression has recently been linked to cognitive decline and neurodegenerative diseases. Inhibition of SHIP2 was shown to reduce tau hyperphosphorylation induced by amyloid ß in Alzheimer's disease mouse models and rescued memory impairment.[42] With the potential for an Alzheimer's disease treatment by targeting SHIP2, interest in SHIP2 inhibitors that cross the blood-brain barrier have been investigated. Lim *et. al.* identified an active SHIP2 inhibitor with an IC_{50} of 2 μM based on the parent small molecule crizotinib. This inhibitor was found through a high-throughput screen and was shown to cross the blood brain barrier. This

inhibitor was shown to be effective in HT22 neuronal cells, reducing SHIP2 activation and $PI(3,4)P_2$ production.[42] Also, suppression of GSK3ß activation, a key signaling event for tau hyperphosphorylation, was also observed in the SHIP2 inhibition in HT22 cells.[42] Further investigations into the development of potent SHIP2 selective inhibitors targeting the brain could play a key role in potential Alzheimer's disease treatments.

SHIP1 may also play a role in the development of Alzheimer's disease. Recently a number of single nucleotide polymorphisms in the INPP5D (SHIP1) gene have been linked with an increase in risk of Alzheimer's disease.[43,44] This suggests that a reduction in SHIP1 activity (as could be envisioned with a small molecule inhibitor) could be a viable therapeutic strategy worth pursuing to treat Alzheimer's disease.[45] This is supported by the role SHIP1 plays in cell signaling in myeloid cells, which include microglial cells in the brain. SHIP1 limits signaling by receptors (TREM2, Dectin1, CCR2) that are key in promoting microglial survival and proliferation in the CNS (TREM2, Dectin1), hindering their effector function including responding to Aβ plaques (TREM2).[46-48] SHIP1 also limits the production of granulocyte colony-stimulating factor (G-CSF) *in vivo.*[21,49] Administration of G-CSF, or its co-administration with stem cell factor (SCF), have been shown to reduce disease severity in multiple murine Alzheimer's disease models.[50,51] Treatment with G-CSF has also been implicated to improve cognitive function in a small clinical trial in humans which explored G-CSF treatment in Alzheimer's patients.[52] Given the significant preliminary data and the growing need for new Alzheimer's disease therapeutics, the development of new small molecule SHIP modulators which cross the blood brain barrier will likely be explored in this area in the near future.

1.7 SHIP Phosphatase Modulation with Small Molecules

Targeting the key inositol phosphatases and kinases present in PI3K cell signaling pathway, PI3K/PTEN/SHIP, has become a pharmaceutically appealing goal as these enzyme regulators are present at the top of the PI3K signaling chain, just inside the cell membrane. This allows for modulation of the signal near it's beginning but avoids issues with trying to influence and/or work with membrane bound proteins which can be time consuming and difficult. Development of PI3K modulators has had some success[5,53,54] but unfortunately in many cases these successes have not been as widespread as was hoped, being only effective in small niche areas. This may be due to the need to target specific PI3K isoforms in order to ensure efficacy. As an alternative way to modulate PI3K signaling, interest has shifted to the development of SHIP agonists and antagonists to help regulate this system. In some ways SHIP represents a more specific target, as SHIP has only two main paralogs where as PI3K has many more. The development of these SHIP modulators will potentially increase the therapeutic advances for new treatments to counter or amplify PI3K signaling. In addition these small molecules can be used as probes to further interrogate the role of SHIP in the PI3K pathway and on cell signaling.

1.8 SHIP Modulation: Small Molecule Agonists

Aberrant activation of PI3K induces tumor growth attributed to the high concentrations of $PI(3,4,5)P_3$ found within the cell. Acting as a negative regulator, SHIP1 can oppose the PI3K-AKT promoted signal by reducing the concentration of $PI(3,4,5)P_3$. This is accomplished by catalyzing the hydrolysis of the 5'-phosphate from $PI(3,4,5)P_3$, generating $PI(3,4)P_2$. To increase the rate of hydrolysis, the development of SHIP agonists have become of interest to reduce PI3K over-activation which is thought to lead to undesired cell division and excessive inflammation.

Small molecule agonists of SHIP1 and their effects on the PI3K pathway have been recently investigated by Anderson and co-workers with their initial identification of the naturally occurring sesquiterpene pelorol **1.1** (Figure 1.3) through a screen of crude marine invertebrates.[5,41,55] Pelorol showed a two-fold increase of SHIP1 activation at 5μg/mL using recombinant purified SHIP1 in the malachite green phosphatase assay. To deliver more material for further biological studies, a nine step synthesis was developed for pelorol **1.1**. This synthesis was then modified to provide a number of analogs, many of which were potent SHIP1 agonists. This study identified multiple new agonists, including AQX-016A **1.2** and AQX-MN100 **1.3**. The tolyl analog AQX-016A **1.2** was synthesized in a 6 step synthetic route starting from (+)-sclareolide by Yang *et al.* and showed a six-fold increase in SHIP1 dephosphorylation in vitro at 2 μM compared to pelorol which showed a two-fold increase at the same concentration.[5,41,55] AQX-016A **1.2** was found to be a selective SHIP1 agonist, selectively activating SHIP1 over SHIP2 by a factor of 5 in vitro.[41] This molecule also was shown to inhibit degranulation and TNFα production in $SHIP^{+/+}$ murine mast cells stimulated with IgE but no activity was observed with $SHIP1^{-/-}$ murine mast cells.[5] When compared to the known anti-inflammatory agent dexamethasone, AQX-016A **1.2** showed similar anti-inflammatory activity.[55] Although showing potent agonistic activity selective for SHIP1, concerns with off-target issues led to the discontinuation of the development of this molecule. Specifically, the presence of a catechol (which is known to cause problems with metal binding and oxidation to the quinone methide in vivo, which can lead to undesired alkylation events) was a major concern. Later studies led to the development of AQX-MN100 **1.3** by the removal of the hydroxyl moiety at C17.[41,56] This compound was also shown to be a potent SHIP1 agonist.

Figure 1.3: Structures of SHIP1 Agonists

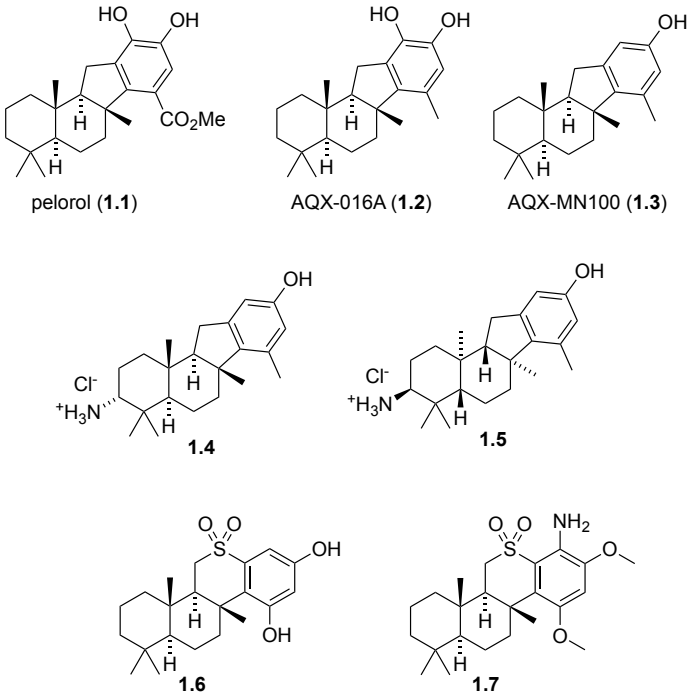

Interestingly, the activation of SHIP1 by AQX-MN100 **1.3** was similar to AQX-016A **1.2** (six-fold activation), but AQX-MN100 showed significantly improved toxicology due to the lack of the catechol.[5] Evaluation of in vitro assays against multiple myeloma cells by Kennah et al. showed AQX-MN100 **1.3** to be active and confirmed the role of a SHIP1 agonist as a potential therapeutic for hematopoietic cancer.[25] Concerns about the water solubility of AQX-MN100 became apparent, as the molecule is quite lipophilic and was difficult to dose orally. These poor solubility properties led Aquinox Pharmaceuticals to develop the amine derivatives of AQX-MN100, **1.4** and **1.5**. While these compounds were more water soluble the SHIP1 agonist activity was weaker.[57] While racemic material was initially tested, separation of the two enantiomers interestingly showed that **1.5** was actually more active than **1.4**. Further synthetic studies on these systems led to the development of the sulfone-containing analogs **1.6** and **1.7**, which were hoped to have better pharmacodynamics properties.[57,58]

At some point Aquinox Pharmaceuticals halted development of the pelorol derivatives and instead focused on the seco-steroidal indene derivative containing an open B-ring, AQX-1125 **1.8** (Figure 1.4).[59] This agonist shows a more moderate 20% activation of SHIP1 at 300 μM (compared to AQX-MN115 **1.9** which shows a 77% increase in SHIP1 activity at 300 μM), however the excellent pharmacological properties and water solubility of AQX-1125 **1.8** led to its advancement to phase II clinical trials as a treatment for asthma and COPD. These types of trials can be difficult to show efficacy, however, as the molecule must work on cells in the lungs which are often difficult to target. Insufficient efficacy was seen in the trial, and the molecule was moved to other trials against other inflammatory disorders. Eventually AQX-1125 **1.8** was advanced to phase III clinical trials for interstitial cystitis/ bladder pain syndrome.[60,61] Although not showing efficacy, AQX-1125 **1.8** has been the only compound targeting SHIP1 to advance to clinical studies and would provide a good standard for further development of a more potent agonist of SHIP1.

Figure 1.4: Structure of SHIP1 Agonists AQX-1125 and AQX-MN115

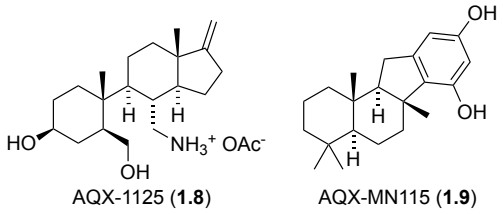

The identification of australin E **1.10** by Anderson and Mui in an isolate from the soft coral *Cladiella* sp. collected in Pohnpei was found to be another class of natural products to agonistically activate SHIP1 (Figure 1.5).[5,62] This eunicellin diterpenoid showed an increase in SHIP1 activation by 12% at 100 μM, while the other isolates australin F **1.11** and G **1.12** showed no activation. This

seemed to indicate that the exocyclic olefin on the cyclohexane ring was key to the SHIP1 agonist activity that was observed.[5]

Figure 1.5: Eunicellin Diterpenoid and Cyclic Depsipeptide SHIP1 Agonists

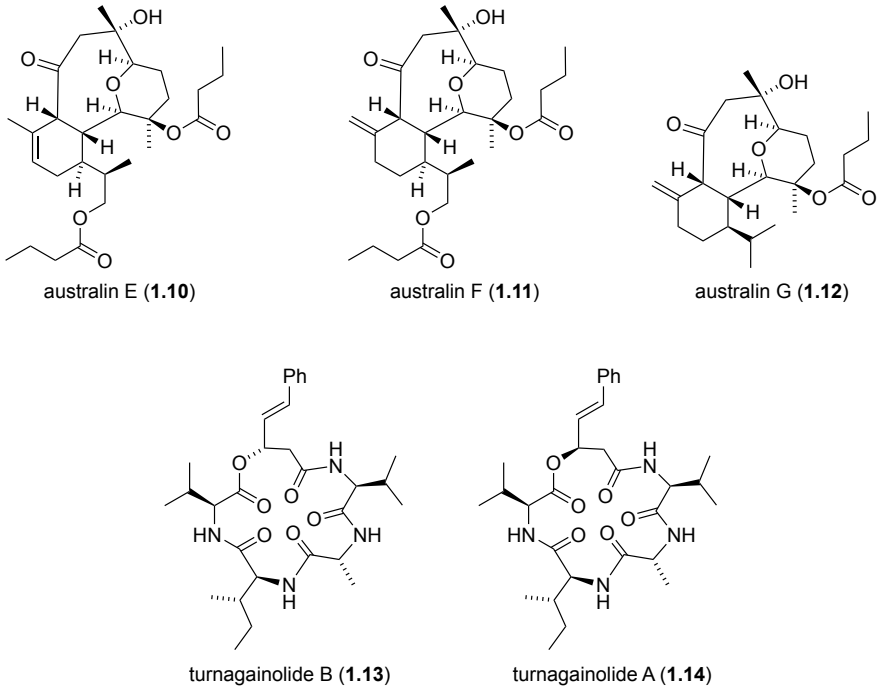

Further screening of natural product isolates provided yet another class of SHIP1 agonists: the cyclic depsipeptide turnagainolide B. Identified in a strain of *Bacullus* sp. cultured from a sediment sample collected from the sea floor, turnagainolide B **1.13** shows similar activity compared to AQX-MN100 **1.3** (12% activation at 10 μM) however, a change in stereochemistry at the lactone moiety of turnagainolide A **1.14** showed no activation of SHIP1. [5,63]

1.9 SHIP1 Modulation: Small Molecule Antagonists

Inhibition of SHIP inositol phosphatase activity using small molecule antagonists may have the potential to treat a number of diseases from cancer[5,16,17] and diabeties,[18,19] to cardiovascular disease and autoimmune disorders.[2] Complicating the development of SHIP inhibitors is the presence of multiple SHIP isoforms in vertebrates. In blood and bone marrow (hematopoietic) cells, the major inositol 5'-phosphatase that generates $PI(3,4)P_2$ is referred to as SHIP1. In other cells this function is typically performed by a similar phosphatase, SHIP2. Selective inhibitors are typically more desirable than pan-inhibitors to minimize side effects, but in some cases pan-inhibitors may also be of interest, especially in cases where resistance can manifest by the cells switching from the use of one paralog of SHIP to the other.

Some of the first SHIP antagonists disclosed were modified analogs of $PI(3,4,5)P_3$ containing a methylenephosphonate (like **1.15**) or phosphorthioate (like **1.16** and **1.17**) at the 5' position. These molecules were developed by the Prestwich laboratory specifically to hinder SHIPs ability to hydrolyze the phosphate at the 5' position (Figure 1.6).[5,64] Evaluation of their effects on SHIP1 and SHIP2 showed 50% inhibition at 10 μM for SHIP1 with some inhibition also occurring for SHIP2.[5] The differences in inhibition of SHIP1 and SHIP2 with these analogs was noteworthy as this was the first evidence that the two paralogs could be selectively inhibited. While these compounds are interesting academically, due to their highly charged nature they cannot cross cell membranes which limits their use as probes of the PI3K pathway in in vivo studies.

Figure 1.6: Analogs of PI(3,4,5)P₃

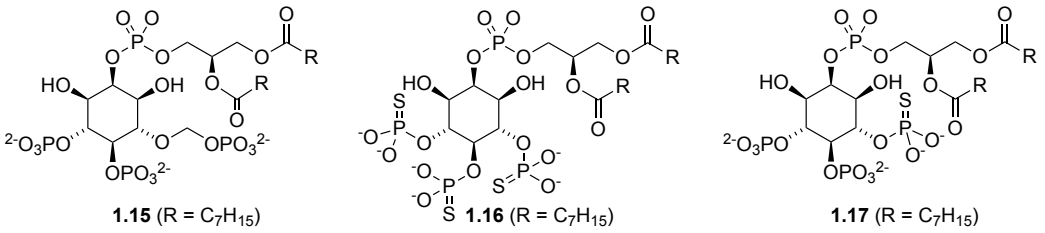

1.15 (R = C_7H_{15}) **1.16** (R = C_7H_{15}) **1.17** (R = C_7H_{15})

In order to find small molecules with more drug like properties, the Kerr group performed a high-throughput screen of a library of compounds from the National Cancer Institute against SHIP1 using a fluorescence polarization assay. Brooks and co-workers found NSC23922 **1.18** to have significant activity for the inhibition of SHIP1 (Figure 1.7).[24] The activity was then confirmed using the colorimetric malachite green phosphatase assay.[65] The α-amine isomer 3α-aminocholestane 3AC **1.19** was found to be more active against one paralog of SHIP, SHIP1, with an inhibition of 50% at 10 μM and no inhibition of SHIP2.[5] Interestingly, using 3AC **1.19,** inhibition of SHIP1 was found to reduce the growth and increase apoptosis of the hematopoietic cancer cell lines AML (acute myelogenous leukemia) KG-1, murine C1498 leukemia cells, and multiple myeloma OPM2 cells with an IC_{50} at 10 μM, establishing that a delicate balance of both PI(3,4,5) and PI(3,4) are needed for cancer survival.[5] Further studies showed that 3AC **1.19** reduced tumor growth and increased survival in vivo in a mouse study where immunosuppressed mice were challenged with OPM2 cells, a multiple myeloma cell line. Some mice still showed significant tumor growth, however, and mice that developed cancer resistant to the treatment showed an increased expression of SHIP2 in the tumor cells which compensated for the SHIP1 inhibtion.[5,31] This study demonstrated the potential for the use of inhibitors that inhibit both SHIP1

and SHIP2 **1.20**,[66] as the cancer cells cannot build resistance to the inhibitor as easily if both isoforms are inhibited.

Figure 1.7: SHIP1 Aminosteroid Inhibitors

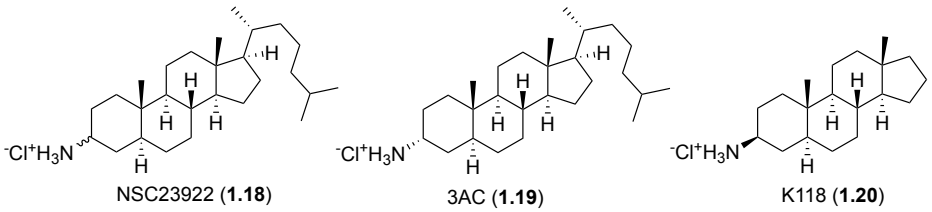

Additional SHIP inhibitors have been developed through three-dimensional modeling of mimics of $PI(3,4,5)P_3$. This led to the discovery of the phosphorylated polyphenols biphenyl(2,3′,4,5′,6)P_5 **1.21**, Bz(1,2,4,5)P_4 **1.22**, and Bz(1,2,3,4)P_4 **1.23**, which were identified to have a high homology to the phosphorylated inositol, and demonstrated activity as SHIP2 inhibitors (Figure 1.8).[5,67] The number and position of the phosphates present were shown to effect the inhibition of SHIP2. Biphenyl(2,3′,4,5′,6)P_5 **1.21** had an IC_{50} of 1.8 μM whereas Bz(1,2,4,5)P_4 **1.22** exhibited an IC_{50} of 11.2 μM and Bz(1,2,3,4)P_4 **1.23** 19.6 μM. However, due to the high polarity of these compounds they are unable to cross the cell membrane, so they cannot be utilized in in vivo studies.[5,67]

Figure 1.8: SHIP2 Phosphorylated Polyphenol Inhibitors

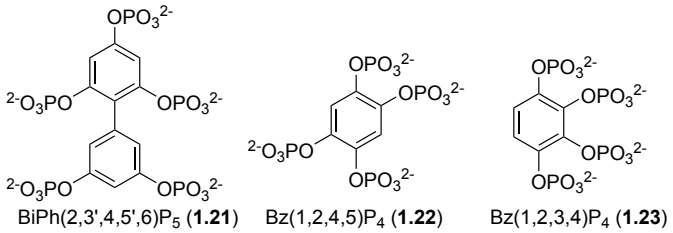

Further work by Potter and coworkers, the biphenyl(2,3′,4,5′,6)P_5 **1.21** ligand (which is quite water soluble) facilitated the determination of a crystal structure of the SHIP2 phosphatase domain with the small molecule bound in the active site (Figure 1.9).[68] While the entire SHIP protein could not be crystallized, a portion of the enzyme containing the phosphatase domain was able to form crystals which provided the data. This section of the enzyme was catalytically active as an inositol phosphatase. The x-ray structure revealed that a flexible loop of the SHIP2 protein acts as a P4-interactive motif (P4IM) where it can fold over the active site, facilitating the interactions leading to hydrolysis. With a crystal structure of the SHIP2 active site identified and having a high homology to SHIP1, the interactions with small molecule modulators can be rationally investigated to better design new SHIP inhibitors.[5]

Figure 1.9: Crystal Structure of the SHIP2 Active Site

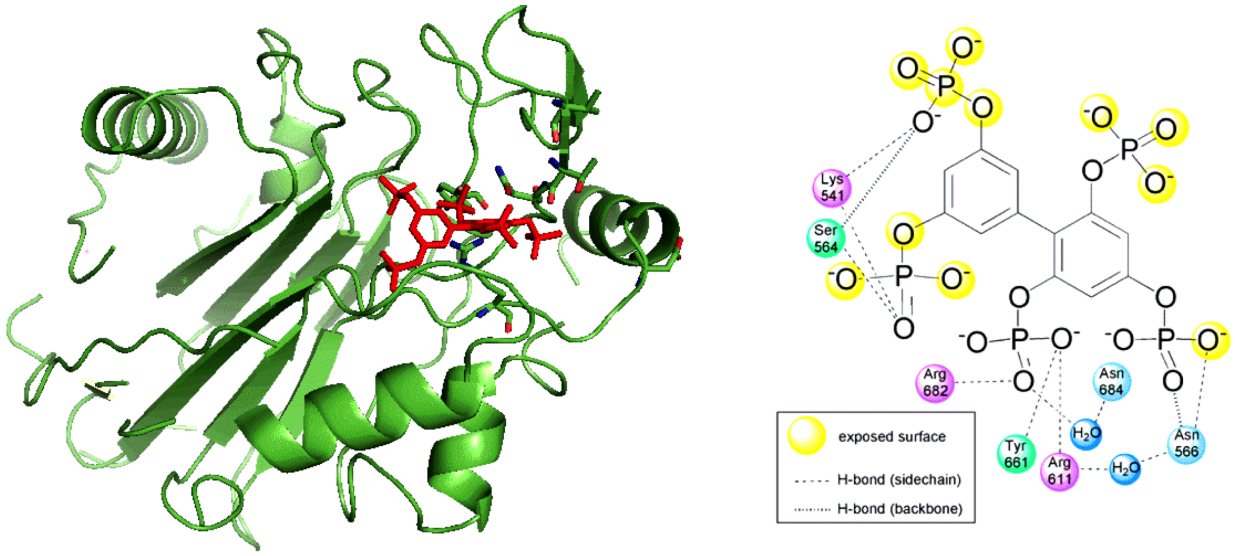

Workers at Astellas Pharmaceuticals identified the thiophene-based small molecule SHIP2 inhibitor, AS1949490 **1.24**, which showed a high selectivity for SHIP2 and an IC_{50} of 0.62 μM (Figure 1.10).[5,37] Upon treatment of L6 myoblasts with AS1949490 **1.24**, an increase in the

activation of AKT was observed, however, the inhibitor was found to only target the isoform of AKT, protein kinase B2 (AKT2), which plays a role in the insulin-signaling pathway.[5,37,69] AS1949490 **1.24** was also found to control gluconeogenesis in vitro and in vivo.[37] Astellas developed a second thiophene-based inhibitor AS1938909 **1.25** which showed similar activity towards SHIP2 with greater selectivity.[5,70] More recent studies suggest that AS1949490 **1.24** may be a potential lead for new therapeutics for the treatment of Alzheimer's disease.[42]

Figure 1.10: SHIP2 Thiophene-Based Inhibitors

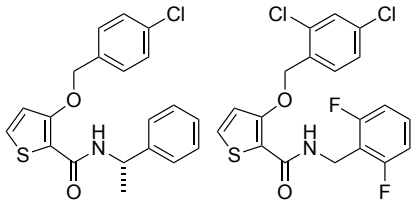

AS1949490 (**1.24**) AS1938909 (**1.25**)

Further screening for SHIP2 antagonists led Neogenesis Pharmaceuticals to perform a high-throughput screen identifying the phenol-based inhibitor NGD61185 **1.26** as a SHIP2 inhibitor. The core of this system is based on salicylic acid, which is somewhat similar to the Astellas compounds from Fig. 1.10 (Figure 1.11). Other inhibitors identified by Neogenesis Pharmaceuticals include NGD61388 **1.27** and NGD62448 **1.28**, which contain a highly functionalized pyrazole core. NGD61388 **1.27** showed to be quite active with an IC_{50} of 1.1 μM against SHIP2.[5,71] The most active compounds found in this screening campaign did not have their structures disclosed, however, so more active inhibitors have been found but their structures remain unknown.

Figure 1.11: SHIP2 Inhibitors Identified by Neogenesis Pharmaceuticals

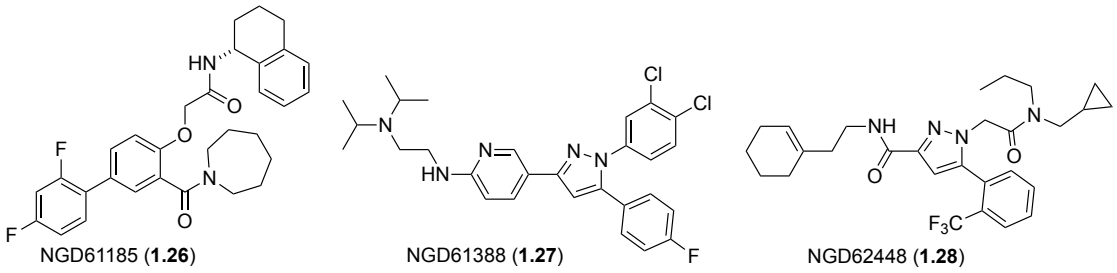

Taking advantage of the inhibitors identified by Astellas and Neogenesis Pharmaceuticals, computational prediction software led to the discovery of the pyridine-based structure **1.29** as a SHIP2 inhibitor, as was determined by researchers at the University of Toyama and Kitasato University (Figure 1.12).[5,72] This structure was based off the hydrogen bond functionality and orientation of the aromatic groups to get the conformation required for a biologically active SHIP2 inhibitor.[5]

Figure 1.12: SHIP2 Pyridine-Based Inhibitor

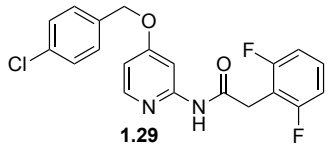

Interest in inhibitors that target both SHIP1 and SHIP2 led to a high-throughput screen performed by the Kerr group to identify pan-inhibitors for both paralogs of SHIP.[5,31] The quinoline aminoalcohols **1.30** and **1.31** as well as the tyrptamine **1.32** were identified (Figure 1.13). Tryptamine **1.32** showed an IC_{50} of 4-5 μM against SHIP1 and 9-10 μM against SHIP2. Each inhibitor was evaluated for its ability to inhibit SHIP1 and SHIP2 in vitro. All three molecules also showed activity against the multiple myeloma cell lines RPM18226, U266, and OPM2 through

inhibition of SHIP1. Activity was also observed against the breast cancer cell lines MDA-MB-231 and MCF-7, which do not express SHIP1 (the SHIP1 selective inhibitor 3AC showed no activity), reducing the cell survival and proliferation using the pan-inhibitors.[5]

Figure 1.13: SHIP1/2 Pan-Inhibitors

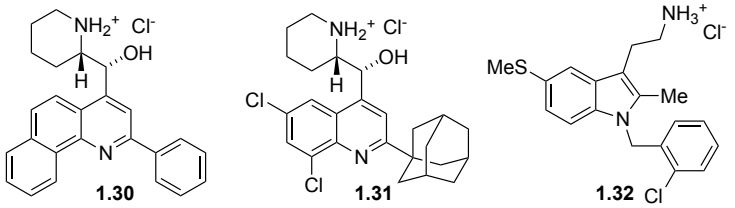

Additional high throughput screening by the De Cammili group at Yale led to the identification of two new classes of SHIP inhibitors: the triazolo[3,4-b][1,3,4] thiadiazoles **1.33**, **1.34** and **1.35** and the benzylic amines **1.36**, **1.37** and **1.38** (Figure 1.14).[73] These compounds not only showed inhibition of SHIP1 and SHIP2, but also showed inhibition of other 5'-inositol phosphatases that are not structurally related to SHIP, namely OCRL and, in the case of the benzylic amines, both OCRL and synaptogenin SJ1. This is unusual as most of the other inhibitors mentioned previously do not inhibit the other 5'-inositol phosphatases. The promiscuity of the inhibition has likely limited the use of these compounds for further studies.

Figure 1.14: SHIP Inhibitors Discovered at Yale University

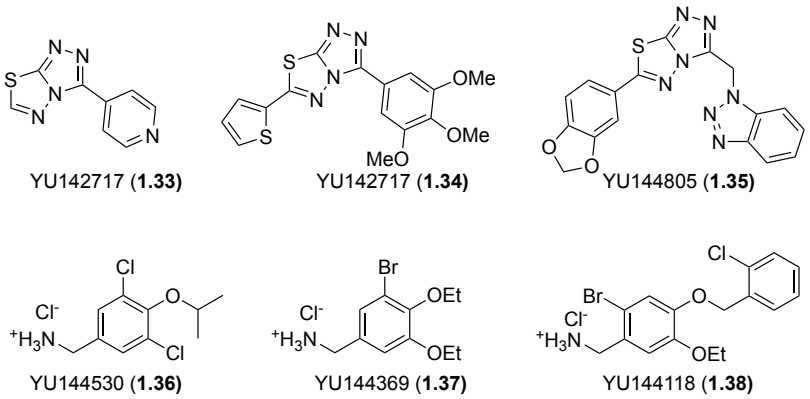

1.10 Summary

The development of isoform specific PI3K inhibitors for the treatment of inflammatory disease and cancer has proven difficult and provided only mixed results. This has led to the exploration of alternative strategies to modulate signaling in this pathway, including targeting the inositol phosphatase SHIP. This mode of attack is not without challenges, however, as multiple isoforms of SHIP are known and SHIP has also been shown to be both an activator and an antagonist of PI3K signaling depending on the environment. Despite these potential issues, a number of approaches has led to the identification of SHIP antagonists and agonists. These molecules have been shown to be not only useful in probing the role of SHIP in cell signaling, but have also been used to provide information on potential treatments for a variety of disorders from cancer to inflammation to Alzheimer's disease. Given the common role PI3K signaling plays in many of these diseases, further study of small molecule modulators of SHIP appears to be justified.

1.11 References

1. Zhang, X.; Majerus, P. W., Phosphatidylinositol signaling reactions. *Semin. CellDev. Biol.* **1998**, *9*, 153-160.

2. Catimel, B.; Yin, M.-X.; Schieber, C.; Condron, M.; Patsiouras, H.; Catimel, J.; Robinson, D. E. J. E.; Wong, L. S.-M.; Nice, E. C.; Holmes, A. B.; Burgess, A. W., PI(3,4,5)P3 Interactome. *J. Proteome Res.* **2009**, *8*, 3712-3726.

3. Cantely, L. C., The phosphoinositide 3-kinase pathway. *Science* **2002**, *296*, 1655-1657.

4. Majerus, P. W.; Kisseleva, M. V.; Norris, F. A., The role of phosphatases in inositol signaling reactions. *J. Biol. Chem.* **1999**, *274*, 10669-10672.

5. Viernes, D. R.; Choi, L. B.; Kerr, W. G.; Chisholm, J. D., Discovery and development of small molecule SHIP phosphatase modulators. *Med. Res. Rev.* **2013**, *34*, 795-824.

6. Marion, F.; Williams, D. E.; Patrick, B. O.; Hollander, I.; Mallon, R.; Kim, S. C.; Roll, D. M.; Feldberg, L.; Van Soest, R.; Anderson, R. J., Liphagal, a selective inhibitor of PI3 kinase a isolated from the sponge akacoralliphaga: structure elucidation and biomimetic synthesis. *Org. Lett.* **2006**, *8*, 321-324.

7. Vivanco, I.; Sawyers, C. L., Phosphatidylinositol 3-kinase AKT pathway in human cancer. *Nat. Rev. Cancer* **2002**, *2*, 489-501.

8. Leslie, N. R.; Biondi, R. M.; Alessi, D. R., Phosphoinositide-regulated kinases and phosphoinositide phosphatases. *Chem. Rev.* **2001**, *101*, 2365-2380.

9. Krystal, G., Lipid phosphatases in the immune system. *Semin. Immunol.* **2000**, *12*, 397-403.

10. Sewell, G. W.; Marks, D. J.; Segal, A. W., The immunopathogenesis of Crohn's disease: A three-stage model. *Curr. Opin. Immunol.* **2009**, *21*, 506-513.

11. Kerr, W. G.; Heller, M.; Herzenberg, L. A., Analysis of lipopolysaccharide-response genes in B-lineage cells demonstrates that they can have differentiation stage-restricted expression and contain SH2 domains. *Proc. Natl. Acad. Sci. USA.* **1996**, *93*, 3947-3952.

12. Damen, J. E.; Liu, L.; Rosten, P.; Humphries, R. K.; Jefferson, A. B.; Majerus, P. W.; Krystal, G., The 145-kDa protein induced to associate with the Shc by multiple cytokines is an inositol tetraphosphate and phosphatidylinositol 3,4,5- trisphosphate 5-phosphatase. *Proc. Natl. Acad. Sci. USA.***1996**, *93*, 1689-1693.

13. Lioubin, M. N.; Algate, P. A.; Tsai, S.; Carlberg, K.; Aebersold, R.; Rohchneider, L. R., p150Ship, a signal transduction molecule with inositol polyphosphate-5-phosphatase activity. *Genes & Dev.* **1996**, *10*, 1084-1095.

14. Zippo, A.; De Robertis, A.; Bardelli, M.; Galvagni, F.; Oliviero, S., Identification of F1K-1 target genes in vasculogenesis: Pim-1 is required for endothelial and mural cell differentiation in vitro. *Blood* **2004**, *103*, 4536-4544.

15. Tu, Z.; Ninos, J. M.; Ma, Z.; Wang, J.; Lemos, M. P.; Desponts, C.; Ghansah, T.; Howson, J. M.; Kerr, W. G., Embryonic and hematopoietic stem cells express a novel SH2-contaning inositol 5'-phosphatase isoform that partners with the Brb2 adapter protein. *Blood* **2001**, *98*, 2028-2038.

16. Hamilton, M. J.; Ho, V. W.; Kuroda, E.; Ruschmann, J.; Antignano, F.; Lam, V.; Krystal, G., Role of SHIP in cancer. *Exp. Hematol.* **2011**, *39*, 2-13.

17. Prasad, K. N., Two diseases with one hit: Inhibiting a potential diabetes target to reduce cancer risk and to improve anti-cancer therapy. *Curr. Cancer Ther. Rev.* **2009**, *5*, 111-121.

18. Clement, S.; Krause, U.; Desmedt, F.; Tanti, J. F.; Behrends, J.; Pesesse, X.; Sasaki, T.; Penninger, J.; Doherty, M.; Malaisse, W.; Dumont, J. E.; Le Marchand-Brustel, Y.; Erneux, C.; Hue, L.; Schurmans, S., The lipid phosphatase SHIP2 controls insulin sensitivity. *Nature* **2001**, *409*, 92-97.

19. Sleeman, M. W.; Wortley, K. E.; Lai, K. M.; Gowen, L. C.; Kintner, J.; Kline, W. O.; Garcia, K.; Stitt, T. N.; Yancopoulos, G. D.; Wiegand, S. J.; Glass, D. J., Absence of the lipid phosphatase SHIP2 confers resistance to dietary obesity. *Nat. Med.***2005**, *11*, 199-205.

20. Kerr, W. G.; Park, M. Y.; Maubert, M.; Engelman, R. W., SHIP deficiency causes Crohn's disease-like ileitis. *Gut.* **2011**, *60*, 177-188.

21. Hazen, A. L.; Smith, M. J.; Desponts, C.; Winter, O.; Moser, K.; Kerr, W. G., SHIP is required for a functional hematopoietic stem cell niche. *Blood* **2009**, *113*, 2924-2933.

22. Hakim, S.; Bertucci, M. C.; Conduit, S. E.; Vuong, D. L.; Mitchell, C. A., Inositol polyphosphate phosphatases in human disease. *Curr. Top. Microbiol. Immunol.* **2012**, *362*, 247-314.

23. Ooms, L. M.; Horan, K. A.; Rahman, P.; Seaton, G.; Gurung, R.; Kethesparan, D. S.; Mitchell, C. A., The role of the inositol polyphosphate 5-phosphatases in cellular function and human disease. *Biochem. J.* **2009**, *419*, 29-49.

24. Brooks, R.; Fuhler, G. M.; Iyer, S.; Smith, M. J.; Park, M.; Paraiso, K.; Engelman, R. W.; G, K. W., SHIP1 inhibition increases immunoregulatory capacity and triggers apoptosis of hematopoietic cancer cells. *J. Immunol.* **2010**, *184*, 3582-3589.

25. Kennah, M.; Yau, T. Y.; Nodwell, M.; Krystal, G.; Anderson, R. J.; Ong, C. J.; Mui, A., Activation of SHIP via a small molecule agonist kills multiple myeloma cells. *Exp. Hematol.* **2009**, *37*, 1274-1283.

26. Prasad, K. N.; Decker, S. J., SH2-containing 5'-inositol phosphatase, SHIP2, regulates cytoskeleton organization and ligand-dependent down-regulation of the epidermal growth factor receptor. *J. Biol. Chem.* **2005**, *280*, 13129-13136.

27. Prasad, K. N.; Tandon, M.; Badve, S.; Snyder, P. W.; Nakshatri, H., Phosphoinositol phosphatase SHIP 2 promotes cancer development and metastasis coupled with alterations in the EGF receptor turnover. *Carcinogenesis* **2008**, *29*, 25-34.

28. Prasad, K. N.; Tandon, M.; Handa, A.; Moore, G. E.; Babbs, C. F.; Snyder, P. W.; Bose, S., High expression of obesity-linked phosphatase SHIP2 in invasive breast cancer correlates with reduced disease-free survival. *Tumor Biol.* **2008**, *29*, 330-341.

29. Prasad, K. N., SHIP2 phosphoinositol phosphatase positively regulates EGFR-Akt pathway, CXCR4 expression, and cell migration in MDA-MB-231 breast cancer cells. *Int. J. Oncol.* **2009**, *34*, 97-105.

30. Hoekstra, E.; Das, A.; Willemsen, M.; Swets, M.; Kuppen, P. J. K.; van der Woude, C. J.; Bruno, M. J.; Shah, J. P.; ten Hagen, T.; Chisholm, J. D.; Kerr, W. G.; Peppelenbosch, M. P.; Fuhler, G. M., Lipid phosphatase SHIP2 functions as oncogene in colorectal cancer by regulating PKB activation. *Oncotarget.* **2016**, *7*, 73525-73540.

31. Fuhler, G. M.; Brooks, R.; Toms, B.; Iyer, S.; Gengo, E. A.; Park, M. Y.; Gumbleton, M.; Viernes, D. R.; Chisholm, J. D.; Kerr, W. G., Therapeutic potential of SH2 domain-containing inositol-5′-phosphatase 1 (SHIP1)and SHIP2 inhibition in cancer. *Mol. Med.* **2012**, *18*, 65-75.

32. Gumbleton, M.; Sudan, R.; Fernandes, S.; Kerr, W. G.; Engelman, R. W.; Russo, C. M.; Chisholm, J. D.; Kerr, W. G., Dual enhancement of T and NK cell function by pulsatile inhibition of SHIP1 improves antitumor immunity and survival. *Sci. Signal* **2017**, *10*, eaam5353.

33. Saz-Leal, P.; Del Fresno, C.; Brandi, P.; Martinez-Cano, S.; Dungan, O. M.; Chisholm, J. D.; Kerr, W. G.; Sancho, D., Targeting SHIP-1 in myeloid cells enhances trained immunity and boosts response toinfection. *Cell Rep.* **2018**, *25*, 1118-1126.

34. Ishihara, H.; Sasaoka, T.; Hori, H.; Wada, T.; Hirari, H.; Haruta, T.; Langlois, W. J.; Kobayashi, M., Molecular cloningof rat SH2-containing inositol phosphatase 2 (SHIP2) and its role in the regulation of insulin signaling. *Biochem. Biophys. Res. Commun.* **1999**, *260*, 256-272.

35. Sleeman, M. W.; Wortley, K. E.; Lai, K. M.; Gowen, L. C.; Kintner, J.; Kline, W. O.; Garcia, K.; Stitt, T. N.; Yancopoulos, G. D.; Wiegand, S. J.; Glass, D. J., Absence of the lipid phosphatase SHIP2 confers resistance to dietary obesity. *Nat. Med.* **2005**, *11*, 199-205.

36. Clement, S.; Krause, U.; Desmedt, F.; Tanti, J. F.; Behrends, J.; Pesesse, X.; Sasaki, T.; Penninger, J.; Doherty, M.; Malaisse, W.; Dumont, J. E.; Le Marchand-Brustel, Y.; Erneux, C.; Hue, L.; Schurmans, S., The lipid phosphatase SHIP2 controls insulin sensitivity. *Nature* **2001**, *409*, 92-97.

37. Suwa, A.; Yamamoto, T.; Sawada, A.; Minoura, K.; Hosogai, N.; Tahara, A.; Kurama, T.; Shimokawa, T.; Aramori, I., Discovery and functional characterization of a novel small molecule inhibitor of the intracellular phosphatase, SHIP2. *Br. J. Pharmacol.* **2009**, *158*, 879-887.

38. Srivastava, N.; Iyer, S.; Sudan, R.; Youngs, C.; Engelman, R. W.; Howard, K. T.; Russo, C. M.; Chisholm, J. D.; Kerr, W. G., A small-molecule inhibitor of SHIP reverse age- and diet-associated obesity and metabolic syndrome. *JCI Insight* **2016**, *1*, e88544.

39. Kerr, W. G., Dual functions for SHIP in immunity and cancer. *Ann. NY. Acad. Sci.* **2011**, *1217*, 1-17.

40. Liu, Q.; Sasaki, T.; Kozieradzki, I.; Wakeham, A.; Itie, A.; Dumont, D. J.; Penninger, J. M., SHIP is a negative regulator of growth factor receptor-mediated PKB/Akt activation and myeloid cell survival. *Genes Dev.* **1999**, *13*, 786-791.

41. Ong, C.; Ming-Lum, A.; Nodwell, M.; Ghanipour, A.; Yang, L.; Williams, D.; Kim, J.; Demirjian, L.; Qasimi, P.; Ruschmann, J.; Cao, L.; Ma, K.; Chung, S.; Duronio, V.; Andersen, R.; Krystal, G.; Mui, A., Small-molecule agonists of SHIP1 inhibit the phosphoinositide 3-kinase pathway in hematopoietic cells. *Blood* **2007**, *110*, 1942-1949

42. Lim, J. W.; Kim, S. K.; Choi, Y. S.; Kim, D. H.; Gadhe, C. G.; Lee, H. N.; Kim, H.-N.; Kim, J.; Cho, S. J.; Hwang, H.; Seong, J.; KJeong, K.-S.; Lee, J. Y.; Lim, S. M.; Lee, J. W.; Pae, A. N., Identification of crizotinib derivatives as potent SHIP2 inhibitors for the treatment of Alzheimer's disease. *Euro. J. Med. Chem.* **2018**, *157*, 405-422.

43. Ruiz, A.; Heilmann, S.; Becker, T.; Hernández, I.; Wagner, H.; Thelen, M.; Mauleón, A.; Rosende-Roca, M.; Bellenguez, C.; Bis, J. C.; Harold, D.; Gerrish, A.; Sims, R.; Sotolongo-Grau, O.; Espinosa, A.; Alegret, M.; Arrieta, J. L.; Lacour, A.; Leber, M.; Becker, J.; Lafuente, A.; Ruiz, S.; Vargas, L.; Rodríguez, O.; Ortega, G.; Dominguez, M.; IGAP; Mayeux, R.; Haines, J. L.; Pericak-Vance, M. A.; Farrer, L. A.; Schellenberg, G. D.; Chouraki, V.; Launer, L. J.; van Duijn, C.; Seshadri, S.; Antúnez, C.; Breteler, M. M.; Serrano-Ríos, M.; Jessen, F.; Tárraga, L.; Nöthen, M. M.; Maier, W.; Boada, M.; Ramírez, A., Follow-up of loci from the International Genomics of Alzheimer's Disease Project identifies TRIP4 as a novel susceptibility gene. *Transl. Psychiatry.* **2014**, *4*, e358.

44. Zhang, M.; Schmitt-Ulms, G.; Sato, C.; Xi, Z.; Zhang, Y.; Zhou, Y.; St George-Hyslop, P.; Rogaeva, E., Drug Repositioning for Alzheimer's Disease Based on Systematic 'omics' Data Mining. *PLOS ONE* **2016**, *11*, e0168812.

45. Yoshino, Y.; Yamazaki, K.; Ozaki, Y.; Sao, T.; Yoshida, T.; Mori, T.; Mori, Y.; Ochi, S.; Iga, J. I.; Ueno, S. I., INPP5D mRNA xxpression and cognitive decline in Japanese Alzheimer's disease dubjects. *J. Alzheimers Dis.* **2017**, *58*, 687-694.

46. Ulland, T. K.; Song, W. M.; Huang, S. C.-C.; Ulrich, J. D.; Sergushichev, A.; Beatty, W. L.; Loboda, A. A.; Zhou, Y.; Cairns, N. J.; Kambal, A.; Loginicheva, E.; Gilfillan, S.; Cella, M.; Virgin, H. W.; Unanue, E. R.; Wang, Y.; Artyomov, M. N.; Holtzman, D. M.; Colonna, M., TREM2 maintains microglial metabolic fitness in Alzheimer's disease. *Cell* **2017**, *170*, 649-663.e13.

47. Ulland, T. K.; Wang, Y.; Colonna, M., Regulation of microglial survival and proliferation in health and diseases. *Semin. Immunol.* **2015**, *27*, 410-415.

48. Wang, Y.; Cella, M.; Mallinson, K.; Ulrich, J. D.; Young, K. L.; Robinette, M. L.; Gilfillan, S.; Krishnan, G. M.; Sudhakar, S.; Zinselmeyer, B. H.; Holtzman, D. M.; Cirrito, J. R.; Colonna, M., TREM2 lipid sensing sustains the microglial response in an Alzheimer's disease model. *Cell* **2015**, *160*, 1061-1071.

49. Iyer, S.; Brooks, R.; Gumbleton, M.; Kerr, W. G., SHIP1-expressing mesenchymal stem cells regulate hematopoietic stem cell homeostasis and lineage commitment during aging. *Stem Cells Dev.* **2015**, *24*, 1073-1081.

50. Prakash, A.; Medhi, B.; Chopra, K., Granulocyte colony stimulating factor (GCSF) improves memory and neurobehavior in an amyloid-β induced experimental model of Alzheimer's disease. *Pharmacol. Biochem. Behav.* **2013**, *110*, 46-57.

51. Tsai, K.-J.; Tsai, Y.-C.; Shen, C.-K. J., G-CSF rescues the memory impairment of animal models of Alzheimer's disease. *J. Exp. Med.* **2007**, *204*, 1273-1280.

52. Sanchez-Ramos, J.; Cimino, C.; Avila, R.; Rowe, A.; Chen, R.; Whelan, G.; Lin, X.; Cao, C.; Ashok, R., Pilot study of granulocyte-colony stimulating factor for treatment of Alzheimer's disease. *J. Alzheimers Dis.* **2012**, *31*, 843-855.

53. Wu, P.; Hu, Y., Small molecules targeting phosphoinositide 3-kinases. *Med. Chem. Comm.* **2012**, *3*, 1337-1355.

54. Marone, R.; Cmilijanovic, V.; Giese, B.; Wymann, M. P., Targeting phosphoinositide 3-kinase—Moving towards therapy. *Biochim. Biophys. Acta.* **2008**, *1784*, 159-185.

55. Yang, L.; Williams, D.; Mui, A.; Ong, C.; Krystal, R.; Andersen, R., Synthesis of pelorol and analogues: activators of inositol 5-phosphatase SHIP. *Org. Lett.* **2005**, *7*, 1073-1076.

56. Goclik, E.; Konig, G. M.; Wright, A. D.; Kaminsky, R., Pelorol from the tropical marine sponge Dacty- lospongia elegans. *J. Nat. Prod.* **2000**, *63*, 1150–1152.

57. Meimetis, L. G.; Nodwell, M.; Yang, L.; Wang, X.; Wu, J.; Harwig, C.; Stenton, G. R.; MacKenzie, L. F.; MacRury, T.; Patrick, B. O.; Ming-Lum, A.; Ong, C. J.; Krystal, G.; Mui, A.; Andersen, R. J., Synthesis of SHIP1-activating analogs of the sponge meroterpenoid pelorol. *Eur. J. Org. Chem.* **2012**, *2012*, 5195-5207.

58. Mackenzie, L.; Macrury, T.; Harwig, C.; Khlebnikov, V.; Shan, R.; Place, S.; Bird, P.; Pettigrew, J.; Bhatti, N. A., SHIP1 modulators and methods related thereto. *Patent. Appl.* **2011**, WO 2011069118.

59. Stenton, G.; Mackenzie, L.; Tam, P.; Cross, J.; Harwig, C.; Raymond, J.; Toews, J.; Wu, J.; Ogden, N.; MacRury, T.; Szabo, C., Characterization of AQX-1125, a small molecule SHIP1 activator Part 1. Effects on inflammatory cell activation and chemotaxi in vitro and pharmocokinetic characterization in vivo. *Br. J. Pharmacol.* **2013**, *168*, 1506-1518.

60. Stenton, G.; Mackenzie, L.; Tam, P.; Cross, J.; Harwig, C.; Raymond, J.; Toews, J.; Chernoff, D.; MacRury, T.; Szabo, C., Characterization of AQX-1125, a small-molecule SHIP1 activator. Part 2. Efficacy studies in allergic and pulmonary inflammation models in vivo . *Br. J. Pharmacol.* **2013**, *168*, 1519-1529.

61. Globe Newswire. Vancouver, British Columbia. Aquinoxs AQX 1125 flunks mid stage study for patients with atopic dermatitis. Nov. 2, **2015**. http://www.biospace.com/News/aquinoxs-aqx-1125-flunks-mid-stage-study-for/397505/

62. Williams, D. E.; Amlani, A.; Dewi, A. S.; Patrick, B. O.; vanOfwegen, L.; Mui, A.; Andersen, R. J., Australin E isolated from the soft coral Cladiella sp. collected in pohnpei activates the inositol 5-phosphatase SHIP1. *Aust. J. Chem.* **2010**, *63*, 895-900.

63. Li, D.; Carr, G.; Zhang, Y.; Williams, D. E.; Amlani, A.; Bottriell, H.; Mui, A.; Andersen, R. J., Turna- gainolides A and B, cyclic depsipeptides produced in culture by a Bacillus sp.: Isolation, structure elucidation, and synthesis. *J. Nat. Prod.* **2011**, *74*, 1093-1099.

64. Zhang, H.; He, J.; Kutateladze, T. G.; Sakai, T.; Sasaki, T.; Markadieu, N.; Erneux, C.; Prestwich, G. D., 5-Stabilized phosphatidylinositol 3,4,5-trisphosphate analogues bind Grp1 PH, inhibit phospho- inositide phosphatases, and block neutrophil migration. *Chem. Biochem.* **2010**, *11*, 388-395.

65. Maehama, T.; Taylor, G. S.; Slama, J. T.; Dixon, J. E., A sensitive assay for phosphoinositide phosphatases. *Anal. Biochem.***2000**, *279*, 248-250.

66. Brooks, R.; Iyer, S.; Akada, H.; Neelam, S.; Russo, C. M.; Chisholm, J. D.; G, K. W., Coordinate expansion of murine hematopoietic and mesenchymal stem cell compartments by SHIPi. *Stem Cells* **2015**, *33*, 848-858.

67. Vandeput, F.; Combettes, L.; Mills, S. J.; Backers, K.; Wohlkonig, A.; Parys, J.; De Smedt, H.; Missiaen, L.; Dupont, G.; Potter, B. V. L.; Erneux, C., Biphenyl 2,3′,4,5′,6-pentakisphosphate, a novel inositol polyphosphate surrogate, modulates Ca2+ responses in rat hepatocytes. *FASEB J.* **2007**, *21*, 1481-1491.

68. Mills, S. J.; Persson, C.; Cozier, G.; Thomas, M. P.; Trésaugues, L.; Erneux, C.; Riley, A. M.; Nordlund, P.; Potter, B. V. L., A synthetic polyphosphoinositide headgroup surrogate in complex with SHIP2 provides a rationale for drug discovery. *ACS Chem. Bio.* **2012**, *7*, 822-828.

69. Sasaoka, T.; Wada, T.; Fukui, K.; Murakami, S.; Ishihara, H.; Suzuki, R.; Tobe, K.; Kadowaki, T.; Kobayashi, M., SH2-containing inositol phosphatase 2 predominantly regulates Akt2, and not Akt1, phos- phorylation at the plasma membrane in response to insulin in 3T3-L1 adipocytes. *J. Biol. Chem.* **2004**, *279*, 14835-14843.

70. Suwa, A.; Kurama, T.; Yamamoto, T.; Sawada, A.; Shimokawa, T.; Aramori, I., Glucose metabolism activation by SHIP2 inhibitors via up-regulation of GLUT1 gene in L6 myotubes. *Eur. J. Pharmacol.* **2010**, *642*, 177-182.

71. Annis, D. A.; Cheng, C. C.; Chuang, C.-C.; McCarter, J. D.; Nash, H. M.; Nazef, N.; Rowe, T.; Kurzeja, R. J. M.; Shipps, G. W. J., Inhibitors of the lipid phosphatase SHIP2 discovered by high throughput affinity selection-mass spectrometry screening of combinatorial libraries. *Comb. Chem. High Throughput Screen* **2009**, *12*, 760-771.

72. Ichihara, Y.; Fujimura, R.; Tsuneki, H.; Wada, T.; Okamoto, K.; Gouda, H.; Hirono, S.; Sugimoto, K.; Matsuya, Y.; Sasaoka, T.; Toyooka, N., Rational design and synthesis of 4-substituted 2-pyridin-2- ylamides with inhibitory effects on SH2 domain-containing inositol 5′-phosphatase 2 (SHIP2). *Eur. J. Med. Chem.* **2013**, *62*, 649-660.

73. Pirruccello, M.; Nandez, R.; Idevall-Hagren, O.; Alcazar-Roman, A.; Abriola, L.; Berwick, S. A.; Lucast, L.; Morel, D.; De Camilli, P., Identification of inhibitors of inositol 5-phosphatases through multiple screening strategies. *ACS Chem. Bio.* **2014**, *9*, 1359-1368.

Chapter 2 - Synthetic Studies on Small Molecule SHIP Inhibitors

Abstract

SHIP is a key regulator in the PI3K cell signaling pathway, influencing the phosphorylation patterns of inositol phospholipids intercalated in the cell membrane which act as second messengers helping transmit signals from outside the cell to the nucleus. Misregulation of SHIP disrupts this signaling, causing changes in many aspects of cellular physiology. These changes have been implicated in a number of human disorders ranging from cell growth diseases (cancer), immune response diseases (autoimmune disease), chronic neurodegenerative diseases (Alzheimer's) and obesity. Since the SHIP enzyme may play a role in the pathogenesis of these conditions, regulation of SHIP with small molecules is an attractive approach to ameliorate any aberrant signaling. Attempts to modulate SHIP activity with small molecules has led us to investigate the synthesis of new aminosteroid SHIP inhibitors. These molecules may then be used to further evaluate the role SHIP plays in this signaling pathway. These studies may also aid in determining the key structure-activity relationships necessary for increased potency and selectivity for inhibition of a specific paralog of SHIP (SHIP1 over SHIP2).

2.1 Introduction

The phosphatase SHIP1 is expressed and utilized in hematopoietic cells, while a paralog enzyme (SHIP2) is utilized in other cells. This difference provides a potentially selective way of targeting PI3K signaling in these specific cell types. The regulation of the SHIP1 enzyme has been shown to play an important role in the cellular physiology of blood and bone marrow cells,[1-3] endothelial cells,[4] and embryonic cells[5] by the effects it invokes on the PI3K signaling pathway. Understanding the role of SHIP modulation may lead to the development of possible therapeutic treatments for a wide spectrum of human disorders[6] ranging from cancer,[7,8] autoimmune diseases,[9] Alzheimer's,[10] as well as obesity.[11] However, isolation and use of small molecule SHIP modulators is complicated by the presence of several isoforms of the SHIP enzyme in vertebrates. The development of selective SHIP inhibitors may have advantages over pan-inhibitors to minimize any side effects in these potential treatments. In order to take advantage of paralog specific inhibition, specific SHIP inhibitors targeting each paralog of SHIP are needed. This can be challenging, as the two enzymes are highly homologous, however recently Astellas divulged some SHIP2 specific inhibitors,[12,13] so specific inhibition of SHIP isoforms has been shown to be possible.

Utilizing a fluorescence polarization assay to detect inhibition activity against recombinant SHIP1, a high-throughput screen identified the aminosteroid NSC23922 **2.1** (Figuer 2.1) from a library of compounds available from the National Cancer Institute. NSC23922 was actually a mixture of the 3α and 3β isomers, but further studies showed that the α-isomer, 3α-aminocholestane 3AC **2.2**, was significantly more active (Figure 2.1).[14] The 3α-aminocholestane **2.2** showed 50% inhibitory activity against the SHIP1 enzyme at 10 μM with inhibitory activity still observed at 2 μM against 0.1 μg of recombinant SHIP .[9,14]

Figure 2.1: Structure of NSC23922 ***2.1****, 3AC* ***2.2****, and Steroid Numbering System*

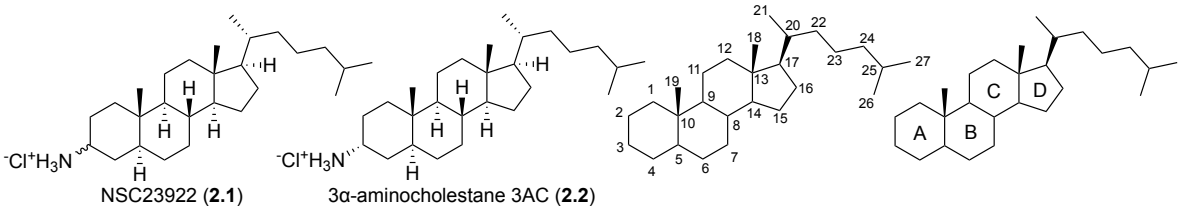

Further evaluation using the colorimetric Malachite Green assay proved 3AC **2.2** to be a selective inhibitor of SHIP1 at 1mM concentration with no inhibition detectable for two other inositol phosphatases, SHIP2 and PTEN, which also hydrolyze $PI(3,4,5)P_3$ (Figure 2.2). This selectivity allows for a greater understanding of the role of SHIP1 in the PI3K cell signaling pathway with less risk of off target effects, as it has been shown that inhibition of PTEN can be detrimental as it acts as a tumor suppressor, inhibiting tumor growth and cell malignancies.[15-17]

Figure 2.2: 3AC is a Selective SHIP1 Inhibitor based on Malachite Green Assay Results[9,14]

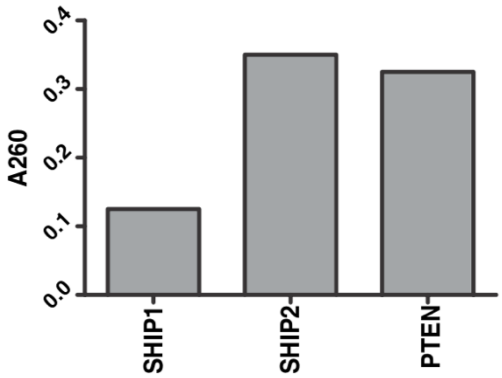

With in vitro data supporting 3AC **2.2** to be a selective SHIP1 inhibitor, in vivo testing in mice was undertaken to show whether or not small molecule inhibition with 3AC showed effects in an animal. Adult mice treated with 60 μM 3AC **2.2** daily for 7 days showed to have a similar increase in $Mac1^+Gr1^+$ myeloid immunoregulatory (MIR) cells comparable to SHIP knockout mice, whereas vehicle mice had no increased response (Figure 2.3).[9,18] Increases in MIR cells in

peripheral lymphoid tissues suppresses allogeneic T cell responses, which is a potential method to treat Graft versus host disease (GvHD) and reduce bone marrow and organ transplant rejection.[9,14,18-20] A similar modified immune system was observed in SHIP1 knockout mice, which accept mismatched bone marrow grafts without rejection.[21] This study was important as it showed that the aminosteroids possessed adequate pharmacodynamic properties to be effective in animal model systems.

*Figure 2.3: $Mac1^{+}Gr1^{+}$ Myeloid Immunoregulatory (MIR) Cells in Spleen (**A**) and Lymph Node (**B**) of Mice Treated with 3AC **2.2** (Compound), Vehicle (Ethanol), and Unmanipulated Control (Normal)*[9,14]

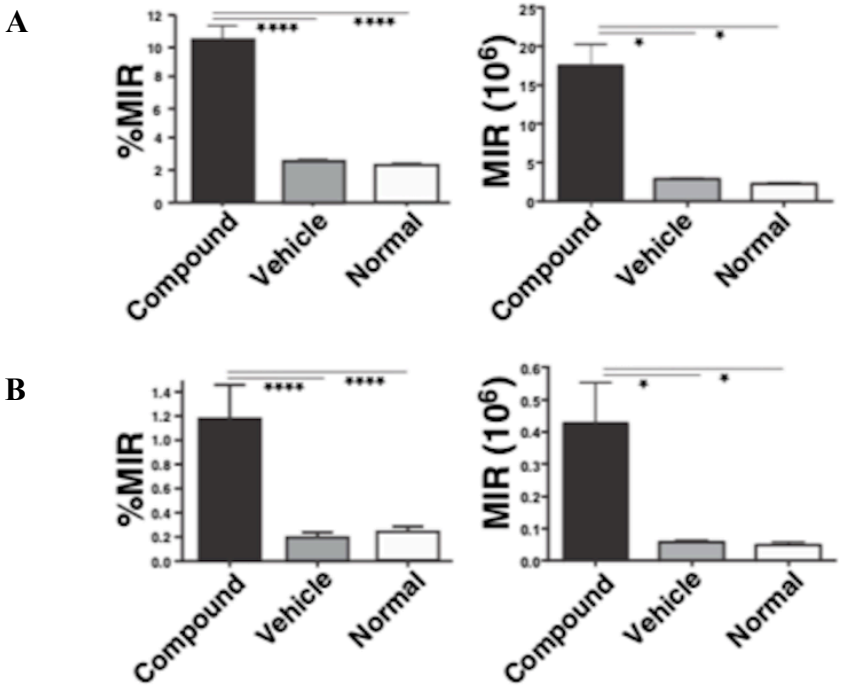

More evidence of SHIP modulation in vivo was observed when mice treated with 3AC **2.2** showed a 4- to 5-fold increase in circulating granulocytes in peripheral blood similar to that of $SHIP^{-/-}$ mice (Figure 2.4).[9,22] However, unlike SHIP knockout mice which show lung defects which

result in the development of pneumonia, mice treated with NSC23922 **2.1** appeared to have normal lung function. Mice treated with 3AC **2.2** did not show any toxic side-effects, nor was there an increase in mortality or body weight fluctuation (Figure 2.5).[9,14,18,19,22]

Figure 2.4: SHIP1 Inhibition Increases Circulating Granuocyte/Neutrophil Numbers[9,14]

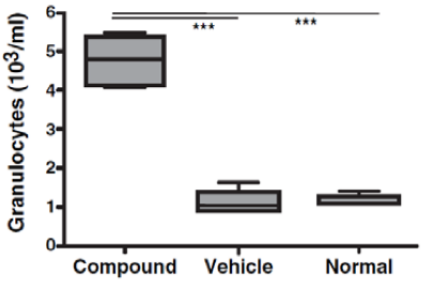

*Figure 2.5: Induction of Lung Pneumonia in SHIP-Deficient Adult Mice (**A-C**). SHIP Inhibition Does Not Induce Myeloid-Associated Lung Pneumonia (**D-F**). No Reduction of Body Weight When Treated with 3AC **2.2** (**G**).*[9,14]

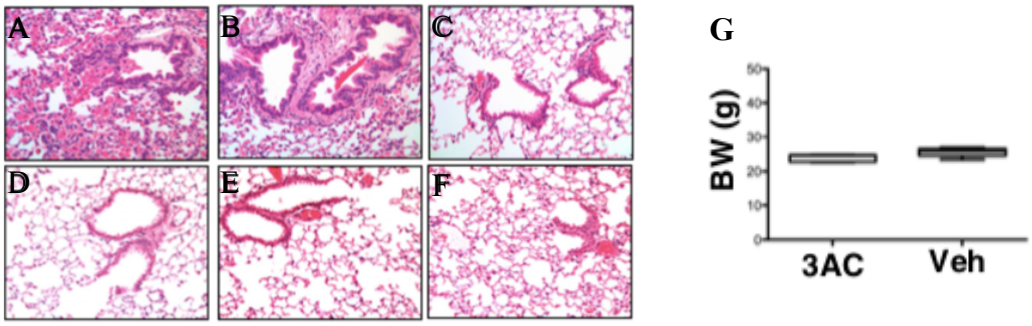

As SHIP can both activate and inhibit PI3K signaling depending on the environment, there was some concern that SHIP inhibitors may act to facilitate tumor growth. To alleviate any concern of potential blood cell cancer promotion and/or enhanced survival, 3AC **2.2** treatment of several cancer cell lines was explored. Both the SHIP1 expressing KG-1 AML cell line and osteosarcoma cells that show no expression of SHIP1 were evaluated in vitro (Figure 2.6).[9] Cell growth and

survival decreased in the KG-1 cells but no effect was observed on the osteosarcoma cells. Murine C1498 leukemia cells were also observed to be responsive to 3AC **2.2** upon treatment, but K562 leukemia cells that only express SHIP2 and PTEN showed no observable effect.[9] SHIP1 inhibition was also shown to cause cell death in multiple myeloma (MM) cell lines using 3AC **2.2** as the SHIP1 inhibitor.[9] It is evident that SHIP1 inhibition through small molecule 3AC **2.2** treatment can be a potential for human blood therapeutic treatments as inhibition leads to a decrease in AKT activation and apoptosis.

*Figure 2.6: Increased 3AC **2.2** Concentration Promotes Cell Death of SHIP1 Expressing KG-1 AML Cells and C1498 Leukemia Cells. No Apoptosis Observed for K562 Leukemia Cells Only Expressing SHIP2 and PTEN.[9]*

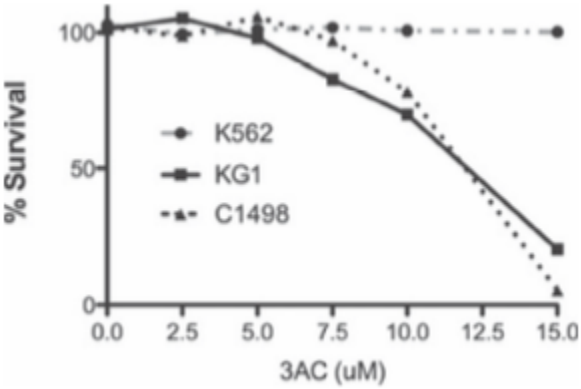

Interestingly, SHIP1 has recently been discovered to play a role in trained immunity and improved cell response to infection through increased activation of the PI3K/AKT/mTOR signaling pathway.[23] In vitro studies identified macrophages from SHIP1-deleted myeloid cells to have an increase in proinflammatory cytokine production through β-glucan induced training when exposed to a lethal dose of lipopolysaccharides.[23] This increased proinflammatory response was

also observed when bone marrow derived macrophages (BMDM) trained with β-glucan were administered 3AC **2.2** before being treated with lipopolysaccharides. The cell response showed a dose-dependent increase in TNFα production (Figure 2.7).[23]

*Figure 2.7: Increasing TNF*α Production from Bone Marrow Derived Macrophages Trained with Increasing Concentrations of 3AC **2.2** [23]

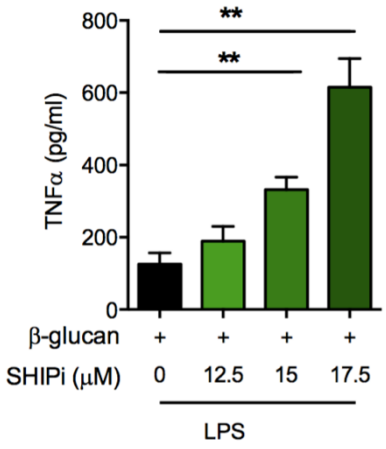

In vivo evaluation of 3AC's **2.2** ability to help boost a trained immunity response to infectious conditions showed that mice treated with 3AC **2.2** twice daily on consecutive days followed by exposure to a low dose of *Candida albicans* followed by a 7-day period before being injected with a lethal dose of the same fungus proved that mice trained with the fungus while being administered the SHIP1 inhibitor 3AC **2.2** had a higher survival rate (Figure 2.8).[23] Mice not trained with the *Candida albicans* fungus but still administered 3AC **2.2** showed no significant increase in survival compared to the control. Mice primed with the fungus but not administered 3AC **2.2** had a higher survival rate compared to the control but not greater than the 3AC **2.2** trained.[23] These results were attributed to the role of SHIP1 in the immune response, where loss of SHIP1 function leads to oversensitive immune cells.[24] By using a transient inhibition of SHIP1,

the immune cells can be hypersensitized for a short time, and then trained with only a mild challenge to target foreign cell like cancer cells or a fungal infection.

*Figure 2.8: Survival Curve of 3AC **2.2** Primed Mice Trained with Candida albicans*[23]

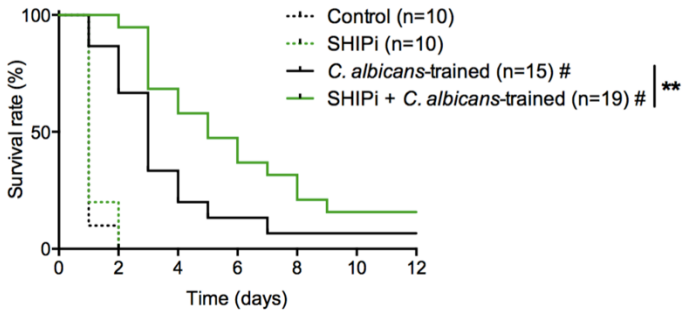

2.2 Objectives

More recent studies on 3AC **2.2** showed that while the compound was still selective for SHIP1, some inhibition of SHIP2 was being observed, with 3AC **2.2** only showing an approximately 3-fold selectivity for SHIP1. While this may have been the result of the use of a different source of the SHIP2 enzyme (the new source was recombinant human SHIP2 instead of the original enzyme, which was derived from a murine source), it may also be due to the testing of a single isomer of the aminosteroid, as the initial testing which showed selective inhibition was performed on NSC23922 **2.1** which is a mixture of isomers (Figure 2.9). Therefore the β-isomer of NSC23922 **2.3** could potentially have been mischaracterized, and should it be a potent SHIP1 inhibitor leading to a reassessment of these inhibitors (Figure 2.9). To investigate these issues, the resynthesis of both **2.2** and **2.3**, as well as the reformulation of the original NSC23922 **2.1** was

undertaken so that all three could be tested against SHIP1 and SHIP2 side by side under exactly the same assay conditions.

Figure 2.9: Structures of NSC23922 ***2.1****, the α-isomer 3AC* ***2.2****, and β-isomer* ***2.3****.*

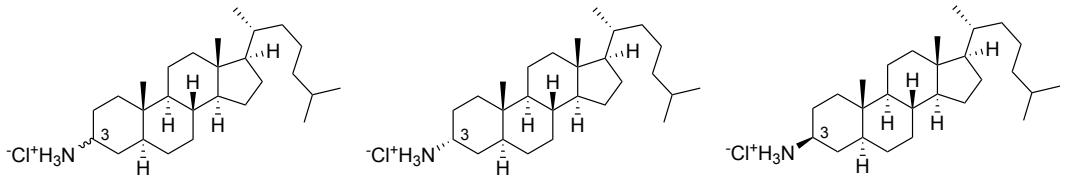

Furthermore, an investigation of structure-activity relationships in aminosteroids was undertaken to determine which functionality was necessary for potency and SHIP1 selectivity. The focus of this study was to increase the potency of the SHIP inhibitors to a sub-micromolar level. Additionally, 3AC **2.2** has poor water solubility properties and therefore some efforts were made into developing analogs that not only had increased potency, but also increased water solubility. Structural information about SHIP would greatly facilitate these studies, but unfortunately no crystal structure of SHIP1 has been determined. Initially, the priority was to increase water solubility. This was achieved by removing the greasy aliphatic carbon chain at C17. Removal of the C17 side chain resulted in the more potent and more water soluble SHIP inhibitors K185 **2.4** and K118 **2.5**, but interestingly these molecules target both SHIP1 and SHIP2, with the SHIP1 selectivity being lost (Figure 2.10).[25] This revelation made it clear that the C17 side chain was important in determining selectivity between the two paralogs.

Figure 2.10: Structure and Selectivity of 3AC ***2.2*** *and Tailless Derivatives K185* ***2.4*** *and K118* ***2.5****.*[25]*(Inhibition of SHIP1 and SHIP1 was determined using the malachite green assay at 1mM concentration).*

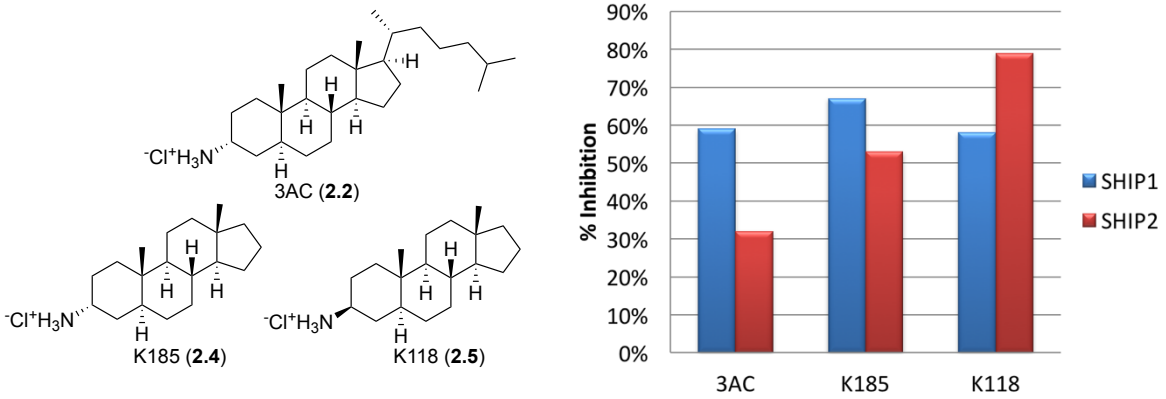

With interest in further understanding the active site of SHIP1, the SHIP2 crystal structure described by Potter and coworkers[26] was modified by threading the SHIP1 amino acid sequence into the structure with hopes that the high homology between SHIP1 and SHIP2 would construct a reasonable model of the SHIP1 phosphatase active site. This model could then be used for evaluation of small molecule docking in the active site (Figure 2.11). The Potter x-ray structure (PDB ID = 4A9C) is missing much of the enzyme including the SH2 and PH protein-protein recognition domains as well as the C2 domain (SHIP is a 145 kDa protein, the structure is only 73 kDa), but does contain the phosphatase domain and is catalytically active. This model revealed that the P4-interactive motif (P4IM) flexible loop could fold over the active site, facilitating the phosphate hydrolysis by interacting with the alkyl chains of $PI(3,4,5)P_3$. This same area may be where the C17 carbon chain of 3AC **2.2** binds to achieve SHIP1 selectivity, as the SHIP1 amino acid sequence is less polar than that of the SHIP2 sequence in this area of the enzyme. When the C17 chain was removed no interaction between the tail and loop can occur, leading to the unselective inhibition of SHIP1 and SHIP2.

Figure 2.11: Model of the SHIP1 Active Site and Docking of 3AC ***2.2***

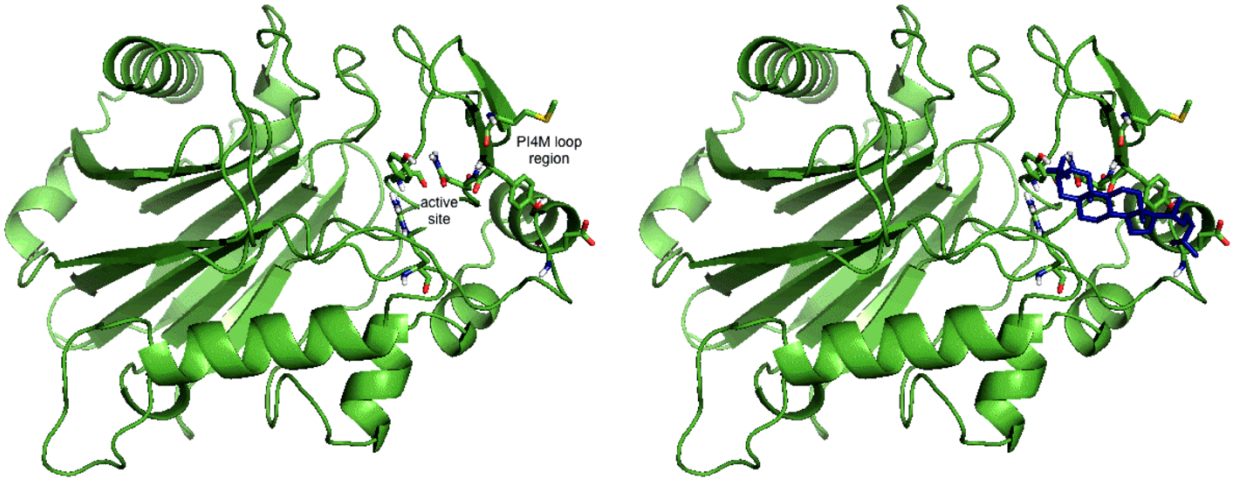

Interest in the effects associated with the substituents at the C17 position (Figure 2.12) has led to the investigation of new aminosteroids containing nonpolar ethers of various sizes at C17 (**2.6**, **2.7**, **2.8**, **2.9**), which will allow us to explore the effect of substituent size on SHIP1/SHIP2 selectivity as well as evaluate water solubility. These studies may also lead to the development of more potent SHIP inhibitors, as proper functionalization of the C17 side chain may lead to better interaction with the enzyme and increased binding and potency.

F*igure 2.12: C-17 Ether Derivatives of 3AC*

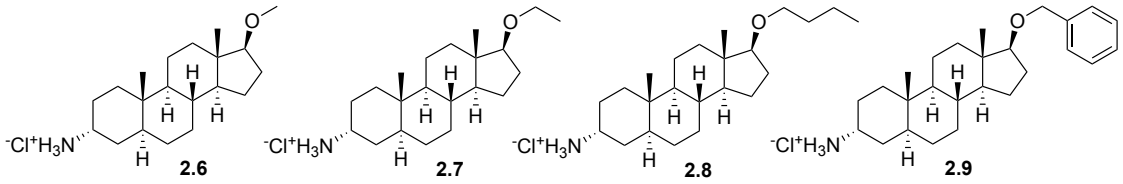

Additionally, this investigation has led to the synthesis of the alkynyl ether **2.10** (Figure 2.13). The alkyne functionality provides an attachment point through click chemistry with

azides,[27,28] which may be useful for the synthesis of fluorescent compounds which may provide a means of following the molecule in its interactions with SHIP and other receptors. Additionally, the alkyne **2.10** may be used in determining if the aminosteroid is binding to other proteins via an azide labelled biotin-streptavidin in pull-down experiments with cell lysates.

*Figure 2.13: C-17 Alkynyl Ether Derivative of 3AC **2.10***

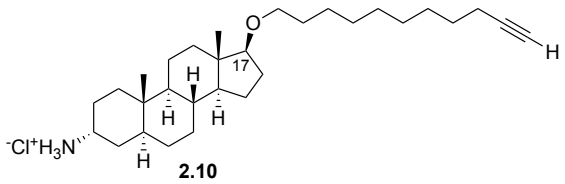

2.10

2.3 Results and Discussion

*Synthesis of the C3α-aminosteroid **2.2***

The synthesis of the C3α-aminosteroid **2.2** was performed to provide material for testing for both the α-azide **2.13** and the mixture of α and β isomers **2.1**. Starting from the commercially available dihydrocohlesterol **2.11**, formation of the mesylate **2.12** was accomplished in 93% yield with methanesulfonyl chloride (MsCl) and triethylamine (Et_3N) (Scheme 2.1). Formation of the mesylate produced a good leaving group, allowing for an S_N2 displacement with sodium azide (NaN_3) in dimethylformamide (DMF) to generate the α-azide isomer **2.13** in 80% yield. This methodology proved more effective than a direct Mitsunobu reaction on alcohol **2.11** previously utilized in the laboratory. Staudinger reduction[29,30] using triphenylphosphine, tetrahydrofuran (THF), and excess water on azide **2.13** provided the 3*α*-amine **2.14** in 55% yield. This route for the reduction allows for milder and safer conditions, compared with the previously used lithium aluminum hydride reduction. Formation of the 3*α*-amine hydrochloride salt 3AC **2.2** was achieved

by bubbling dry hydrogen chloride gas into a solution of **2.14** in diethyl ether (Et_2O) providing the α-salt **2.2** in 65% yield.[31]

*Scheme 2.1: Synthesis of 3AC **2.2***

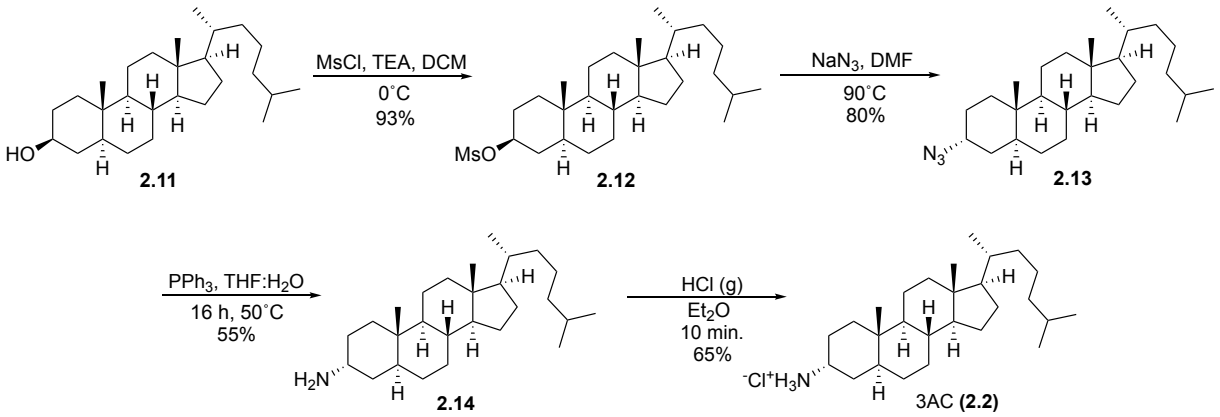

*Synthesis of the C3β-aminosteroid **2.3***

Synthesis of the 3β-amino isomer **2.3** began by first performing a Mitsunobu reaction[32] with triphenylphosphine, diisopropyl azodicarboxylate (DIAD), and methyl iodide on commercially available dihydrocholesterol **2.11** producing 3α-iodo-5α-cholestane **2.15** in 90% yield (Scheme 2.2). An S_N2 reaction with on the iodide with sodium azide in dimethylformamide was then performed to provide 3β-azido-5α-cholestane **2.16** in 82% yield. The Staudinger reduction reaction was again utilized to reduce azide **2.16** to give the 3β-amine **2.17** in 85% yield. Formation of the 3β-amine hydrochloride salt **2.3** was achieved by bubbling dry hydrogen chloride gas into a solution of **2.17** in diethyl ether (Et_2O) providing the β-salt **2.3** in 83% yield.

Scheme 2.2: Synthesis of β-amine Isomer **2.3**

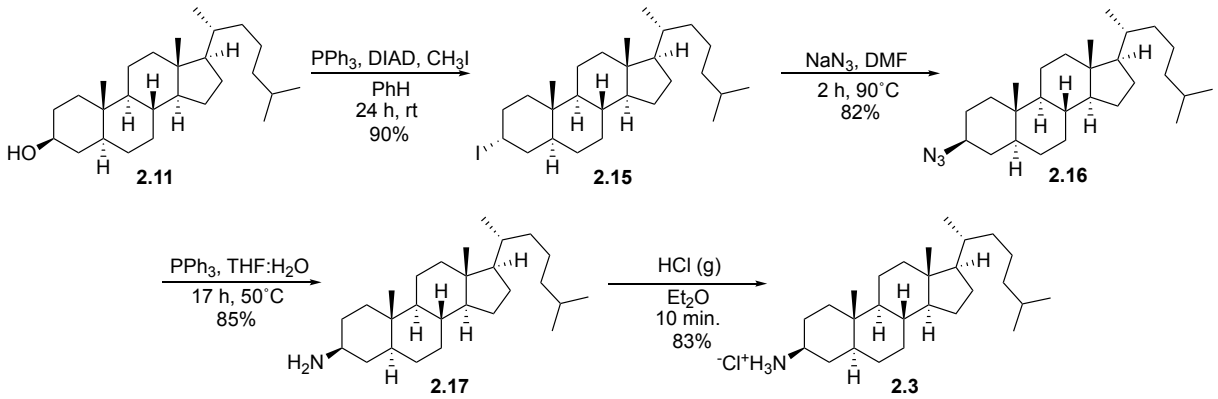

Synthesis of β-amine salt K118 ***2.5***

Aminosteroid **2.5** was synthesized from epiandrosterone **2.18** by initially performing a Wolff-Kishner[33] reduction to generate alcohol **2.19** in 95% yield (Scheme 2.3). A Mitsunobu reaction was then performed using triphenylphosphine, diisopropyl azodicarboxylate (DIAD), and methyl iodide to produce iodide **2.20** in 60% yield. Using sodium azide in dimethylformamide, a S_N2 reaction was performed on **2.20** to give azide **2.21** in 76% yield. Again, utilizing the mild Staudinger reduction with triphenylphosphine, tetrahydrofuran (THF), and excess water on azide **2.21** produced the amine **2.22** in 95% yield. Finally, bubbling dry hydrogen chloride gas into a solution of **2.22** and diethyl ether provided the amine hydrochloride salt **2.5** in 93% yield.

Scheme 2.3: Synthesis of K118 ***2.5***

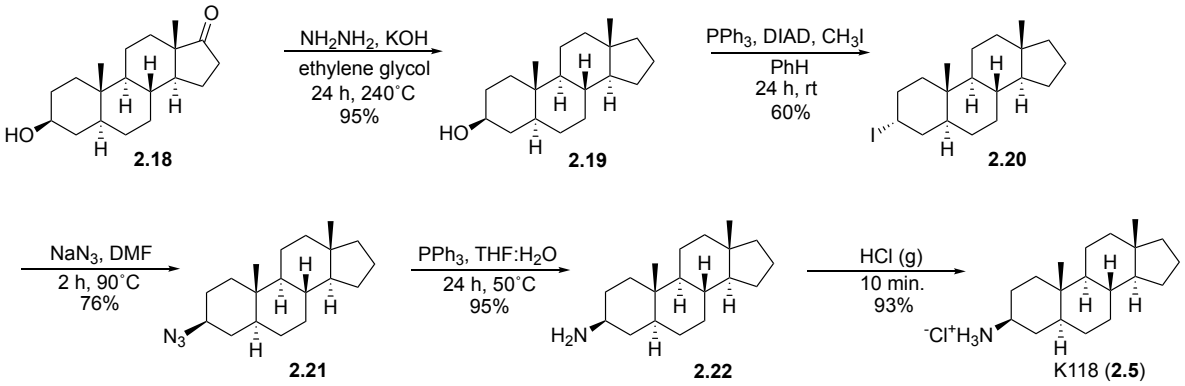

Synthesis of α-isomer aminosteroid analogs ***2.6, 2.7, 2.8***

With interest in the ether formation at C17, epiandrosterone **2.18** was utilized for the starting material. Formation of the 3β-mesylate **2.23** was achieved in 91% yield (Scheme 2.4). An S_N2 reaction using sodium azide in dimethylformamide then provided azide **2.24** in 88% yield. The pure α-azido ketone **2.24** was diastereoselectively reduced to the α-azido alcohol **2.25** using sodium borohydride ($NaBH_4$) in methanol in 77% yield.

Scheme 2.4: Synthesis of Alcohol Intermediate ***2.25***

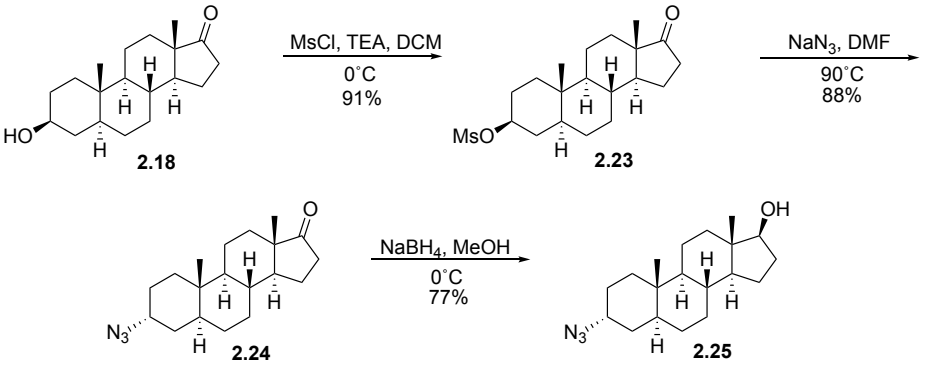

With similar stereoselective reductions at C17 having been reported,[34,35] the selectivity is most likely due to the presence of the axial methyl group at C13 hindering the β-face and forcing the pseudoequatorial hydride delivery to the α-face of the ketone **2.24**, producing the C17 β-alcohol **2.25** as the sole observed product (Figure 2.14).

Figure 2.14: Possible Mechanistic Approach for Hydride Delivery

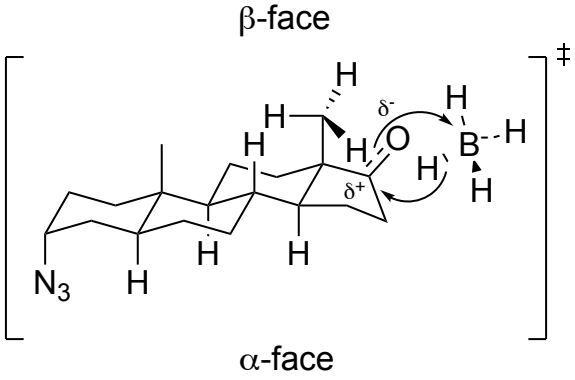

The formation of the methyl ether **2.26**, ethyl ether **2.27**, and *n*-butyl ether **2.28** was achieved through a Williamson ether synthesis,[36] utilizing a number of alkyl halide electrophiles (Scheme 2.5). This gave yields of 54%, 80%, and 70% with methyl iodide, ethyl bromide and butyl bromide respectively. The newly synthesized 3α-azido C17-ethers could be readily reduced to the 3α-amines **2.29**, **2.30**, and **2.31** using the Staudinger reduction conditions with yields of 89%, 76%, and 78%, respectively. Formation of the 3α-amine ether hydrochloride salts **2.6**, **2.7**, and **2.8** was then achieved by reaction with dry hydrogen chloride gas, producing yields of 72%, 82%, and 72%, respectively. These compounds are now undergoing testing for their ability to inhibit SHIP1 and SHIP2 *in vitro*.

Scheme 2.5: Synthesis of Ether derivatives

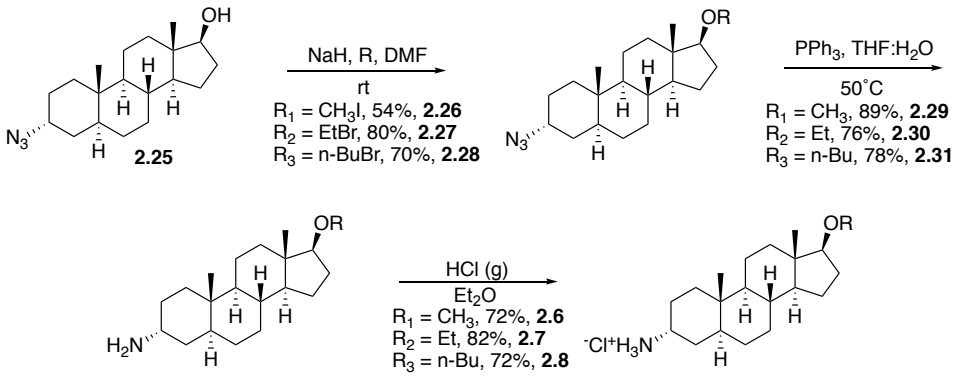

*Synthesis of C3α-aminocholestane alkynyl ether aminosteroid analog **2.10***

With a useful synthetic route for the ether analogs in place, attention was turned to the synthesis of the alkynyl ether **2.10** (Scheme 2.6). Utilizing the key intermediate alcohol **2.25** (derived from epiandrosterone) with the mesylate from 10-undecyn-1-ol[37] **2.32** provided azide **2.33** in 80% yield. Following the previously identified route for reduction of the azide **2.33** by Staudinger reduction produced amine **2.34** in 62% yield. Bubbling dry hydrogen chloride gas into a solution of **33** and diethyl ether generated the alkynyl ether hydrochloride salt **2.10** in 35% yield. The lower yield of the salt in this case may be due to the greater solubility of the long chain alkyne amine salt in organic solvents.

*Scheme 2.6: Synthesis of Alkyne Ether Derivative **2.10***

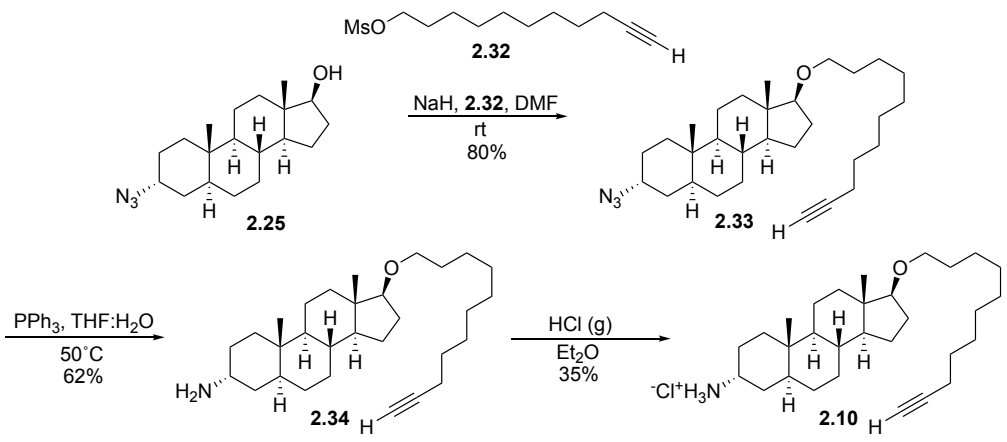

2.4 Conclusion

The successful synthesis of the α-isomer **2.2** and the β-isomer **2.3** allows for the further evaluation of their activity and selectivity of these compounds to provide further insight into these small molecule inhibitors of SHIP. Along with the isomers of NSC29322 **2.1**, the original isomer mixture identical to NSC29322 **2.1** (Scheme 2.7**)**, as well as the α-azide **2.13** and the β-iodide **2.16** will be tested for activity. Along with these molecules, the newly synthesized aminosteroids containing ethers at C-17 will be evaluated for SHIP activity as well. Depending on the results of the assay studies, a variety of compounds could easily be accessed by utilizing the etherification process. These studies will provide information about the structure activity relationships and may also lead to more potent SHIP inhibitors.

Scheme 2.7: Original Mixture of NSC29322 ***2.1***

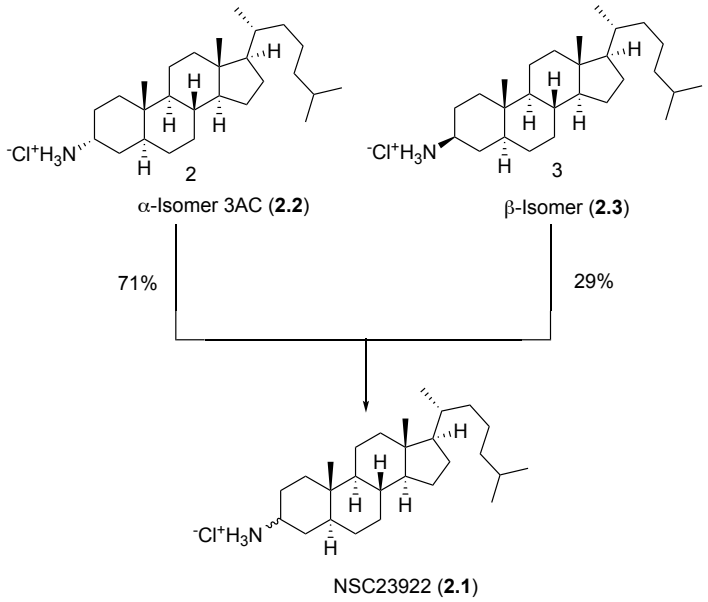

The synthesis of alkyne ether **2.10** was also accomplished. This alkyne functionality in this molecule allows for its use in pull down assay studies through the use of click chemistry. Detailed information about the aminosteroid scaffolds selectivity towards not only SHIP but a wide range of other proteins, may now be examined. The alkyne **2.10** may also be utilized to incorporate fluorescent tags on the inhibitor. These fluorescent molecules may be also used to evaluate the binding of the aminosteroid to different proteins.

2.5 Experimental

General Methods: All anhydrous reactions were run under a positive pressure of argon. All syringes, needles, and reaction flasks required for anhydrous reactions were dried in an oven and cooled under an N_2 atmosphere or in a desiccator. Dichloromethane and THF were dried by passage through an alumina column following the method of Grubbs (Pangborn, A. B.; Giardello, M. A.; Grubbs, R. H.; Rosen, R. K.; Timmers, F. J. *Organometallics* **1996,** *15*, 1518). All other reagents and solvents were purchased from commercial sources and used without further purification.

Analysis and Purification. Analytical thin layer chromatography (TLC) was performed on precoated glass backed plates (silica gel 60 F_{254}; 0.25 mm thickness). The TLC plates were visualized by UV illumination and by staining. Solvents for chromatography are listed as volume:volume ratios. Flash column chromatography was carried out on silica gel (40-63 μm). Melting points were recorded using an electrothermal melting point apparatus and are uncorrected. Elemental analyses were performed on an elemental analyzer with a thermal conductivity detector and 2 meter GC column maintained at 50 °C.

Identity. Proton (^{1}H NMR) and carbon (^{13}C NMR) nuclear magnetic resonance spectra were recorded at 300 or 400 MHz and 75 or 100 MHz respectively. The chemical shifts are given in parts per million (ppm) on the delta (δ) scale. Coupling constants are reported in hertz (Hz). The spectra were recorded in solutions of deuterated chloroform ($CDCl_3$), with residual chloroform (δ 7.26 ppm for ^{1}H NMR, δ 77.23 ppm for ^{13}C NMR) or tetramethylsilane (δ 0.00 for ^{1}H NMR, δ 0.00 ppm for ^{13}C NMR) as the internal reference. Data are reported as follows: (s = singlet; d = doublet; t = triplet; q = quartet; p = pentet; dd = doublet of doublets; dt = doublet of triplets; td = triplet of doublets; tt = triplet of triplets; qd = quartet of doublets; ddd = doublet of doublet of

doublets; br s = broad singlet). Where applicable, the number of protons attached to the corresponding carbon atom was determined by DEPT 135 NMR. Infrared (IR) spectra were obtained as thin films on NaCl plates by dissolving the compound in CH_2Cl_2 followed by evaporation or as KBr pellets.

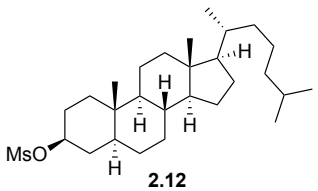

2.12

5 α -cholestane-3 β -ol-3-methanesulfonate (2.12)[38]

Lit. Ref.: Sugandhi, E. W.; Slebodnick, C.; Falkinham, J. O.; Gandour, R. D., Synthesis and antimicrobial evaluation of water-soluble, dendritic derivatives of epimeric 5α-cholestan-3-amines and 5α-cholestan-3-yl aminoethanoates. *Steroids* **2007**, *72*, 615-626.

A solution of 5α-cholestan-3β-ol **2.11** (0.500 g, 1.29 mmol) in 13 mL DCM was cooled to 0 ˚C. Et_3N (0.360 mL, 2.58 mmol) was added to the cooled solution followed by slow addition of MsCl (0.120 mL, 1.55 mmol). The reaction mixture was stirred for approximately 30 min before 12 mL of water was added and the aqueous phase separated and extracted with DCM (2 x 12 mL). The organic extracts were collected and washed with brine (2 x 12 mL), dried over Na_2SO_4, filtered and concentrated. The residue was purified by column chromatography on silica gel using 100% hexanes as the eluent to produce 5α-cholestane-3β-ol-3-methanesulfonate **2.12** (0.444 g, 93%). m.p. = 107-110 ˚C; TLC R_f = 0.68 (hexane:EtOAc, 3:1); ^{1}H NMR (400 MHz, $CDCl_3$) δ 4.67-4.54 (m, 1H), 3.01 (s, 3H), 1.93-2.10 (m, 2H), 1.72-1.86 (m, 3H), 1.61-1.71 (m, 2H), 1.57-1.60 (m, 1H), 1.54-1.56 (m, 4), 1.42-1.53 (m, 3H), 1.29-1.37 (m, 4H), 1.19-1.28 (m, 3H), 1.04-1.17 (m, 6H),

0.93-1.03 (m, 3H), 0.89 (d, *J* = 6.6 Hz, 3H), 0.86 (d, *J* = 1.8 Hz, 3H), 0.85 (d, *J* = 1.8 Hz, 3H), 0.82 (s, 3H), 0.64 (s, 3H).

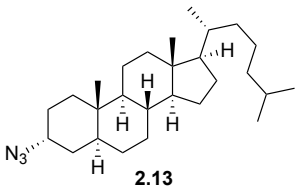

2.13

3 α -azido-5 α -cholestane (2.13)[14,38]

Lit. Ref: Viernes, D. R., "Synthesis, design, and biological evaluation of inhibitors and activators of Src Homology 2 domain-containing inositol phosphatase (SHIP) and synthetic studies of apicularen A and maoecrystal V" *Syracuse University Dissertations*, *Department of Chemistry* **2012**.

5α-cholestane-3β-ol-3-methanesulfonate **2.12** (2.12 g, 4.55 mmol) was dissolved in 45 mL DMF and stirred at room temperature. NaN_3 (0.592 g, 9.10 mmol) was added and the reaction mixture was heated to 90˚C. After approximately 5 h the reaction was allowed to cool to room temperature and 45 mL of water was slowly added to quench the reaction. The reaction mixture was extracted with ethyl acetate (3 x 14 mL) and the combined organic extracts were washed with water (3 x 14 mL), brine (3 x 14 mL), dried over sodium sulfate, filtered and concentrated. Purification with column chromatography on silica gel using 100% hexanes as the eluent provided 3α-azide **2.13** (1.73 g, 80%). m.p. = 44-50 ˚C; TLC R_f = 0.61 (hexane); ^{1}H NMR (400 MHz, $CDCl_3$) δ 3.88 (t, *J* = 2.8 Hz, 1H), 1.96 (dt, *J* = 12.2, 3.0 Hz, 1H), 1.86-1.76 (m, 1H), 1.73-1.65 (m, 2H), 1.64-1.61 (m, 1H) 1.59-1.54 (m, 3H), 1.53-1.49 (m, 2H), 1.48-1.45 (m, 2H), 1.43-1.40 (m, 1H), 1.39-1.35 (m, 1H), 1.34-1.30 (m, 3H), 1.29-1.23 (m, 2H), 1.22-1.17 (m, 3H), 1.16-1.06 (m, 5H), 1.05-0.93 (m, 3H), 0.90 (d, *J* = 6.6 Hz, 3H), 0.88 (d, *J* = 1.9 Hz, 3H), 0.85 (d, *J* = 1.9 Hz, 3H), 0.78 (s, 3H),

0.77-0.69 (m, 1H), 0.65 (s, 3H). Anal calcd for $C_{27}H_{47}N_3$: C, 78.39; H, 11.45; N, 10.16. Found: C, 78.22; H, 11.64; N, 10.27.

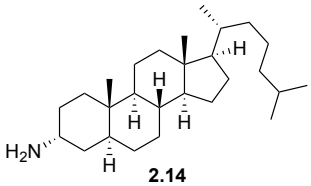

2.14

3 α -Amino-5 α -cholestane (2.14)[14,38]

Lit. Ref: Viernes, D. R., "Synthesis, design, and biological evaluation of inhibitors and activators of Src Homology 2 domain-containing inositol phosphatase (SHIP) and synthetic studies of apicularen A and maoecrystal V" *Syracuse University Dissertations*, *Department of Chemistry* **2012**.

To a solution of α-azide **2.13** (1.21 g, 2.91 mmol) in 15 mL of anhydrous THF was added triphenylphosphine (1.15 g, 4.37 mmol). The solution was heated to 50˚C with the addition of water (0.100 mL, 5.55 mmol) in excess and stirred overnight (approx. 17 h). The reaction mixture was concentrated, and the residue purified by silica gel column chromatography, initially using 90:10 DCM:MeOH solution as the eluent, then 90:9:1 DCM: methanol: 40% aq. ammonium hydroxide as the eluent to produce the α-amine **2.14** (0.621 g, 55%) as a white solid. m.p. = 71-76˚C; TLC R_f = 0.38 (DCM:MeOH:NH_4OH, 90:9:1); ^{1}H NMR (300 MHz, $CDCl_3$) δ 3.14 (bs, 1H), 1.96 (dt, *J* = 6.1, 3.4 Hz, 1H), 1.88-1.70 (m, 2H), 1.69-1.64 (m, 1H), 1.63-1.58 (m, 1H), 1.62-1.51 (m, 6H), 1.50-1.42 (m, 4H), 1.41-1.35(m, 4H), 1.29-1.16 (m, 5H), 1.15-1.02 (m, 6H), 1.01-0.90 (m, 4H), 0.88 (d, *J* = 6.6 Hz, 3H), 0.86 (d, *J* = 1.8 Hz, 3H), 0.83 (d, *J* = 1.6 Hz, 3H), 0.78 (s, 3H), 0.65 (s, 3H).

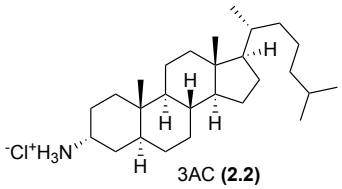

3AC **(2.2)**

3 α -Amino-5 α -cholestane hydrochloride 3AC (2.2)[14]

Lit. Ref: Viernes, D. R., "Synthesis, design, and biological evaluation of inhibitors and activators of Src Homology 2 domain-containing inositol phosphatase (SHIP) and synthetic studies of apicularen A and maoecrystal V" *Syracuse University Dissertations*, *Department of Chemistry* **2012**.

α-amine **2.14** (0.621 g, 1.60 mmol) was dissolved in 20 mL of Et_2O and allowed to stir while dry HCl gas was purged into the reaction mixture by the reaction of concentrated sulfuric acid and sodium chloride. During this time a precipitate formed. After approx. 5 min the reaction mixture was filtered and the white precipitate was collected and dried under vacuum producing the α-amine hydrochloride salt **2.2** (0.443 g, 65%) as a white solid. m.p. = 253˚C (dec.); ^{1}H NMR (300 MHz, $CDCl_3$) δ 8.47 (bs, 3H), 3.61 (bs, 1H), 1.94 (d, *J* = 10.3 Hz, 1H), 1.86–1.78 (m, 2H), 1.66–1.61 (m, 2H), 1.56–1.43 (m, 6H), 1.40–1.30 (m, 7H), 1.27– 1.25 (m, 1H), 1.21–1.17 (m, 4H), 1.13–1.10 (m, 4H), 1.04–0.93 (m, 5H), 0.90 (s, 3H), 0.86 (d, *J* = 1.4 Hz, 3H), 0.84 (d, *J* = 1.4 Hz, 3H), 0.78 (s, 3H), 0.63 (s, 3H); Anal calcd for $C_{27}H_{50}ClN$: C, 76.46; H, 11.88; N, 3.30. Found: C, 76.18; H, 11.76; N, 3.63. Anal calcd for $C_{27}H_{50}ClN$: C, 76.46; H, 11.88; N, 3.30. Found: C, 76.70; H, 11.88; N, 3.50.

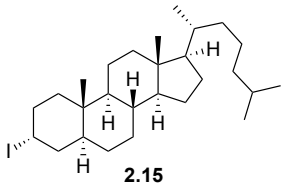

2.15

3 α -Iodo-5 α -cholestane (2.15)[14,39]

Lit. Ref: Viernes, D. R., "Synthesis, design, and biological evaluation of inhibitors and activators of Src Homology 2 domain-containing inositol phosphatase (SHIP) and synthetic studies of apicularen A and maoecrystal V" *Syracuse University Dissertations*, *Department of Chemistry* **2012**.

To a solution of 5α-cholestan-3β-ol **2.11** (2.00 g, 5.15 mmol) and triphenylphosphine (1.48 g, 5.67 mmol) in 28 mL benzene was added a solution of DIAD (1.10 mL, 5.67 mmol) in 12 mL of benzene dropwise. The resulting yellow solution was stirred at room temperature for 15 min before a solution of iodomethane (0.350 mL, 5.67 mmol) in 12 mL of benzene was slowly added dropwise. The reaction mixture was allowed to stir continuously for approx. 6 h before addition of another equiv of triphenylphosphine, DIAD, and iodomethane. The reaction was allowed to stir overnight for approx. 24 h before it was concentrated under reduced pressure, and purified by chromatography on silica gel using 100% hexanes as the eluent to afford the α-iodide **2.15** (2.32 g, 90%) as an off white solid. m.p. = 105-109 ˚C; TLC R_f = 0.92 (hexane:EtOAc, 3:1); ^{1}H NMR (400 MHz, $CDCl_3$) δ 4.94-4.91 (m, 1H), 2.10-1.94 (dt, *J* = 12.0, 2.8 Hz, 1H), 1.93-1.88 (dt, *J* = 14.8, 2.5 Hz, 1H), 1.87-1.75 (m, 1H), 1.74-1.69 (m, 1H), 1.68-1.65 (m, 2H), 1.64-1.60 (m, 1H), 1.59-1.53 (m, 3H), 1.52-1.49 (m, 1H) 1.48-1.46 (m, 1H), 1.45-1.39 (m, 1H), 1.38-1.31 (m, 4H), 1.30-1.28 (m, 1H), 1.27-1.25 (m, 1H), 1.24-1.18 (m, 3H), 1.17-1.06 (m, 5H), 1.05-0.94 (m, 4H),

0.90 (d, *J* = 6.6 Hz, 3H), 0.88 (d, *J* = 1.9 Hz, 3H), 0.85 (d, *J* = 1.9 Hz, 3H), 0.79 (s, 3H), 0.65 (s, 3H); Anal calcd for $C_{27}H_{47}I$: C, 65.04; H, 9.50. Found: C, 65.09; H, 9.74.

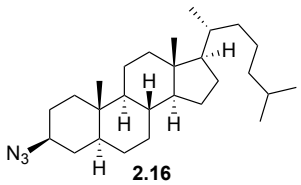

2.16

3 β -Azido-5 α -cholestane (2.16)[14]

Lit. Ref: Viernes, D. R., "Synthesis, design, and biological evaluation of inhibitors and activators of Src Homology 2 domain-containing inositol phosphatase (SHIP) and synthetic studies of apicularen A and maoecrystal V" *Syracuse University Dissertations*, *Department of Chemistry* **2012**.

A suspension of α-iodide **2.15** (2.25 g, 4.52 mmol) and NaN_3 (2.94 g, 45.2 mmol) in 113 mL DMF was warmed to 90˚C in a round bottom flask. After approx. 2 h, the solution was cooled to room temperature diluted with 113 mL of water. The resulting solution was extracted with Et_2O (3 x 100 mL) and the combined organic layers were washed with a solution of brine (3 x 100 mL), dried over sodium sulfate, and filtered, and concentrated. Purification with flash column chromatography on silica gel using 100% hexanes as the eluent afforded the β-azide **2.16** (1.53 g, 82%). m.p. = 56-59˚C; TLC R_f = 0.41 (hexanes); ^{1}H NMR (400 MHz, $CDCl_3$) δ 3.29-3.17 (m, 1H), 1.97 (dt, *J* = 12.8, 3.3 Hz, 1H), 1.86-1.72 (m, 3H), 1.71-1.63 (m, 1H), 1.62-1.44 (m, 5H), 1.37-1.23 (m, 9H), 1.18-1.04 (m, 6H), 1.03-0.94 (m, 4H) 0.93-0.88 (m, 4H), 0.88 (d, *J* = 1.7 Hz, 3H), 0.86 (d, *J* = 1.7 Hz, 3H), 0.79 (s, 3H), 0.65 (s, 4H); Anal calcd for $C_{27}H_{47}N_3$: C, 78.39; H, 11.45; N, 10.16. Found: C, 78.75; H, 11.54; N, 10.28.

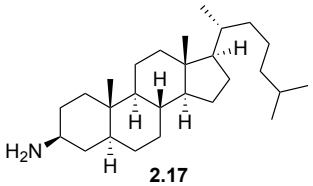

2.17

3 β -Amino-5 α -cholestane (2.17)[14]

Lit. Ref: Viernes, D. R., "Synthesis, design, and biological evaluation of inhibitors and activators of Src Homology 2 domain-containing inositol phosphatase (SHIP) and synthetic studies of apicularen A and maoecrystal V" *Syracuse University Dissertations*, *Department of Chemistry* **2012**.

To a solution of β-azide **2.16** (1.46 g, 3.57 mmol) in 18 mL of anhydrous THF was added triphenylphosphine (1.40 g, 5.35 mmol). The solution was heated to 50˚C with the addition of water (0.100 mL, 5.55 mmol) in excess and stirred overnight (approx. 17 h). The reaction mixture was concentrated, and the residue purified by silica gel column chromatography, initially using 90:10 DCM:MeOH solution as the eluent, then 90:9:1 DCM: methanol: 40% aq. ammonium hydroxide as the eluent to produce the β-amine **2.17** (1.18 g, 85%) as a white solid. m.p. = 154 ˚C (dec.); TLC R_f = 0.33 (DCM:MeOH;NH_4OH, 90:9:1); ^{1}H NMR (400 MHz, $CDCl_3$) δ 2.71-2.61 (m, 2H), 1.96 (dt, *J* = 12.8, 3.4 Hz, 1H), 1.88-1.74 (m, 1H), 1.72-1.69 (m, 1H), 1.68-1.65 (m, 1H), 1.64-1.59 (m, 5H), 1.57-1.40 (m, 4H), 1.39-1.30 (m, 4H), 1.29-1.16 (m, 5H), 1.14-1.04 (m, 6H), 1.03-0.92 (m, 4H), 0.89 (d, *J* = 6.6 Hz, 3H), 0.87 (d, *J* = 1.8 Hz, 3H), 0.85 (d, *J* = 1.6 Hz, 3H), 0.78 (s, 3H), 0.65 (s, 3H).

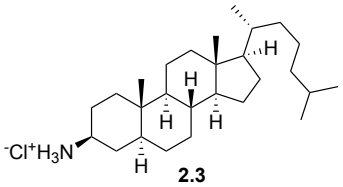

2.3

3 β -Amino-5 α -cholestane hydrochloride (2.3)[14]

Lit. Ref: Viernes, D. R., "Synthesis, design, and biological evaluation of inhibitors and activators of Src Homology 2 domain-containing inositol phosphatase (SHIP) and synthetic studies of apicularen A and maoecrystal V" *Syracuse University Dissertations*, *Department of Chemistry* **2012**.

β-amine **2.17** (1.18 g, 3.04 mmol) was dissolved in 20 mL of Et_2O and allowed to stir while dry HCl gas was purged into the reaction mixture by the reaction of concentrated sulfuric acid and sodium chloride. During this time a precipitate formed. After approx. 5 min the reaction mixture was filtered and the white precipitate was collected and dried under vacuum producing the β-amine hydrochloride salt **2.3** (1.08 g, 83%) as a white solid. m.p. = 228˚C (dec.); ^{1}H NMR (400 MHz, $CDCl_3$) δ 8.29 (bs, 3H), 3.12 (bs, 1H), 2.03-1.92 (m, 2H), 1.86-1.69 (m, 3H), 1.68-1.64 (m, 1H), 1.63-1.59 (m, 2H), 1.58-1.41 (m, 4H), 1.40-1.27 (m, 6H), 1.26-1.21 (m, 3H), 1.20-1.05 (m, 6H), 1.04-0.93 (m, 4H), 0.89 (d, J = 6.4 Hz, 3H), 0.86 (d, J = 1.8 Hz, 3H), 0.85 (d, J = 1.8 Hz, 3H), 0.82 (s, 3H), 0.64 (s, 3H); Anal calcd for $C_{27}H_{50}ClN$: C, 76.46; H, 11.88; N, 3.30. Found: C, 76.18; H, 11.76; N, 3.63.

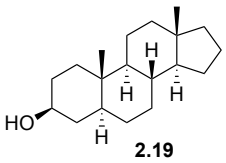

2.19

5α-androstane-3β-ol (2.19)[14,33]

Lit. Ref: Viernes, D. R., "Synthesis, design, and biological evaluation of inhibitors and activators of Src Homology 2 domain-containing inositol phosphatase (SHIP) and synthetic studies of apicularen A and maoecrystal V" *Syracuse University Dissertations*, *Department of Chemistry* **2012**.

KOH (5.79 g, 103.3 mmol) was added to 30 mL diethylene glycol and heated until dissolved with a heat gun. Once the solution of KOH in diethylene glycol cooled to rt epiandrosterone **2.18** (6.00 g, 20.7 mmol) and hydrazine hydrate (4.05 mL, 82.6 mmol) were added. With a reflux condenser attached the solution was heated to 245˚C and stirred continuously for 24 h. The condenser was removed and a distillate column attached to distill off diethylene glycol. The reaction was then cooled to rt and 100 mL MTBE and 100 mL brine were added and the solution stirred overnight. The aqueous phase was extracted with MTBE (10 x 60 mL). The collected organic phase was washed with brine (5 x 60 mL), dried with sodium sulfate, and concentrated down to produce **2.19** (5.49 g, 95%) as a white solid. m.p. 148.4-150.2˚C; TLC R_f = 0.40 (hexane:EtOAc, 7:3); ^{1}H NMR (400 MHz, $CDCl_3$) δ 3.62-3.59 (m, 1H), 1.82-1.76 (m, 1H), 1.70-1.67 (m, 2H), 1.67-1.62 (m, 1H), 1.61-1.58 (m, 1H), 1.57-1.51 (m, 4H), 1.50-1.48 (m, 1H), 1.49-1.36 (m, 2H), 1.35-1.29 (m, 2H), 1.28-1.284 (m, 4H), 1.17-1.13 (m, 1H), 1.12-1.02 (m, 2H), 1.01-0.96 (m, 1H), 0.95-0.84 (m, 2H), 0.82 (s, 3H), 0.70 (s, 3H), 0.67-0.60 (m, 1H).

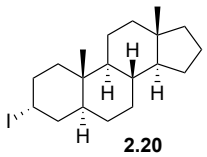

2.20

3 α -Iodo-5 α -androstane (2.20)[14]

Lit. Ref: Viernes, D. R., "Synthesis, design, and biological evaluation of inhibitors and activators of Src Homology 2 domain-containing inositol phosphatase (SHIP) and synthetic studies of apicularen A and maoecrystal V" *Syracuse University Dissertations*, *Department of Chemistry* **2012**.

To a solution of 5α-androstane-3β-ol **2.19** (5.50 g, 19.9 mmol) and triphenylphosphine (10.7 g, 41.8 mmol) in 120 mL benzene was added a solution of DIAD (8.45 mL, 41.8 mmol) in 12 mL of benzene dropwise. The resulting yellow solution was stirred at room temperature for 15 min before a solution of iodomethane (2.60 mL, 41.8 mmol) in 12 mL of benzene was slowly added dropwise. The reaction mixture was allowed to stir continuously for approx. 6 h before addition of another equiv of triphenylphosphine, DIAD, and iodomethane. The reaction was allowed to stir overnight for approx. 24 h before it was concentrated under reduced pressure, and purified by chromatography on silica gel using 100% hexanes as the eluent to afford the α-iodide **2.20** (4.51 g, 60%) as an off white solid. m.p. = ; TLC R_f = 0.73; ^{1}H NMR (300 MHz, $CDCl_3$) δ 4.94-4.91 (m, 1H), 1.92 (dt, *J* = 15.4, 3.3 Hz, 1H), 1.77-1.65 (m, 5H), 1.64-1.54 (m, 1H), 1.53-1.51 (m, 2H), 1.47 (t, *J* = 2.2 Hz, 1H), 1.46-1.38 (m, 2H), 1.37-1.22 (m, 4H), 1.21-1.05 (m, 4H), 1.04-0.98 (m, 1H), 0.97-0.87 (m, 2H), 0.86-0.84 (m, 1H), 0.79 (s, 3H), 0.69 (s, 3H).

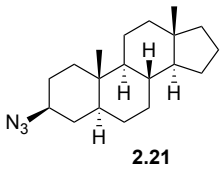

2.21

3β-azido-5 α -androstane (2.21)[14]

Lit. Ref: Viernes, D. R., "Synthesis, design, and biological evaluation of inhibitors and activators of Src Homology 2 domain-containing inositol phosphatase (SHIP) and synthetic studies of apicularen A and maoecrystal V" *Syracuse University Dissertations*, *Department of Chemistry* **2012**.

To a solution of the 3β-iodo-5 α -androstane **2.20** (4.50 g, 11.6 mmol) in 290 mL DMF was added NaN_3 (3.77 g, 58 mmol). The reaction mixture was heated to 90˚C and stirred overnight, with the addition of another 0.5 equiv of NaN_3. The reaction was allowed to cool to room temperature and quenched with the addition of 80 mL water. The reaction was extracted with ethyl acetate (3 x 50 mL). The combined organic extracts were then washed with water (3 x 50 mL) and brine (3 x 50 mL), dried over sodium sulfate and concentrated. Purification using chromatography on silica gel using 3:1 hexanes:EtOAc as eluent gave 3α-azide **2.21** (2.66 g, 76%). m.p. = 124 (dec.); TLC R_f = 0.90; ^{1}H NMR (400 MHz, $CDCl_3$) δ 3.25 (m, 1H), 1.86-1.78 (m, 1H), 1.76-1.67 (m, 3H), 1.65-1.61 (m, 1H), 1.60-1.54 (m, 2H), 1.53-1.51 (m, 1H), 1.50-1.38 (m, 3H), 1.37-1.33 (m, 1H), 1.32-1.29 (m, 1H), 1.28-1.26 (m, 2H), 1.25-1.19 (m, 1H), 1.18-1.04 (m, 4H), 1.01-0.92 (m, 1H), 0.91-0.84 (m, 2H), 0.81 (s, 3H), 0.70 (s, 3H), 0.69-0.63 (m, 1H).

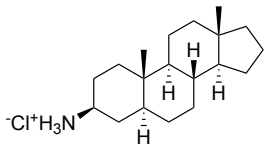

K118 (**2.5**)

3β-amino-5 α -androstane hydrochloride K118 (2.5)[14]

Lit. Ref: Viernes, D. R., "Synthesis, design, and biological evaluation of inhibitors and activators of Src Homology 2 domain-containing inositol phosphatase (SHIP) and synthetic studies of apicularen A and maoecrystal V" *Syracuse University Dissertations*, *Department of Chemistry* **2012**.

3β-azido-5 α -androstane **2.22** (2.31 g, 8.40 mmol) was dissolved in 15 mL Et_2O and stirred at room temperature as dry HCl gas, generated from the reaction of concentrated sulfuric acid and sodium chloride, was purged into the reaction mixture. The resulting precipitate was collected by vacuum filtration, washed with ethyl ether, and dried under vacuum to produce the 3α-amino-5α-androstan-17-ethyl-ether hydrochloride salt **2.5** (2.44 g, 93%) m.p. = 254˚C (dec.); ^{1}H NMR (300 MHz, $CDCl_3$) δ 8.31 (bs, 3H), 3.14 (bs, 1H), 2.10 (d, 1H), 1.81-1.65 (m, 6H), 1.64-1.55 (m, 3H), 1.50-1.35 (m, 2H), 1.34-1.20 (m, 4H), 1.19-1.01 (m, 5H), 1.00-0.87 (m, 3H), 0.83 (s, 3H), 0.68 (s, 3H). ^{13}C NMR (100 MHz, $CDCl_3$) δ 54.5, 54.3, 51.3, 45.1, 40.8, 40.4, 38.8, 36.7, 35.8, 35.5, 33.2, 32.2, 28.3, 26.9, 25.5, 21.1, 20.5, 17.6, 12.3. Anal calcd for $C_{19}H_{34}ClN$: C, 73.16; H, 10.99; N, 4.49. Found: C, 73.37; H, 11.11; N, 4.15.

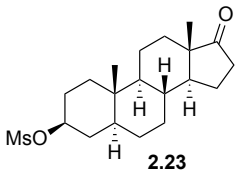

2.23

3 β -ol-5 α -androstan-17-one 3-methanesulfonate (2.23)[40]

Lit. Ref: Wang, Y.; Ji, S.; Wei, K.; Lin, J., Epiandrosterone-derived prolinamide as an efficient asymmetric catalyst for Michael addition reactions of aldehydes to nitroalkenes. *RSC Adv.* **2014**, *4*, 30850-30856.

Et_3N (4.80 mL, 34.4 mmol) was added to a cooled, 0˚C, solution of 3β-hydroxy-5α-androstan-17-one **2.18** (5.00 g, 17.2 mmol) in 172 mL DCM. MsCl (1.60 mL, 20.7 mmol) was slowly added into the reaction mixture. After approximately 3 h the reaction was quenched with 172 mL of water. The reaction was extracted with DCM (3 x 100 mL), and the combined organic extracts washed with water (3 x 100 mL) and brine (3 x 100 mL), dried over sodium sulfate and concentrated. Purification through chromatography on silica gel using 100% hexanes as the eluent, provided 3β-mesylate **2.23** (5.78 g, 91%). m.p. = 155-157 ˚C; TLC R_f = 0.67 (hexane:EtOAc, 1:1); ^{1}H NMR (300 MHz, $CDCl_3$) δ 4.69-4.58 (m, 1H), 3.00 (s, 3H), 2.47 (dd, *J* = 19.2, 8.7 Hz, 1H), 2.17-1.18 (m, 3H), 1.85-1.76 (m, 4H), 1.75-1.61 (m, 3H), 1.60-1.53 (m, 1H), 1.52-1.43 (m, 1H), 1.41-1.34 (m, 2H), 1.33-1.16 (m, 4H), 1.14-1.02 (m, 1H), 1.01-0.90 (m, 1H), 0.85 (s, 6H), 0.79-0.65 (m, 1H).

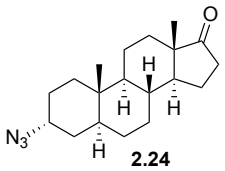

2.24

3 α -azido-5 α -androstan-17-one (2.24)[40]

Lit. Ref: Wang, Y.; Ji, S.; Wei, K.; Lin, J., Epiandrosterone-derived prolinamide as an efficient asymmetric catalyst for Michael addition reactions of aldehydes to nitroalkenes. *RSC Adv.* **2014**, *4*, 30850-30856.

To a solution of the 3β-mesylate **2.23** (5.78 g, 15.7 mmol) in 50 mL DMF was added NaN_3 (2.04 g, 31.4 mmol). The reaction mixture was heated to 90˚C and stirred overnight, with the addition of another 0.5 equiv of NaN_3. The reaction was allowed to cool to room temperature and quenched with the addition of 80 mL water. The reaction was extracted with ethyl acetate (3 x 50 mL). The combined organic extracts were then washed with water (3 x 50 mL) and brine (3 x 50 mL), dried over sodium sulfate and concentrated. Purification using chromatography on silica gel using 3:1 hexanes:EtOAc as eluent gave 3α-azide **2.24** (4.35 g, 88%). m.p. = 110-113˚C; TLC R_f = 0.66 (hexane:EtOAc, 3:1); ^{1}H NMR (400 MHz, $CDCl_3$) δ 3.88 (t, *J* = 2.8 Hz, 1H), 2.44 (dd, *J* = 19.2, 8.9 Hz, 1H), 2.13-2.02 (m, 1H), 1.97-1.89 (m, 1H), 1.83-1.77 (m, 2H), 1.74-1.69 (m, 1H), 1.68-1.64 (m, 1H), 1.60-1.56 (m, 1H), 1.55-1.51 (m, 2H), 1.50-1.47 (m, 2H), 1.46-1.39 (m, 2H), 1.34-1.25 (m, 4H), 1.24-1.16 (m, 3H), 1.02 (qd, *J* = 12.5, 4.8 Hz, 1H), 0.87 (s, 3H), 0.81 (s, 3H).

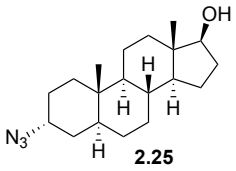

2.25

3 α -azido-5 α -androstan-17-ol (2.25)[41]

Lit. Ref.: Amiranashvili, L. Sh.; Sladkov, V. I.; Levina, I. I.; Men'shova, N. I.; Suvorov, N. N. *J. Org. Chem*. *USSR*. **1990**, *26*, 1629-1632.

A suspension of 3α-azide **2.24** (4.35 g, 13.8 mmol) in 138 mL methanol was cooled to 0˚C and $NaBH_4$ (0.310 g, 8.27 mmol) was added. After approximately 4 h, the reaction was quenched with the addition of 27 mL 1M HCl and 137 mL NH_4Cl. The methanol was removed in vacuo, and the resulting suspension extracted with ethyl acetate (3 x 100 mL). The combined organic extracts were washed with water (2 x 100 mL) and brine (3 x 100 mL), dried over sodium sulfate and concentrated down. After purification using chromatography on silica gel with 3:1 hexanes:EtOAc as the eluent provided 3α-azido-5α-androstan-17-ol **2.25** (3.39 g, 77%) as a white solid. m.p. = 134-137˚C; TLC R_f = 0.43 (hexane:EtOAc, 3:1); ^{1}H NMR (400 MHz, $CDCl_3$) δ 3.88 (t, *J* = 2.8 Hz, 1H), 3.63 (t, *J* = 8.44 Hz, 1H), 2.21-2.09 (m, 1H), 1.79 (dt, *J* =12.4, 2.9 Hz, 1H), 1.74-1.60 (m, 3H), 1.59-1.46 (m, 4H), 1.45-1.33 (m, 5H), 1.30-1.24 (m, 2H), 1.23-1.21 (m, 4H), 1.04 (td, *J* = 12.6, 4.0 Hz, 1H), 0.99-0.93 (m, 1H), 0.92-0.89 (m, 1H), 0.80 (s, 3H), 0.73 (s, 4H); ^{13}C NMR (100 MHz, $CDCl_3$) δ 81.9, 58.2, 54.3, 51.1, 43.0, 40.2, 36.7, 36.0, 35.5, 32.9, 32.6, 31.5, 30.5, 28.2, 25.6, 23.4, 20.4, 11.6, 11.2.

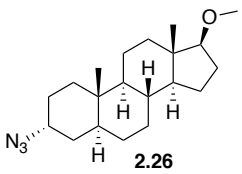

2.26

3 α -azido-5 α -androstan-17-methyl-ether (2.26)

3α-azido-5α-androstan-17-ol **2.25** (0.546 g, 1.72 mmol) was dissolved in 4 mL DMF. NaH (0.248 g, 10.32 mmol) was then added. After 1 h iodomethane (0.960 mL, 15.48 mmol) was added to the reaction mixture and then stirred overnight (approx. 18 h). Addition of 16 mL 1 M HCl and 16 mL DCM was then followed by separation of the organic layer. The aqueous phase was extracted using DCM (3 x 16 mL), the organic extracts combined, washed with water (3 x 15 mL) and brine (3 x 15 mL), dried over sodium sulfate, filtered and concentrated. The residue was purified by column chromatography on silica gel using 15% ethyl acetate:85% hexanes as the eluent to produce 3α-azido-5α-androstan-17-methyl-ether **2.26** (0.305 g, 54%). m.p. = 103-109 ˚C; TLC R_f = 0.78 (hexane:EtOAc, 3:1); IR (KBr) 2933 2089, 1687, 1451, 1360, 1269, 1100, 993, 663 cm^{-1}; ^1H NMR (400 MHz, $CDCl_3$) δ 3.88 (t, *J* = 2.8 Hz, 1H), 3.45 (s, 3H), 3.22 (t, *J* = 8.4 Hz, 1H), 2.05-1.95 (m, 1H), 1.90 (dt, *J* = 11.6, 2.7 Hz, 1H), 1.75-1.63 (m, 3H), 1.62-1.33 (m, 8H) 1.32-1.09 (m, 7H), 1.02-0.84 (m, 2H), 0.77 (s, 3H), 0.73 (s, 3H); ^{13}C NMR (100 MHz, $CDCl_3$) δ 90.8, 58.2, 57.9, 54.3, 51.3, 43.0, 40.1, 38.1, 36.0, 35.3, 32.9, 32.6, 31.5, 28.2, 27.7, 25.6, 23.4, 20.5, 11.6, 11.5; Anal calcd for $C_{20}H_{33}N_3O$: C, 72.46; H, 10.03; N, 12.68. Found: C, 72.82; H, 9.63; N, 12.28.

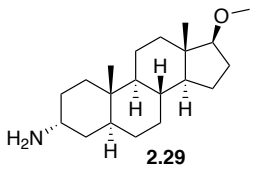

2.29

3 α -amino-5 α -androstan-17-methyl-ether (2.29)

A solution of 3α-azido-5α-androstan-17-methyl-ether **2.26** (0.305 g, 0.920 mmol) was dissolved in 4.6 mL of anhydrous THF and triphenylphosphine (0.362 g, 1.38 mmol) was added. Water (0.100 mL, 5.55 mmol) was then added and the reaction mixture was warmed to 50 ˚C. After approx. 4 h the reaction was concentrated and the residue purified by column chromatography on silica gel initially using 90:10 DCM:MeOH solution as the eluent followed by a solution of 90:9:1 DCM:MeOH:NH_4OH to produce the white solid 3α-amino-5α-androstan-17-methyl-ether **2.29** (0.251 g, 89%). m.p. = 105-107˚C; TLC R_f = 0.24 (DCM:MeOH:NH_4OH, 90:9:1); IR (KBr) 3449 3367, 3300, 2969, 2914, 2870, 2848, 2821, 1604, 1458, 1385, 1098, 890 cm^{-1}; ^1H NMR (400 MHz, $CDCl_3$) δ 3.35 (s, 3H), 3.27 (bs, 1H), 3.22 (t, *J* = 8.4 Hz, 1H) 2.94 (bs, 2H), 2.05-1.95 (m, 1H), 1.90 (dt, *J* = 11.6, 2.6 Hz, 1H), 1.75 (tt, *J* = 14.2, 4.2 Hz, 1H), 1.69-1.62 (m, 1H), 1.61-1.33 (m, 9H) 1.32-1.09 (m, 7H), 1.04-0.85 (m, 2H), 0.77 (s, 3H), 0.73 (s, 3H); ^{13}C NMR (100 MHz, $CDCl_3$) δ 90.9, 57.8, 54.4, 51.3, 46.1, 42.9, 39.1, 38.1, 36.4, 35.4, 35.3, 32.1, 31.6, 28.6, 28.3, 27.7, 23.3, 20.5, 11.7, 11.4; Anal calcd for $C_{20}H_{35}NO$: C, 78.53; H, 11.56; N, 4.58. Found: C, 78.65; H, 11.56; N, 4.57.

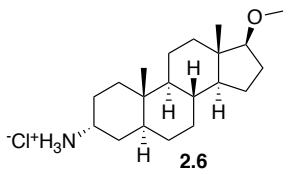

2.6

3 α -amino-5 α -androstan-17-methyl-ether hydrochloride (2.6)

3α-amino-5α-androstan-17-methyl-ether **2.29** (0.251 g, 0.822 mmol) was suspended in 10 mL Et_2O. Dry HCl gas, produced by the reaction of concentrated sulfuric acid and sodium chloride, was purged into the reaction mixture for approx. 5 min. A precipitate formed during the gas purge. The precipitate was collected by vacuum filtration and washed with ethyl ether and dried under vacuum to produce the 3α-amino-5α-androstan-17-methyl-ether hydrochloride salt **2.6** (0.203 g, 72%) as a white solid. m.p. = 254˚C (dec.); IR (KBr) 3460, 2928, 2017, 1604, 1503, 1458, 1382, 1109, 675 cm^{-1}; ^{1}H NMR (400 MHz, DMSO-d_6) δ 8.03 (bs, 3H), 3.37 (s, 3H), 3.29-3.14 (m, 4H), 2.03-1.89 (m, 1H), 1.84 (d, J = 11.2 Hz, 1H), 1.78-1.67 (m, 1H), 1.66-1.59 (m, 2H), 1.58-1.43 (m, 4H), 1.42-1.27 (m, 4H), 1.26-1.03 (m, 5H), 1.02-0.89 (m, 1H) 0.88-0.79 (m, 1H), 0.77 (s, 3H), 0.68 (s, 3H); ^{13}C NMR (100 MHz, DMSO-d_6) δ 90.3, 57.5, 53.6, 51.3, 46.7, 43.0, 38.4, 38.0, 36.1, 35.2, 31.5, 31.2, 30.9, 28.1, 27.6, 24.3, 23.4, 20.4, 12.1, 11.5; Anal calcd for $C_{20}H_{36}ClNO$: C, 70.25; H, 10.61; N, 4.10. Found: C, 69.95; H, 10.56; N, 4.03.

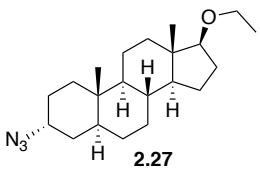

2.27

3 α -azido-5 α -androstan-17-ethyl-ether (2.27)

A solution of 3α-azido-5α-androstan-17-ol **2.25** (0.750 g, 2.36 mmol) was dissolved in 4 mL DMF and NaH (0.340 g, 14.2 mmol) was added. The reaction mixture was stirred for 1 h, after which ethyl bromide (1.58 mL, 21.3 mmol) was added. After approximately 14 h 15 mL of 1M aq. HCl solution was added. The reaction mixture was then extracted with DCM (3 x 10 mL). The combined organic extracts were washed with water (3 x 10 mL) and brine (3 x 10 mL), dried with sodium sulfate and concentrated. Purification of the residue by column chromatography on silica gel using 80% hexanes:20% ethyl acetate produced the product 3α-azido-5α-androstan-17-ethyl-ether **2.27** (0.651 g, 80%). m.p. = 91-93˚C; TLC R_f = 0.82 (hexane:EtOAc, 3:1); IR (KBr) 2917, 2874, 2852, 2077, 1442, 1405, 1379, 1263, 1123, 973 cm^{-1}; ^1H NMR (400 MHz, $CDCl_3$) δ 3.88 (t, *J* = 2.8 Hz, 1H), 3.59-3.43 (m, 2H), 3.30 (t, *J* = 8.3 Hz, 1H), 2.04-1.94 (m, 1H), 1.88 (dt, *J* = 11.7, 2.9 Hz, 1H), 1.75-1.67 (m, 2H), 1.66-1.63 (m,1H), 1.55-1.47 (m, 4H), 1.46-1.29 (m, 4H), 1.28-1.12 (m, 9H), 1.00-0.83 (m, 2H), 0.79 (s, 3H), 0.77-0.71 (m, 4H); ^{13}C NMR (100 MHz, $CDCl_3$) δ 89.0, 65.4, 58.2, 54.4, 51.4, 43.0, 40.1, 38.2, 35.9, 35.3, 32.9, 32.5, 31.5, 28.2, 28.2, 25.6, 23.3, 20.5, 15.8, 11.7, 11.6; Anal calcd for $C_{21}H_{35}N_3O$: C, 73.00; H, 10.21; N, 12.16. Found: C, 72.77; H, 10.42; N, 11.88.

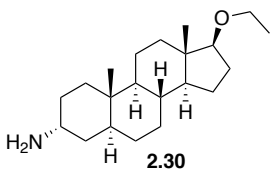

2.30

3 α -amino-5 α -androstan-17-ethyl-ether (2.30)

3α-azido-5α-androstan-17-ethyl-ether **2.27** (0.600 g, 1.73 mmol) was dissolved in 9 mL of anhydrous THF and heated to 50 ˚C. Triphenylphosphine (0.911 g, 3.47 mmol) and water (0.100 mL, 5.55 mmol) were then added and the reaction mixture was stirred for approximately 4 h. The solvent was then removed *in vacuo* and the residue purified by column chromatography on silica gel using 90:10 DCM:MeOH initially as the eluent, followed by a 90:9:1 solution of DCM:MeOH: 40% aq. ammonium hydroxide to produce the product 3α-amino-5α-androstan-17-ethyl-ether **2.30** (0.420 g, 76%) as a white solid. m.p. = 88-92˚C; TLC R_f = 0.31 (DCM:MeOH:NH_4OH, 90:9:1); ^{1}H NMR (400 MHz, $CDCl_3$) δ 3.59-3.42 (m, 2H), 3.30 (t, *J* = 8.3 Hz, 1H), 3.22 (bs, 1H), 2.32 (bs, 2H), 2.05-1.94 (m, 1H), 1.89 (dt, *J* = 11.8, 2.8 Hz, 1H), 1.81-1.62 (m, 2H), 1.61-1.32 (m, 8H) 1.32-1.10 (m, 10H), 1.01-0.83 (m, 2H), 0.79 (s, 3H), 0.75 (s, 4H); ^{13}C NMR (75 MHz, $CDCl_3$) δ 89.0, 65.3, 62.6, 54.5, 51.4, 46.0, 43.0, 39.2, 38.2, 36.4, 35.4, 32.1, 31.6, 28.7, 28.6, 28.3, 23.3, 20.5, 15.7, 11.7, 11.3; Anal calcd for $C_{21}H_{37}NO$: C, 78.94; H, 11.67; N, 4.38. Found: C, 78.75; H, 11.67; N, 4.58.

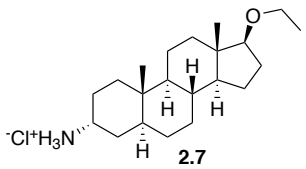

2.7

3 α -amino-5 α -androstan-17-ethyl-ether hydrochloride (2.7)

3α-amino-5α-androstan-17-ethyl-ether **2.30** (0.420 g, 0.131 mmol) was dissolved in 10 mL Et_2O and stirred at room temperature as dry HCl gas, generated from the reaction of concentrated sulfuric acid and sodium chloride, was purged into the reaction mixture. The resulting precipitate was collected by vacuum filtration, washed with ethyl ether, and dried under vacuum to produce the 3α-amino-5α-androstan-17-ethyl-ether hydrochloride salt **2.7** (0.385 g, 82%). m.p. = 241˚C (dec.); TLC R_f = 0.21 (DCM:MeOH:NH_4OH, 90:9:1); IR (KBr) 3329, 2945, 2032, 1618, 1494, 1458, 1445, 1380, 1110, 674 cm^{-1}; ^1H NMR (300 MHz, DMSO-d_6) δ 7.87 (bs, 3H), 3.47-3.36 (m, 4H), 2.03-1.28 (m, 15H), 1.22-1.013 (m, 4H), 1.07 (t, J = 6.9 Hz, 4H), 1.01-0.83 (m, 2H), 0.76 (s, 3H), 0.68 (s, 3H); ^{13}C NMR (100 MHz, DMSO-d_6) δ 89.5, 79.8, 64.9, 53.7, 51.3, 46.8, 43.1, 38.6, 38.1, 36.1, 35.3, 31.6, 31.2, 31.0, 28.2, 24.3, 23.4, 20.4, 16.2, 12.2, 11.5. Anal calcd for $C_{21}H_{28}ClNO$: C, 70.85; H, 10.76; N, 3.93. Found: C, 70.84; H, 10.4; N, 3.70.

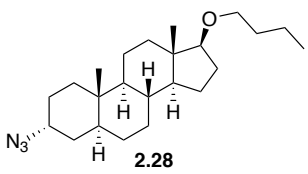

2.28

3 α -azido-5 α -androstan-17-*n*-butyl-ether (2.28)

NaH (0.378 g, 15.7 mmol) was added to a solution of 3α-azido-5α-androstan-17-ol **2.25** (0.500 g, 1.57 mmol) in 3.6 mL DMF. After 1 h *n*-butyl bromide (1.70 mL, 15.7 mmol) and tetra-butyl-ammonium iodide (0.02 g) were added, and the reaction mixture was stirred. After approx. 5 h addition of another equiv of *n*-butyl bromide was added and the reaction was stirred overnight for approx. 23 h. 15 mL of 1M HCl was added slowly followed by 15 mL ethyl acetate, and the aqueous phase separated. The organic phase was washed with brine (3 x 15 mL), dried with sodium sulfate, concentrated down, and ran purified through column chromatography using 100% hexanes as the eluent to produce 3α-azido-5α-androstan-17-*n*-butyl-ether **2.28** (0.414 g, 70%). m.p. = 75-78˚C; TLC R_f = 0.76 (hexane:EtOAc, 3:1); IR (KBr) 2925 2845, 2112, 2086, 1458, 1268, 1112, 978, 620 cm^{-1}; ^1H NMR (400 MHz, $CDCl_3$) δ 3.88 (t, *J* = 2.8 Hz, 1H), 3.49-3.36 (m, 2H), 3.28 (t, *J* = 8.2 Hz, 1H), 2.03-1.92 (m, 1H), 1.88 (dt, *J* = 11.9, 3.0 Hz, 1H), 1.74-1.61 (m, 3H), 1.73-1.46 (m, 6H), 1.45-1.29 (m, 6H), 1.28-1.08 (m, 6H), 0.99-0.83 (m, 5H), 0.79 (s, 3H), 0.74 (s, 4H); ^{13}C NMR (100 MHz, $CDCl_3$) δ 89.1, 69.9, 58.2, 54.4, 51.3, 43.1, 40.1, 38.1, 35.9, 35.3, 32.9, 32.6, 32.4, 31.5, 28.2, 28.2, 25.7, 23.3, 20.5, 19.4, 13.9, 11.7, 11.6; Anal calcd for $C_{23}H_{39}N_3O$: C, 73.95; H, 10.52; N, 11.25. Found: C, 73.83; H, 10.63; N, 10.79.

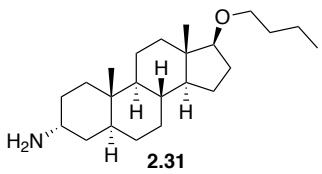

2.31

3 α -amino-5 α -androstan-17-*n*-butly-ether (2.31)

3α-azido-5α-androstan-17-*n*-butyl-ether **2.28** (0.368 g, 0.985 mmol) was dissolved in 5 mL anhydrous THF. Triphenylphosphine (0.388 g, 1.48 mmol) was added and the reaction mixture was heated to 50 ˚C. Water (0.100 mL, 5.55 mmol) was then added and the reaction stirred for 5 h. The reaction was allowed to cool to room temp and the solvent was removed in vacuo. Purification by column chromatography on silica gel using 90:10 DCM:MeOH as the initial eluent, followed by a 90:9:1 solution of DCM:MeOH:NH_4OH produced 3α-amino-5α-androstan-17-*n*-butyl-ether **2.31** (0.266 g, 78%) as a white solid. m.p. = 132 (dec.); TLC R_f = 0.27 (DCM:MeOH:NH_4OH, 90:9:1); ^{1}H NMR (400 MHz, $CDCl_3$) δ 3.48-3.37 (m, 2H), 3.34 (bs, 1H), 3.27 (t, *J* = 8.6 Hz, 1H), 2.79 (bs, 2H), 2.05-1.92 (m, 1H), 1.87 (dt, *J* = 11.9, 2.9 Hz, 1H), 1.78 (tt, *J* = 14.4, 4.0 Hz, 1H), 1.70-1.61 (m, 1H) 1.60-1.57 (m, 1H) 1.56-1.44 (m, 7H), 1.43-1.28 (m, 6H), 1.27-1.05 (m, 5H) 1.03-0.93 (m, 1H), 0.91 (t, *J* = 7.4 Hz, 4H), 0.79 (s, 4H), 0.74 (s, 3H); ^{13}C NMR (100 MHz, $CDCl_3$) δ 89.1, 69.9, 54.2, 51,3, 46.5, 43.1, 39.1, 38.1, 36.3, 35.4, 34.4, 32.4, 31.9, 31.6, 28.5, 28.2, 27.4, 23.4, 20.5, 19.5, 14.0, 11.7, 11.4; Anal calcd for $C_{23}H_{41}NO$: C, 79.48; H, 11.89; N, 4.03. Found: C, 79.11; H, 11.98; N, 4.00.

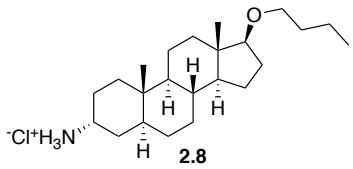

3 α -amino-5 α -androstan-17-*n*-butyl-ether hydrochloride (2.8)

3α-amino-5α-androstan-17-*n*-butyl-ether **2.31** (0.221 g, 0.636 mmol) was suspended in 10 mL Et_2O and stirred at room temperature as dry HCl gas, produced from the reaction of concentrated sulfuric acid and sodium chloride, was purged into the reaction mixture for approximately 5 min. The resulting precipitate was collected by vacuum filtration, washed with ethyl ether and dried under vacuum to produce the 3α-amino-5α-androstan-17-*n*-butyl-ether hydrochloride salt **2.8** (0.176 g, 72%) as a white solid. m.p. = 186 °C (dec.); TLC R_f = 0.27 (DCM:MeOH: 40% aq. ammonium hydroxide, 90:9:1); IR (KBr) 3335, 2944, 2566, 2032, 1619, 1495, 1458, 1445, 1263, 1218, 1125 cm^{-1}; ^1H NMR (400 MHz, DMSO-d_6) δ 7.98 (bs, 3H), 3.48-3.33 (m, 3H), 3.26 (t, J = 8.2 Hz, 1H), 2.01-1.89 (m, 1H), 1.81 (d, J = 11.4 Hz, 1H), 1.71 (d, J =14.1 Hz, 1H), 1.67-1.57 (m, 2H), 1.56-1.39 (m, 8H), 1.38-1.27 (m, 5H), 1.26-1.09 (m, 5H), 0.91-0.88 (m, 2H), 0.87 (t, J = 7.6, 3H), 0.80-0.71 (m, 4H), 0.69 (s, 3H); ^{13}C NMR (100 MHz, DMSO-d_6) δ 88.6, 69.3, 53.7, 51.3,46.7, 43.0, 38.5, 38.0, 35.9, 35.2, 32.3, 31.5, 31.2, 30.9, 28.1, 28.1, 24.3, 23.4, 20.4, 19.4, 14.2, 12.1, 11.5; Anal calcd for $C_{23}H_{42}ClNO$: C, 71.93; H, 11.02; N, 3.65. Found: C, 71.57; H, 10.83; N, 3.35.

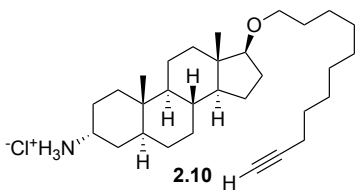

3 α -amino-5 α -androstan-17-undecyn-ether hydrochloride (2.10)

3α-amino-5α-androstan-17-*undecyn*-ether **2.35** (0.41 g, 0.930 mmol) was suspended in 10 mL Et_2O and stirred at room temperature as dry HCl gas, produced from the reaction of concentrated sulfuric acid and sodium chloride, was purged into the reaction mixture for approximately 5 min. The resulting precipitate was collected by vacuum filtration, washed with ethyl ether and dried under vacuum to produce the 3α-amino-5α-androstan-17-undecyn-ether hydrochloride salt **2.10** (1.57 g, 35%) as a white solid. m.p. = 243°C (dec.); TLC R_f = 0.27 (DCM:MeOH: 40% aq. ammonium hydroxide, 90:9:1); ^{1}H NMR (400 MHz, $CDCl_3$) δ 8.42 (bs, 3H), 3.61 (bs, 1H), 3.48-3.32 (m, 2H), 3.24 (t, *J* = 8.2 Hz, 1H), 2.18 (td, *J* = 10.3, 5.8 Hz, 2H), 1.93 (t, *J* =2.6 Hz, 2H), 1.92-1.80 (m, 3H), 1.79-1.60 (m, 4H), 1.52-1.43 (m, 7H), 1.42-1.32 (m, 4H), 1.31-1.09 (m, 13H), 1.08-0.87 (m, 4H), 0.79 (s, 3H), 0.73 (s, 3H); ^{13}C NMR (100 MHz, $CDCl_3$) δ 89.2, 84.8, 77.2, 70.3, 68.1, 53.0, 50.9, 47.7, 43.1, 38.7, 37.9, 36.1, 35.3, 31.4, 31.3, 30.2, 29.5, 29.4, 29.1, 28.8, 28.5, 28.2, 26.3, 24.7, 23.3, 20.5, 18.4, 11.7, 11.23, 1.02; Anal calcd for $C_{30}H_{52}ClNO$: C, 75.35; H, 10.96; N, 2.93. Found: C, 75.3; H, 10.9; N, 2.62.

2.6 References

1. Kerr, W. G.; Heller, M.; Herzenberg, L. A., Analysis of lipopolysaccharide-response genes in B-lineage cells demonstrates that they can have differentiation stage-restricted expression and contain SH2 domains. *Proc. Natl. Acad. Sci. USA.* **1996**, *93*, 3947-3952.

2. Damen, J. E.; Liu, L.; Rosten, P.; Humphries, R. K.; Jefferson, A. B.; Majerus, P. W.; Krystal, G., The 145-kDa protein induced to associate with the Shc by multiple cytokines is an inositol tetraphosphate and phosphatidylinositol 3,4,5- trisphosphate 5-phosphatase. *Proc. Natl. Acad. Sci. USA.***1996**, *93*, 1689-1693.

3. Lioubin, M. N.; Algate, P. A.; Tsai, S.; Carlberg, K.; Aebersold, R.; Rohchneider, L. R., p150Ship, a signal transduction molecule with inositol polyphosphate-5-phosphatase activity. *Genes & Dev.* **1996**, *10*, 1084-1095.

4. Zippo, A.; De Robertis, A.; Bardelli, M.; Galvagni, F.; Oliviero, S., Identification of F1K-1 target genes in vasculogenesis: Pim-1 is required for endothelial and mural cell differentiation in vitro. *Blood* **2004**, *103*, 4536-4544.

5. Tu, Z.; Ninos, J. M.; Ma, Z.; Wang, J.; Lemos, M. P.; Desponts, C.; Ghansah, T.; Howson, J. M.; Kerr, W. G., Embryonic and hematopoietic stem cells express a novel SH2-contaning inositol 5'-phosphatase isoform that partners with the Brb2 adapter protein. *Blood* **2001**, *98*, 2028-2038.

6. Fuhler, G. M.; Brooks, R.; Toms, B.; Iyer, S.; Gengo, E. A.; Park, M. Y.; Gumbleton, M.; Viernes, D. R.; Chisholm, J. D.; Kerr, W. G., Therapeutic potential of SH2 domain-containing inositol-5′-phosphatase 1 (SHIP1)and SHIP2 inhibition in cancer. *Mol. Med.* **2012**, *18*, 65-75.

7. Hamilton, M. J.; Ho, V. W.; Kuroda, E.; Ruschmann, J.; Antignano, F.; Lam, V.; Krystal, G., Role of SHIP in cancer. *Exp. Hematol.* **2011**, *39*, 2-13.

8. Catimel, B.; Yin, M.-X.; Schieber, C.; Condron, M.; Patsiouras, H.; Catimel, J.; Robinson, D. E. J. E.; Wong, L. S.-M.; Nice, E. C.; Holmes, A. B.; Burgess, A. W., PI(3,4,5)P3 Interactome. *J. Proteome Res.* **2009**, *8*, 3712-3726.

9. Brooks, R.; Fuhler, G. M.; Iyer, S.; Smith, M. J.; Park, M.; Paraiso, K.; Engelman, R. W.; G, K. W., SHIP1 inhibition increases immunoregulatory capacity and triggers apoptosis of hematopoietic cancer cells. *J. Immunol.* **2010**, *184*, 3582-3589.

10. Lim, J. W.; Kim, S. K.; Choi, Y. S.; Kim, D. H.; Gadhe, C. G.; Lee, H. N.; Kim, H.-N.; Kim, J.; Cho, S. J.; Hwang, H.; Seong, J.; KJeong, K.-S.; Lee, J. Y.; Lim, S. M.; Lee, J. W.; Pae, A. N., Identification of crizotinib derivatives as potent SHIP2 inhibitors for the treatment of Alzheimer's disease. *Euro. J. Med. Chem.* **2018**, *157*, 405-422.

11. Srivastava, N.; Iyer, S.; Sudan, R.; Youngs, C.; Engelman, R. W.; Howard, K. T.; Russo, C. M.; Chisholm, J. D.; Kerr, W. G., A small-molecule inhibitor of SHIP reverse age- and diet-associated obesity and metabolic syndrome. *JCI Insight* **2016,** *1*, e88544.

12. Suwa, A.; Yamamoto, T.; Sawada, A.; Minoura, K.; Hosogai, N.; Tahara, A.; Kurama, T.; Shimokawa, T.; Aramori, I., Discovery and functional characterization of a novel small molecule inhibitor of the intracellular phosphatase, SHIP2. *Br. J. Pharmacol.* **2009**, *158*, 879-887.

13. Suwa, A.; Kurama, T.; Shimokawa, T., SHIP2 and its involvement in various diseases. *Expert Opinion on Therapeutic Targets* **2010**, *14*, 727-737.

14. Viernes, D. R., "Synthesis, design, and biological evaluation of inhibitors and activators of Src Homology 2 domain-containing inositol phosphatase (SHIP) and synthetic studies of apicularen A and maoecrystal V" *Syracuse University Dissertations, Department of Chemistry* **2012**.

15. Yuan, T. L.; Cantely, L. C., PI3K pathway alterations in cancer: variations on a theme. *Oncogene* **2008**, *27*, 5497-5510.

16. Zhang, J.; Grindley, J. C.; Yin, T.; Jayasinghe, S.; He, X. C.; Ross, J. T.; Haug, J. S.; Rupp, D.; Porter-Westpfahl, K. S.; Wiedemann, L. M.; Wu, H.; Li, L., PTEN maintains haematopoietic stem cells and acts in lineage choic and leukaemia prevention. *Nature* **2006**, *441*, 518-522.

17. Yilmaz, O. H.; Valdez, R.; Theisen, B. K.; Guo, W.; Ferguson, D. O.; Wu, H.; Morrison, S. J., PTEN dependence distinguishes haematopoietic stem cells from leukaemia-initiatin cells. *Nature* **2006**, *441*, 475-482.

18. Ghansah, T.; Paraiso, K. H. T.; Highfill, S.; Desponts, C.; May, S.; McIntosh, J. K.; Wang, J.-W.; Ninos, J.; Brayer, J.; Cheng, F.; Sotomayor, E.; Kerr, W. G., Expansion of Myeloid Suppressor Cells in SHIP-Deficient Mice Represses Allogeneic T Cell Responses. *J. Immunol.* **2004**, *173*, 7324-7330.

19. Paraiso, K.; Ghansah, T.; Costello, A.; Robert, E. W.; Kerr, W. G., Induced SHIP deficiency expands myeloid regulatory cells and abrogates graft- versus-host disease. *J. Immunol.* **2007**, *178*, 2893-2900.

20. MacDonald, K. P.; Rowe, V.; Clouston, A. D.; Welply, J. K.; Kuns, R. D.; Ferrara, J. L.; Thomas, R.; Hill, G. R., Cytokine expanded myeloid precursors function as regulatory antigen-presenting cells and promote tolerance through IL-10-producing regulatory T cells. *J. Immunol.* **2005**, *174*, 1841-1850.

21. Wang, J.-W.; Howson, J. M.; Ghansah, T.; Desponts, C.; Ninos, J. M.; May, S. L.; Nguyen, K. H. T.; Toyama-Sorimachi, N.; Kerr, W. G., Influence of SHIP on the NK repertoire and allogeneic bone marrow transplantation. *Science* **2002**, *295*, 2094-2097.

22. Helgason, C. D.; Damen, J. E.; Rosten, P.; Grewal, R.; Sorensen, P.; Chappel, S. M.; Borowski, A.; Jirik, F.; Krystal, G.; Humphries, R. K., Targeted disruption of SHIP leads to hemopoietic perturbations, lung pathology, and a shortened life span. *Genes & Dev.* **1998**, *12*, 1610-1620.

23. Saz-Leal, P.; Del Fresno, C.; Brandi, P.; Martinez-Cano, S.; Dungan, O. M.; Chisholm, J. D.; Kerr, W. G.; Sancho, D., Targeting SHIP-1 in myeloid cells enhances trained immunity and boosts response toinfection. *Cell Rep.* **2018**, *25*, 1118-1126.

24. Gumbleton, M.; Sudan, R.; Fernandes, S.; Kerr, W. G.; Engelman, R. W.; Russo, C. M.; Chisholm, J. D.; Kerr, W. G., Dual enhancement of T and NK cell function by pulsatile inhibition of SHIP1 improves antitumor immunity and survival. *Sci. Signal* **2017**, *10*, eaam5353.

25. Howard, K. T., "Convenient etherification using trichloroacetimidates and synthesis of aminosteroid SHIP inhibitors". *Syracuse University Dissertations, Department of Chemistry* **2016**.

26. Mills, S. J.; Persson, C.; Cozier, G.; Thomas, M. P.; Trésaugues, L.; Erneux, C.; Riley, A. M.; Nordlund, P.; Potter, B. V. L., A synthetic polyphosphoinositide headgroup surrogate in complex with SHIP2 provides a rationale for drug discovery. *ACS Chem. Bio.* **2012**, *7*, 822-828.

27. Kolb, H. C.; Sharpless, K. B., The growing impact of click chemistry on drug discovery. *Drug Discovery Today* **2003**, *8*, 1128-1137.

28. Tornøe, C. W.; Christensen, C.; Meldal, M., Peptidotriazoles on solid phase: [1,2,3]-triazoles by regiospecific copper(I)-catalyzed 1,3-dipolar cycloadditions of terminal alkynes to azides. *J. Org. Chem* **2002**, *67*, 3057-3064.

29. Gololobov, Y. G.; Kasukhin, L. F., Recent advances in the staudinger reaction. *Tetrahedron* **1992**, *48*, 1353-1406.

30. Zhao, Y.; Zhong, Z., Oligomeric cholates: amphiphilic foldamers with nanometer-sized hydrophilic cavities. *J. Am. Chem. Soc.* **2005**, *127*, 17894-17901.

31. Arnáiz, F. J., A convenient way to generate hydrogen chloride in the freshman lab. *J. Chem. Ed.* **1995**, *72*, 1139.

32. Swamy, K. C. K.; Kumar, N. N. B.; Balaraman, E.; Kumar, K. V. P. P., Mitsunobu and related reactions: Advances and applications. *Chem. Rev.* **2009**, *109*, 2551-2651.

33. Norden, S.; Bender, M.; Rullkotter, J.; Christoffers, J., Androstanes with modified carbon skeletons. *Eur. J. Org. Chem.* **2011**, 4543-4550.

34. Purushottamachar, P.; Njar, V. C. O., A new simple and high-yield synthesis of 5α-dihydrotestosterone (DHT), a potent androgen receptor agonist. *Steroids* **2012**, *77*, 1530-1534.

35. Liu, X.-K.; Ye, B.-J.; Wu, Y.; Nan, J.-X.; Lin, Z.-H.; Piao, H.-R., Synthesis and antitumor activity of dehydroepiandrosterone derivatives on Es-2, A549, and HepG2 cells in vitro. *Chem. Biol. Drug Des.* **2012**, *79*, 523-529.

36. Prokai, L.; Oon, S.-M.; Prokai-Tatrai, K.; Abboud, K. A.; Simpkins, J. W., Synthesis and biological evaluation of 17β-alkoxyestra-1,3,5(10)-trienes as potential neuroprotectants against oxidative stress. *J. Med. Chem* **2001**, *44*, 110-114.

37. McGuigan, C.; Hinsinger, K.; Farleigh, L.; Pathirana, R. N.; Bugert, J. J., Novel antiviral activity of l-dideoxy bicyclic nucleoside analogues versus vaccinia and measles viruses in vitro. *J. Med. Chem.* **2013**, *56*, 1311-1322.

38. Sugandhi, E. W.; Slebodnick, C.; Falkinham, J. O.; Gandour, R. D., Synthesis and antimicrobial evaluation of water-soluble, dendritic derivatives of epimeric 5α-cholestan-3-amines and 5α-cholestan-3-yl aminoethanoates. *Steroids* **2007**, *72*, 615-626.

39. Loibner, H.; Zbiral, E., Reaktionen mit phosphororganischen Verbindungen. XLI[1]. Neuartige synthetische Aspekte des Systems Triphenylphosphin-Azodicarbonsäureester-Hydroxyverbindung. *Helv. Chim. Acta.* **1976**, *59*, 2100-2113.

40. Wang, Y.; Ji, S.; Wei, K.; Lin, J., Epiandrosterone-derived prolinamide as an efficient asymmetric catalyst for Michael addition reactions of aldehydes to nitroalkenes. *RSC Adv.* **2014**, *4*, 30850-30856.

41. Amiranashvili, L. S.; Sladkov, V. I.; Levina, I. I.; Men'shova, N. I.; Suvorov, N. N., *J. Org. Chem. USSR* **1990**, *26*, 1629-1632.

Chapter 3 - Development of a New Synthesis of AQX-1125

Abstract

Increasing the phosphatase activity of SHIP1 through activation with an allosteric agonist may reduce PI3K signaling. SHIP1 is allosterically activated as its own product, $PI(3,4)P_2$, binds to the enzyme and increases activity. This upregulation of SHIP1 further increases the rate of hydrolysis of $PI(3,4,5)P_3$, reducing the activation of protein kinase AKT from binding of $PI(3,4,5)P_3$ but promoting signaling from the interaction of $PI(3,4)P_2$ with AKT. With this understanding the potential for small molecules to allosterically bind and accelerate SHIP1 phosphatase activity will further drive the hydrolysis of $PI(3,4,5)P_3$. The complicated nature of these interactions demonstrates the need for small molecule SHIP1 agonists to investigate the role of SHIP1 in PI3K signaling. Several small molecule SHIP1 agonists have been reported in the literature. These studies culminated in the identification by Aquinox Pharmaceuticals of AQX-1125, which recently underwent clinical evaluation for interstitial cystitis / bladder pain syndrome. To facilitate our own studies on SHIP1 signaling, a new synthetic route to the SHIP1 agonist AQX-1125 has been developed. This route is significantly more rapid than the previously published route (17 steps), requiring only 12 steps from the commercially available dehydroepiandrosterone.

3.1 Introduction

Investigations into the inhibition of PI3K have been pursued with some isoform-specific inhibitors being developed and proceeding through clinical trials.[1-4] One difficulty in targeting PI3K is with the off-target effects caused by the inhibition of an undesired PI3K isoform. However, regulation of the intercellular signaling responses through the PI3K pathway can also be achieved by targeting SHIP, the negative regulator of $PI(3,4,5)P_3$, and this enzyme only exists in two isoforms, SHIP1 and SHIP2. Expressed primarily in hematopoietic cells,[5] SHIP1 plays a key role in blood and bone marrow cellular physiology, whereas the other paralog SHIP2 is utilized for a similar role in other cells.[6-10] Modulating SHIP could allow for the development of alternative therapeutic treatments for multiple human disorders[11] such as cancer,[3,12-16] autoimmune disease,[13,14] cardiovascular disease,[13,14] obesity,[17,18] and chronic inflammatory conditions.[14,15,19]

Interest in modulation of SHIP to influence the PI3K signaling pathway led Andersen, Krystal and Mui to screen a library consisting of roughly 2000 marine invertebrate extracts. This screening led to the identification of the meroterpenoid pelorol **3.1** from the Papua New Guinea sponge *Dactylospongia elegans* as a SHIP1 agonist (Figure 3.1). This molecule was shown to act as a selective SHIP1 agonist in a chromogenic enzyme assay.[20] Although pelorol was independently isolated and identified by Golcik *et al.*[21] and Kwak *et al.*,[22] these studies just described the isolation and characterization of pelorol, and did not mention the activation of SHIP1 enzymatic activity.[20] Further evaluation of the agonist activity demonstrated by pelorol towards SHIP1 was facilitated by a total synthesis of the molecule which was developed by Yang and co-workers. This synthesis utilized the commercially available and inexpensive terpenoid (+)-sclareolide **3.2** as the starting material.[14,15,20,23]

*Figure 3.1: Structure of Pelorol **3.1** Synthesized from (+)-Sclareolide **3.2***

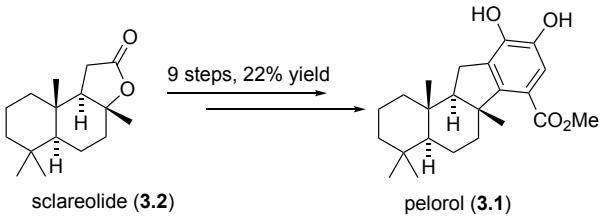

Evaluation of synthetic pelorol **3.1**, the intermediates from the total synthesis as well as a number of pelorol analogs led to the identification of AQX-016A **3.3** as an even more potent SHIP1 agonist. This molecule was reported to be approximately three times more active than pelorol when tested against SHIP1 at the same concentration. A number of further studies were then performed using the more potent agonist AXQ-016A **3.3** (Figure 3.2).[14,20,23,24] To address selectivity concerns on other inositol phosphatases, AQX-016A **3.3** was tested against the other paralog of SHIP, SHIP2. Using a number of in vitro enzyme assays, the phosphatase activity of SHIP1 showed an increase with increasing concentration of AQX-016A **3.3** but no increase was observed for SHIP2 phosphatase activity.[14,20] Therefore it was concluded that these agonists exert their biological effects through interactions solely with SHIP1.

*Figure 3.2: Structure of AQX-016A **3.3** (A) Activity Towards SHIP Enzyme (B) Selectivity for SHIP1 vs SHIP2 [20]*

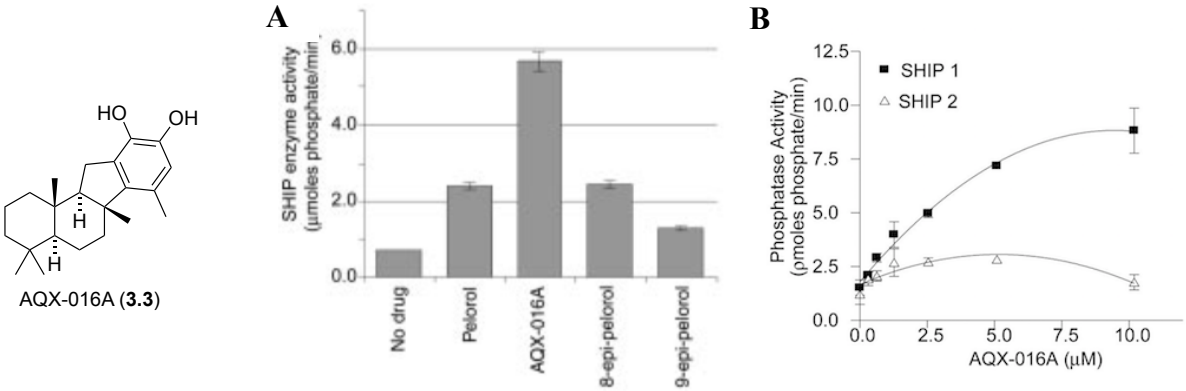

Furthermore, analysis of the ability of AQX-016A **3.3** to upregulate SHIP1 activity in the PI3K signaling pathway in cells was investigated. Prior experiments demonstrated that macrophages stimulated with lipopolysaccharides (LPS) activate PI3K signaling and generate a 3- to 5-fold increase in $PI(3,4,5)P_3$, which drives an inflammatory response.[20] Upon treatment with AQX-016A **3.3**, $PI(3,4,5)P_3$ levels in LPS treated macrophages decreased, as was expected since increasing SHIP1 activity will convert the $PI(3,4,5)P_3$ to the hydrolyzed product $PI(3,4)P_2$ (Figure 3.3).[20] As a positive control, LPS stimulated macrophages were also treated with a known PI3K inhibitor LY294002.[25] The PI3K inhibitor showed a similar result with no $PI(3,4,5)P_3$ observed, signifying that both LY294002 and AQX-016A **3.3** are targeting the PI3K signaling pathway.[20] Additional support that AQX-016A **3.3** was targeting SHIP1 was obtained from measuring the amount of $PI(3,4)P_2$ after treatment of the cells with LY294002 and AQX-016A **3.3**. As a 5' inositol phosphatase, treatment of the cells with a SHIP1 agonist should lead to a significant increase in the amount of $PI(3,4)P_2$ in the cells. The PI3K inhibitor LY294002 should not show this increase, since it is stopping formation of the $PI(3,4,5)P_3$ by halting addition of the 3' phosphate to the inositol via inhibition of the parent kinase PI3K. These expectations are consistent with the results shown in Figure 3.3B, where treatment with AQX-016A **3.3** provides significantly more $PI(3,4)P_2$ than treatment with LY294002, but both lead to a drop in $PI(3,4,5)P_3$.

Figure 3.3: $PI(3,4,5)P_3$ (A) vs $PI(3,4)P_2$ (B) Concentrations in AQX-016A **3.3** Treated Macrophages Stimulated with LPS[20]

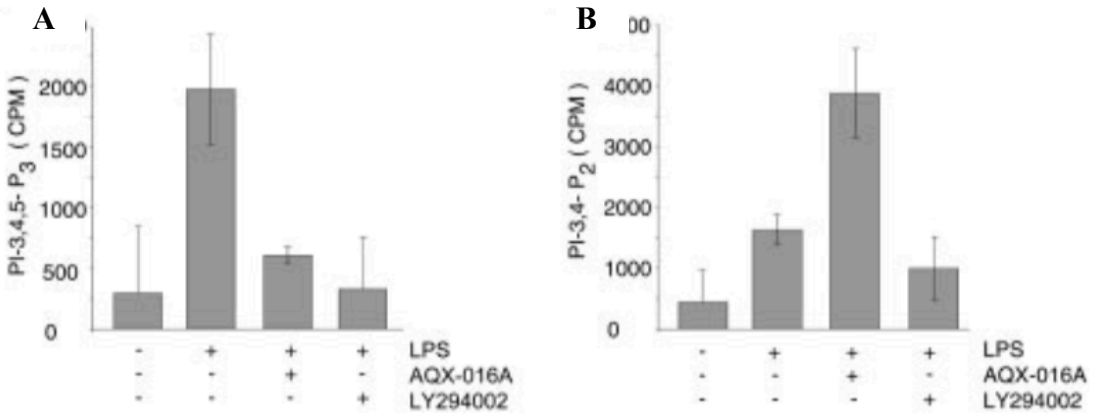

Another recognizable response to LPS stimulated macrophages is an increase in PI3K induced production of proinflammatory cytokines such as TNFα.[26] Increased cell concentrations of $PI(3,4,5)P_3$ activate an inflammatory response, and therefore an LPS challenge increases TNFα production and leads to inflammation. Treatment with a SHIP1 agonist should drive the hydrolysis of the 5' phosphate from the inositol and lower the amount of $PI(3,4,5)P_3$ present, leading to less TNFα and acting as an anti-inflammatory agent. This reduction in TNFα production can easily be measured with an antibody using a commercially available ELISA kit, providing an assay for new small molecules with anti-inflammatory properties. Evaluation of AQX-016A **3.3** in this assay demonstrated a 30% decrease in TNFα at 3μM and 50% decrease at 15 μM.(Figure 3.4).[20] This study was performed using LPS challenged bone marrow-derived macrophages (BMDM) that express SHIP1 ($SHIP^{+/+}$). To further validate the role of AQX-016A **3.3** in reducing TNFα by activating SHIP1, BMDM that were modified to be SHIP1 deficient ($SHIP^{-/-}$) gave no observed decrease in TNFα, signifying that AQX-016A **3.3** was specifically modulating SHIP1 activity in these systems.[20] A comparison study using LY294002 gave a similar result showing a decrease in

TNFα (40% at 15 μM) due to a lack of PI(3,4,5)P_3. Again, this was due to a lack of PI(3,4,5)P_3 as the PI3K kinase enzyme being inhibited, so the 3'-phosphate could not be installed. Using LY294002 the decrease in TNFα was observed in both $SHIP^{+/+}$ and $SHIP^{-/-}$ BMDM, demonstrating that the PI3K inhibitor was active through a different mechanism than AQX-016A **3.3** .[20]

*Figure 3.4: Reduction of TNF*α in BMDM Treated with AQX-016A **3.3**[20]

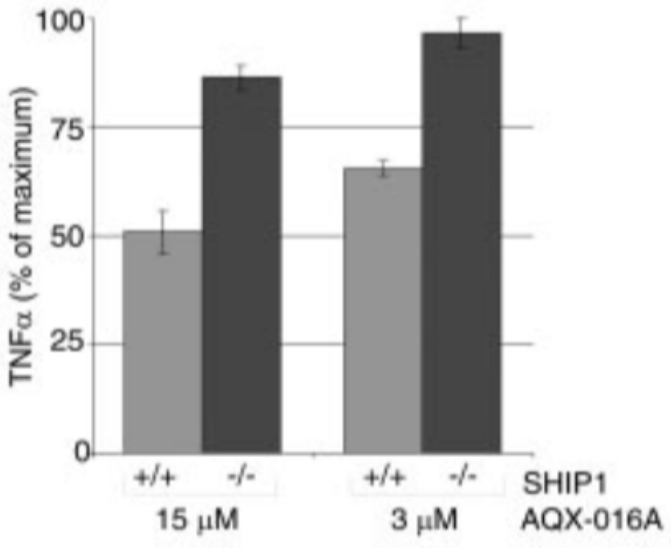

While the in vitro studies were quite promising, AQX-MN100 and the other pelorol analogs had yet to show if they were active and robust enough to activate SHIP1 in a whole animal. In vivo studies were then undertaken in mice. These studies showed that AQX-016A **3.3** was able to reduce an inflammatory response induced from LPS injections.[20] Mice pretreated with AQX-016A **3.3** orally 30 minutes prior to the injection showed a decreased amount of serum TNFα levels (Figure 3.5).[20] This reduced level of TNFα was comparable to mice treated with dexamethasone, a known macrophage inhibitor.[20] These studies showed that AQX-016A could function as a SHIP1 agonist in an animal and, importantly, also demonstrated that the small molecule was active through oral dosing.

*Figure 3.5: In vivo Reduction of Serum TNF*α of Mice Treated with SHIP1 Agonist AQX-016A **3.3** Comparable to Mice Treated with Macrophage Inhibitor Dexamethasone [20]

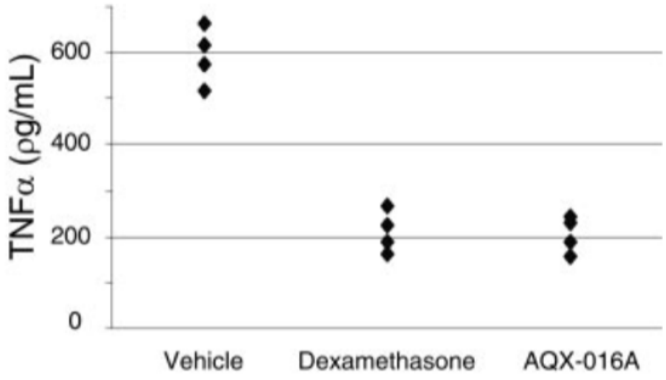

Although the molecule was demonstrated to be an orally bioavailable, potent and selective agonist for SHIP1, the catechol functionality in AQX-016A **3.3** gave rise to concerns over toxicity and potential side effects. Catechols are well known to bind metals and/or are easily oxidized to orthoquinones under physiological conditions by cytochrome P450 enzymes, which are near ubiquitous. These orthoquinones can cause covalent modifications to proteins and DNA through Michael reactions.[14,20] To overcome these issues, further structure activity studies were performed on the pelorol system. Eventually the phenol AQX-MN100 **3.4** was developed. This molecule was similar to AQX-016A but lacked the hydroxyl functionality at C17. AQX-MN100 showed equivalent selectivity as AQX-016A **3.3** (Figure 3.6)[14,20,21] for SHIP1, and actually appeared to be a slightly more potent agonist.

Figure 3.6: Structure of AQX-MN100 ***3.4*** *and (A) Comparison of SHIP1 Activity to AQX-016A* ***3.3*** *(B) TNFα Reduction with AQX-MN100* ***3.4*** *(C) Agonist Activity Occurs Through Allosteric Activation at the C2 Domain of SHIP1*[20]

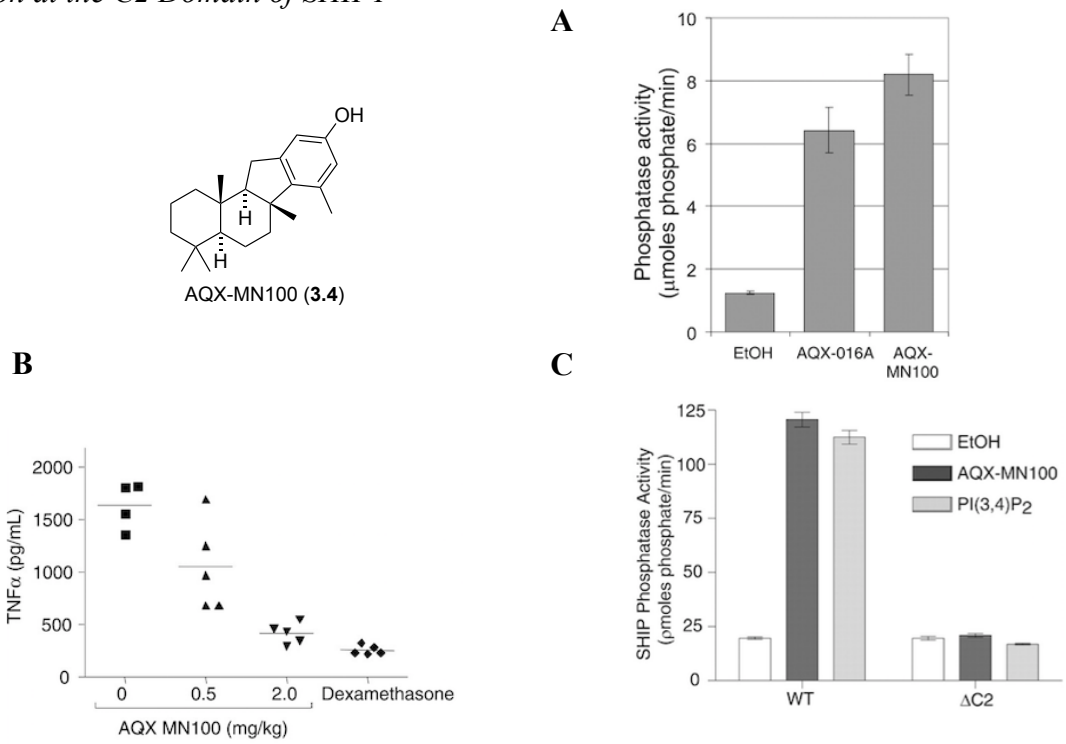

Further studies with AQX-MN100 **3.4** as a SHIP1 agonist revealed that the allosteric recognition site (where the agonist binds to the enzyme to increase activity) is localized on the C2-domian of the protein (Figure 3.7).[14,20] To determine the location of the allosteric agonist binding site, Anderson and co-workers analyzed SHIP1 phosphatase activity towards the wild-type enzyme or a C2-domain deleted SHIP1 mutant. Treatment with AQX-MN100 **3.4** led to increased activity for the wild-type SHIP1 enzyme, but no increase was demonstrated for the C2-domain deleted mutant protein.[20] Interestingly the product of SHIP1 hydrolysis, $PI(3,4)P_2$, also was shown to cause an increase in phosphatase activity. This demonstrates that the SHIP1 product is likely the endogenous ligand for the allosteric site on the C2 domain, with some of the product of the

hydrolysis of $PI(3,4,5)P_3$ binding to the enzyme and increasing the rate of hydrolysis of more $PI(3,4,5)P_3$.[20] While these pelorol derivatives were the first small molecules which were shown to be SHIP1 agonists, their development was eventually discontinued due to concerns about their pharmacodynamics, which appeared to be poor as the molecules are quite nonpolar.

Figure 3.7: AQX-MN100 ***3.4*** *Increases SHIP1 Activity Allosterically Through the C2-Domain*

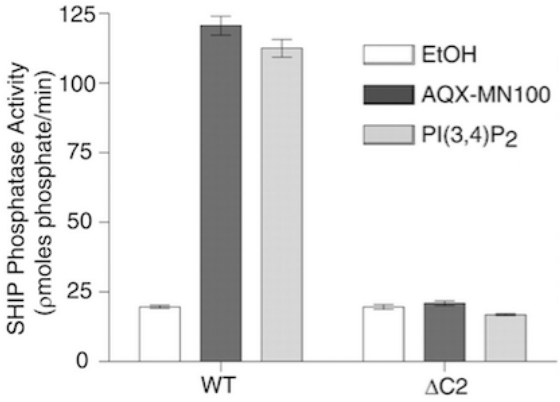

Continued efforts in developing new SHIP1 agonists by Aquinox Pharmaceuticals led to the undisclosed identification of AQX-MN115 **3.5** and the seco-steroidal indene AQX-1125 **3.6**, potentially through a screen of indene analogs developed by Inflazyme Pharmaceuticals (Figure 3.8).[27] While AQX-MN115 **3.5** showed an increase in SHIP1 activity by 77% at 300 μM, AQX-1125 **3.6** only showed a 20% increase at the same concentration.[28] Although less potent, AQX-1125 **3.6** displays exceptional pharmacokinetics and was therefore advanced as the new lead compound. A patented 17 step synthesis of AQX-1125 **3.6** was developed from commercially available dehydroepiandrosterone with an overall yield of 13%.[29]

Figure 3.8: Structure of AQX-MN115 ***3.5*** *and AQX-1125* ***3.6*** *(Synthesized from Dehydroepiandrosterone* ***3.7****)*

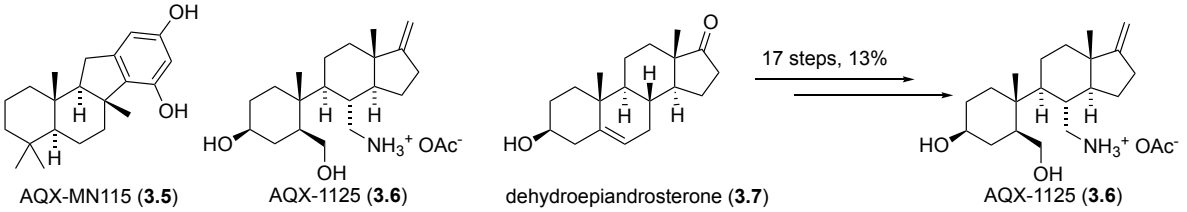

AQX-1125 **3.6** showed no toxicity in a phase I clinical trial, and was quickly moved on to a phase II clinical trial to test for anti-asthmatic properties.[28,30] AQX-1125 **3.6** is the first SHIP1 modulator to reach clinical trials. However, while the phase I trial demonstrated safety and did seem to show some efficacy, the later phase II trials did not show sufficient evidence of efficacy for treatment of COPD.[31] The molecule is now being evaluated for a number of other inflammatory conditions. For example, AQX-1125 **3.6** was recently evaluated in a phase III clinical trial for the treatment of bladder pain syndrome/interstitial cystitis (BPS/IC), a chronic inflammatory bladder disease.[32] Again the molecule did not demonstrate efficacy in this clinical trial. The reason for the lack of efficacy in these clinical settings is currently unclear, but AQX-1125 **3.6** has shown only a 20% increase in SHIP1 activity at 300 μM and this may not be potent enough activity to show an anti-inflammatory effect at the organismal level. Aquinox appears to be continuing development of AQX-1125 **3.6** and other SHIP1 agonists as anti-inflammatories.

Initially, the Aquinox synthesis of AQX-1125 **3.6** begins with the commercially available dehydroepiandrosterone **3.7** (Scheme 3.1). Using ethylene glycol and *p*-toluenesulfonic acid a ketal was installed from the C17 ketone leading to structure **3.8**. Protection of the C3 hydroxy group as the *tert*-butyldimethylsilyl ether **3.9** was then executed with TBDMSCl and imidazole. This was followed by the allylic oxidation of alkene **3.10** with a ruthenium catalyst generating

ketone **3.10**. While this oxidation is well precedented in the literature, it is known to proceed in moderate yield as there are many allylic positions in the molecule and the selectivity of this process is problematic. Reduction of enone **3.10** using Luche conditions[33] leads to the allylic alcohol **3.11**.[29]

*Scheme 3.1: Aquinox Synthesis Formation of the Allylic Alcohol **3.11***

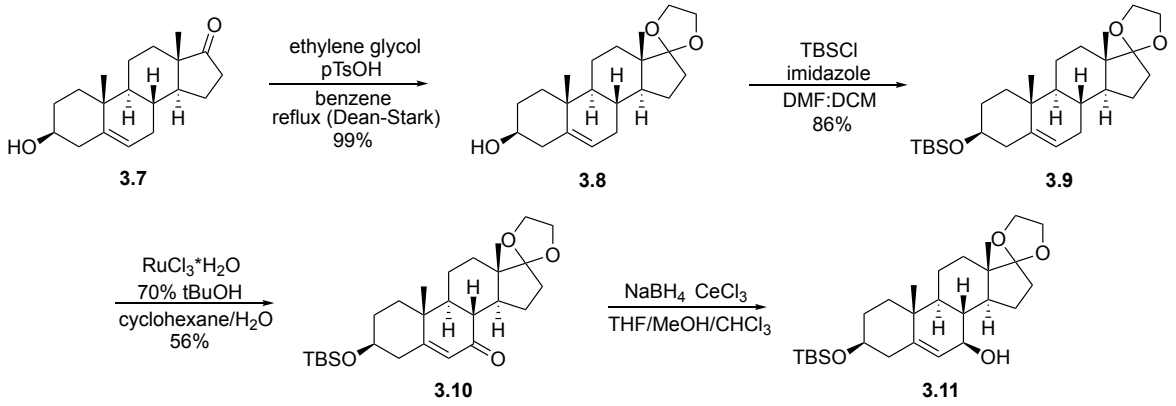

Hydroboration-oxidation of the allylic alcohol **3.11** then accessed the diol **3.12** (Scheme 3.2). Deprotection of the C17 ketal and the TBDMS group was accomplished using 80% aq. acetic acid, which formed ketone **3.13**. The diol was then protected as an acetonide to provide the ketone **3.14**.[29]

*Scheme 3.2: Aquinox Synthesis Formation of the Acetonide **3.14***

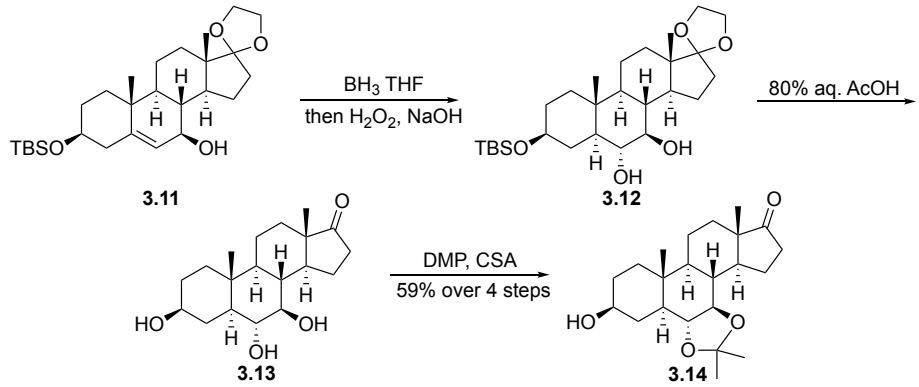

A Wittig reaction was then performed on the **3.14** carbonyl at C17 to generate the exocyclic olefin **3.15** (Scheme 3.3). The protection of the C3 alcohol as the acetate **3.16** was then accomplished with acetic anhydride and pyridine. This was followed by acid promoted hydrolysis of the acetonide, producing diol **3.17**. Oxidative cleavage of the diol with sodium periodate opened the steroid B ring to provide dialdehyde **3.18**.[29]

Scheme 3.3: *Aquinox Synthesis Formation of the Dialdehyde **3.18***

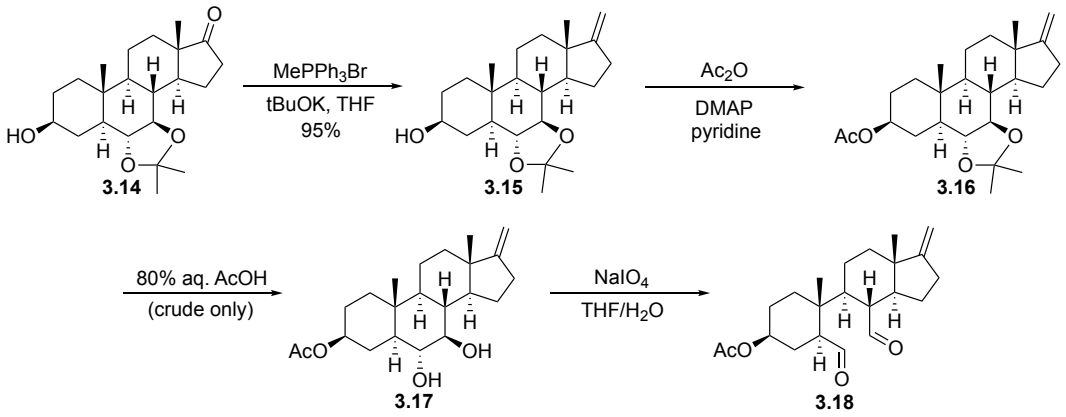

Dialdehyde **3.18** was then reduced using sodium borohydride to generate intermediate diol **3.19**. This diol was then selectively protected as the monoacetate **3.20** (Scheme 3.4). This monoprotection reaction was claimed to be selective, but no reasoning for this selectivity was given in the patent. The less reactive alcohol was then activated as the mesylate with methanesulfonyl chloride and triethylamine to provide mesylate **3.21**. Displacement of the mesylate **3.21** was accomplished using sodium azide in DMF, providing the azide **3.22**.[29]

Scheme 3.4: *Aquinox Synthesis Formation of the Azide **3.22***

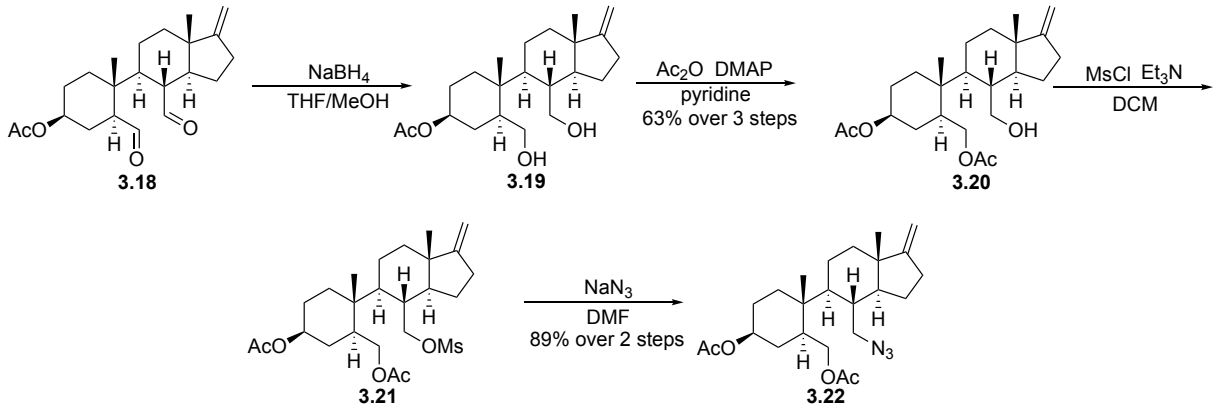

This azide **3.22** was then was reduced to the primary amine **3.23** with lithium aluminum hydride (Scheme 3.5). This reduction was also effective in removing the acetate from the C3 alcohol. To complete the synthesis the acetate salt of the free amine **3.23** was formed generating AQX-1125 **3.6**.[29,34]

*Scheme 3.5: Aquinox Synthesis Formation of the AQX-1125 **3.6***

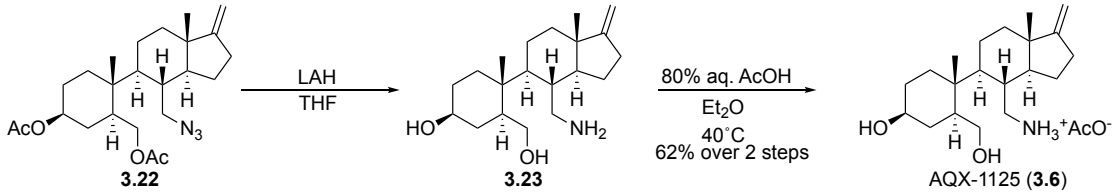

Even though AQX-1125 **3.6** has performed poorly in clinical trials, [28,30-32] it remains the only compound targeting SHIP1 to advance to the clinic. Given its ability to activate SHIP1 and its excellent pharmacodynamic properties, the molecule may still be useful as a reagent to probe the role of SHIP1 on signaling in the PI3K pathway, especially in murine settings. Given our own studies on the role of SHIP modulation in human disease,[35-37] we undertook a synthesis of AQX-

1125 **3.6** to provide material for to further study the effects of upregulating SHIP1. Given the length of the synthesis developed by Aquinox, some effort was expended into developing a shorter synthesis of the molecule so that it could be produced more quickly and efficiently.

3.2 Development of a New Synthetic Route to AQX-1125

A new synthetic route to the SHIP1 agonist AQX-1125 **3.6** has been developed. Some initial studies on this route were performed previously by lab colleague Dr. Brian C. Duffy.[34] This route is significantly more rapid than the previously published route, requiring only 12 steps from the commercially available dehydroepiandrosterone **3.7**. Retrosynthetically the new route utilizes the lactone intermediate **3.25** which facilitates differentiation of the C6 and C7 positions (steroid numbering). This results in a completely regioselective synthesis of this complex molecule (Scheme 3.6). In addition, some intermediates and analogs have been prepared, providing evidence that the C17 alkene is not relevant for maintaining SHIP1 agonist activity in preliminary malachite green assays.

Scheme 3.6: Proposed Retrosynthetic Analysis of AQX-1125 ***3.6***

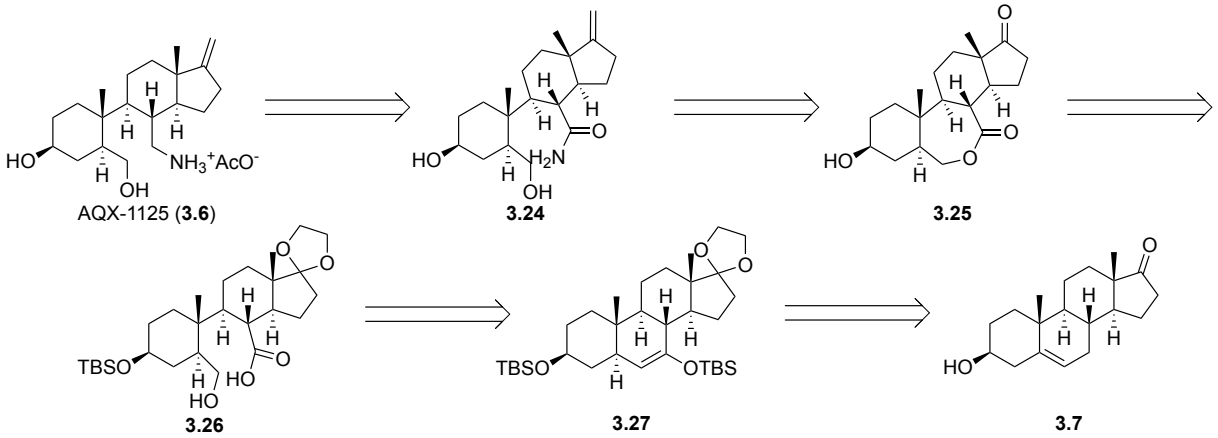

3.3 Results and Discussion

The first three steps of the new synthesis of AQX-1125 follow from the literature. First the ketal **3.8** is produced using a catalytic amount of toluenesulfonic acid**,** ethylene glycol, and benzene at reflux using a Dean-Stark trap (Scheme 3.7) to remove water from the reaction mixture. The alcohol on the C3 position was then protected as the TBS ether **3.9**. Both of these steps proceeded with good conversion. No purification was required over these first two steps, with the crude product being pure enough to go on to the next step. The allylic oxidation using a ruthenium catalyst was then performed on alkene **3.9** to generate the α,β-unsaturated ketone **3.10**. The yield of this reaction is generally moderate due to the multiple allylic sites and harsh oxidation conditions producing a mixture of products.[29,34,38,39] However, purification via recrystallization allowed for the product **3.10** to be easily separated from the byproducts produced in the reaction.[29,38] This is convenient as ketone **3.10** can be isolated on large scale (3.41 g **3.10**) from starting dehydroepiandrosterone **3.7** without chromatography.[29,38] From here the synthetic route diverges from the Aquinox route. Using 10% palladium on carbon in ethyl acetate a hydrogenation of the unsaturated ketone **3.10** produced the favored trans-decalin **3.28**. The delivery of the hydrogen from the bottom face of the steroid is consistent with the angular methyl groups blocking the top face of the molecule from attack. Similar stereochemistry has been generated by hydrogenation of C5-C6 alkenes is other steroid systems.[39]

*Scheme 3.7: Synthesis of Ketone Intermediate **3.28***

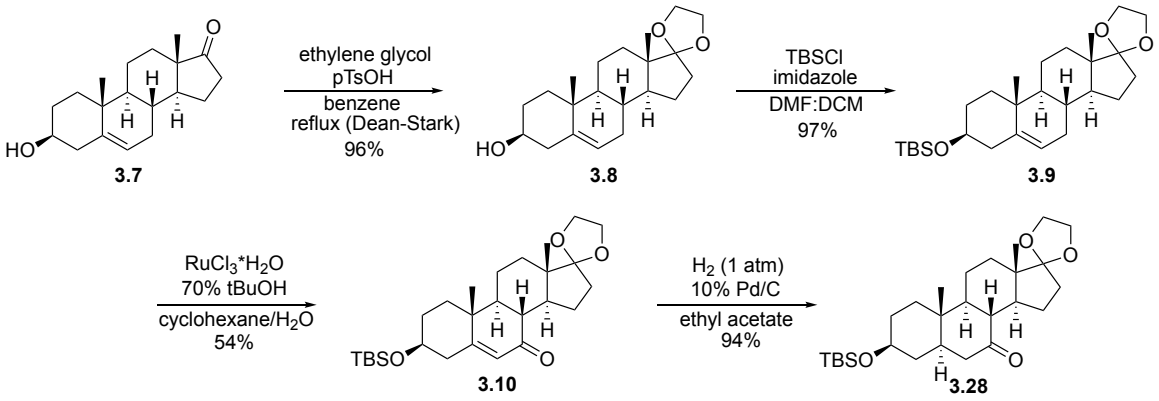

The ketone **3.28** was then transformed into the silyl enol ether **3.27** in good yields using tert-butyldimethylsilyl trifluoromethanesulfonate and triethylamine in dichloromethane (Scheme 3.8). This reaction was selective for formation of the less highly substituted silyl enol ether, as is consistent with literature reports in similar systems.[40] Purification by column chromatography is required to remove the byproducts produced during the silyl enol ether formation. Previous work attempted to oxidatively cleave the TBS enol ether through ozonolysis[34] without purification, which led to issues with isolation and confirmation of the acid product **3.26**. Therefore initially a synthetic alternative was investigated. Using the silyl enol ether **3.27**, a Rubottom oxidation[41] was performed using *m*-CPBA and $NaHCO_3$ in DCM at 0˚C (Scheme 3.8) followed by deprotection using 10% aq. HCl **3.29**. An oxidative cleavage with sodium periodate $NaIO_4$[29] of **3.29** to generate the free acid/alcohol **3.30** system was found to show no reaction.

Scheme 3.8: *Synthesis of Acid Intermediate* ***3.31***

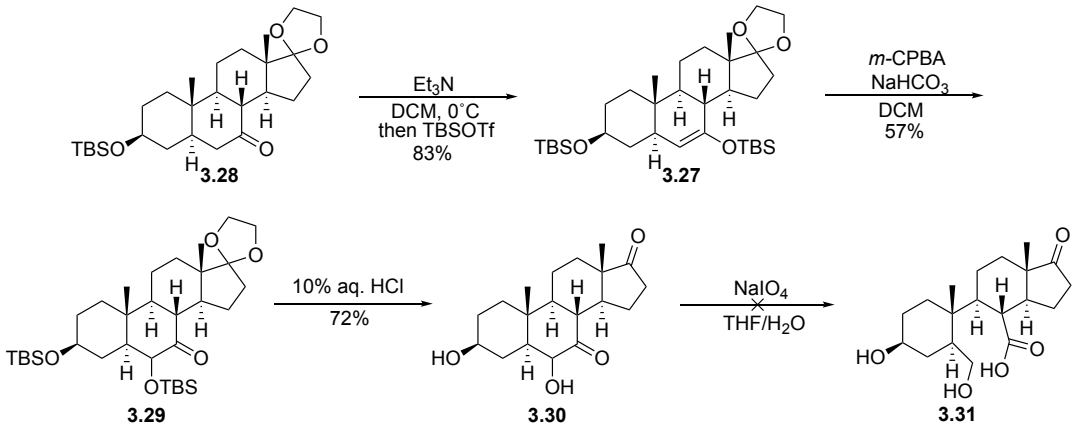

With the alternative route being problematic, reevaluation of the ozonoylsis was attempted. The goal was to fully identify and confirm product formation by following the reaction as it progressed through TLC and crude proton NMR examination. To further confirm the ozonolysis was in fact generating the product, a quick check was performed on the crude product by esterification of the potentially formed carboxylic acid with diphenylmethyl (DPM) imidate (Scheme 3.9).[42] DPM imidate has been shown to esterify carboxylic acids like **3.30** to generate the DPM ester **3.32** and trichloroacetamide byproduct **3.33** under mild reaction condition even in the presence of alcohols.

Scheme 3.9: General Esterification with Diphenylmethyl Imidate ***3.33***

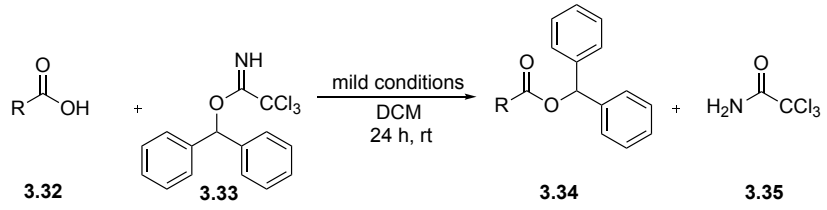

After acidic workup and isolation of the crude product of **3.31** generated from the ozonolysis reaction, the crude sample of **3.31** was dissolved in DCM followed by the addition of DPM imidate **3.33** and the reaction mixture was allowed to stir for 24 h (Scheme 3.10). Upon examination of the crude proton NMR key peaks were identified (Figure 3.9). The singlet proton at 6.87 ppm identifies as the proton on the methyl of the DPM ester **3.36** and the two proton peaks at 6.59 ppm and 5.78 ppm represent the protons of the amide trichloroacetamide byproduct **3.35**.

*Scheme 3.10: Esterification with Diphenylmethyl Imidate **3.33***

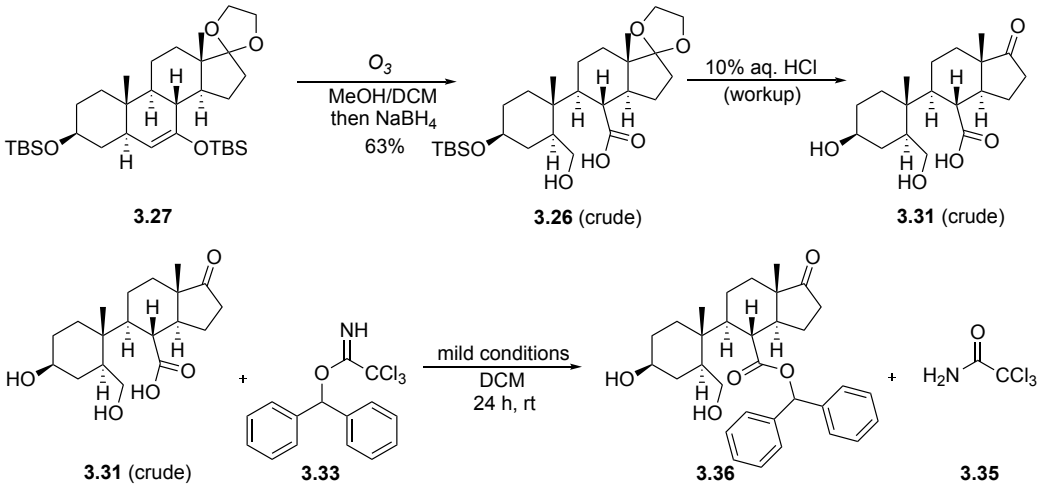

*Figure 3.9: Key Peaks of DPM Ester **3.36** Formation [1]HNMR Peak*

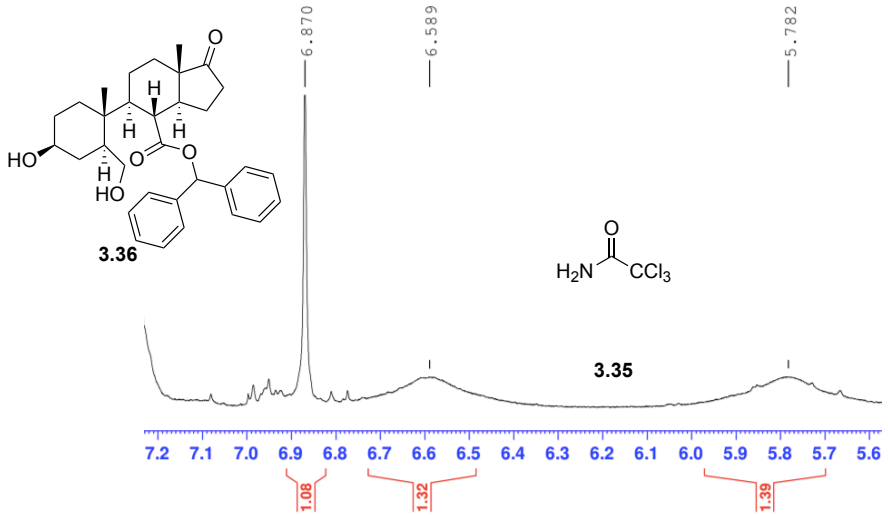

Along with showing the formation of the DPM ester **3.36**, careful monitoring of the esterification reaction by TLC identified the free acid **3.31**. This information was then used to identify the formation of the acid **3.26** as the silyl enol ether **3.27** is being exposed to ozone generating the alcohol/carboxylic acid intermediate. Once the intermediate was observed and the starting material disappeared, the ozonolysis could be halted using sodium borohydride to reduce the ozonide.[34]

The ozonolysis is a key step in the new synthetic route because it produces the necessary oxygen-containing functionality at C6 and C7 in different oxidation states, allowing for more a selective incorporation of the amine in the final product. Purification of the free acid can be performed by column chromatography accessing product **3.26** (Scheme 3.11). Deprotection of the ketal and the TBDMS group could be achieved from the hydroxy acid although the yield was low, possibly due to the incomplete deprotection of both the TBS protecting group and the ketal, or the high solubility of the free acid **3.31** in water.

However, the ozonolysis product **3.26** can be used without purification in an intramolecular lactonization reaction between the free alcohol and the carboxylic acid generated in the ozonolysis to form the 7-member cyclic lactone **3.37.** This can be accomplished in high yield using EDCl (1-ethyl-3-(3-dimethylaminopropyl) carbodiimide) and 4-dimethylaminopyridine in DCM.[43] Once the lactone is formed the deprotection of the 3β alcohol and ketal can be achieved by suspending lactone **3.37** in methanol and adding 10% aqueous hydrochloric acid dropwise until the TLC shows no more starting material. The lactone **3.25** is easily separable from the minor impurities with column chromatography, and is not water soluble like the diol carboxylic acid **3.31** which facilitates the removal of impurities by extraction.

*Scheme 3.11: Ozonolysis and Lactone **3.25** Formation*

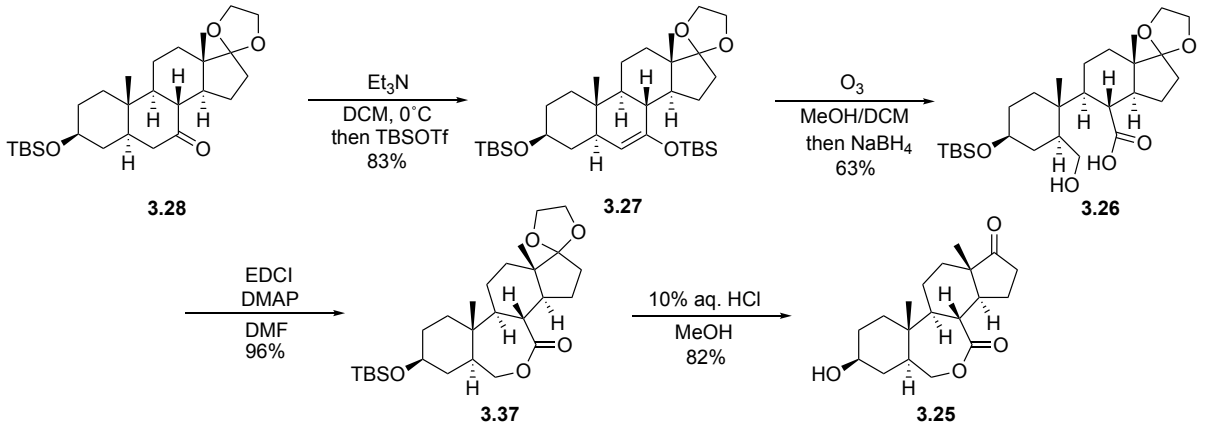

Installation of the C17 exocyclic alkene was then explored. A Wittig reaction was performed on lactone **3.25** to generate the exocyclic olefin **3.38** using methyltriphenylphosphonium bromide and n-butyllithium in refluxing tetrahydrofuran (Scheme 3.12). Initial attempts using KOH as the base proved to be of issue as no product was formed and starting material was lost in side reactions. This may be due to hydrolysis of the lactone.

Scheme 3.12: *Wittig Formation of Exocyclic Olefin **3.37***

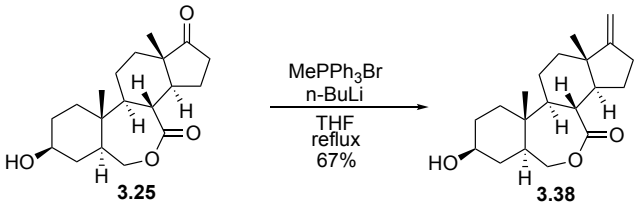

In an effort to conserve the key intermediate, further investigations into the Wittig reaction were first performed on a model system using the commercially available epiandrosterone **3.39** (Scheme 3.13).[44] The key doublet at 4.67 ppm identified the olefin protons using the *n*-BuLi conditions, providing evidence of the formation of **3.40** (Figure 3.10).

*Scheme 3.13: Epiandrosterone **3.39** Wittig Model*

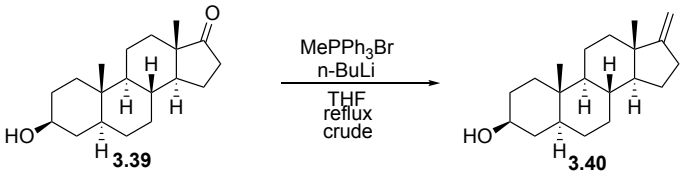

Figure 3.10: *Key Model Wittig Product **3.40** [1]HNMR Peak*

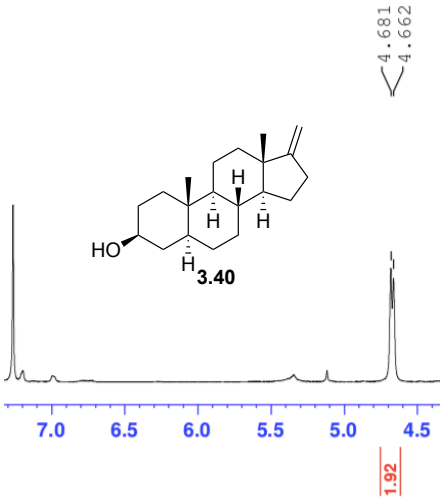

With the Wittig reaction complete and alkene installed at C17, formation of the amide **3.24** was undertaken. Attempts to break open the lactone **3.38** using ammonia in MeOH were initially investigated (Scheme 3.14). Treating ammonium in methanol with lactone **3.38** in a sealed tube with heating did not generate the amide, with the methyl ester **3.41** being identified as the major product from the crude ^{1}H NMR (Figure 3.11). Although not the expected product, this did however prove that the lactone **3.38** could be opened to give the free alcohol. Reaction of the lactone **3.38** in THF while bubbling ammonia in to the system also proved to be ineffective as only starting material was only recovered. Alternatively, by reaction with $LiNH_2$ (formed in situ from ammonia and n-BuLi), the lactone **3.38** was opened to give the amide product **3.24**.

*Scheme 3.14:Formation of Methyl Ester **3.41** and Key Amide Intermediate **3.24***

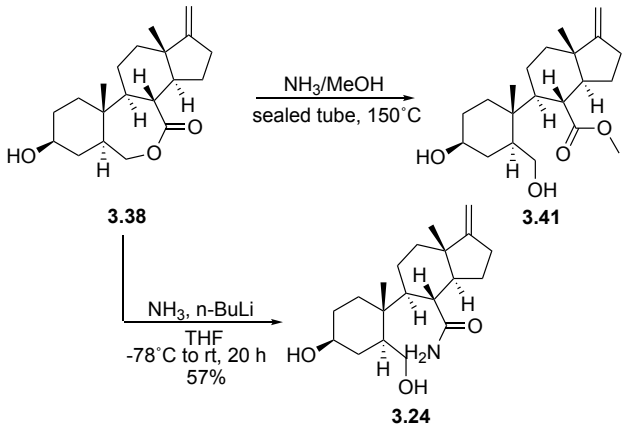

*Figure 3.11: Key Methyl Ester **3.41** [1]HNMR Peak*

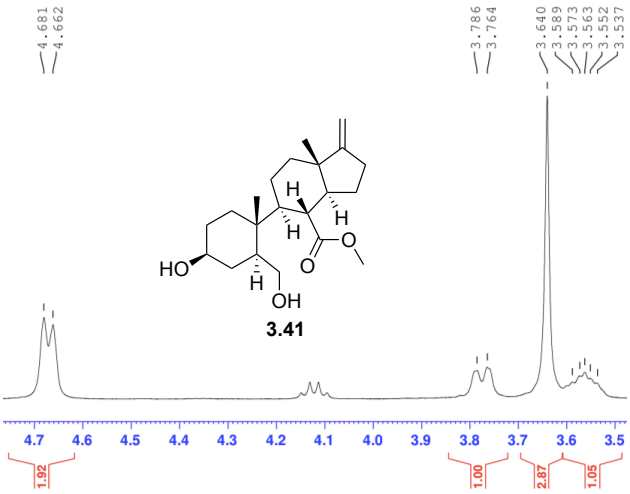

With the formation of the amide **3.24** a free alcohol at C6 is also generated. The newly formed amide intermediate **3.24** could be exposed to reducing conditions using lithium aluminum hydride in THF to give the free amine **3.42** (Scheme 3.15), with the free alcohols and alkene unaffected. Alternate methods were investigated using Red-Al as the reducing agent but a complex mixture of products formed. Salt formation using acetic acid and heat generated the final product AQX-1125 **3.6**. With this newly developed synthetic sequence the synthesis of AQX-1125 **3.6** has

been reduced from the 17 step Aquinox procedure to approximately 12 linear steps, cutting the time and cost to produce AQX-1125 **3.6**.

Scheme 3.15: Final Steps to AQX-1125 ***3.6***

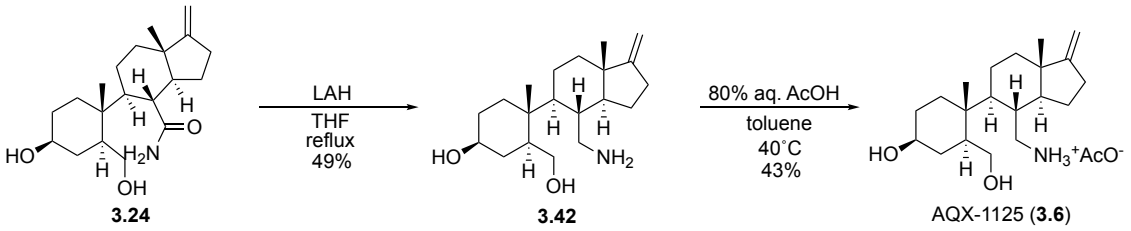

With the newly developed synthesis for AQX-1125 **3.6** in place we wished to utilize it to understand the role of the olefin functionality at the C17 position on the SHIP1 agonist activity. The synthesis of compound **3.43** (Figure 3.12) was therefore undertaken. The activity of **3.43** will be compared to the parent AQX-1125 **3.6** to determine whether or not the alkene plays a critical role in the binding to the allosteric site of SHIP1. We hope that removing this functionality will give similar if not better activity, allowing for even quicker access to an active SHIP1 agonist for future development of more active compounds.

Figure 3.12: Structure of Olefin-less Analog of AQX-1125 ***3.42***

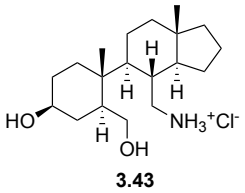

To access compound **3.43** the C17 ketone was removed from epiandrosterone. This was accomplished with a Wolff-Kishner reduction[45] on the commercially available ketone **3.7** in place of the ketal formation to remove the carbonyl functionality at the C17 position **3.44** (Scheme 3.16). With the removal of the carbonyl we avoid the protection/deprotection and Wittig reactions

necessary in the original synthesis, making the synthesis of this analog even more rapid and less complex. The synthesis then proceeds in a similar fashion to that of the newly utilized AQX-1125 **3.6** synthesis discussed above. The alcohol **3.44** is protected as the TBS ether **3.45** followed by the ruthenium catalyzed allylic oxidation to give the unsaturated ketone **3.46**. Purification again can be achieved through recrystallization as mentioned in the other route. Hydrogenation of the unsaturated ketone is then performed to yield the saturated carbonyl **3.47**.

*Scheme 3.16: Synthesis of Analogue Ketone **3.46***

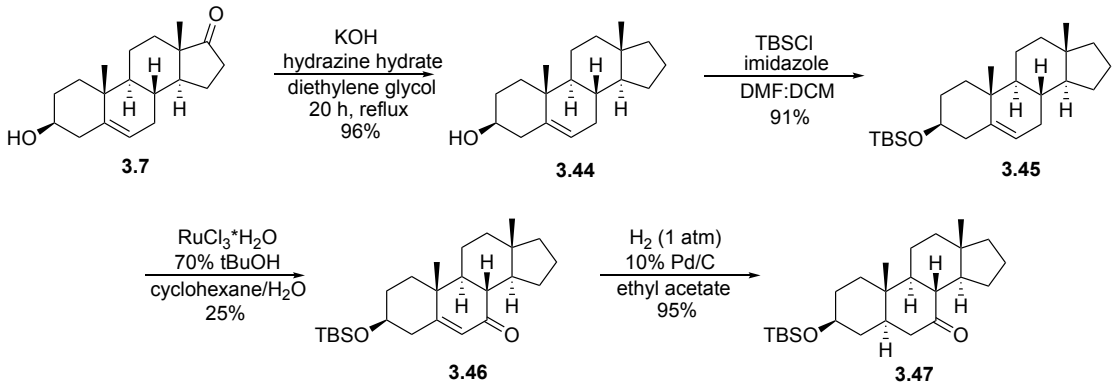

Formation of the silyl enol ether **3.48** was then accomplished utilizing TBSOTf and triethylamine (Scheme 3.17). Employing the ozonolysis reaction on **3.48** to generate the carboxylic acid intermediate **3.49** was followed by the formation of the lactone **3.50** with EDCl. Deprotection of the TBS group was then accomplished under acidic conditions to provide alcohol **3.51**.

*Scheme 3.17: Synthesis of Analog Lactone **3.51***

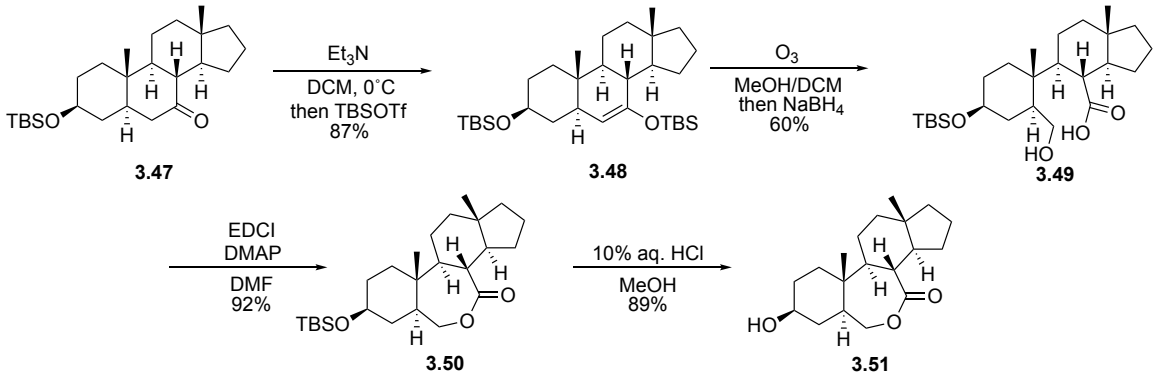

Here, the Wittig originally performed on the parent compound is not necessary so amide formation can be directly engaged to generate amide **3.52** by addition of ammonia to the lactone (Scheme 3.18). Amide reduction to the free amine **3.53** using LAH reducing conditions similar to the parent synthesis followed by HCl salt formation generates the analog **3.43**.

*Scheme 3.18: Final steps to AQX-1125 Analog **3.44***

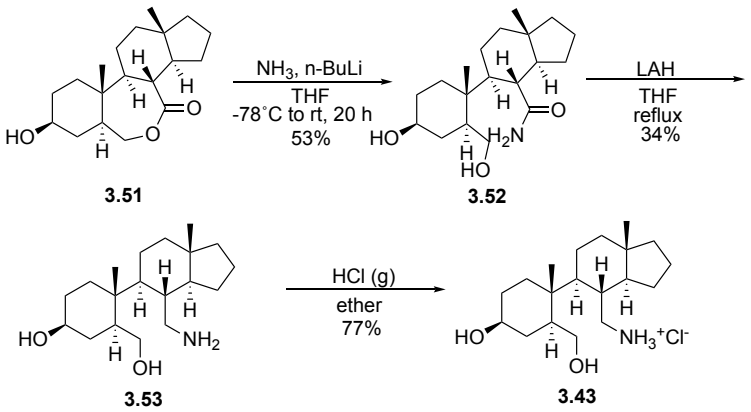

3.4 Conclusion

The development of a new 12 step synthetic sequence to AQX-1125 **3.6** from dehydroepiandrosterone **3.7** (Figure 3.13) will allow for quicker access to material for future comparison of AQX-1125 to other potential agonists of SHIP1. The new synthesis utilizes the

ozonolysis reaction of a silyl enol ether to generate the key alcohol and carboxylic acid functionalities. The different oxidation states on carbons 5 and 6 allow for a more selective and controlled synthesis. Access to the lactone pseudo-protecting group allows for formation of the exocyclic olefin and quick formation of the amide to generate the open B ring with the necessary oxygen and nitrogen functionality in their correct localities. Reduction and salt formation then complete the synthesis of the final product AQX-1125 **3.6**. This synthetic sequence was also applied to form the analog **3.43** lacking the olefin at C17 to evaluate some key structure-activity relationships of the allosteric site and the necessity of the alkene.

Figure 3.13: Synthesis of AQX-1125 ***3.6*** *and Analog* ***3.43*** *from Dehydroepiandrosterone* ***3.7***

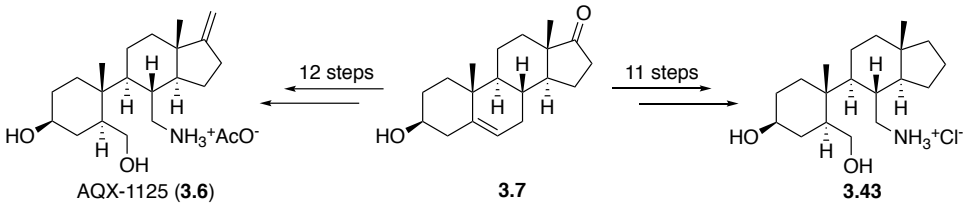

In addition to preparing material for a standard for testing new SHIP1 agonists, structure-activity relationships of the AQX-1125 intermediates and analogs (**3.24**, **3.31**, **3.38**, **3.51**, **3.52**, **3.54**) will be evaluated for SHIP1 agonist activity (Figure 3.14). These analogs will be tested initially in the malachite green phosphatase assay to determine if any of these molecules can increase SHIP1 phosphatase activity and act as SHIP1 agonists. This will help further our investigation into the development of more selective and active modulators.

Figure 3.14: SHIP1 Agonist AQX-1125 ***3.6*** *Analogs for Evaluation*

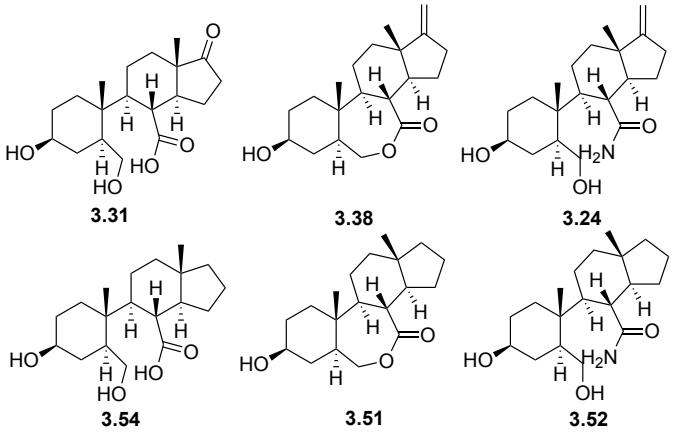

3.5 Experimental

General Methods: All anhydrous reactions were run under a positive pressure of argon. All syringes, needles, and reaction flasks required for anhydrous reactions were dried in an oven and cooled under an N_2 atmosphere or in a desiccator. Dichloromethane and THF were dried by passage through an alumina column following the method of Grubbs (Pangborn, A. B.; Giardello, M. A.; Grubbs, R. H.; Rosen, R. K.; Timmers, F. J. *Organometallics* **1996,** *15*, 1518). All other reagents and solvents were purchased from commercial sources and used without further purification.

Analysis and Purification. Analytical thin layer chromatography (TLC) was performed on precoated glass backed plates (silica gel 60 F_{254}; 0.25 mm thickness). The TLC plates were visualized by UV illumination and by staining. Solvents for chromatography are listed as volume:volume ratios. Flash column chromatography was carried out on silica gel (40-63 μm). Melting points were recorded using an electrothermal melting point apparatus and are uncorrected. Elemental analyses were performed on an elemental analyzer with a thermal conductivity detector and 2 meter GC column maintained at 50 °C.

Identity. Proton (^{1}H NMR) and carbon (^{13}C NMR) nuclear magnetic resonance spectra were recorded at 300 or 400 MHz and 75 or 100 MHz respectively. The chemical shifts are given in parts per million (ppm) on the delta (δ) scale. Coupling constants are reported in hertz (Hz). The spectra were recorded in solutions of deuterated chloroform ($CDCl_3$), with residual chloroform (δ 7.26 ppm for ^{1}H NMR, δ 77.23 ppm for ^{13}C NMR) or tetramethylsilane (δ 0.00 for ^{1}H NMR, δ 0.00 ppm for ^{13}C NMR) as the internal reference. Data are reported as follows: (s = singlet; d = doublet; t = triplet; q = quartet; p = pentet; dd = doublet of doublets; dt = doublet of triplets; td = triplet of doublets; tt = triplet of triplets; qd = quartet of doublets; ddd = doublet of doublet of

doublets; br s = broad singlet). Where applicable, the number of protons attached to the corresponding carbon atom was determined by DEPT 135 NMR. Infrared (IR) spectra were obtained as thin films on NaCl plates by dissolving the compound in CH_2Cl_2 followed by evaporation or as KBr pellets.

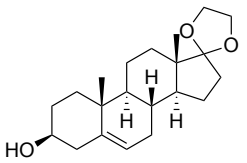

3.8

5-androsten-3β-ol-17-ethylene ketal (3.8)[29]

Lit. Ref: Raymond, J.; Han, K.; Zhou, Y.; He, Y.; Noren, B.; Yee, J. G. K., Indene derivatives as pharmaceutical agents. *Patent. Appl.* **2004**; EP2277848A1.

Trans-dehydroandrosterone **3.7** (5.00 g, 17.3 mmol) was added to a 250 mL flame dried round-bottom flask. 50 mL of dry Benzene was added to suspend the trans-dehydroandrosterone. p-Toluene sulfonic acid monohydrate (0.114 g, 0.66 mmol) and ethylene glycol (5.00 mL) were then added to the reaction. This reaction mixture was heated to reflux under a Dean-Stark trap for 24 hours under argon. The mixture was removed from heat and allowed to cool to rt. The excess benzene was removed under reduced pressure. The remaining contents were diluted with diethyl ether (150 mL) and washed successively with saturated $NaHCO_3$ (2 x 75 mL) and saturated NaCl (75 mL). The organic layer was dried with anhydrous $NaSO_4$ and removed under reduced pressure. Purification by column chromatography (30% EtOAc /70% Hexane) to yield ketal **3.8** as a white colored solid (0.553 g, 96%). TLC R_f = 0.28 (30% EtOAc /70% Hexane); ^1H NMR (400 MHz, $CDCl_3$) δ 5.40-5.32 (m, 1H), 3.99–3.81 (m, 4H), 3.61–3.46 (m, 1H), 2.39–2.17 (m, 2H), 2.09–1.95

(m, 2H), 1.92–1.76 (m, 3H), 1.75–1.66 (m, 1H), 1.65-1.57 (m, 2H), 1.51-1.36 (m, 6H), 1.34-1.18 (m, 2H), 1.13-1.03 (m, 1H), 1.01 (s, 3H), 0.99-0.93 (m, 1H), 0.86 (s, 3H).

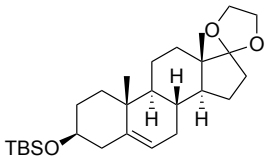

3.9

5-androsten-3β-ol-17-ethylene ketal tert-butyldimethylsilyl ether (3.9)[29]

Lit. Ref: Raymond, J.; Han, K.; Zhou, Y.; He, Y.; Noren, B.; Yee, J. G. K., Indene derivatives as pharmaceutical agents. *Patent. Appl.* **2004**; EP2277848A1.

Ketal **3.8** (5.00 g, 15.0 mmol) was added to a 250 mL flame dried round-bottom flask. 27 mL of DMF and 27 mL of CH_2Cl_2 were added to dissolve the ketal. Imidazole (2.51 g, 36.8 mmol) and tert-butyl (chloro) dimethyl silane (3.51 g, 23.3 mmol) were then added to the reaction. This reaction mixture was allowed to stir at rt for 20 hours under argon. The excess solvent was removed under reduced pressure. The remaining contents were diluted with diethyl ether (150 mL) and washed successively with 5% aqueous HCl (2 x 75 mL), saturated $NaHCO_3$ (2 x 75 mL) and saturated NaCl (75 mL). The organic layer was dried with anhydrous $NaSO_4$ and removed under reduced pressure to yield silyl ether **3.9** as a white colored solid (6.53 g, 97%). TLC R_f = 0.74 (30% EtOAc /70% Hexane); ^{1}H NMR (300 MHz, $CDCl_3$) δ 5.36 – 5.34 (m, 1H), 3.95 – 3.84 (m, 4H), 3.57 – 3.49 (m, 1H), 2.33 – 2.04 (m, 2H), 2.02 – 1.88 (m, 2H), 1.87-1.66 (m, 4H), 1.65-1.58 (m, 2H), 1.52-1.37 (m, 4H), 1.35-1.19 (m, 2H), 1.01 (s, 3H), 0.89 (s, 9H), 0.86 (s, 3H), 0.06 (s, 6H).

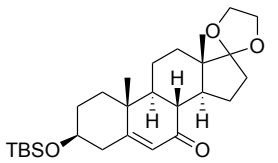

3.10

5-androsten-7-one-3β-ol 17-ethylene ketal tert-butyldimethylsilyl ether (3.10)[29,38]

Lit. Ref: Raymond, J.; Han, K.; Zhou, Y.; He, Y.; Noren, B.; Yee, J. G. K., Indene derivatives as pharmaceutical agents. *Patent. Appl.* **2004**; EP2277848A1.

Burgoyne, D. L.; Shen, Y.; Langlands, J. M.; Rogers, C.; Chau, J. H.-L.; Piers, E.; Salari, H., 6,7-oxygenated steroids and uses related thereto. *Patent. Appl.* **1997**; 6,046,185.

tert-butyldimethylsilyl ether **3.9** (6.00 g, 13.4 mmol) was added to a 100 mL flame dried round-bottom flask. 24 mL of cyclohexane and 3 mL of water were added to dissolve the ketal. Ruthenium trichloride hydrate (0.022 g, catalytic) was then added to the reaction. 70% tert-Butyl hydroperoxide (14 mL) was added drop wise. This reaction stirred for 22 hours under argon. Then an additional 5 mL of cyclohexane was added and this was allowed to stir at rt for 2 additional hours. The mixture was diluted with ethyl acetate (100 mL) and filtered over celite. The collected organic was washed successively with 25% aqueous Na_2SO_4 (2 x 75 mL) and saturated NaCl (75 mL). The organic layer was dried with anhydrous $NaSO_4$ and removed under reduced pressure. Recrystallized using hot EtoAc to yield the unsaturated ketone **3.10** as a pale-yellow solid (3.34 g, 54%). ^{1}H NMR (400 MHz, $CDCl_3$) δ 5.67 (s, 1 H), 3.99 – 3.74 (m, 4 H), 3.68 – 3.55 (m, 1 H), 2.56 – 2.433(m, 3H), 2.29 – 2.18 (m, 1H), 2.06-1.88 (m, 2H), 1.87-1.73 (m, 3H), 1.69-1.59 (m, 2H), 1.54-1.38 (m, 5H), 1.23-1.15 (m, 4H), 0.89 (s, 9 H), 0.86 (s, 3 H), 0.06 (s, 6 H).

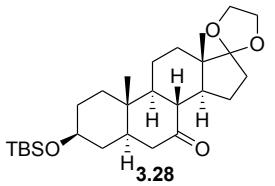

5-androsta-7-one-3β-ol 17-ethylene ketal tert-butyldimethylsilyl ether (3.28)[29]

Lit. Ref: Raymond, J.; Han, K.; Zhou, Y.; He, Y.; Noren, B.; Yee, J. G. K., Indene derivatives as pharmaceutical agents. *Patent. Appl.* **2004**; EP2277848A1.

To a 250 mL flame-dried round bottom flask, **3.10** (2.13g, 4.62 mmol) was dissolved in 140 mL of ethyl acetate. 10% Pd/C (0.45 g) was added to the reaction. This was placed under vacuum until bubbling occurred in which a hydrogen balloon was added. This was allowed to stir for 20 hours at rt. The reaction was then filtered through celite, rinsing with ethyl acetate. This was concentrated under reduced pressure to yield ketone **3.28** as a white colored solid (2.02 g, 94%). mp = 198.5 – 200.3°C; TLC R_f = 0.30 (10% EtOAc /90% Hexane); IR (neat) 2979, 1698, 1091 cm^{-1}; ^1H NMR (400 MHz, $CDCl_3$) 3.98 – 3.78 (m, 4 H), 3.61 – 3.48 (m, 1 H), 2.33 (t, *J* = 11.8 Hz, 2 H), 2.29-2.18 (m, 1H), 2.04-1.88 (m, 2H), 1.87-1.72 (m, 2H), 1.76-1.67 (m, 2H), 1.66-1.61 (m, 1H), 1.51-1.45 (m, 5H), 1.39-1.18 (m, 4H), 1.07 (s, 3H), 1.05-0.92 (m, 1H), 0.87 (s, 9H), 0.83 (s, 3H), 0.04 (s, 6H).

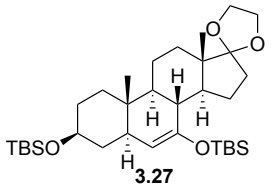

5-androsta -7 – tert-butyldimethyl oxysilane -3β-ol 17-ethylene ketal tert-butyldimethylsilyl enol ether (3.27)[34]

Lit. Ref: Duffy, B., Thioetherification and etherification utilizing trichloroacetimidates under thermal conditions & progress towards an efficient synthesis of AQX-1125. *Syracuse University Dissertations, Department of Chemistry* **2016**.

3.28 (3.30 g, 7.13 mmol) was dissolved in 65 mL of CH_2Cl_2. 38.8 mL of triethylamine (278 mmol) was added drop wise at 0˚C. This was allowed to stir at this temperature for 15 minutes. Tert-butyldimethylsilyl trifluoromethane sulfonate (9.80 mL, 42.8 mmol) was then added to the reaction, maintaining 0°C. This reaction mixture was placed at rt and allowed to stir for 20 hours under argon. This was re-placed at 0°C and isopropyl alcohol (1.1 mL) was then added. The reaction was then diluted with DCM (150 mL) and saturated $NaHCO_3$ (150 mL). The aqueous phase was extracted 2x with DCM (100 mL) collected and the organic layer was washed with saturated $NaHCO_3$ (1x 100 mL) and brine (1x 100 mL) (This was concentrated under reduced pressure and subjected to column chromatography (10% EtOAc/90% Hexane) to yield silyl enol ether **3.27** as a pale-yellowish solid (3.40 g, 83%). TLC R_f = 0.58 (10% EtOAc /90% Hexane); ^{1}H NMR (300 MHz, $CDCl_3$) δ 4.38 (s, 1H), 3.96 – 3.79 (m, 4H), 3.58 (septet, J = 15.5, 10.5, 5.25 Hz, 1H), 1.99 – 1.85 (m, 4 H), 1.82 – 1.57 (m, 6 H), 1.52 – 1.45 (m, 2 H), 1.42 – 1.15 (m, 4 H), 1.12-0.97 (m, 2H), 0.91 (s, 9 H), 0.88 (s, 12 H), 0.74 (s, 3H), 0.12 (d, J = 4.35 Hz, 6H), 0.06 (s, 6H).

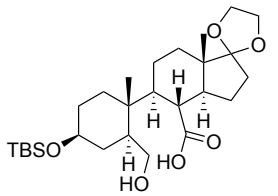

3.26

(7a'S)-5'-((1R,4S)-4-((tert-butyldimethylsilyl)oxy)-2-(hydroxymethyl)-1-methylcyclohexyl)-7a'-methyloctahydrospiro[[1,3]dioxolane-2,1'-indene]-4'-carboxylic acid (3.26)

tert-butyldimethylsilyl enol ether **3.27** (4.41 g, 7.64 mmol) was dissolved in methanol (122 mL) and CH_2Cl_2 (122 mL) and was treated with excess O_3 at -78 °C until the solution turned blue. After purging with argon, the blue color dissipated. This was placed at 0 °C and sodium borohydride (0.866 g, 22.9 mmol) was added. This was then placed at rt and allowed to stir for 20 hours. Another equivalent of $NaBH_4$ was added and stirred for another 3 hours. After the solvent was evaporated on a rotary evaporator, DCM was added (150 mL) and water (150 mL). The solution foamed from the evolution of H_2 gas so 10% HCl was added drop wise until the foaming stopped. The DCM layer was removed and the aqueous layer extracted with CH_2Cl_2 (3 × 75 mL). The organic layers were collected and washed with saturated NaCl (2x 75 mL). The organic layer was dried with anhydrous $NaSO_4$ and removed under reduced pressure. Purification by column chromatography (10% MeOH/ 90% DCM)) to yield acid **3.26** as a cream colored solid (2.39 g, 63%). TLC R_f = 0.47 (10% MeOH/ 90% DCM); IR (neat) 3404, 1701, 1053 cm^{-1}; 1H NMR (400 MHz, $CDCl_3$) δ 6.57 (bs, 1 H), 3.96-3.77 (m, 4 H), 3.71 (d, *J* = 9.2 Hz, 1 H), 3.49 (bs, 1 H), 3.25 (s, 1 H), 2.29 (t, *J* = 10.8 Hz, 1 H), 2.04-1.82 (m, 4 H), 1.81-1.69 (m, 3 H), 1.68-1.45 (m, 4 H), 1.44-1.18 (m, 7 H), 0.86 (s, 12 H), 0.79 (s, 3 H) 0.03 (s, 6 H). ^{13}C NMR (100 MHz, $CDCl_3$): δ 182.1, 118.7, 71.0, 65.2, 64.6, 62.6, 47.5, 45.5, 45.1, 45.0, 42.1, 37.7, 34.4, 33.6, 31.2, 29.9, 25.9,

22.9, 20.7, 19.3, 18.2, 13.7, -4.58. Anal calcd for $C_{18}H_{28}O_4$: C, 65.28; H, 9.74 Found: C, 65.25; H, 9.76.

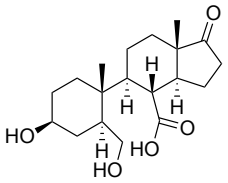

3.31

(7a*S*)-5-[(1*R*,4*S*)-4-Hydroxy-2-(hydroxymethyl)-1-methylcyclohexyl]-7a-methyl-1-oxo-2,3,3a,4,5,6,7,7a-octahydroindene-4-carboxylic acid (3.31)

Carboxylic acid **3.26** (0.399 g, 0.803 mmol) was dissolved in tetrahydrofuran (13 mL) and was treated with 4.5 mL of 10% HCl at rt for 5h. The solution was extracted with EtoAc (3 × 100 mL). The organic layers were collected and washed with saturated NaCl (2x 50 mL). The organic layer was dried with anhydrous $NaSO_4$ and removed under reduced pressure to yield acid **3.31** as a white solid (0.090 g, 33%). TLC R_f = 0.20 (10% MeOH/ 90% DCM); IR (neat) 3441, 3293, 1736, 1696 cm^{-1}; 1H NMR (400 MHz, MeOD) δ 3.73 (d, *J* = 8.00 Hz, 1H), 3.59-3.40 (m, 1H), 3.13 (t, *J* = 10.3 Hz, 1H), 2.58-2.42 (m, 2H), 2.22-2.06 (m, 2H), 2.05-1.96 (m, 1H), 1.95-1.88 (m, 1H), 1.87-1.74 (m, 5H), 1.74-1.62 (m, 2H), 1.61-1.47 (m, 2H), 1.44-1.25 (m, 3H), 0.96 (s, 3H), 0.88 (s, 3H). ^{13}C NMR (100 MHz, MeOD): δ 178.0, 69.3, 60.55, 48.2, 46.1, 45.8, 44.1, 41.8, 36.9, 34.4, 33.0, 29.8, 29.5, 21.5, 19.8, 17.8, 11.6. Anal calcd for $C_{18}H_{28}O_4$: C, 67.43; H, 8.94 Found: C, 67.77; H, 8.62.

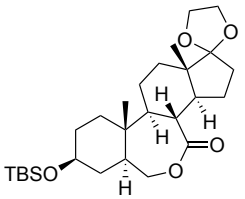

3.37

(2'*R*,5'*S*,16'*S*)-5'-((tert-butyldimethylsilyl)oxy)-2',16'-dimethylspiro[1,3-dioxolane-2,15'-[9]oxatetracyclo[9.7.0.0^{2,7}.0^{12,16}]octadecan]-10'-lactone (3.37)

Carboxylic acid **3.26** (1.50 g, 3.02 mmol) was dissolved in 45 mL of DCM followed by the addition of DMAP (0.074 g, 0.604 mmol). After stirring for 5 minutes, 1-Ethyl-3-(3-dimethylaminopropyl)carbodiimide (0.94 g, 6.04 mmol) was then added. This was allowed to stir at rt for 24 hours. The reaction was diluted with DCM (150 mL) and washed successively with saturated $NaHCO_3$ (2 x 50 mL), 10% aqueous HCl (2 x 50 mL), and saturated NaCl (50 mL). The organic layer was dried with anhydrous $MgSO_4$ and solvent removed under reduced pressure. This was subjected to column chromatography using (20% EtOAc/80% Hexane) to yield lactone **3.37** as a white solid (1.39 g, 96%). TLC R_f = 0.51 (20% EtOAc /80% Hexane); IR (neat) 2979, 1716, 1095, 1044 cm^{-1}; ^{1}H NMR (300 MHz, $CDCl_3$) δ 4.31 (dd, *J* = 12.7, 7.2 Hz, 1 H), 3.98-3.80 (m, 4H), 3.60 (d, *J* = 12.7 Hz, 1H), 3.57-3.46 (m, 1H), 2.56 (t, *J* = 2.6 Hz, 1H), 2.36-2.21 (m, 1H), 2.00, 1.76 (m, 5H), 1.75-1.58 (m, 3H), 1.56-1.48 (m, 2H), 1.45-1.24 (m, 5H), 1.23-1.05 (m, 2H), 1.03 (s, 3H), 0.88 (s, 9H), 0.84 (s, 3H), 0.05 (s, 6H). ^{13}C NMR (100 MHz, $CDCl_3$): δ 176.5, 118.7, 70.9, 68.2, 65.2, 64.5, 47.2, 46.6, 44.7, 44.0, 42.3, 38.6, 37.6, 37.3, 33.5, 31.3, 29.2, 25.7, 24.7, 21.5, 18.2, 12.9, 13.4, -4.67.

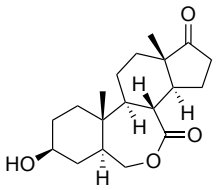

3.25

((2*R*,5*S*,16*S*)-5-Hydroxy-2,16-dimethyl-9-oxatetracyclo[9.7.0.0^{2,7}.0^{12,16}]octadecane-15-one-10'-lactone (3.25)

Lactone **3.37** (0.200 g, 0.42 mmol) was added to a 100 mL flame dried round-bottom flask. 10.0 mL of methanol and 6.0 mL of 10% aq. HCl was added to the solution. This reaction mixture was allowed to stir at rt for 4 hours. The reaction mixture was concentrated down and the contents diluted with ethyl acetate (75 mL) and water (75 mL). The aqueous phase was extracted with ethyl acetate (2 x 50 mL) and the collected organic was washed successively with saturated aqueous $NaHCO_3$ (2 x 50 mL) and NaCl (1 x 50 mL), The organic layer was dried with anhydrous $MgSO_4$ and removed under reduced pressure. Purification through column chromatography (80% EtOAc: 20% Hexane) yielded lactone **3.25** as a white colored solid (0.11 g, 82%). TLC R_f = 0.34 (100% EtOAc); IR (neat) 3478, 1739, 1697 $^{cm-1}$;1H NMR (400 MHz, $CDCl_3$) δ 4.37 (q, *J* = 7.75 Hz, 1 H), 3.67 (d, *J* = 13.1 Hz, 1 H), 3.64-3.56 (m, 1 H), 2.74 (t, *J* = 10.7 Hz, 1 H), 2.51-2.38 (m, 1 H), 2.26-2.00 (m, 3 H), 1.99-1.86 (m, 2 H), 1.86-1.72 (m, 3H), 1.66-1.56 (m, 2H), 1.51-1.22 (m, 6H), 1.13-1.02 (m, 1H), 1.06 (s, 3H), 0.86 (s, 3H); ^{13}C NMR (100 MHz, $CDCl_3$): δ 219.7, 175.9, 69.9, 68.3, 47.2, 46.4, 45.9, 45.8, 41.6, 38.8, 37.2, 36.6, 35.4, 30.7, 30.3, 23.6, 21.6, 13.2, 13.2; Anal calcd for $C_{18}H_{28}O_4$: C, 71.22; H, 8.81 Found: C, 71.26; H, 8.64.

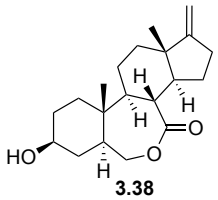

3.38

(2*R*,5*S*,16*S*)-5-Hydroxy-2,16-dimethyl-15-methylene-9-oxatetracyclo[9.7.0.0^{2,7}.0^{12,16}]octadecan-10'-lactone (3.38)

Methyltriphenylphosphonium bromide (10.6 g, 29.6 mmol) was suspended in 56.7 mL dry THF under argon. n-BuLi (11.2 mL, 2.5 M) was added dropwise to the stirring solution to generate the ylide. This stirred for 15 min at rt before being heated to 40˚C. Lactone **3.25** (1.90 g, 5.93 mmol) was dissolved in 69.3 mL dry THF and added dropwise into the stirring reaction. The temperature was increased to reflux and the reaction ran for 24 h. The flask was then removed from heat and allowed to cool down to rt before water (75.0 mL) was added dropwise to quench the reaction. Ethyl acetate (100 mL) and water (75.0 mL) was added and the layers separated. The aqueous phase was extracted with ethyl acetate (2 x 100 mL). The collected organic phase was washed with water (2 x 75 mL) followed by brine (2 x 75100 mL). The organic layer was dried with anhydrous $MgSO_4$ and removed under reduced pressure. This was subjected to column chromatography using (25% Et_2O/75% EtOAc) to yield lactone **3.38** as a white solid (1.28 g, 67%). TLC R_f = 0.51 (100% EtOAc); IR (neat) 3510, 3074, 1701, 1675 cm^{-1}; ^{1}H NMR (400 MHz, $CDCl_3$) δ 4.65 (d, *J* = 8.93 Hz, 2 H), 4.33 (dd, *J* = 12.6, 7.80 Hz, 1 H), 3.68-3.50 (m, 2 H), 2.59 (t, *J* = 10.8 Hz, 1 H), 2.52-2.39 (m, 1 H), 2.37-2.22 (m, 1 H), 2.11-2.01 (m, 1H), 1.98-1.67 (m, 7 H), 1.66-1.46 (m, 2 H), 1.44-1.12 (m, 5 H), 1.03 (s, 4 H), 0.76 (s, 3 H). ^{13}C NMR (100 MHz, $CDCl_3$): δ 177.0, 160.0, 101.8, 69.9, 68.2, 48.4, 47.1, 46.5, 42.0, 41.7, 38.7, 37.3, 36.6, 34.2, 30.7, 28.8, 26.1, 22.0, 17.9, 13.2. Mass Spec *m/z* $C_{20}H_{30}O_3$ Exact Mass 318.2195; Observed 318.2192.

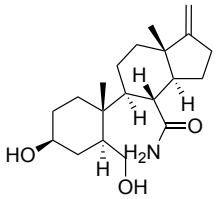

3.24

(3a*S*,4*R*,5*S*,7a*S*)-5-[(1*R*,2*S*,4*S*)-4-Hydroxy-2-(hydroxymethyl)-1-methylcyclohexyl]-7a-methyl-1-methylene-2,3,3a,4,5,6,7,7a-octahydroindene-4-carboxamide (3.24)

A solution of ammonia in THF (5.3 mL, 0.5 M) was cooled to -78˚C. n-BuLi (1.0 mL, 2.5 M) was added dropwise and allowed to stir for 30 min. Lactone **3.38** (0.169 g, 0.53 mmol) was dissolved in a solution of 2.0 mL dry THF and added dropwise into the reaction before allowing the reaction to warm to rt The reaction continued for 24 hours. The reaction was diluted with $NH_4^+Cl^-$ (50 mL) and extracted successively with EtOAc (2 x 75 mL). The collected organic was washed with saturated NaCl (2 x 50 mL). The organic layer was dried with anhydrous $MgSO_4$ and solvent removed under reduced pressure. This was subjected to column chromatography using (90% EtoAc/10% MeOH) to yield amide **3.24** as a white solid (0.101 g, 57%). TLC R_f = 0.51 (80% EtOAc /20% MeOH); ^{1}H NMR (300 MHz, CD_3OD) δ 4.69 (s, 2 H), 3.77 (dd, *J* = 10.7, 3.1 Hz, 1 H), 3.55-3.39 (m, 1 H), 3.12 (t, *J* = 10.7 Hz, 1 H), 2.59-2.46 (m, 1 H), 2.41 (t, *J* = 10.4 Hz, 1 H), 2.34-2.07 (m, 2 H), 2.03-1.95 (m, 1H), 1.94-1.74 (m, 4H), 1.73-1.55 (m, 3H), 1.54-1.30 (m, 6H), 0.97 (s, 3H), 0.84 (s, 3H). ^{13}C NMR (75MHz, $CDCl_3$): δ 180.4, 160.4, 100.9, 70.0, 60.9, 51.5, 44.6, 44.5, 42.7, 42.3, 37.4, 35.1, 33.5, 30.4, 29.9, 28.5, 24.7, 20.9, 18.3, 16.9. Anal calcd for $C_{18}H_{28}O_4$: C, 71.6; H, 9.92; N, 4.18 Found: C, 71.20; H, 9.63; N, 4.28.

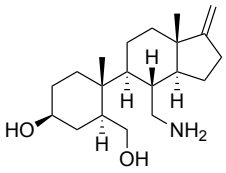

3.42

(1*S*,3*S*,4*R*)-4-[(3a*S*,4*R*,5*S*,7a*S*)-4-(aminomethyl)-7a-methyl-1-methylene-2,3,3a,4,5,6,7,7a-octahydroinden-5-yl]-3-(hydroxymethyl)-4-methylcyclohexanol (3.42)

Amide **3.24** (0.350 g, 1.25 mmol) was dissolved in 12.0 mL of THF and cooled to 0˚C. LAH (25.0 mL, 1.0M in THF) was added dropwise to the stirring solution. The temperature was increased to reflux for 20 h. The reaction was cooled to rt and diluted with THF before being cooled to 0˚C. Fieser method was used to work up the reaction. The filtered product was dried with $MgSO_4$ and concentrated down to give the crude amine. Purification through column chromatography (10% methanol: 89% EtOAc: 1% $NH_4^+OH^-$) yield the amine **3.42** as a white gum (0.164 g, 49%). TLC R_f = 0.23 (89% EtOAc /10% MeOH/ 1% NH_4OH); ^1H NMR (300 MHz, MeOD) δ 4.65 (s, 2H), 3.75(dd, *J* = 10.8, 2.17 Hz, 1H), 3.56-3.39 (m,1H), 3.25-3.00 (m, 2H), 2.74 (d, *J* = 14.4 Hz, 1H), 2.63-2.43 (m, 1H), 2.42-2.24 (m, 1H), 2.32-2.10 (m, 1H), 1.94-1.74 (m, 5H), 1.74-1.21 (m, 11H), 1.11 (s, 3H), 0.84 (s, 3H). ^{13}C NMR (100 MHz, $CDCl_3$): δ 161.2, 101.2, 70.2, 62.8, 49.9, 43.3, 41.9, 38.7, 37.1, 35.9, 34.4, 31.1, 30.7, 29.7, 29.1, 24.7, 23.2, 21.1, 18.3, 14.1.

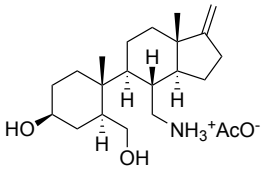

AQX-1125 (**3.6**)

(1*S*,3*S*,4*R*)-4-[(3a*S*,4*R*,5*S*,7a*S*)-4-(aminomethyl)-7a-methyl-1-methylene-2,3,3a,4,5,6,7,7a-octahydroinden-5-yl]-3-(hydroxymethyl)-4-methylcyclohexanol ammonium acetate

AQX-1125 (3.6)

Lit. Ref: Raymond, J.; Han, K.; Zhou, Y.; He, Y.; Noren, B.; Yee, J. G. K., Indene derivatives as pharmaceutical agents. *Patent. Appl.* **2004**; EP2277848A1.

Amine **3.42** (0.100 g, 0.311 mmol) was dissolved in 5.0 mL 80% Acetic acid and heated to 40˚C while stirring for 1 ½ hr. The reaction was cooled to rt before 10.0 mL toluene was added. The solution was concentrated down 3 times with toluene and the residue was washed with diethyl ether 3 times. to yield amine salt **3.6** as a white solid (0.052 g, 43%). ^{1}H NMR (300 MHz, MeOD) δ 4.69 (s, 2 H), 3.73 (dd, *J* = 11.0, 2.56 Hz, 1 H), 3.59-3.42 (m, 1 H), 3.17 (t, *J* = 10.4 Hz, 1 H), 3.06 (dd, *J* = 13.9, 2.78 Hz, 1 H), 2.69-2.50 (m, 1 H), 2.45-2.27 (m, 1 H), 2.26-2.13 (m, 1 H), 1.99-1.94 (m, 1 H), 1.93 (s, 3 H), 1.92-1.79 (m, 5 H), 1.68-1.56 (m, 2 H), 1.55-1.38 (m, 4 H), 1.37-1.21 (m, 4 H), 1.19 (s, 3 H), 0.87 (s, 3 H). ^{13}C NMR (75 MHz, MeOD): δ 160.6, 100.6, 69.6, 61.3, 49.7, 44.2, 43.4, 43.3, 41.1, 36.9, 36.7, 35.4, 33.7, 30.6, 28.6, 24.1, 22.7, 20.3, 17.2. Mass Spec *m/z* $C_{20}H_{36}NO_2$ Exact Mass 322.274056; Observed 322.274010. Anal calcd for $C_{18}H_{28}O_4$: C, 69.25; H, 10.30; N, 3.61 Found: C, 69.28; H, 10.25; N, 3.30.

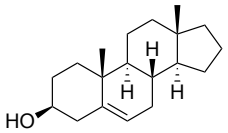

3.44

5-androsten-3β-ol (3.44)[46]

Lit. Ref: Mori, K.; Nakayama, T.; Sakuma, M., Synthesis of some analogues of blattellastanoside A, the steroidal aggregation pheromone of the German cockroach. *Bioorg. Med. Chem.* **1996,** *4*, 401-408.

KOH (4.90 g, 86.7 mmol) was added to 25 mL diethylene glycol and heated until dissolved with a heat gun. Once the solution of KOH in diethylene glycol cooled to rt dehydroepiandrosterone **3.7** (5.00 g, 17.3 mmol) and hydrazine hydrate (3.4 mL, 69.3 mmol) were added. With a reflux condenser attached the solution was heated to 245˚C and stirred continuously for 24 h. The condenser was removed and a distillate column attached to distill off diethylene glycol. The reaction was then cooled to rt and 100 mL MTBE and 100 mL brine were added and the solution stirred overnight. The aqueous phase was extracted with MTBE (10 x 60 mL). The collected organic phase was washed with brine (5 x 60 mL), dried with sodium sulfate, and concentrated down. Column chromatography (30% EtOAc/70% Hexane) yielded alcohol **3.44** as a white colored solid (4.59 g, 96%). TLC R_f = 0.24 (30% EtOAc /70% Hexane); ^{1}H NMR (400 MHz, $CDCl_3$) δ 5.39 – 5.31 (m, 1H), 3.58 – 3.48 (m, 1H), 2.39-2.13 (m, 2H), 2.06-1.97 (m, 1H), 1.90-1.79 (m, 2H), 1.78-1.71 (m, 1H), 1.70-1.63 (m, 2H), 1.62-1.59 (m, 1H), 1.54-1.51 (m, 1H), 1.50-1.47 (m, 1H), 1.46-1.37 (m, 3H), 1.31-1.05 (m, 5H), 1.02 (s, 3H), 0.99-0.84 (m, 3H), 0.72 (s, 3H). ^{13}C NMR (100 MHz, $CDCl_3$): δ 140.8, 121.7, 71.8, 54.9, 50.5, 42.3, 40.6, 40.3, 38.7, 37.4, 36.7, 32.2, 32.1, 231.7, 25.6, 21.1, 20.5, 19.4, 17.3.

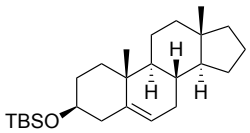

3.45

5-androsten-3β-ol- tert-butyldimethylsilyl ether (3.45)[24]

3.44 (3.64 g, 13.3 mmol) was added to a 250 mL flame dried round-bottom flask. 44 mL of DMF and 44 mL of CH_2Cl_2 were added to dissolve the ketal. Imidazole (2.21 g, 32.5 mmol) and tert-butyl (chloro) dimethyl silane (3.10 g, 20.6 mmol) were then added to the reaction. This reaction mixture was allowed to stir at rt for 20 hours under argon. The excess solvent was removed under reduced pressure. The remaining contents were diluted with diethyl ether (150 mL) and washed successively with 5% aqueous HCl (2 x 75 mL), saturated $NaHCO_3$ (2 x 75 mL) and saturated NaCl (75 mL). The organic layer was dried with anhydrous $NaSO_4$ and removed under reduced pressure to yield the silyl ether **3.45** as a white colored solid (4.67 g, 91%). TLC R_f = 0.89 (10% EtOAc/90% Hexane); IR (neat) 2952, 1091 cm^{-1}; ^1H NMR (400 MHz, $CDCl_3$) δ 5.32 (d, *J* = 5.14, 1H), 3.48 (septet, *J* = 15.8, 10.8, 4.6, 1H), 2.32 – 2.22 (m, 1H), 2.17 (ddd, *J*= 13.1, 4.9, 2.1, 1H), 2.06 – 1.96 (m, 1H), 1.82 (dt, *J* = 16.7, 3.5, 1H), 1.78 – 1.62 (m, 4H), 1.61-1.55 (m, 2H), 1.54-1.50 (m. 2H), 1.49-1.34 (m, 3H), 1.27-1.10 (m, 3H), 1.09-1.03 (dd, *J* = 13.6, 3.7, 1H), 1.01 (s, 3H), 0.99-0.92 (dd, *J* = 11.8, 5.2, 1H), 0.91-0.86 (m, 10H), 0.71 (s, 3H), 0.06 (s, 6H). ^{13}C NMR (100 MHz, $CDCl_3$): δ 141.6, 121.2, 72.7, 54.9, 50.54, 42.85, 40.6, 40.3, 38.8, 37.5, 36.8, 32.3, 32.2, 32.1, 25.9, 25.6, 21.1, 20.5, 19.5, 18.3, 17.3, -4.6.

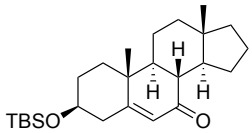

3.46

5-androsten-7-one-3β-ol tert-butyldimethylsilyl ether (3.46)[24]

tert-butyldimethylsilyl ether **3.46** (9.02 g, 23.2 mmol) was added to a 250 mL flame dried round-bottom flask. 37 mL of cyclohexane and 4.5 mL of water were added to dissolve the ketal. Ruthenium trichloride hydrate (0.039 g, catalytic) was then added to the reaction. 70% tert-Butyl hydroperoxide (26 mL) was added drop wise. This reaction stirred for 24 hours under argon. Then an additional 5 mL of cyclohexane was added and this was allowed to stir at rt for 2 additional hours. The mixture was diluted with ethyl acetate (100 mL) and washed successively with 25% aqueous Na_2SO_4 (2 x 60 mL) and saturated NaCl (60 mL). The organic layer was dried with anhydrous $NaSO_4$ and removed under reduced pressure. Recrystallization by hot EtOAc to yield the unsaturated ketone **3.46** as a pale-yellow solid (2.35 g, 25%). TLC R_f = 0.89 (100% Hexane); IR (neat) 2938, 1656, 1058 cm^{-1}; ^1H NMR (400 MHz, $CDCl_3$) δ 5.68 (d, *J* = 1.34, 1H), 3.60 (septet, *J* = 15.8, 10.3, 5.5, 1H), 2.57-2.31 (m, 3H), 2.19 (t, *J* = 11.2, 1H), 1.92 (dt, *J* = 13.7, 3.52, 1H), 1.86-1.78 (m, 1H), 1.74 (dt, *J* = 13.0, 3.26, 1H), 1.69-1.64 (m, 2H), 1.63-1.57 (m, 3H), 1.55-1.47 (m, 2H), 1.46-1.28 (m, 2H), 1.27-1.21 (m, 1H), 1.19 (s, 3H), 1.17-1.07 (m, 2H), 0.89 (s, 9H), 0.72 (s, 3H), 0.66 (s, 6H). ^{13}C NMR (100 MHz, $CDCl_3$): δ 202.3, 166.2, 125.7, 71.3, 50.3, 48.1, 45.8, 42.6, 41.3, 39.2, 38.5, 37.8, 36.5, 31.8, 27.6, 25.8, 21.3, 20.6, 18.1, 17.3, 17.2, -4.64. Anal calcd for $C_{25}H_{42}O_2Si$: C, 74.57; H, 10.51 Found: C, 74.62; H, 10.42.

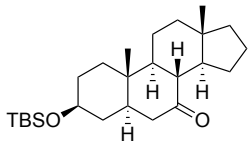

3.47

5-androsta-7-one-3β-ol tert-butyldimethylsilyl ether (3.47)

To a 250 mL flame-dried round bottom flask, tert-butyldimethylsilyl ether **3.46** (2.25g, 5.58 mmol) was dissolved in 154 mL of ethyl acetate. 10% Pd/C (0.26 g) was added to the reaction. This was placed under vacuum until bubbling occurred in which a hydrogen balloon was added. This was allowed to stir for 20 hours at rt. The reaction was then filtered through celite, rinsing with ethyl acetate. This was concentrated under reduced pressure to yield ketone **3.47** as a white colored solid (2.14 g, 95%). mp = 198.5 – 200.3°C; TLC R_f = 0.67 (15% EtOAc /85% Hexane); IR (neat) 2929, 1707, 1096 cm^{-1}; ^1H NMR (400 MHz, $CDCl_3$) 3.55 (septet, *J* = 15.1, 10.5, 4.17, 1H), 2.44-2.18 (m, 3H), 2.07-1.95 (m, 1H), 1.78-1.68 (m, 3H), 1.67-1.57 (m, 3H), 1.54-1.37 (m, 6H), 1.36-1.21(m, 2H), 1.20-1.10 (m, 2H), 1.08 (s, 3H), 1.07-0.92 (m, 2H), 0.88 (s, 9H), 0.68 (s, 3H) 0.04 (s, 6H). ^{13}C NMR (100 MHz, $CDCl_3$): δ 212.3, 71.5, 55.8, 50.4, 47.0, 46.9, 46.1, 40.8, 39.4, 38.5, 37.8, 36.3, 36.1, 31.6, 26.3, 25.9, 21.9, 20.6, 18.2, 17.4, 11.9, -4.63. Anal calcd for $C_{25}H_{44}O_2Si$: C, 74.20; H, 10.96 Found: C, 74.08; H, 10.84.

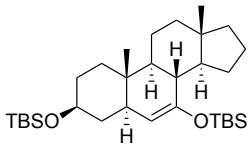

3.48

5-androsta -7 – tert-butyldimethyl oxysilane -3β-ol tert-butyldimethylsilyl ether (3.48)

Ketone **3.47** (0.76 g, 1.87 mmol) was dissolved in 15.3 mL of CH_2Cl_2. 10.2 mL of triethylamine (74.0 mmol) was added drop wise at 0˚C. This was allowed to stir at this temperature for 15 minutes. tert-butyldimethylsilyl trifluoromethane sulfonate (2.15 mL, 9.37 mmol) was then added to the reaction, maintaining 0°C. This reaction mixture was placed at rt and allowed to stir for 20 hours under argon. This was re-placed at 0°C and isopropyl alcohol (1.1 mL) was then added. The reaction was then diluted with DCM (100 mL) and saturated $NaHCO_3$ (50 mL). The aqueous phase was extracted 2x with DCM (100 mL) collected and the organic layer was washed with saturated $NaHCO_3$ (1x 50 mL) and brine (1x 50 mL) and dried over $MgSO_4$ (This was concentrated under reduced pressure and subjected to column chromatography (1% EtOAc/99% Hexane) to yield silyl enol ether **3.48** as a pale yellowish-white colored solid (0.85 g, 87%). TLC R_f = 0.58 (1% EtOAc /99% Hexane); IR (neat) 2928, 1082 cm^{-1}; ^1H NMR (400 MHz, $CDCl_3$) δ 4.41 (s, 1H), 3.59 (septet, *J* = 15.3, 10.5, 5.27, 1H), 1.98-1.78 (m, 3H), 1.77-1.68 (m, 2H), 1.67-1.56 (m, 3H), 1.52-1.45 (m, 2H), 1.44-1.18 (m, 5H), 1.17-0.96 (m, 5H), 0.92 (s, 9H), 0.89 (s, 9H), 0.74 (s, 3H), 0.73 (s, 3H), 0.12 (d, *J* = 8.13, 6H), 0.06 (d, *J* = 0.82, 6H). ^{13}C NMR (100 MHz, $CDCl_3$): δ 152.6, 108.5, 72.2, 54.6, 52.4, 43.6, 42.5, 42.3, 39.8, 39.4, 34.3, 31.9, 28.5, 26.1, 25.9, 21.5, 29.2, 18.2, 18.1, 11.3, -3.89, -4.22, -4.57. Mass Spec *m/z* $C_{31}H_{58}O_2Si_2$ Exact Mass 518.3975; Observed 518.3975.

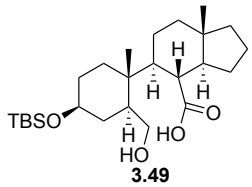

3.49

(7a*S*)-5-[(1*R*,4*S*)-4-((tert-butyldimethylsilyl)oxy)-1-methylcyclohexyl]-7a-methylperhydro-1*H*-indene-4-carboxylic acid (3.49)

Silyl enol ether, **3.48** (1.30 g, 2.50 mmol) was dissolved in methanol (40 mL) and CH_2Cl_2 (40 mL) and was treated with excess O_3 at -78 °C until the solution turned blue. After purging with argon, the blue color dissipated. This was placed at 0 °C and sodium borohydride (0.38 g, 10.0 mmol) was added. This was then placed at rt and allowed to stir for 20 hours. Another equivalent of $NaBH_4$ was added and stirred for another 3 hours. After the solvent was evaporated on a rotary evaporator, DCM was added (50 mL) and water (50 mL). The DCM layer was removed and the aqueous layer extracted with CH_2Cl_2 (3 × 50 mL). The organic layers were collected and washed with saturated NaCl (2x 50 mL). The organic layer was dried with anhydrous $MgSO_4$ and removed under reduced pressure to yield acid **3.49** as a cream colored foam (0.659 g, 60%). TLC R_f = 0.49 (10% MeOH/ 90% DCM). 1H NMR (400 MHz, $CDCl_3$) δ 3.75 (dd, *J* = 10.9, 3.1 Hz, 1H), 3.53 (bs, 1H), 3.31 (t, *J* = 8.9 Hz, 1H), 2.29 (t, *J* = 10.9 Hz, 1H), 2.07-1.89 (m, 3H), 1.80-1.73 (m, 3H), 1.71-1.65 (m, 3H), 1.64-1.57 (m, 3H), 1.52-1.46 (m, 2H), 1.42 (t, *J* = 7.1 Hz, 3H), 1.35-1.18 (m, 5H), 0.90 (s, 3H), 0.89 (s, 9H), 0.71 (s, 3H), 0.06 (s, 6H).

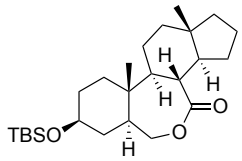

3.50

(2*R*,5*S*,16*S*)-5-((tert-butyldimethylsilyl)oxy)-2,16-dimethyl-9-oxatetracyclo[9.7.0.0^{2,7}.0^{12,16}]octadecan-10-lactone (3.50)

Carboxylic acid **3.49** (0.27 g, 0.62 mmol) was dissolved in 9.2 mL of DCM followed by the addition of DMAP (0.015 g, 0.12 mmol). After stirring for 5 minutes, 1-Ethyl-3-(3-dimethylaminopropyl)carbodiimide (0.19 g, 1.23 mmol) was then added. This was allowed to stir at rt for 24 hours. The reaction was diluted with DCM (75 mL) and washed successively with saturated $NaHCO_3$ (2 x 25 mL), 10% aqueous HCl (2 x 25 mL), and saturated Aq. NaCl (25 mL). The organic layer was dried with anhydrous $MgSO_4$ and solvent removed under reduced pressure. This was subjected to column chromatography using (20% EtOAc/80% Hexane) to yield protected lactone **3.50** as a white solid (0.24 g, 92%). TLC R_f = 0.42 (10% EtOAc /90% Hexane); IR (neat) 2972, 1732, 1093 cm^{-1}; ^{1}H NMR (400 MHz, $CDCl_3$) δ 4.33 (dd, *J* = 12.9, 7.54, 1H), 3.61 (d, *J* = 12.8, 1H), 3.53 (septet, *J* = 15.4, 10.7, 4.72, 1H), 2.50 (t, *J* = 11.1, 1H), 1.95-1.83 (m, 2H), 1.82-1.74 (m, 2H), 1.73-1.60 (m, 5H), 1.52-1.15 (m, 8H), 1.12-1.05 (m, 1H), 1.03 (s, 3H), 1.02-0.97 (m, 1H), 0.87 (s, 9H), 0.71 (s, 3H), 0.05 (s,6H). ^{13}C NMR (100 MHz, $CDCl_3$): δ 177.6, 70.9, 68.3, 48.5, 47.4, 46.7, 41.9, 39.8, 38.7, 38.7, 37.5, 37.3, 37.2, 31.3, 27.5, 25.9, 22.2, 19.9, 18.2, 16.7, 13.3, -4.7. Mass Spec *m/z* $C_{25}H_{44}O_3Si$ Exact Mass 420.3060; Observed 420.3054.

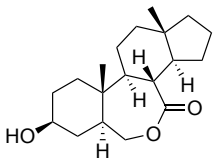

3.51

(2*R*,5*S*,16*S*)-5-Hydroxy-2,16-dimethyl-9-oxatetracyclo[9.7.0.0^{2,7}.0^{12,16}]octadecan-10-one (3.51)

Lactone **3.50** (0.19 g, 0.19 mmol) was added to a 100 mL flame dried round-bottom flask. 5.0 mL of methanol and 6.0 mL of 10% aq. HCl was added to reaction. The reaction mixture was allowed to stir at rt for 4 hours. The solution was concentrated down and the contents diluted with ethyl acetate (50 mL) and water (50 mL). The aqueous phase was extracted with ethyl acetate (2 x 50 mL) and the collected organic was washed successively with saturated aqueous $NaHCO_3$ (2 x 25 mL) and NaCl (1 x 25 mL), The organic layer was dried with anhydrous $MgSO_4$ and removed under reduced pressure. Purification through column chromatography (80% EtOAc: 20% Hexane) yielded lactone **3.51** as a white colored solid (0.123 g, 89%). TLC R_f = 0.42 (50% EtOAc /50% Hexane); IR (neat) 3276, 1733, 1032 cm^{-1}; ^{1}H NMR (300 MHz, $CDCl_3$) δ 4.34 (dd, *J* = 12.9, 7.9 Hz, 1 H), 3.67-3.49 (m, 2 H), (t, *J* = 10.6 Hz, 1 H), 1.96-1.86 (m, 2 H), 1.85-1.72 (m, 5 H), 1.70-1.58 (m, 4H), 1.53-1.41 (m, 2H), 1.40-1.13 (m, 6H), 1.13-1.10 (m, 1H), 1.07 (s, 3 H), 0.71 (s, 3 H). Mass Spec *m/z* $C_{19}H_{30}O_3$ Exact Mass 306.2195; Observed 306.2195.

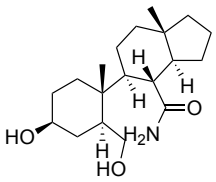

3.52

(7a*S*)-5-[(1*R*,4*S*)-4-Hydroxy-2-(hydroxymethyl)-1-methylcyclohexyl]-7a-methylperhydro-1*H*-indene-4-carboxamide (3.52)

A solution of ammonia in THF (9.12 mL, 0.5 M) was cooled to -78˚C. n-BuLi (1.7 mL, 2.5 M) was added dropwise and allowed to stir for 30 min. Lactone **3.51** (0.350 g, 1.14 mmol) was dissolved in a solution of 5.0 mL THF and added dropwise into the reaction before allowing the reaction to warm to rt The reaction continued for 24 hours. The reaction was diluted with $NH_4^+Cl^-$ (20 mL) and extracted successively with EtOAc (2 x 25 mL) The collected organic was washed with saturated NaCl (25 mL). The organic layer was dried with anhydrous $MgSO_4$ and solvent removed under reduced pressure. This was subjected to column chromatography using (90% EtoAc/10% MeOH) to yield amide **3.52** as a white solid (0.195 g, 53%). TLC R_f = 0.45 (90% ethyl acetate /10% methanol); IR (neat) 3333, 3196, 1651 cm^{-1}; ^1H NMR (300 MHz, CD_3OD) δ 5.29 (d, *J* = 40.7 Hz, 2H), 3.87-3.73 (m, 1H), 3.66-3.51 (m, 1H), 3.29 (t, *J* = 9.25 Hz, 1H), 2.18-2.05 (m, 2H), 2.04-1.95 (m, 1H), 1.89-1.74 (m, 3H), 1.73-1.56 (m, 6H), 1.50-1.37 (m, 6H), 1.36-1.30 (m, 2H), 1.23-1.13 (m, 2H), 0.96 (s, 3H), 0.69 (s, 3H). ^{13}C NMR (75 MHz, $CDCl_3$): δ 180.9, 69.9, 61.1, 51.2, 44.7, 44.6, 42.4, 39.8, 39.4, 38.1, 37.4, 33.5, 30.4, 29.9, 26.1, 21.0, 19.6, 18.3, 15.8. Mass Spec *m/z* $C_{19}H_{33}NO_3$ Exact Mass 323.2460; Observed 323.2456.

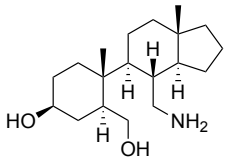

3.53

(1*S*,4*R*)-4-[(7a*S*)-4-(aminomethyl)-7a-methylperhydro-1*H*-inden-5-yl]-3-(hydroxymethyl)-4-methylcyclohexanol (3.53)

Amide **3.52** (0.100 g, 0.31 mmol) was dissolved in 3.0 mL of dry THF and cooled to 0˚C. LAH (4.64 mL, 1.0 M in THF) was added dropwise to the stirring solution. The temperature was increased to reflux for 20 h. The reaction was cooled to rt and diluted with THF before being cooled to 0˚C. Fieser method was used to work up the reaction. The filtered product was dried with $MgSO_4$ and concentrated down to give the crude amine. Purification through column chromatography (9% methanol: 90% EtOAc: 1% $NH_4^+OH^-$) yield amine **3.53** as a clear oil (0.033 g, 34%). ^{1}H NMR (300 MHz, MeOD) δ 3.75 (dd, *J* = 10.8, 1.8 Hz, 1H), 3.47 (septet, *J* = 15.2, 10.9, 4.4 Hz, 1H), 3.22-3.08 (m, 2H), 2.75 (d, *J* = 14.4 Hz, 1H), 2.17 (d, *J* = 12.4 Hz, 1H), 1.86-1.67 (m, 8H), 1.60-1.54 (m, 3H), 1.51-1.42 (m, 3H), 1.37-1.30 (m, 3H), 1.28-1.18 (m, 3H), 1.11 (s, 3H), 0.79 (s, 3H). ^{13}C NMR (100 MHz, $CDCl_3$): δ 697, 61.4, 49.7, 44.0, 43.4, 41.8, 40.2, 40.0, 38.8, 38.7, 36.6, 33.8, 30.7, 25.6, 22.9, 20.0, 19.8, 16.2, 16.1.

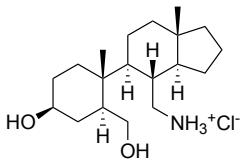

3.43

(1*S*,4*R*)-4-[(7a*S*)-4-(Aminomethyl)-7a-methylperhydro-1*H*-inden-5-yl]-3-(hydroxymethyl)-4-methylcyclohexanol ammonium chloride (3.43)

Amine **3.53** (0.022 g, 0.071mmol) was dissolved in 3.0 mL Et_2O. The reaction was stirred at rt while HCl (g) was bubbled into the solution. The solution was concentrated and the residue was washed with diethyl ether (2x) to yield the amine salt **3.43** as a white solid (0.019 g, 77%). ^{1}H NMR (300 MHz, MeOD) δ 3.71 (dd, *J* = 11.0, 2.5 Hz, 1H), 3.45-3.35 (m, 1H), 3.21-3.00 (m, 2H), 2.15 (d, *J* = 12.3 Hz, 1H), 1.91-1.67 (m, 8H), 1.63-1.38 (m, 6H), 1.36-1.18 (m, 6H), 1.07 (s, 3H), 0.78 (s, 3H). ^{13}C NMR (75 MHz, MeOD): δ 70.8, 62.6, 51.0, 45.6, 46.6, 43.0, 41.6, 41.2, 39.6, 38.1, 37.4, 35.0, 31.9, 26.8, 24.0, 21.9, 21.1, 17.3, 15.4. Mass Spec *m/z* $C_{19}H_{35}NO_2$ Exact Mass 309.2668; Observed 309.2671.

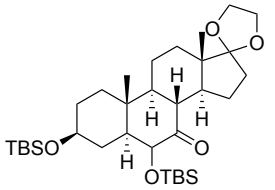

3.29

5-androsta-7-one-3β,6-diol 17-ethylene ketal 3,6-di-tert-butyldimethylsilyl ether (3.29)

A solution of tert-butyldimethylsilyl enol ether **3.27** (0.100 g, 0.17 mmol) in 3.0 mL DCM was cooled to 0˚C. $NaHCO_3$ (0.122g, 1.45 mmol) was added and the reaction stirred 10 min before the addition of *m*-CPBA (0.45g, 0.260 mmol) in 3.0 mL DCM dropwise. After stirring for 30 min, aq. $Na_2S_2O_4$ was added and the organic layer was collected. Organic was extracted with $NaHCO_3$ (1x 25 mL) and brine (1x 25 mL), dried with Na_2SO_4 and concentrated under reduced pressure. **3.29** (0.059 g, 57%). ^{1}H NMR (400 MHz, $CDCl_3$) δ 3.94-3.74 (m, 5H), 3.47 (septet, J = 15.3, 10.3, 4.6 Hz, 1H), 2.30-2.18 (m, 2H), 2.17-2.07 (m, 1H), 1.98-1.84 (m, 2H), 1.83-1.75 (m, 1H), 1.72-1.64 (m, 3H), 1.52-1.22 (m, 7H), 1.13-1.02 (m, 5H), 0.86 (s, 9H), 0.83 (S, 9H), 0.79 (s, 3H), 0.07- -0.08 (m, 12H). ^{13}C NMR (100 MHz, $CDCl_3$): δ 209.3, 118.7, 71.7, 65.2, 64.5, 55.0, 53.4, 48.2, 45.5, 42.9, 36.9, 36.4, 34.1, 33.9, 31.4, 29.7, 25.9, 25.8, 23.5, 21.3, 18.7, 18.3, 14.4, 13.3, -4.42.

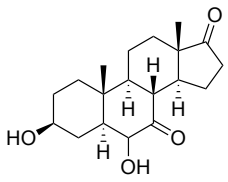

3.30

5-androsta-7,17-dione-3β,6-diol (3.30)

3.29 (0.059 g, 0.10 mmol) was dissolved in 2.0 mL dioxane and 2.0 mL MeOH and 10% aq. HCl was added dropwise. Reaction stirred for 2 h before EtOAc was added. Organic was washed with aq. NaCl (1 x 10 mL) and dried over Na_2SO_4. Concentration under reduced pressure (0.023 g, 72%). ^{1}H NMR (400 MHz, $CDCl_3$) δ 3.96 (d, *J* = 11.7 Hz, 1H), 3.68-3.41 (m, 2H), 2.69-2.55 (m, 2H), 2.47 (dd, *J* = 19.4, 8.8 Hz, 1H), 2.32-2.08 (m, 2H), 2.03-1.70 (m, 6H), 1.63-1.40 (m, 4H), 1.33-1.21 (m, 2H), 1.16 (s, 3H), 1.13-0.97 (m, 1H), 0.88 (s, 3H). ^{13}C NMR (100 MHz, $CDCl_3$): δ 211.0, 75.2, 70.5, 55.7, 54.3, 47.3, 47.0, 44.3, 36.5, 36.3, 36.2, 35.5, 33.4, 30.7, 30.6, 22..5, 21.2, 13.8, 13.1.

3.6 References

1. Workman, P.; Clarke, P. A.; Guillard, S.; Raynaud, F. I., Drugging the PI3 kinome. *Nat. Biotechnol.* **2006**, *24*, 794-796.

2. Simon, J. A., Using isoform-specific inhibitors to target lipid kinases. *Cell* **2006**, *125*, 647-649.

3. Hennessy, B. T.; Smith, D. L.; Ram, P. T.; Lu, Y.; Mills, G. B., Exploiting the PI3K/AKT pathway for cancer drug discovery. *Nat. Rev. Drug Discov.* **2005**, *4*, 988-1004.

4. Knight, Z. A.; Gonzalez, B.; Feldman, M. E.; Zunder, E. R.; Goldenberg, D. D.; Williams, O.; Loewith, R.; Stokoe, D.; Balla, A.; Toth, B.; Balla, T.; Weiss, W.; Williams, R.; Shokat, K. M., A pharmacological map of the PI3-K family dfines a role for p110alpha in insulin signaling. *Cell.* **2006**, *125*, 733-747.

5. Hazen, A. L.; Smith, M. J.; Desponts, C.; Winter, O.; Moser, K.; Kerr, W. G., SHIP is required for a functional hematopoietic stem cell niche. *Blood* **2009**, *113*, 2924-2933.

6. Kerr, W. G.; Heller, M.; Herzenberg, L. A., Analysis of lipopolysaccharide-response genes in B-lineage cells demonstrates that they can have differentiation stage-restricted expression and contain SH2 domains. *Proc. Natl. Acad. Sci. USA.* **1996**, *93*, 3947-3952.

7. Damen, J. E.; Liu, L.; Rosten, P.; Humphries, R. K.; Jefferson, A. B.; Majerus, P. W.; Krystal, G., The 145-kDa protein induced to associate with the Shc by multiple cytokines is an inositol tetraphosphate and phosphatidylinositol 3,4,5- trisphosphate 5-phosphatase. *Proc. Natl. Acad. Sci. USA.***1996**, *93*, 1689-1693.

8. Lioubin, M. N.; Algate, P. A.; Tsai, S.; Carlberg, K.; Aebersold, R.; Rohchneider, L. R., p150Ship, a signal transduction molecule with inositol polyphosphate-5-phosphatase activity. *Genes & Dev.* **1996**, *10*, 1084-1095.

9. Zippo, A.; De Robertis, A.; Bardelli, M.; Galvagni, F.; Oliviero, S., Identification of F1K-1 target genes in vasculogenesis: Pim-1 is required for endothelial and mural cell differentiation in vitro. *Blood* **2004**, *103*, 4536-4544.

10. Tu, Z.; Ninos, J. M.; Ma, Z.; Wang, J.; Lemos, M. P.; Desponts, C.; Ghansah, T.; Howson, J. M.; Kerr, W. G., Embryonic and hematopoietic stem cells express a novel SH2-contaning inositol 5'-phosphatase isoform that partners with the Brb2 adapter protein. *Blood* **2001**, *98*, 2028-2038.

11. Fuhler, G. M.; Brooks, R.; Toms, B.; Iyer, S.; Gengo, E. A.; Park, M. Y.; Gumbleton, M.; Viernes, D. R.; Chisholm, J. D.; Kerr, W. G., Therapeutic potential of SH2 domain-containing inositol-5′-phosphatase 1 (SHIP1)and SHIP2 inhibition in cancer. *Mol. Med.* **2012**, *18*, 65-75.

12. Hamilton, M. J.; Ho, V. W.; Kuroda, E.; Ruschmann, J.; Antignano, F.; Lam, V.; Krystal, G., Role of SHIP in cancer. *Exp. Hematol.* **2011**, *39*, 2-13.

13. Catimel, B.; Yin, M.-X.; Schieber, C.; Condron, M.; Patsiouras, H.; Catimel, J.; Robinson, D. E. J. E.; Wong, L. S.-M.; Nice, E. C.; Holmes, A. B.; Burgess, A. W., PI(3,4,5)P3 Interactome. *J. Proteome Res.* **2009**, *8*, 3712-3726.

14. Viernes, D. R.; Choi, L. B.; Kerr, W. G.; Chisholm, J. D., Discovery and development of small molecule SHIP phosphatase modulators. *Med. Res. Rev.* **2013**, *34*, 795-824.

15. Kerr, W. G., Dual functions for SHIP in immunity and cancer. *Ann. NY. Acad. Sci.* **2011**, *1217*, 1-17.

16. Brooks, R.; Fuhler, G. M.; Iyer, S.; Smith, M. J.; Park, M.; Paraiso, K.; Engelman, R. W.; G, K. W., SHIP1 inhibition increases immunoregulatory capacity and triggers apoptosis of hematopoietic cancer cells. *J. Immunol.* **2010**, *184*, 3582-3589.

17. Clement, S.; Krause, U.; Desmedt, F.; Tanti, J. F.; Behrends, J.; Pesesse, X.; Sasaki, T.; Penninger, J.; Doherty, M.; Malaisse, W.; Dumont, J. E.; Le Marchand-Brustel, Y.; Erneux, C.; Hue, L.; Schurmans, S., The lipid phosphatase SHIP2 controls insulin sensitivity. *Nature* **2001**, *409*, 92-97.

18. Sleeman, M. W.; Wortley, K. E.; Lai, K. M.; Gowen, L. C.; Kintner, J.; Kline, W. O.; Garcia, K.; Stitt, T. N.; Yancopoulos, G. D.; Wiegand, S. J.; Glass, D. J., Absence of the lipid phosphatase SHIP2 confers resistance to dietary obesity. *Nat. Med.***2005**, *11*, 199-205.

19. Kerr, W. G.; Park, M. Y.; Maubert, M.; Engelman, R. W., SHIP deficiency causes Crohn's disease-like ileitis. *Gut.* **2011**, *60*, 177-188.

20. Ong, C.; Ming-Lum, A.; Nodwell, M.; Ghanipour, A.; Yang, L.; Williams, D.; Kim, J.; Demirjian, L.; Qasimi, P.; Ruschmann, J.; Cao, L.; Ma, K.; Chung, S.; Duronio, V.; Andersen, R.; Krystal, G.; Mui, A., Small-molecule agonists of SHIP1 inhibit the phosphoinositide 3-kinase pathway in hematopoietic cells. *Blood* **2007**, *110*, 1942-1949.

21. Goclik, E.; Konig, G. M.; Wright, A. D.; Kaminsky, R., Pelorol from the tropical marine sponge Dacty- lospongia elegans. *J. Nat. Prod.* **2000**, *63*, 1150–1152.

22. Kwak, J. H.; Schmitz, F. J.; Kelly, M., Sesquiterpene quinols/quinones from the Micronesian sponge Petrosaspongia metachromia. *J. Nat. Prod.* **2000**, *63*, 1153-1156.

23. Yang, L.; Williams, D.; Mui, A.; Ong, C.; Krystal, R.; Andersen, R., Synthesis of pelorol and analogues: activators of inositol 5-phosphatase SHIP. *Org. Lett.* **2005**, *7*, 1073-1076.

24. Meimetis, L. G.; Nodwell, M.; Yang, L.; Wang, X.; Wu, J.; Harwig, C.; Stenton, G. R.; MacKenzie, L. F.; MacRury, T.; Patrick, B. O.; Ming-Lum, A.; Ong, C. J.; Krystal, G.;

Mui, A.; Andersen, R. J., Synthesis of SHIP1-activating analogs of the sponge meroterpenoid pelorol. *Eur. J. Org. Chem.* **2012**, *2012*, 5195-5207.

25. Vlahos, C. J.; Matter, W. F.; Hui, K. Y.; Brown, R. F., A specific inhibitor of phosphatidylinositol 3-kinase, 2-(4-morpholinyl)-8-phenyl-4H-1-benzopyran-4-one (LY294002). *J. Biol. Chem.* **1994**, *269*, 5241-5248.

26. Sly, L. M.; Rauh, M. J.; Kalesnikoff, J.; Song, C. H.; Krystal, G., LPS-induced upregulation of SHIP1 is essential for endotoxin tolerance. *Immunity* **2004**, *21*, 227-239.

27. Shen, Y.; Burgoyne, D. L., Efficient synthesis of IPL576,092: A novel anti-asthma agent. *J. Org. Chem* **2002**, *67*, 3909-3910.

28. Stenton, G.; Mackenzie, L.; Tam, P.; Cross, J.; Harwig, C.; Raymond, J.; Toews, J.; Wu, J.; Ogden, N.; MacRury, T.; Szabo, C., Characterization of AQX-1125, a small molecule SHIP1 activator Part 1. Effects on inflammatory cell activation and chemotaxi in vitro and pharmocokinetic characterization in vivo. *Br. J. Pharmacol.* **2013**, *168*, 1506-1518.

29. Raymond, J.; Han, K.; Zhou, Y.; He, Y.; Noren, B.; Yee, J. G. K., Indene derivatives as pharmaceutical agents. *Patent. Appl.* **2004**; EP2277848A1.

30. Stenton, G.; Mackenzie, L.; Tam, P.; Cross, J.; Harwig, C.; Raymond, J.; Toews, J.; Chernoff, D.; MacRury, T.; Szabo, C., Characterization of AQX-1125, a small-molecule SHIP1 activator. Part 2. Efficacy studies in allergic and pulmonary inflammation models in vivo . *Br. J. Pharmacol.* **2013**, *168*, 1519-1529.

31. Globe Newswire. Vancouver, British Columbia. Aquinoxs AQX 1125 flunks mid stage study for patients with atopic dermatitis. Nov. 2, **2015**. http://www.biospace.com/News/aquinoxs-aqx-1125-flunks-mid-stage-study-for/397505/

32. Aquinox Pharmaceuticals. Vancouver, British Columbia. Aquinox announces update on development program for AQX-1125 following meeting with FDA. Jan. 11, **2016**. http://investor.aqxpharma.com/news-releases/news-release-details/aquinox-announces-update-development-program-aqx-1125-following

33. Luche, J. L., Lanthanides in organic chemistry. 1. Selective 1,2 reductions of conjugated ketones. *J. Am. Chem. Soc.* **1978,** *100*, 2226-2227.

34. Duffy, B., Thioetherification and etherification utilizing trichloroacetimidates under thermal conditions & progress towards an fficient synthesis of AQX-1125. *Syracuse University Dissertations, Department of Chemistry* **2016**.

35. Saz-Leal, P.; Del Fresno, C.; Brandi, P.; Martinez-Cano, S.; Dungan, O. M.; Chisholm, J. D.; Kerr, W. G.; Sancho, D., Targeting SHIP-1 in myeloid cells enhances trained immunity and boosts response toinfection. *Cell Rep.* **2018**, *25*, 1118-1126.

36. Hoekstra, E.; Das, A.; Willemsen, M.; Swets, M.; Kuppen, P. J. K.; van der Woude, C. J.; Bruno, M. J.; Shah, J. P.; ten Hagen, T.; Chisholm, J. D.; Kerr, W. G.; Peppelenbosch, M. P.; Fuhler, G. M., Lipid phosphatase SHIP2 functions as oncogene in colorectal cancer by regulating PKB activation. *Oncotarget.* **2016**, *7*, 73525-73540.

37. Russo, C. M.; Adhikari, A. A.; Wallach, D. R.; Fernandes, S.; Balch, A. N.; Kerr, W. G.; Chisholm, J. D., Synthesis and initial evaluation of quinoline-based inhibitors of the SH2-containing inositol 5′-phosphatase (SHIP). *Bioorg. Med. Chem. Lett.* **2015**, *25*, 5344-5348.

38. Burgoyne, D. L.; Shen, Y.; Langlands, J. M.; Rogers, C.; Chau, J. H.-L.; Piers, E.; Salari, H., 6,7-oxygenated steroids and uses related thereto. *Patent. Appl.* **1997**; 6,046,185.

39. Ricco, C.; Revial, G.; Ferroud, C.; Hennebert, O.; Morfin, R., Synthesis of 7β-hydroxy-epiandrosterone. *Steroids* **2011**, *76*, 28-30.

40. Zhang, H.; M, S. R.; Phoenix, S.; Deslongchamps, P., Total synthesis of ouabagenin and ouabain. *Angew. Chem. Int. Ed.* **2008**, *47*, 1272-1275.

41. Rubottom, G. M.; Vazquez, M. A.; Pelegrina, D. R., Peracid oxidation of trimethylsilyl enol ethers: A facile α-hydroxylation procedure. *Tetrahedron Lett.* **1974**, *15*, 4319-4322.

42. Adhikari, A. A.; Shah, J. P.; Howard, K. T.; Russo, C. M.; Wallach, D. R.; Linaburg, M. R.; Chisholm, J. D., Convenient formation of diphenylmethyl esters using diphenylmethyl trichloroacetimidate. *Synlett.* **2014**, *25*, 283-287.

43. Neises, B.; Steglich, W., Esterification of carboxylic acids with dicyclohexylcarbodiimide/4-dimethylaminopyridine: tert-Butyl ethyl fumarate. *Org. Synth.* **1985**, *63*, 183.

44. Howard, K. T., "Convenient etherification using trichloroacetimidates and synthesis of aminosteroid SHIP inhibitors". *Syracuse University Dissertations, Department of Chemistry* **2016**.

45. Norden, S.; Bender, M.; Rullkotter, J.; Christoffers, J., Androstanes with modified carbon skeletons. *Eur. J. Org. Chem.* **2011**, 4543-4550.

46. Mori, K.; Nakayama, T.; Sakuma, M., Synthesis of some analogues of blattellastanoside A, the steroidal aggregation pheromone of the German cockroach. *Bioorg. Med. Chem.* **1996**, *4*, 401-408.

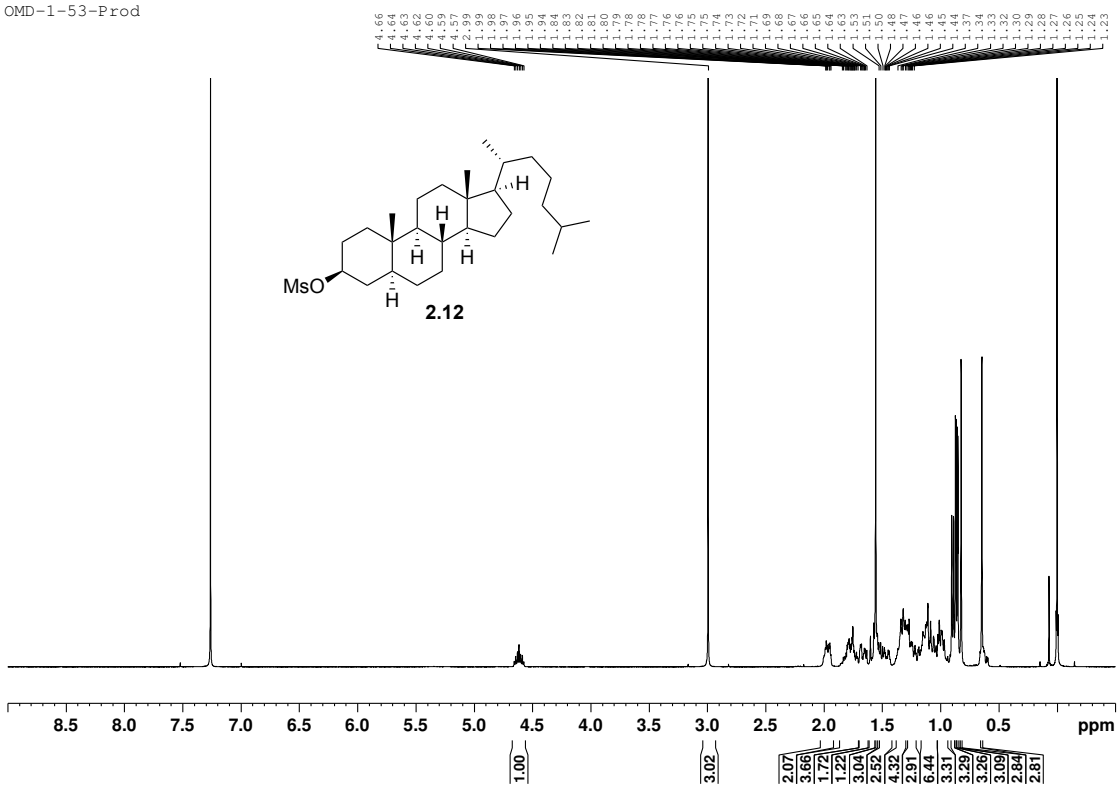
OMD-1-53-Prod
MsO
H
2.12
8.5 8.0 7.5 7.0 6.5 6.0 5.5 5.0 4.5 4.0 3.5 3.0 2.5 2.0 1.5 1.0 0.5 ppm
1.00
3.02
2.07 3.66 1.72 1.22 3.04 2.52 4.32 2.91 6.44 3.31 3.29 3.26 3.09 2.84 2.81

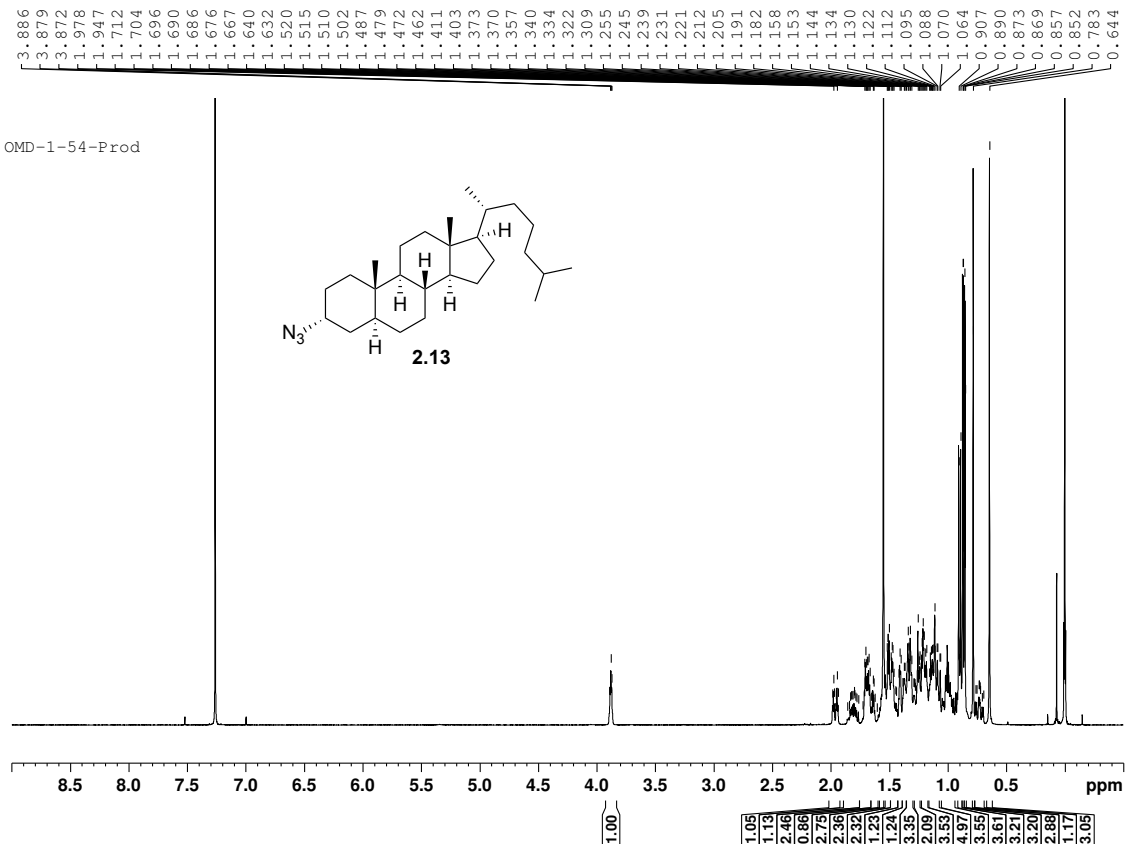
OMD-1-54-Prod
2.13
ppm

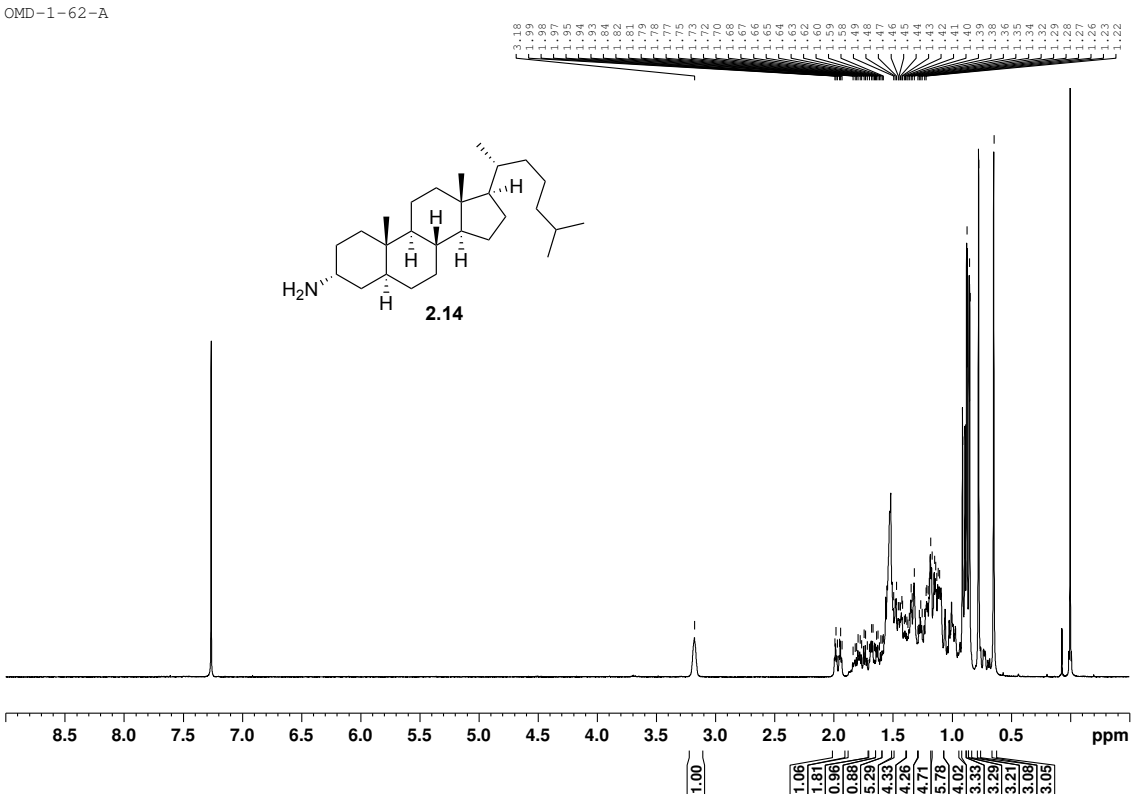
OMD-1-62-A
3.18 1.99 1.98 1.97 1.95 1.94 1.93 1.84 1.82 1.81 1.79 1.78 1.77 1.75 1.73 1.72 1.70 1.68 1.67 1.66 1.65 1.64 1.63 1.62 1.60 1.59 1.58 1.49 1.48 1.47 1.46 1.45 1.44 1.43 1.42 1.41 1.40 1.39 1.38 1.36 1.35 1.34 1.32 1.29 1.28 1.27 1.26 1.23 1.22
H
H
H
H
H2N
H
2.14
8.5 8.0 7.5 7.0 6.5 6.0 5.5 5.0 4.5 4.0 3.5 3.0 2.5 2.0 1.5 1.0 0.5 ppm
1.00
1.06 1.81 0.96 0.88 5.29 4.33 4.26 4.71 5.78 4.02 3.33 3.29 3.21 3.08 3.05

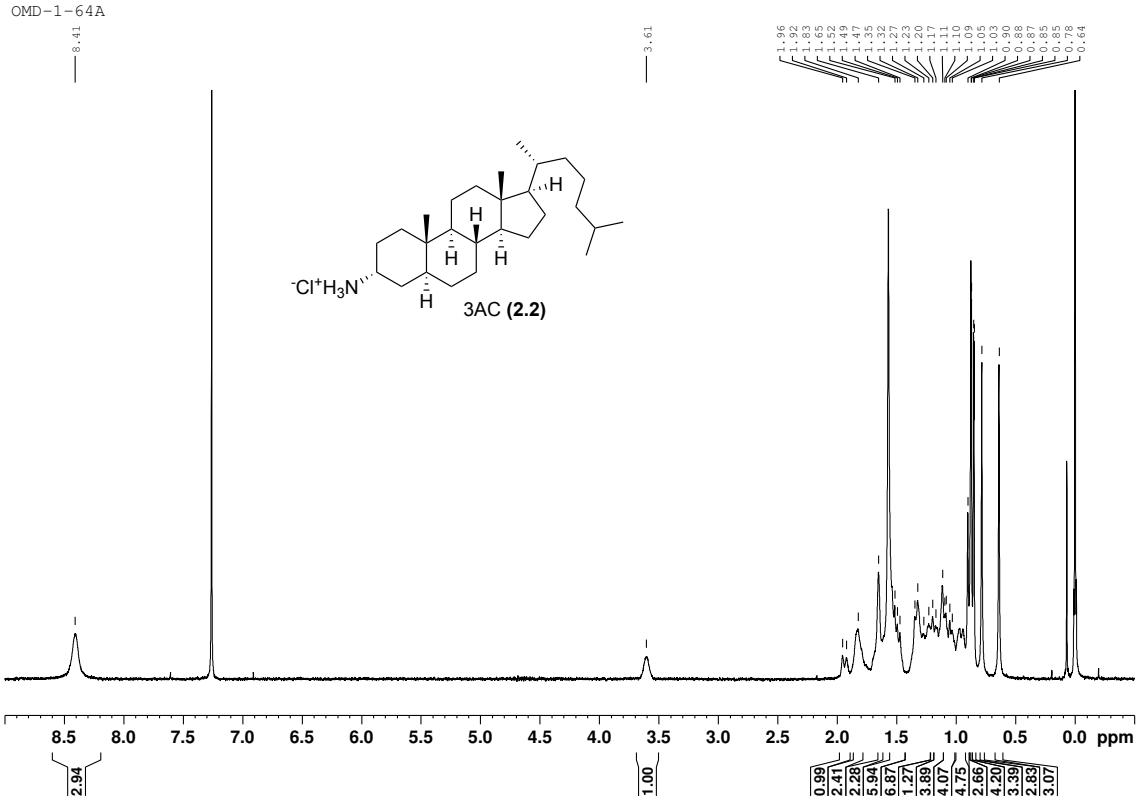
OMD-1-64A
8.41
3.61
1.96
1.92
1.83
1.65
1.52
1.49
1.47
1.35
1.32
1.27
1.23
1.20
1.17
1.11
1.10
1.09
1.05
1.03
0.90
0.88
0.87
0.85
0.78
0.64
H
H
H
H
$^{-}Cl^{+}H_3N$
H
3AC (2.2)
8.5
8.0
7.5
7.0
6.5
6.0
5.5
5.0
4.5
4.0
3.5
3.0
2.5
2.0
1.5
1.0
0.5
0.0
ppm
2.94
1.00
0.99
2.41
2.28
5.94
6.87
1.27
3.89
4.07
4.75
2.66
4.20
3.39
2.83
3.07

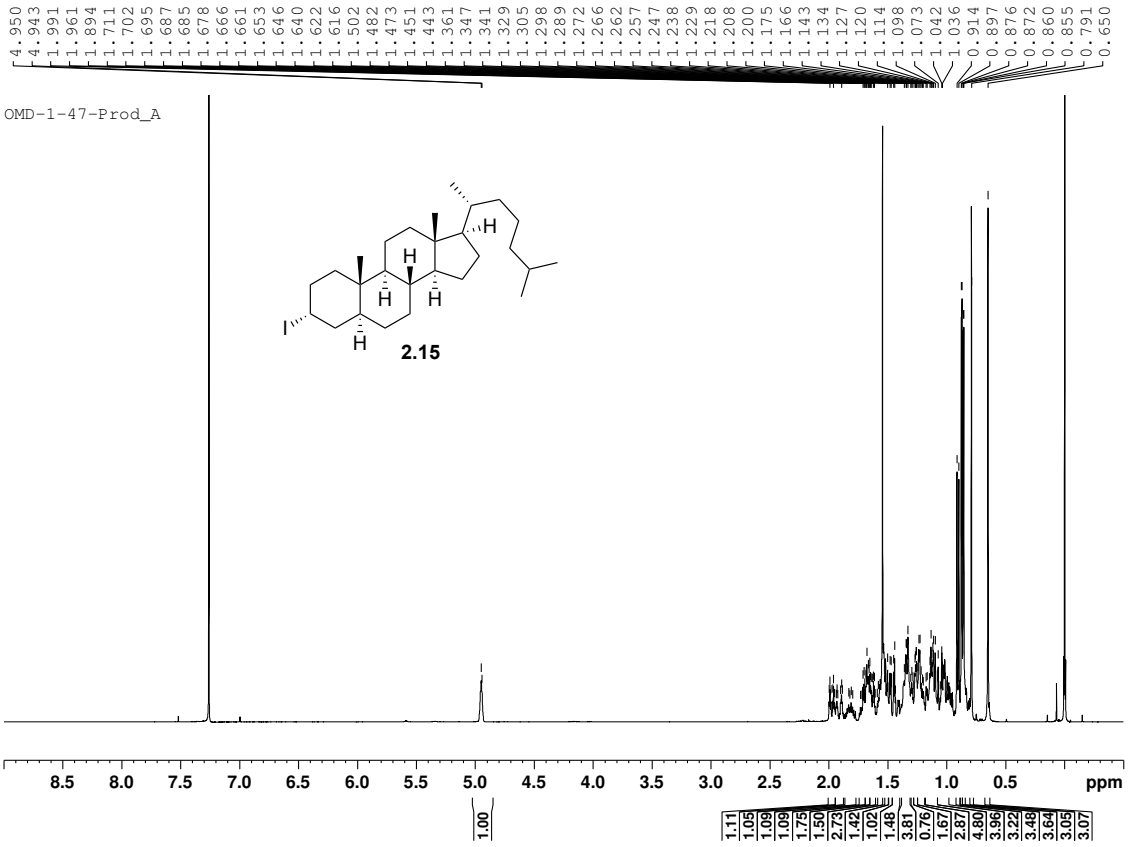
OMD-1-47-Prod_A
2.15
ppm

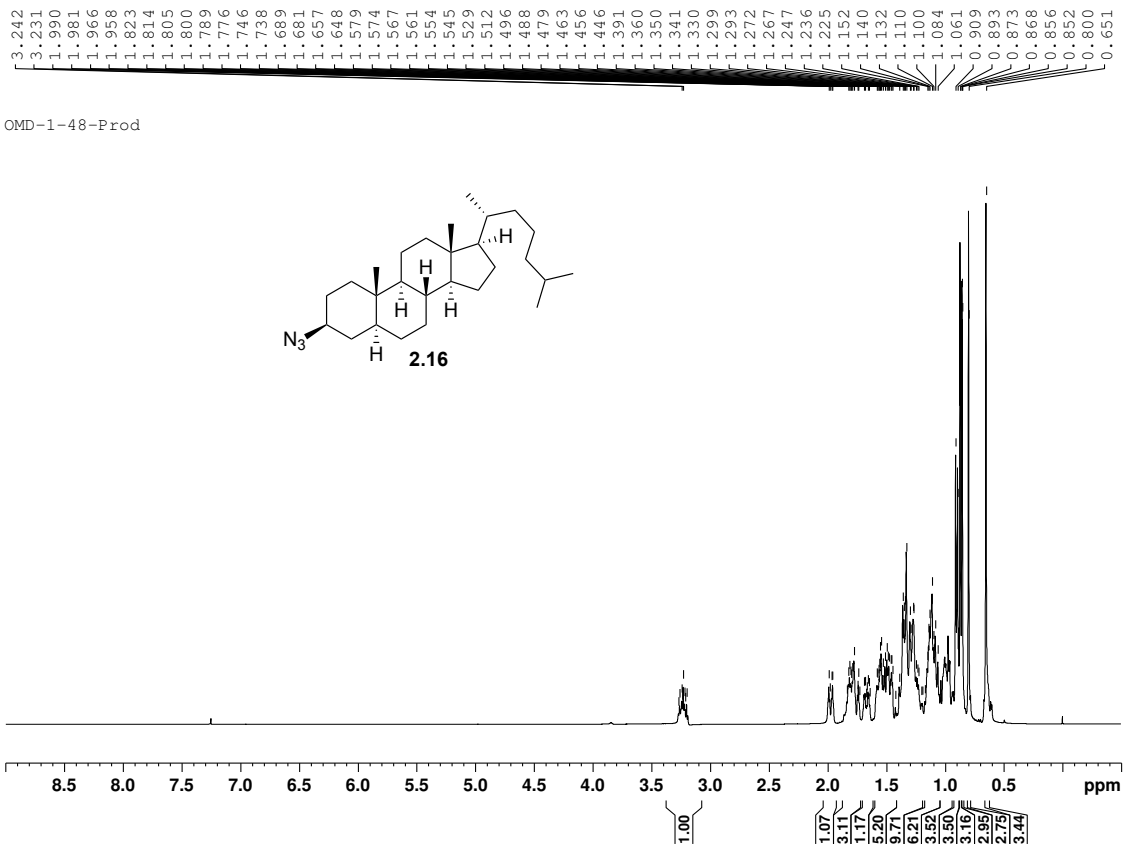
3.242
3.231
1.990
1.981
1.966
1.958
1.823
1.814
1.805
1.800
1.789
1.776
1.746
1.738
1.689
1.681
1.657
1.648
1.579
1.574
1.567
1.561
1.554
1.545
1.529
1.512
1.496
1.488
1.479
1.463
1.456
1.446
1.391
1.360
1.350
1.341
1.330
1.299
1.293
1.272
1.267
1.247
1.236
1.225
1.152
1.140
1.132
1.110
1.100
1.084
1.061
0.909
0.893
0.873
0.868
0.856
0.852
0.800
0.651
OMD-1-48-Prod
N3
2.16
8.5
8.0
7.5
7.0
6.5
6.0
5.5
5.0
4.5
4.0
3.5
3.0
2.5
2.0
1.5
1.0
0.5
ppm
1.00
1.07
3.11
1.17
5.20
9.71
6.21
3.52
3.50
3.16
2.95
2.75
3.44

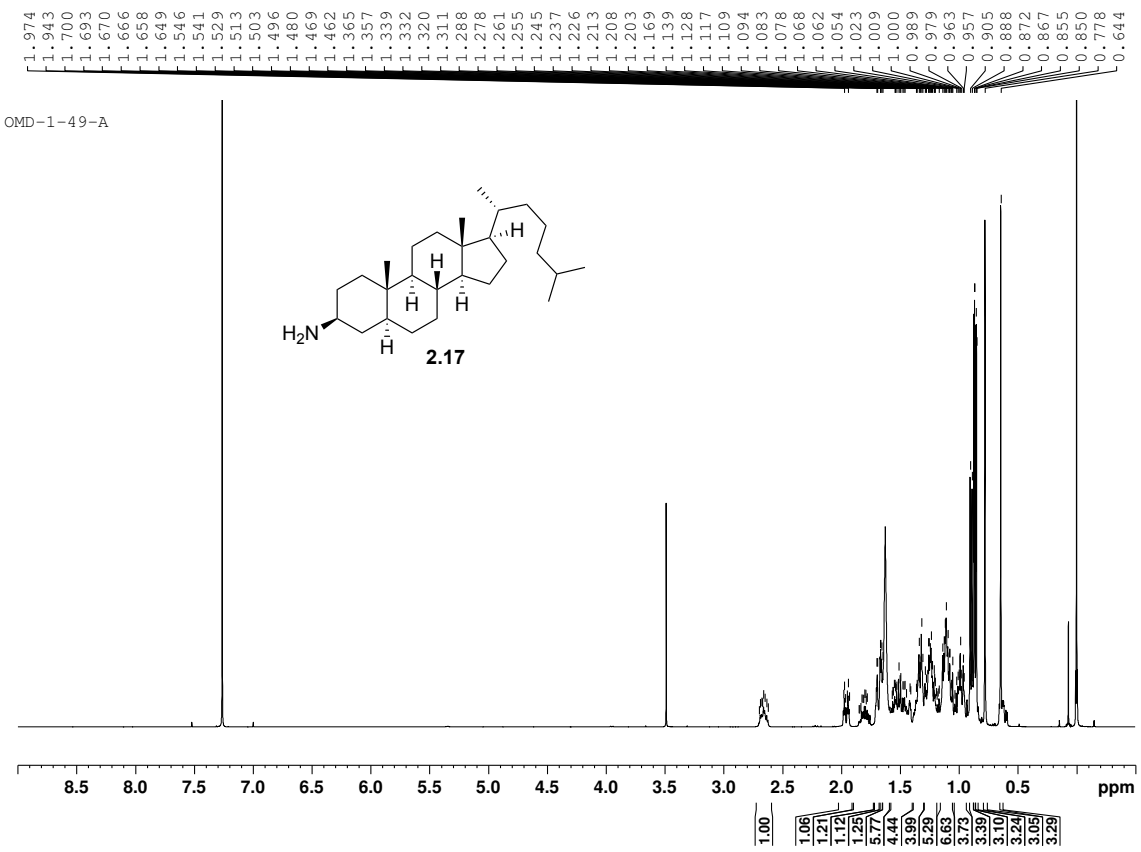
1.974
1.943
1.700
1.693
1.670
1.666
1.658
1.649
1.546
1.541
1.529
1.513
1.503
1.496
1.480
1.469
1.462
1.365
1.357
1.339
1.332
1.320
1.311
1.288
1.278
1.261
1.255
1.245
1.237
1.226
1.213
1.208
1.203
1.169
1.139
1.128
1.117
1.109
1.094
1.083
1.078
1.068
1.062
1.054
1.023
1.009
1.000
0.989
0.979
0.963
0.957
0.905
0.888
0.872
0.867
0.855
0.850
0.778
0.644
OMD-1-49-A
H
H
H
H
H2N
H
2.17
8.5
8.0
7.5
7.0
6.5
6.0
5.5
5.0
4.5
4.0
3.5
3.0
2.5
2.0
1.5
1.0
0.5
ppm
1.00
1.06
1.21
1.12
1.25
5.77
4.44
3.99
5.29
6.63
3.73
3.39
3.10
3.24
3.05
3.29

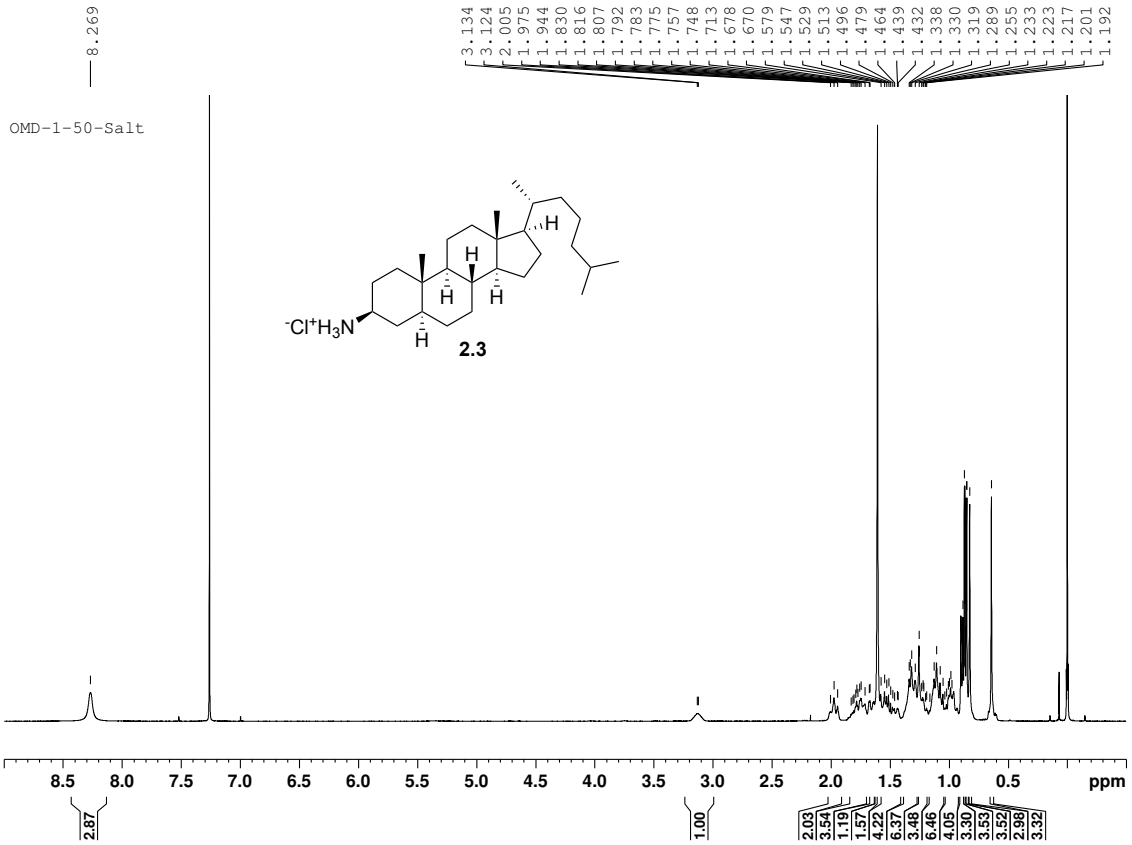
8.269
3.134
3.124
2.005
1.975
1.944
1.830
1.816
1.807
1.792
1.783
1.775
1.757
1.748
1.713
1.678
1.670
1.579
1.547
1.529
1.513
1.496
1.479
1.464
1.439
1.432
1.338
1.330
1.319
1.289
1.255
1.233
1.223
1.217
1.201
1.192
OMD-1-50-Salt
-Cl+H3N
2.3
8.5
8.0
7.5
7.0
6.5
6.0
5.5
5.0
4.5
4.0
3.5
3.0
2.5
2.0
1.5
1.0
0.5
ppm
2.87
1.00
2.03
3.54
1.19
1.57
4.22
6.37
3.48
6.46
4.05
3.30
3.53
3.52
2.98
3.32

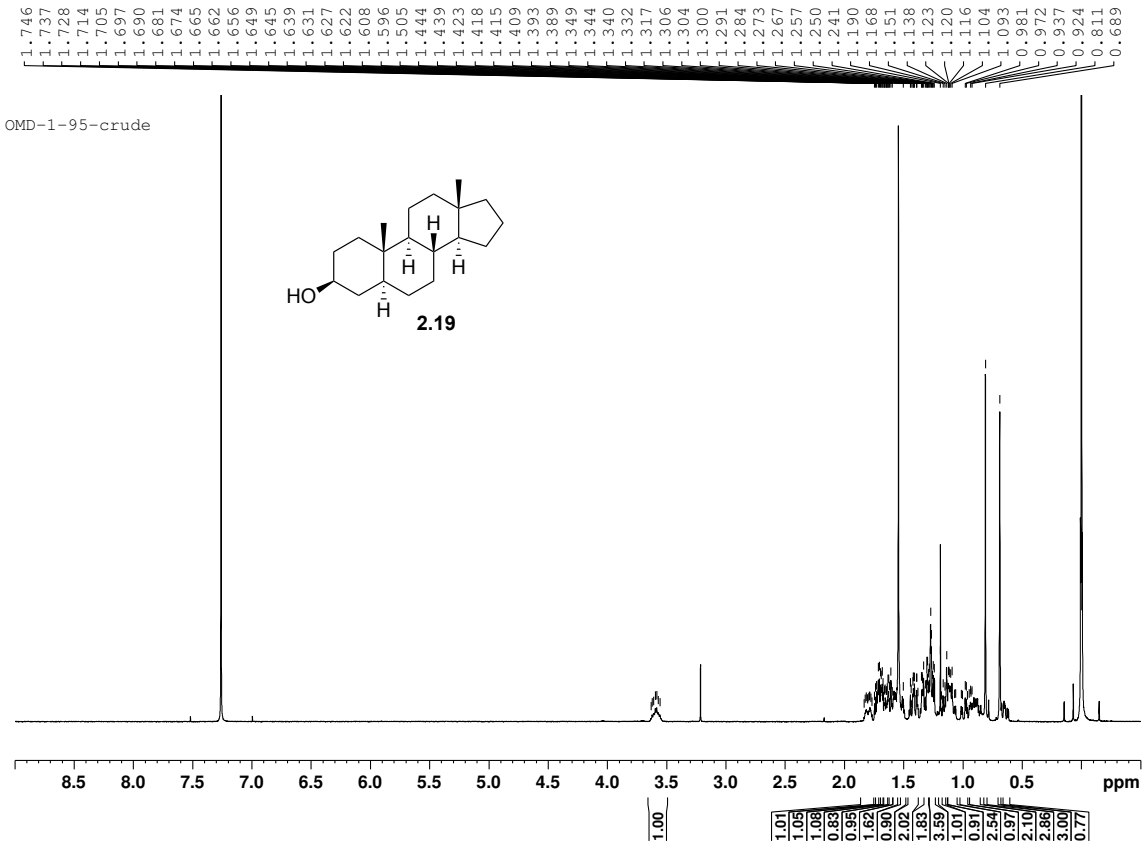
1.746
1.737
1.728
1.714
1.705
1.697
1.690
1.681
1.674
1.665
1.662
1.656
1.649
1.645
1.639
1.631
1.627
1.622
1.608
1.596
1.505
1.444
1.439
1.423
1.418
1.415
1.409
1.393
1.389
1.349
1.344
1.340
1.332
1.317
1.306
1.304
1.300
1.291
1.284
1.273
1.267
1.257
1.250
1.241
1.190
1.168
1.151
1.138
1.123
1.120
1.116
1.104
1.093
0.981
0.972
0.937
0.924
0.811
0.689
OMD-1-95-crude
HO
H
H
H
H
2.19
8.5
8.0
7.5
7.0
6.5
6.0
5.5
5.0
4.5
4.0
3.5
3.0
2.5
2.0
1.5
1.0
0.5
ppm
1.00
1.01
1.05
1.08
0.83
0.95
1.62
0.90
2.02
1.83
3.59
1.01
0.91
2.54
0.97
2.10
2.86
3.00
0.77

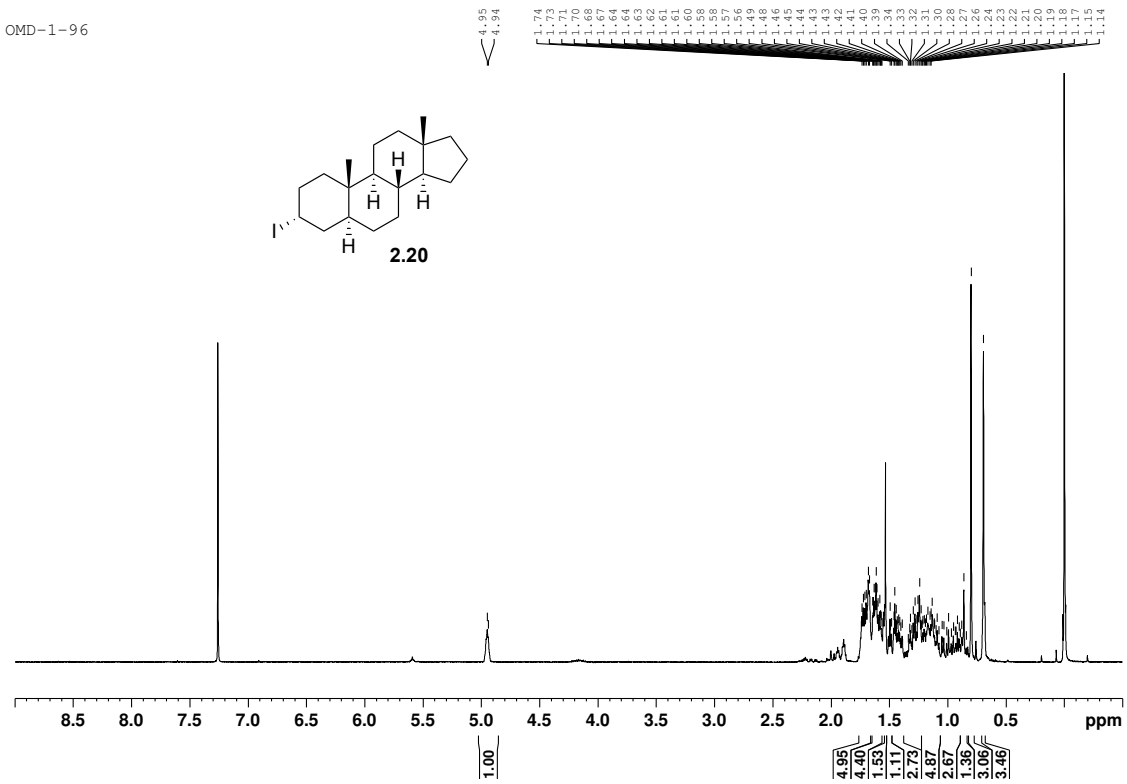
OMD-1-96
4.95
4.94
1.74
1.73
1.71
1.70
1.68
1.67
1.64
1.64
1.63
1.62
1.61
1.61
1.60
1.58
1.58
1.57
1.56
1.49
1.48
1.46
1.45
1.44
1.43
1.43
1.42
1.41
1.40
1.39
1.34
1.33
1.32
1.31
1.30
1.28
1.27
1.26
1.24
1.23
1.22
1.21
1.20
1.19
1.18
1.17
1.15
1.14
H
H
H
H
I
2.20
8.5
8.0
7.5
7.0
6.5
6.0
5.5
5.0
4.5
4.0
3.5
3.0
2.5
2.0
1.5
1.0
0.5
ppm
1.00
4.95
4.40
1.53
1.11
2.73
4.87
2.67
1.36
3.06
3.46

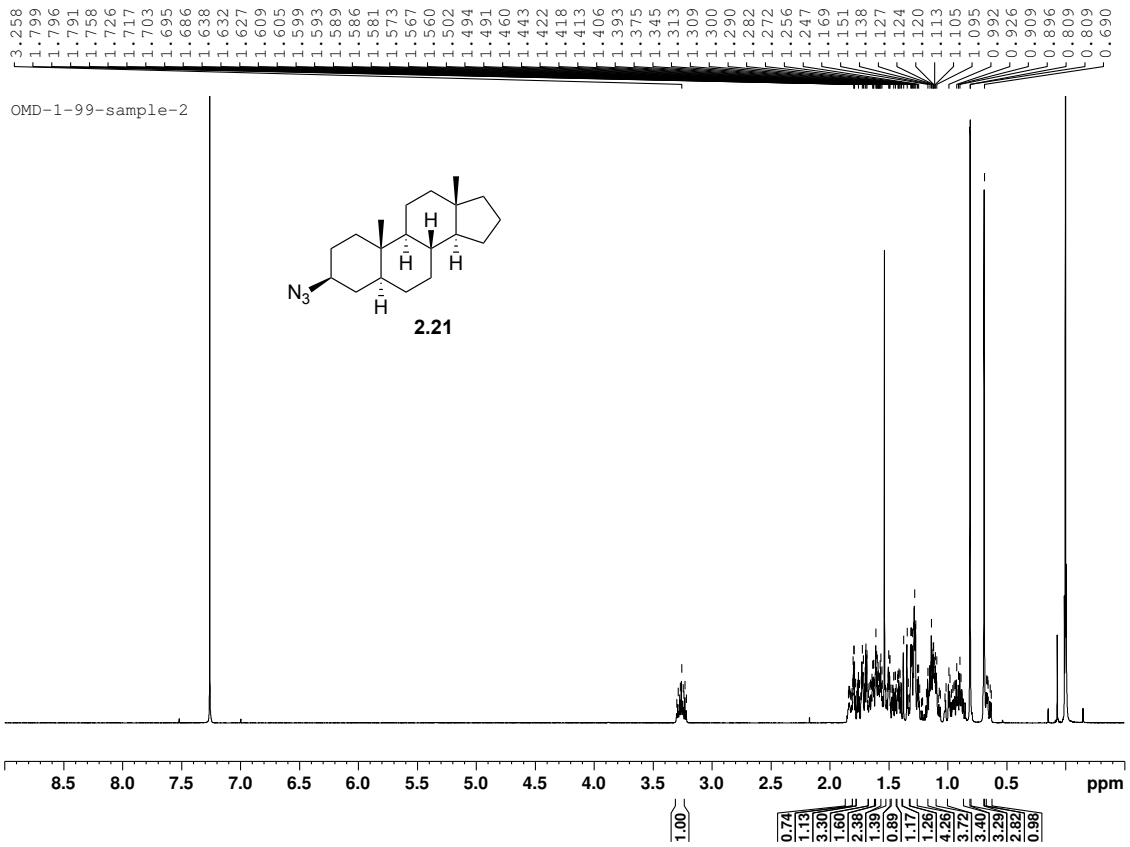
3.258
1.799
1.796
1.791
1.758
1.726
1.717
1.703
1.695
1.686
1.638
1.632
1.627
1.609
1.605
1.599
1.593
1.589
1.586
1.581
1.573
1.567
1.560
1.502
1.494
1.491
1.460
1.443
1.422
1.418
1.413
1.406
1.393
1.375
1.345
1.313
1.309
1.300
1.290
1.282
1.272
1.256
1.247
1.169
1.151
1.138
1.127
1.124
1.120
1.113
1.105
1.095
0.992
0.926
0.909
0.896
0.809
0.809
0.690
OMD-1-99-sample-2
H
H
H
N3
H
2.21
8.5
8.0
7.5
7.0
6.5
6.0
5.5
5.0
4.5
4.0
3.5
3.0
2.5
2.0
1.5
1.0
0.5
ppm
1.00
0.74
1.13
3.30
1.60
2.38
1.39
0.89
1.17
1.26
4.26
3.72
3.40
3.29
2.82
0.98

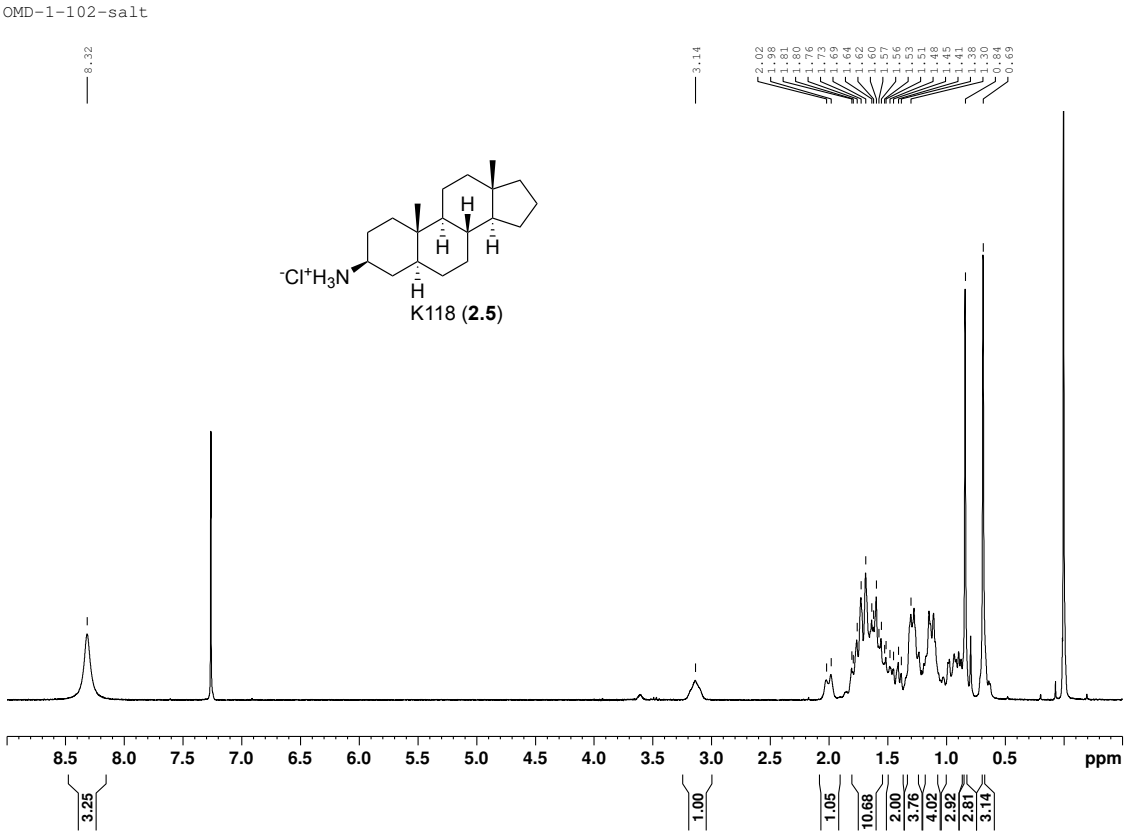
OMD-1-102-salt
8.32
3.14
2.02
1.98
1.81
1.80
1.76
1.73
1.69
1.64
1.62
1.60
1.57
1.56
1.53
1.51
1.48
1.45
1.41
1.38
1.30
0.84
0.69
H
H
H
H
-Cl+H3N
K118 (2.5)
8.5
8.0
7.5
7.0
6.5
6.0
5.5
5.0
4.5
4.0
3.5
3.0
2.5
2.0
1.5
1.0
0.5
ppm
3.25
1.00
1.05
10.68
2.00
3.76
4.02
2.92
2.81
3.14

OMD-1-89-salt-carbon

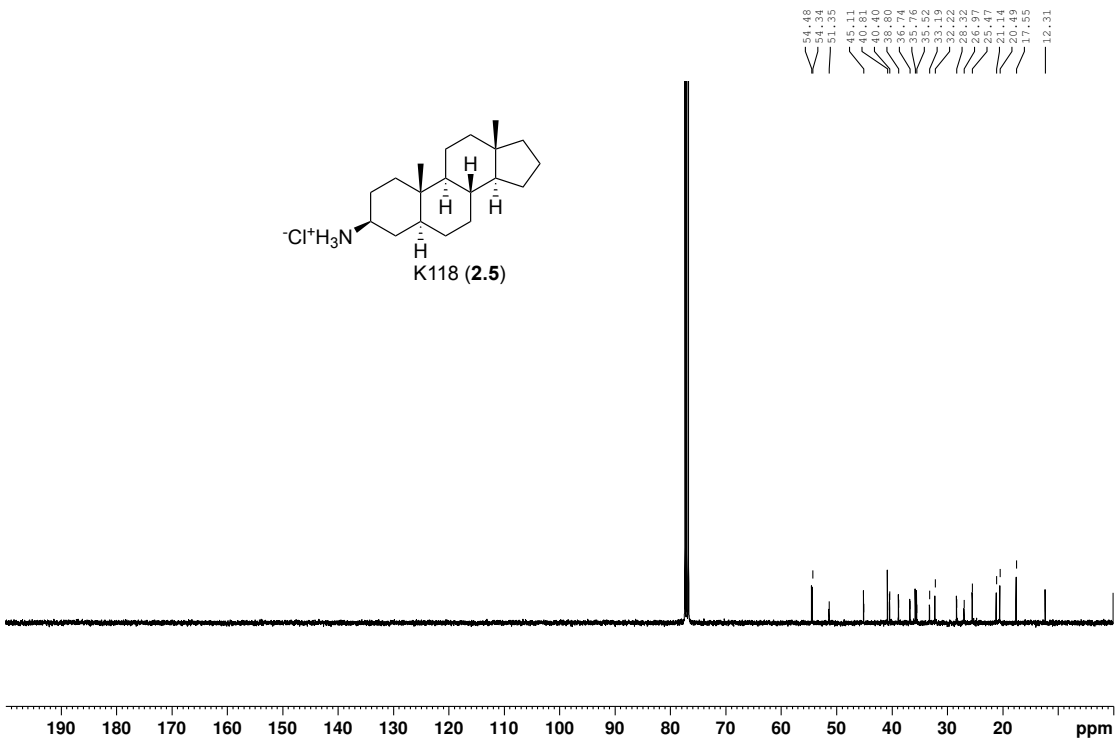

K118 (**2.5**)

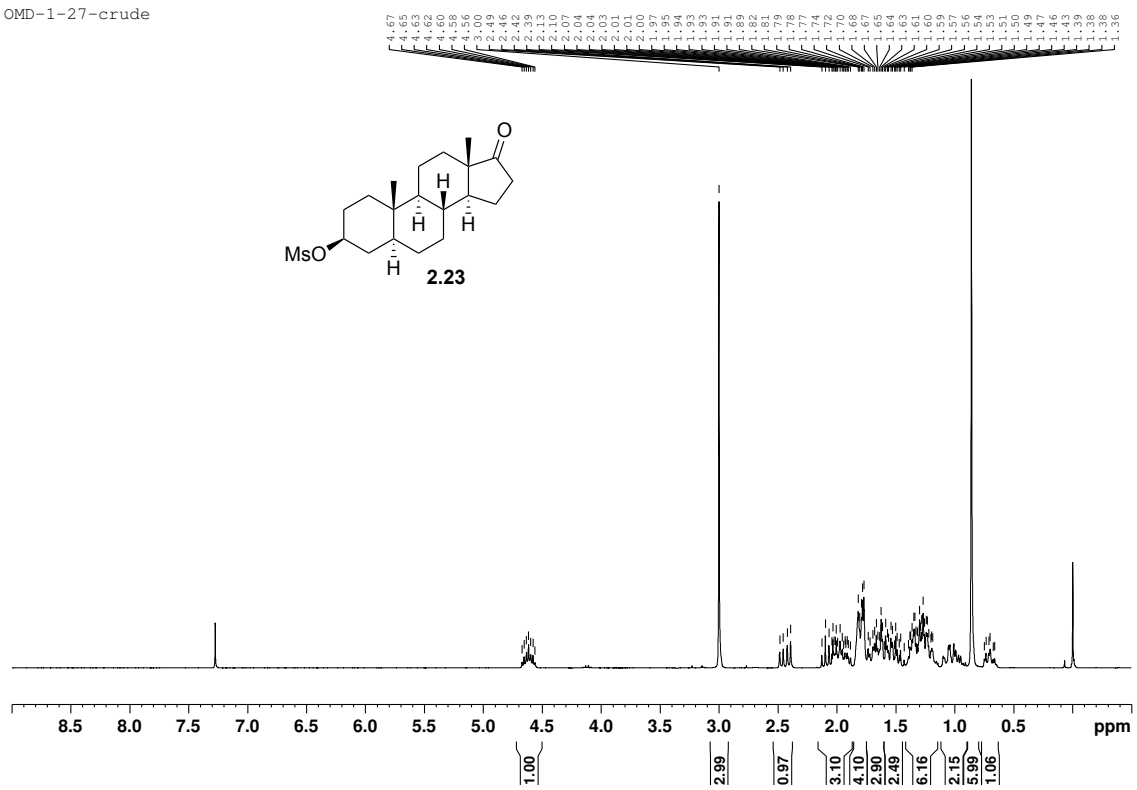
OMD-1-27-crude
4.67 4.65 4.63 4.62 4.60 4.58 4.56 4.50 2.49 2.46 2.42 2.39 2.13 2.10 2.07 2.04 2.03 2.01 2.00 1.97 1.95 1.94 1.93 1.91 1.91 1.89 1.82 1.81 1.79 1.78 1.77 1.74 1.72 1.70 1.68 1.67 1.65 1.64 1.63 1.61 1.60 1.59 1.57 1.56 1.54 1.53 1.51 1.50 1.49 1.47 1.46 1.43 1.39 1.38 1.36
O
H
H
H
MsO
H
2.23
8.5 8.0 7.5 7.0 6.5 6.0 5.5 5.0 4.5 4.0 3.5 3.0 2.5 2.0 1.5 1.0 0.5 ppm
1.00 2.99 0.97 3.10 4.10 2.90 2.49 6.16 2.15 5.99 1.06

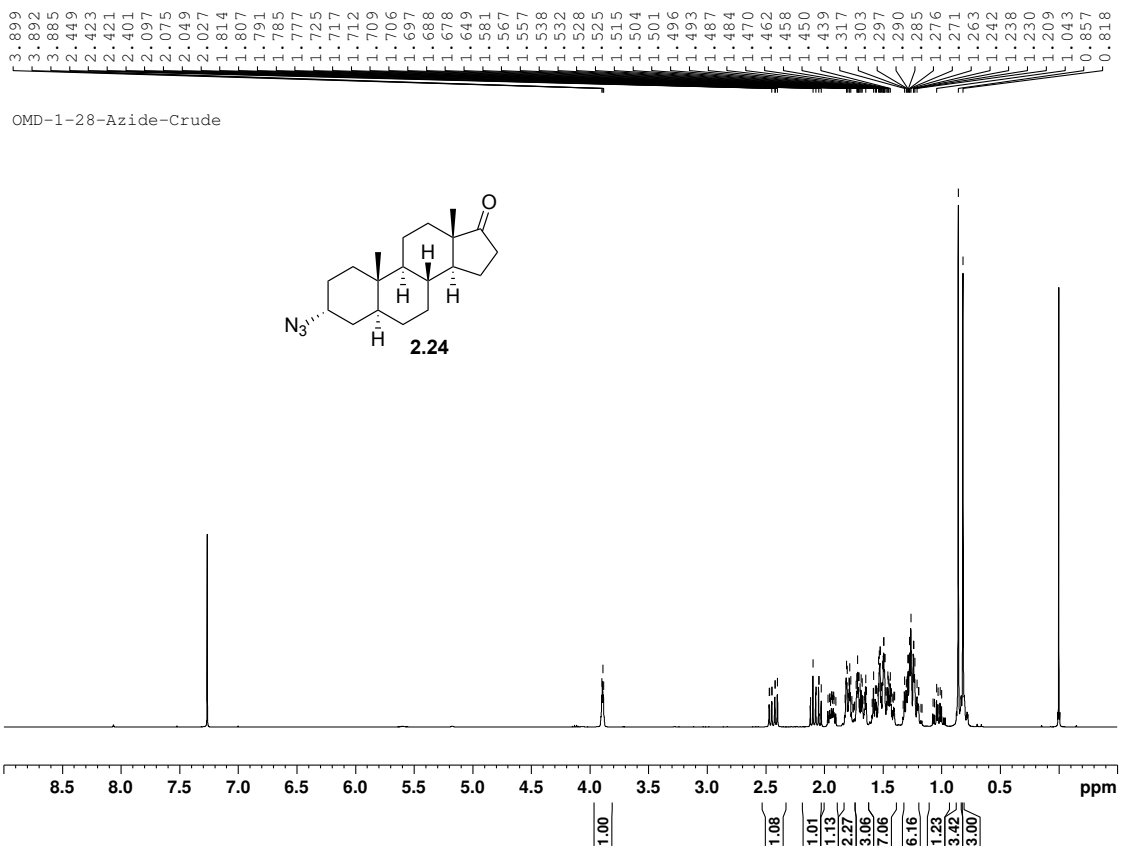
3.899
3.892
3.885
2.449
2.423
2.421
2.401
2.097
2.075
2.049
2.027
1.814
1.807
1.791
1.785
1.777
1.725
1.717
1.712
1.709
1.706
1.697
1.688
1.678
1.649
1.581
1.567
1.557
1.538
1.532
1.528
1.525
1.515
1.504
1.501
1.496
1.493
1.487
1.484
1.470
1.462
1.458
1.450
1.439
1.317
1.303
1.297
1.290
1.285
1.276
1.271
1.263
1.242
1.238
1.230
1.209
1.043
0.857
0.818
OMD-1-28-Azide-Crude
O
H
H
H
N3
H
2.24
8.5
8.0
7.5
7.0
6.5
6.0
5.5
5.0
4.5
4.0
3.5
3.0
2.5
2.0
1.5
1.0
0.5
ppm
1.00
1.08
1.01
1.13
2.27
3.06
7.06
6.16
1.23
3.42
3.00

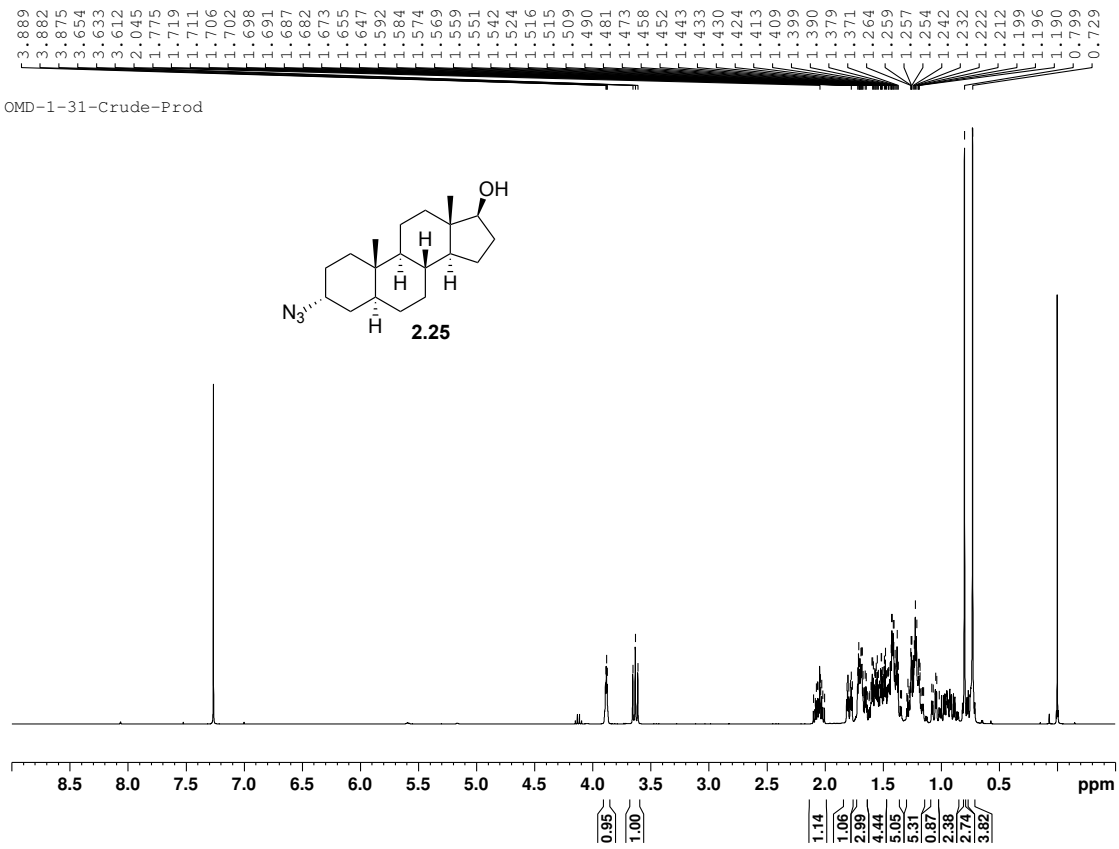
3.889
3.882
3.875
3.654
3.633
3.612
2.045
1.775
1.719
1.711
1.706
1.702
1.698
1.691
1.687
1.682
1.673
1.655
1.647
1.592
1.584
1.574
1.569
1.559
1.551
1.542
1.524
1.516
1.515
1.509
1.490
1.481
1.473
1.458
1.452
1.443
1.433
1.430
1.424
1.413
1.409
1.399
1.390
1.379
1.371
1.264
1.259
1.257
1.254
1.242
1.232
1.222
1.212
1.199
1.196
1.190
0.799
0.729
OMD-1-31-Crude-Prod
OH
H
H
H
N3
H
2.25
8.5
8.0
7.5
7.0
6.5
6.0
5.5
5.0
4.5
4.0
3.5
3.0
2.5
2.0
1.5
1.0
0.5
ppm
0.95
1.00
1.14
1.06
2.99
4.44
5.05
5.31
0.87
2.38
2.74
3.82

OMD-1-17-CARBON

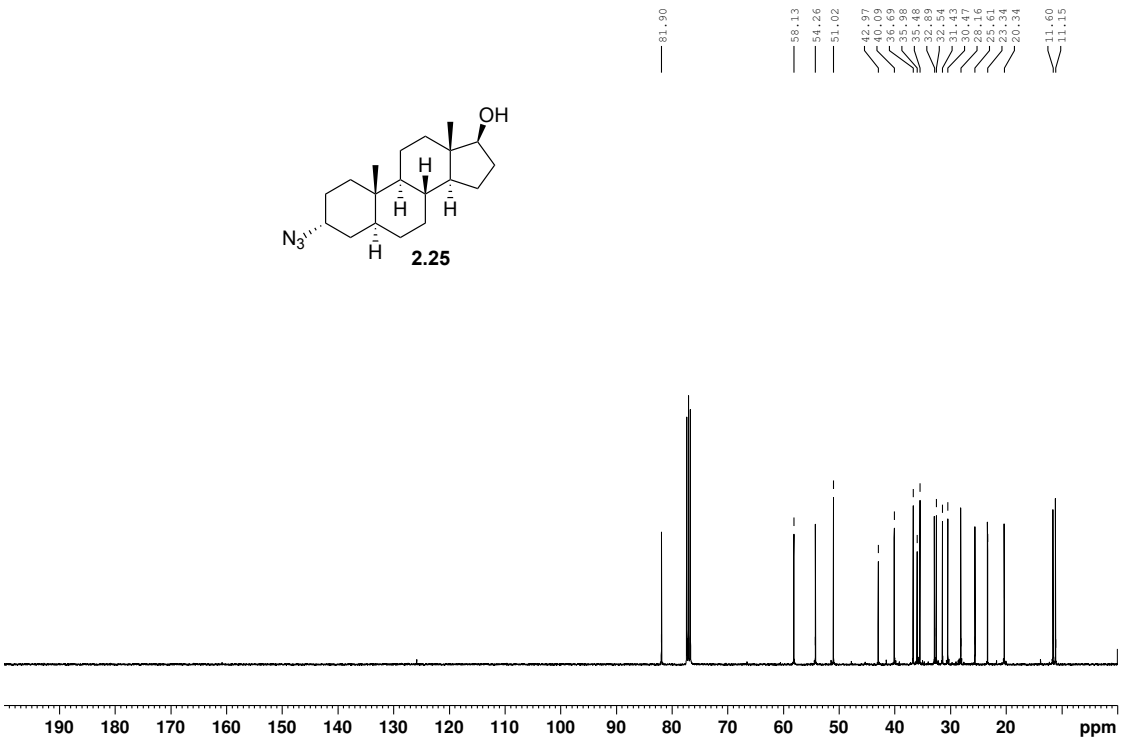

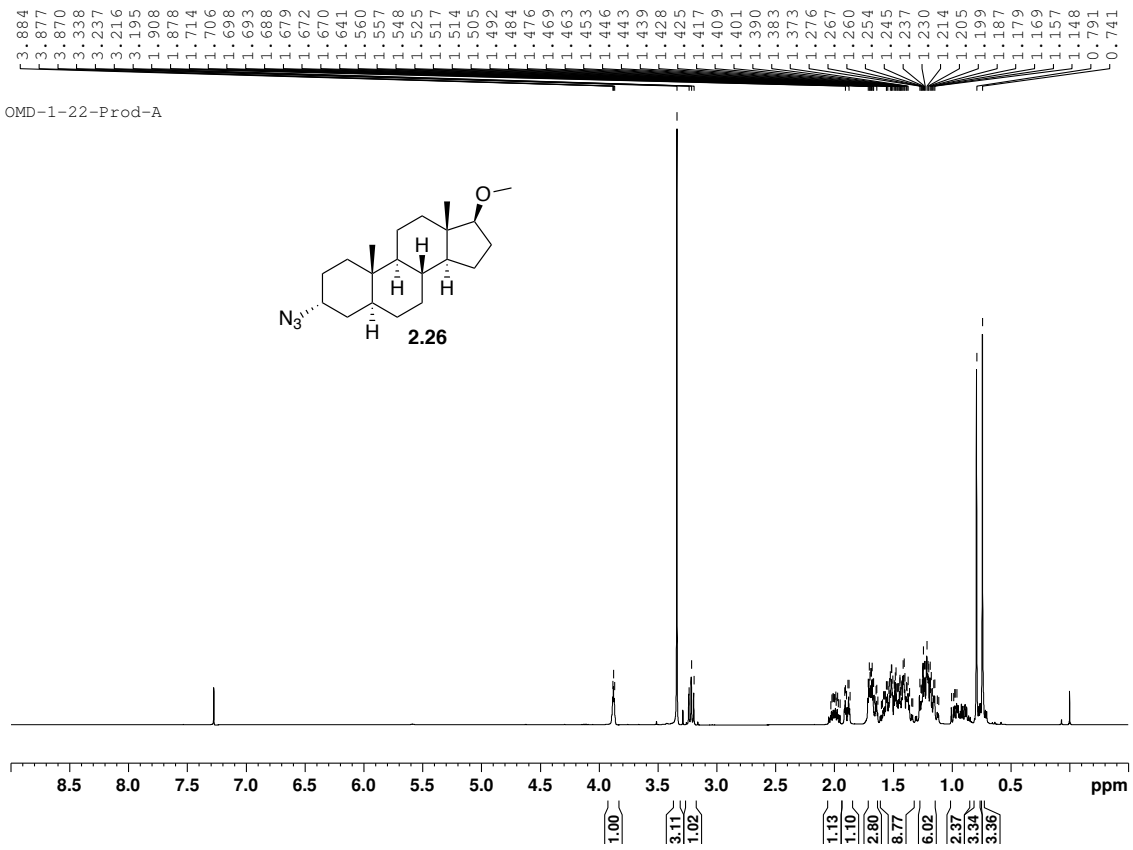
3.884
3.877
3.870
3.338
3.237
3.216
3.195
1.908
1.878
1.714
1.706
1.698
1.693
1.688
1.679
1.672
1.670
1.641
1.560
1.557
1.548
1.525
1.517
1.514
1.505
1.492
1.484
1.476
1.469
1.463
1.453
1.446
1.443
1.439
1.428
1.425
1.417
1.409
1.401
1.390
1.383
1.373
1.276
1.267
1.260
1.254
1.245
1.237
1.230
1.214
1.205
1.199
1.187
1.179
1.169
1.157
1.148
0.791
0.741
OMD-1-22-Prod-A
O
H
H
H
N3
H
2.26
8.5
8.0
7.5
7.0
6.5
6.0
5.5
5.0
4.5
4.0
3.5
3.0
2.5
2.0
1.5
1.0
0.5
ppm
1.00
3.11
1.02
1.13
1.10
2.80
8.77
6.02
2.37
3.34
3.36

OMD-1-42-Methyl-Ether-CNMR

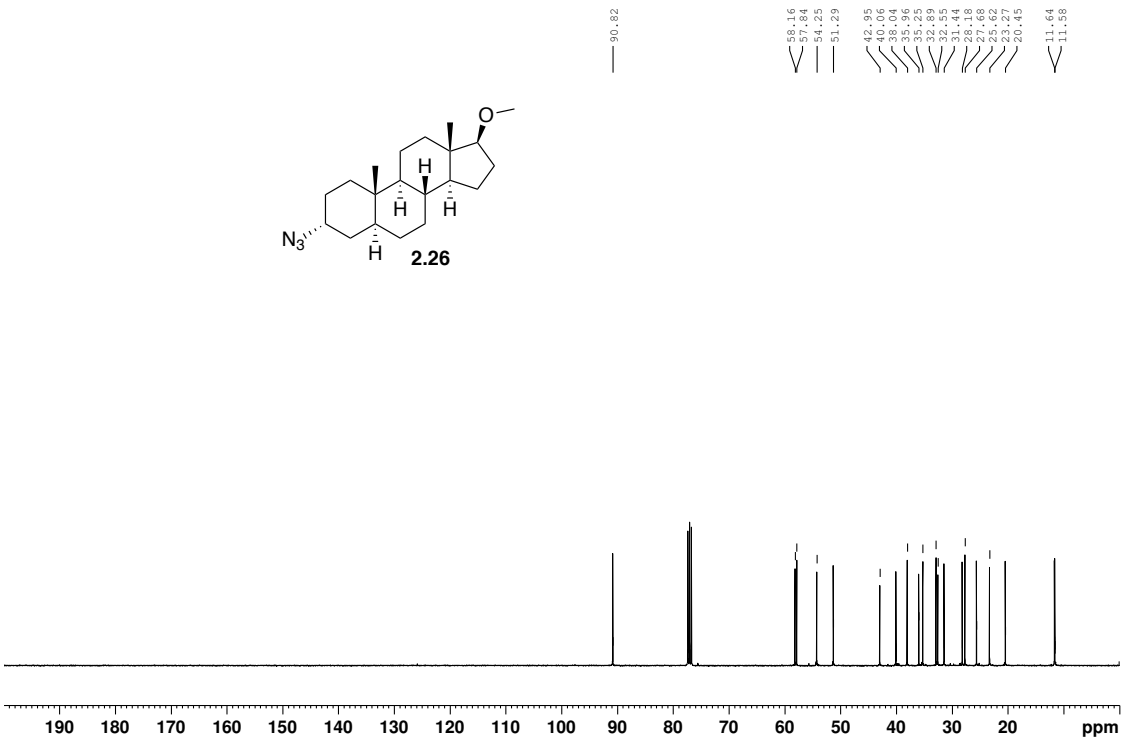

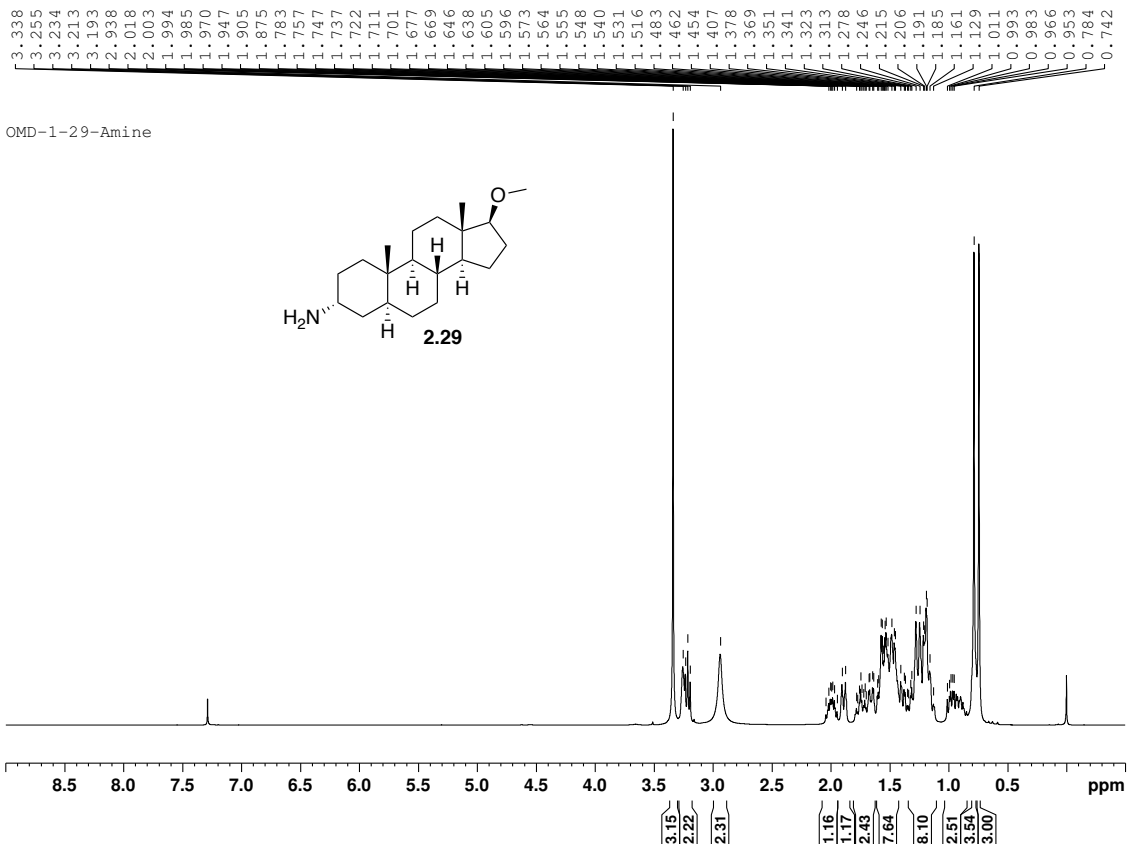
3.338
3.255
3.234
3.213
3.193
2.938
2.018
2.003
1.994
1.985
1.970
1.947
1.905
1.875
1.783
1.757
1.747
1.737
1.722
1.711
1.701
1.677
1.669
1.646
1.638
1.605
1.596
1.573
1.564
1.555
1.548
1.540
1.531
1.516
1.483
1.462
1.454
1.407
1.378
1.369
1.351
1.341
1.323
1.313
1.278
1.246
1.215
1.206
1.191
1.185
1.161
1.129
1.011
0.993
0.983
0.966
0.953
0.784
0.742
OMD-1-29-Amine
O
H
H
H
H
H2N
2.29
8.5
8.0
7.5
7.0
6.5
6.0
5.5
5.0
4.5
4.0
3.5
3.0
2.5
2.0
1.5
1.0
0.5
ppm
3.15
2.22
2.31
1.16
1.17
2.43
7.64
8.10
2.51
3.54
3.00

OMD-1-29-Amine-CNMR

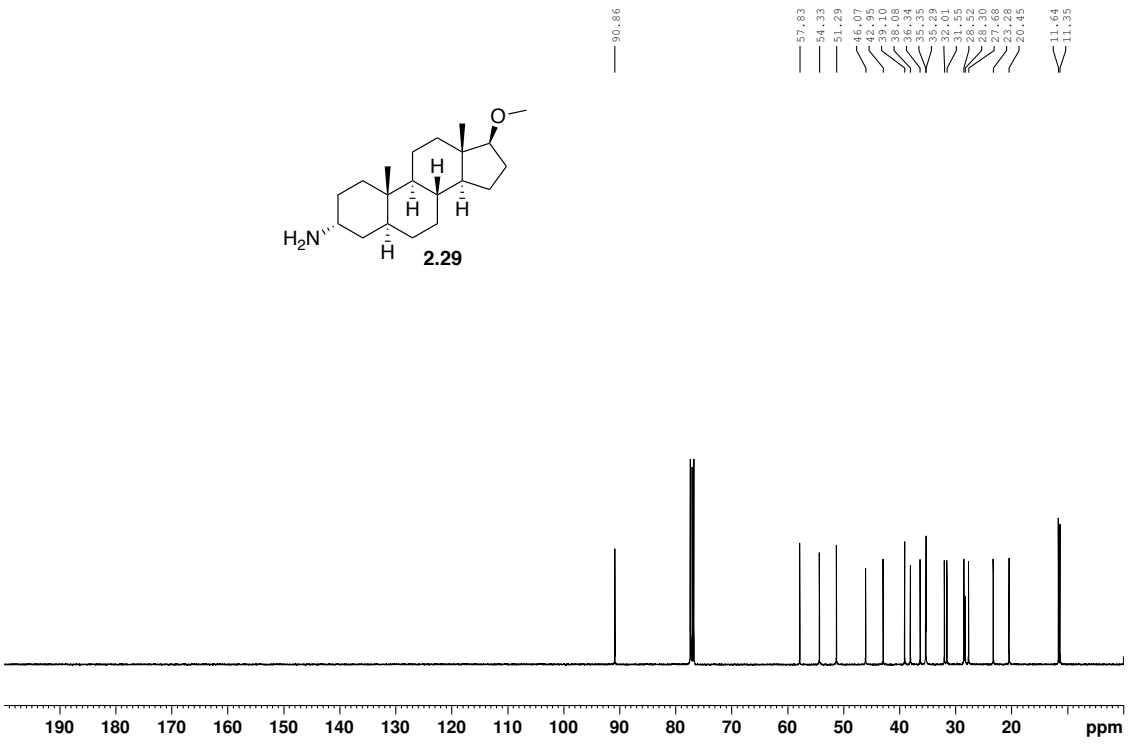

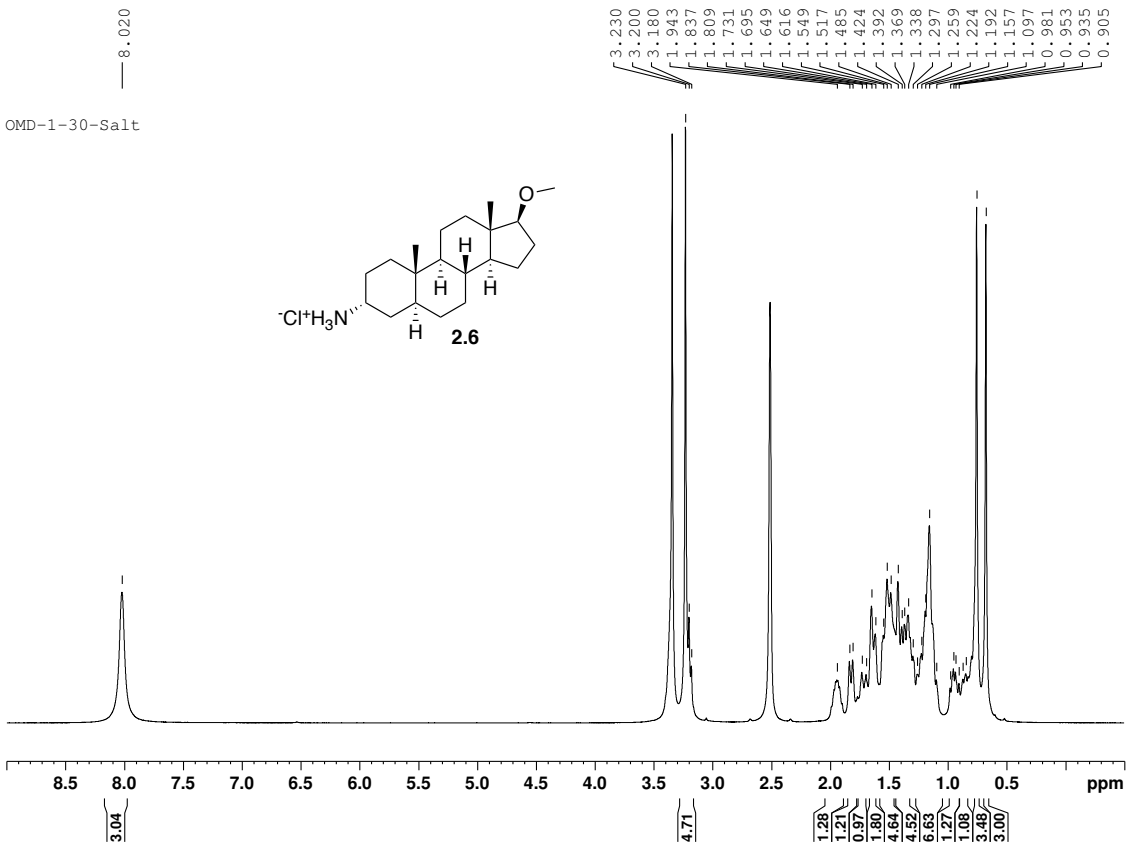
8.020
3.230
3.200
3.180
1.943
1.837
1.809
1.731
1.695
1.649
1.616
1.549
1.517
1.485
1.424
1.392
1.369
1.338
1.297
1.259
1.224
1.192
1.157
1.097
0.981
0.953
0.935
0.905
OMD-1-30-Salt
O
H
H
H
-Cl+H3N
H
2.6
8.5
8.0
7.5
7.0
6.5
6.0
5.5
5.0
4.5
4.0
3.5
3.0
2.5
2.0
1.5
1.0
0.5
ppm
3.04
4.71
1.28
1.21
0.97
1.80
4.64
4.52
6.63
1.27
1.08
3.48
3.00

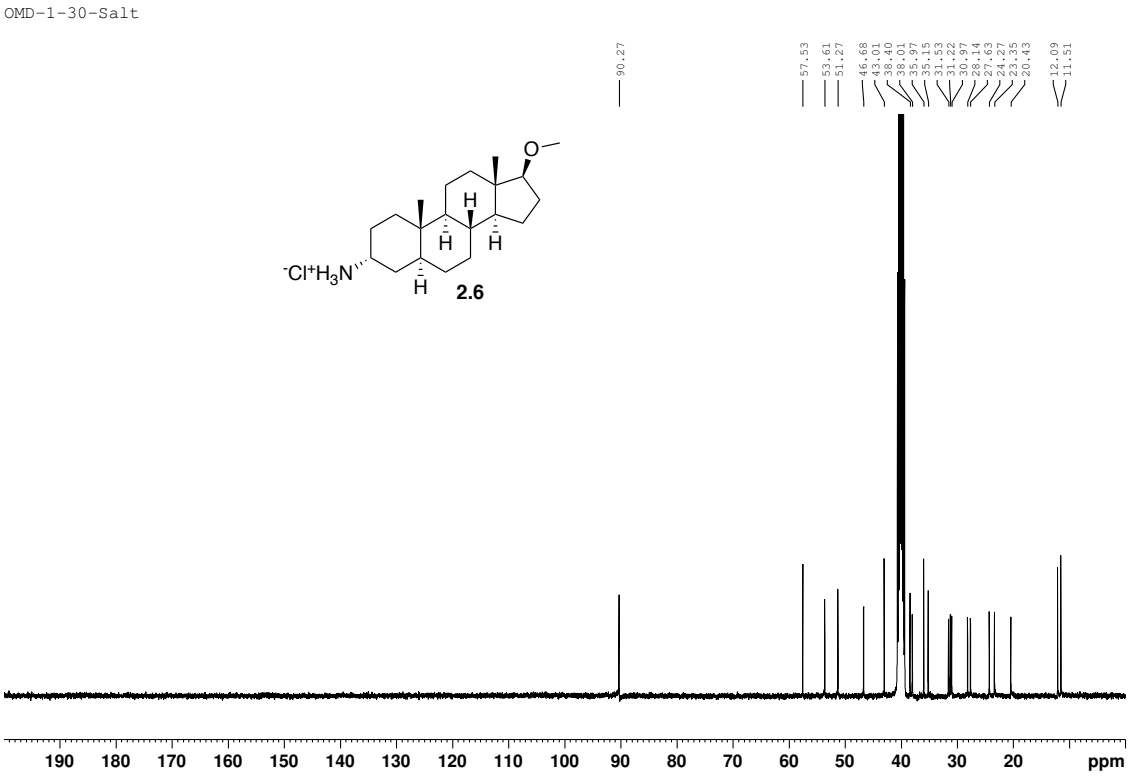
OMD-1-30-Salt
90.27
57.53
53.61
51.27
46.68
43.01
38.40
38.01
35.97
35.15
31.53
31.22
30.97
28.14
27.63
24.27
23.35
20.43
12.09
11.51
O
H
H
H
H
-Cl+H3N
2.6
190
180
170
160
150
140
130
120
110
100
90
80
70
60
50
40
30
20
ppm

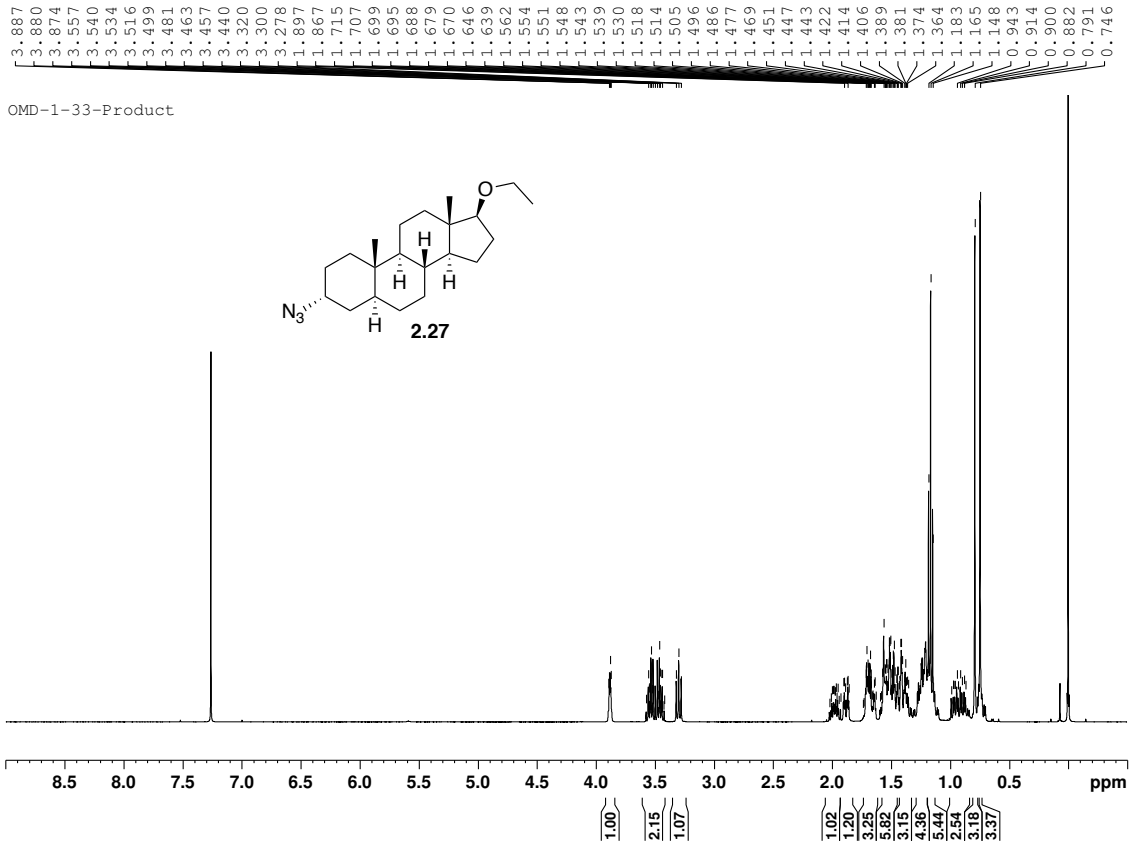
3.887
3.880
3.874
3.557
3.540
3.534
3.516
3.499
3.481
3.463
3.457
3.440
3.320
3.300
3.278
1.897
1.867
1.715
1.707
1.699
1.695
1.688
1.679
1.670
1.646
1.639
1.562
1.554
1.551
1.548
1.543
1.539
1.530
1.518
1.514
1.505
1.496
1.486
1.477
1.469
1.451
1.447
1.443
1.422
1.414
1.406
1.389
1.381
1.374
1.364
1.183
1.165
1.148
0.943
0.914
0.900
0.882
0.791
0.746
OMD-1-33-Product
O
H
H
H
H
N3
2.27
8.5
8.0
7.5
7.0
6.5
6.0
5.5
5.0
4.5
4.0
3.5
3.0
2.5
2.0
1.5
1.0
0.5
ppm
1.00
2.15
1.07
1.02
1.20
3.25
5.82
3.15
4.36
5.44
2.54
3.18
3.37

OMD-1-33-Product-CNMR

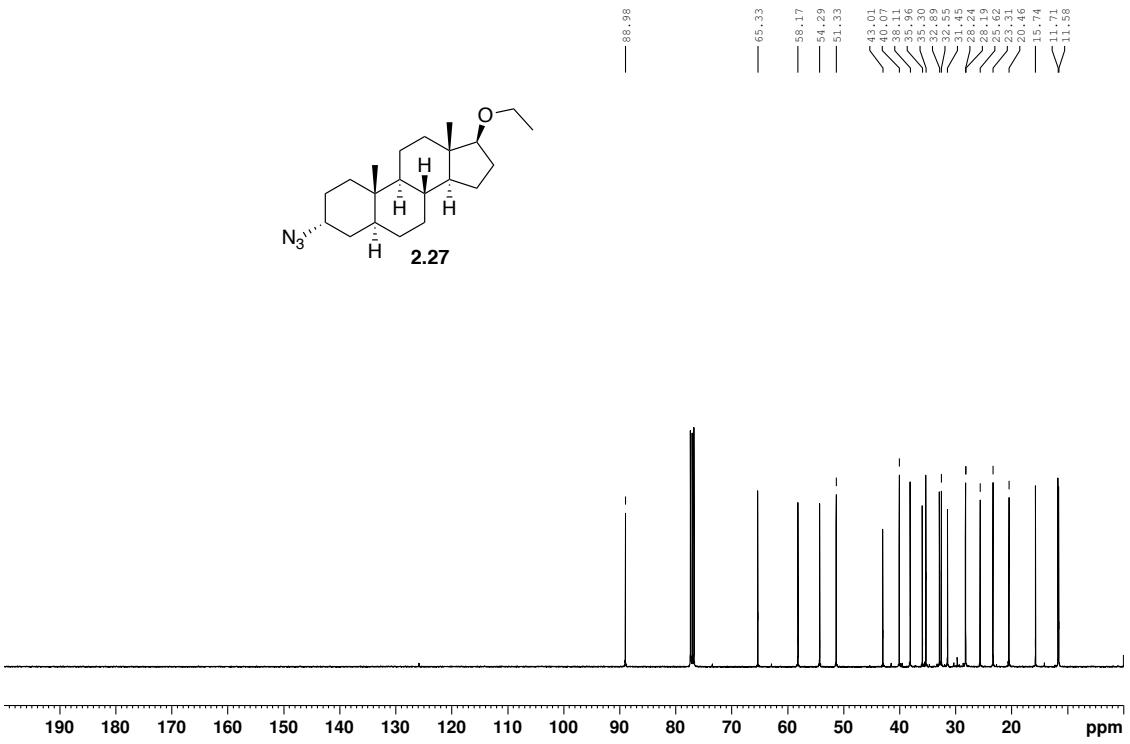

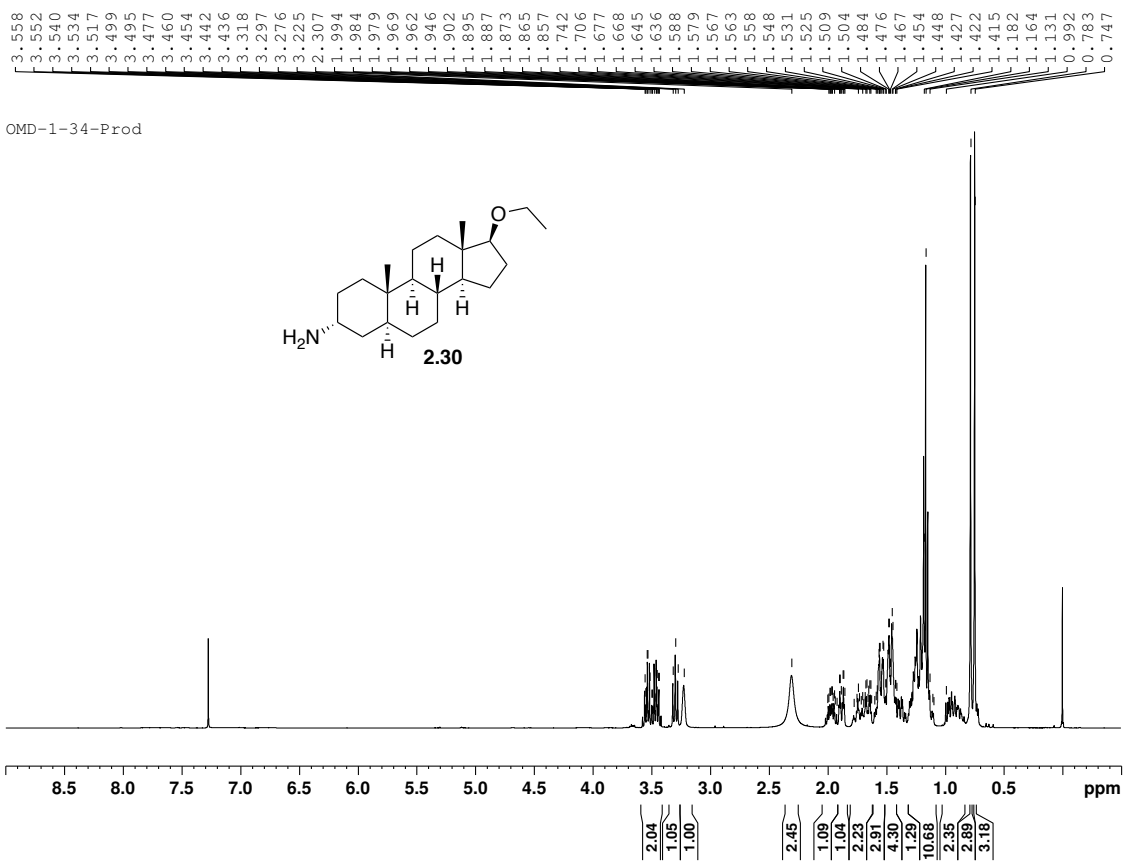
3.558
3.552
3.540
3.534
3.517
3.499
3.495
3.477
3.460
3.454
3.442
3.436
3.318
3.297
3.276
3.225
2.307
1.994
1.984
1.979
1.969
1.962
1.946
1.902
1.895
1.887
1.873
1.865
1.857
1.742
1.706
1.677
1.668
1.645
1.636
1.588
1.579
1.567
1.563
1.558
1.548
1.531
1.525
1.509
1.504
1.484
1.476
1.467
1.454
1.448
1.427
1.422
1.415
1.182
1.164
1.131
0.992
0.783
0.747
OMD-1-34-Prod
O
H
H
H
H2N
H
2.30
8.5
8.0
7.5
7.0
6.5
6.0
5.5
5.0
4.5
4.0
3.5
3.0
2.5
2.0
1.5
1.0
0.5
ppm
2.04
1.05
1.00
2.45
1.09
1.04
2.23
2.91
4.30
1.29
10.68
2.35
2.89
3.18

OMD-1-34-Prod-CNMR

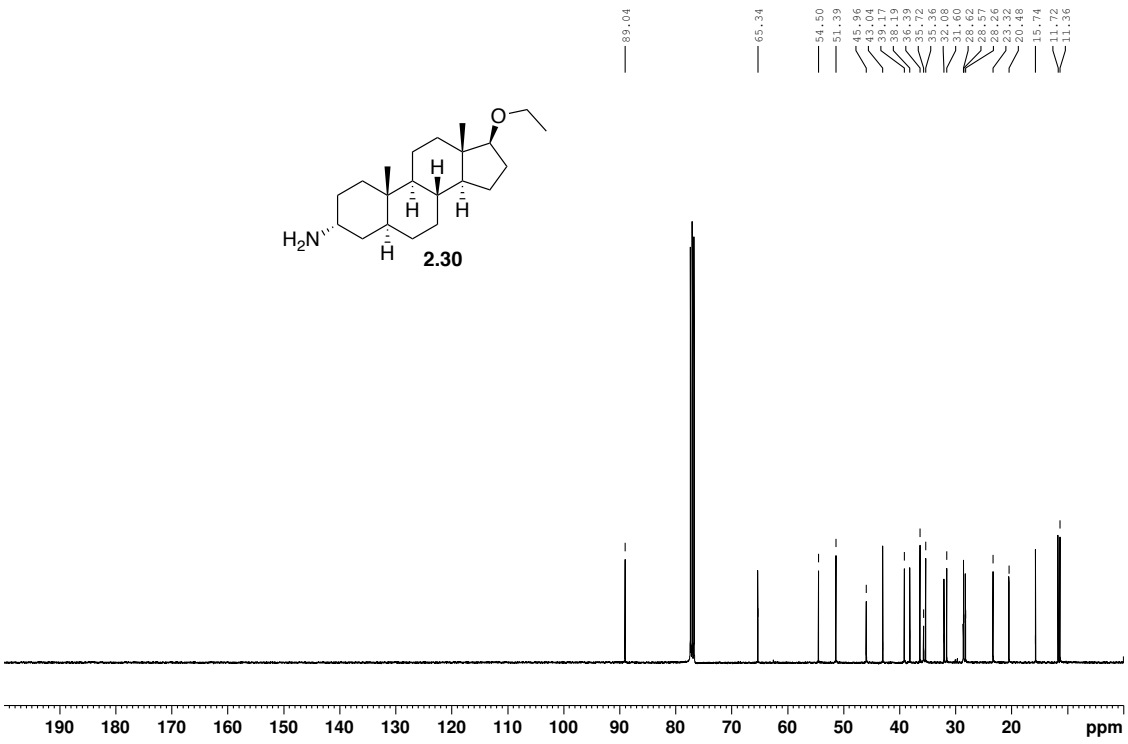

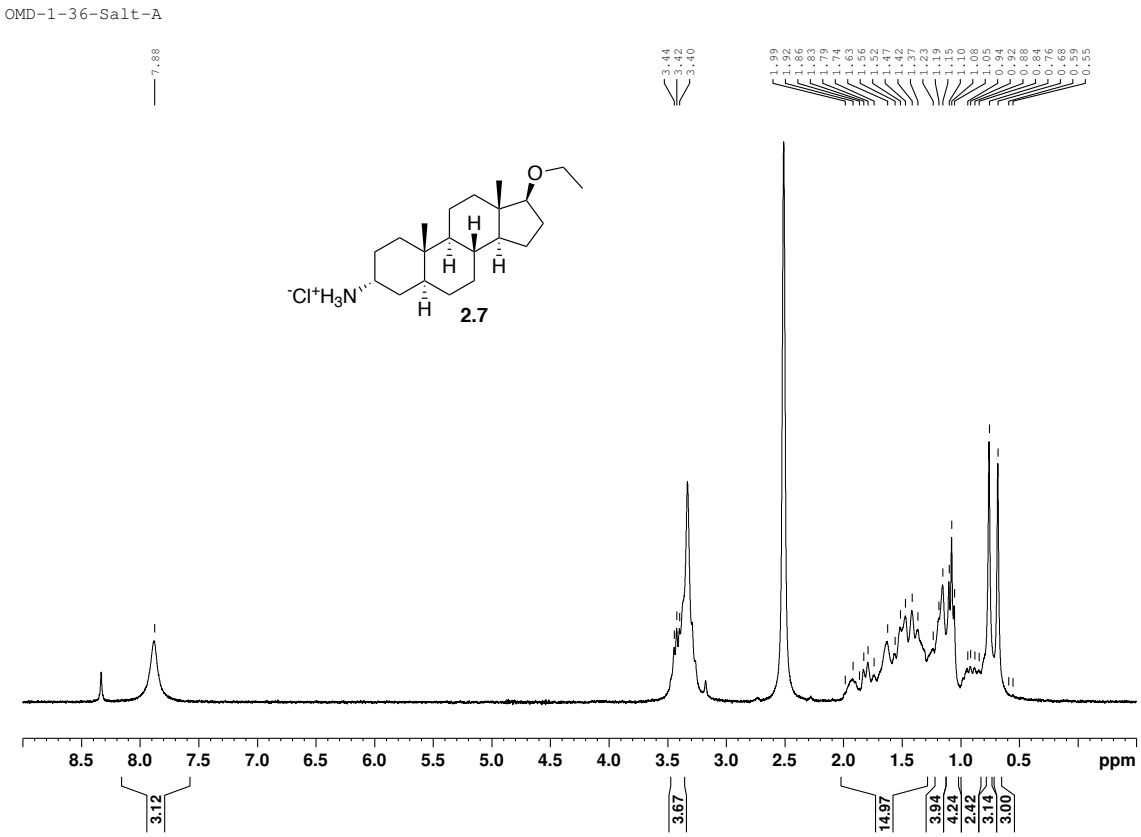
OMD-1-36-Salt-A
7.88
3.44
3.42
3.40
1.99
1.92
1.86
1.83
1.79
1.74
1.63
1.56
1.52
1.47
1.42
1.37
1.23
1.19
1.15
1.10
1.08
1.05
1.04
0.92
0.88
0.84
0.76
0.68
0.59
0.55
O
H
H
H
H
-Cl+H3N
2.7
8.5
8.0
7.5
7.0
6.5
6.0
5.5
5.0
4.5
4.0
3.5
3.0
2.5
2.0
1.5
1.0
0.5
ppm
3.12
3.67
14.97
3.94
4.24
2.42
3.14
3.00

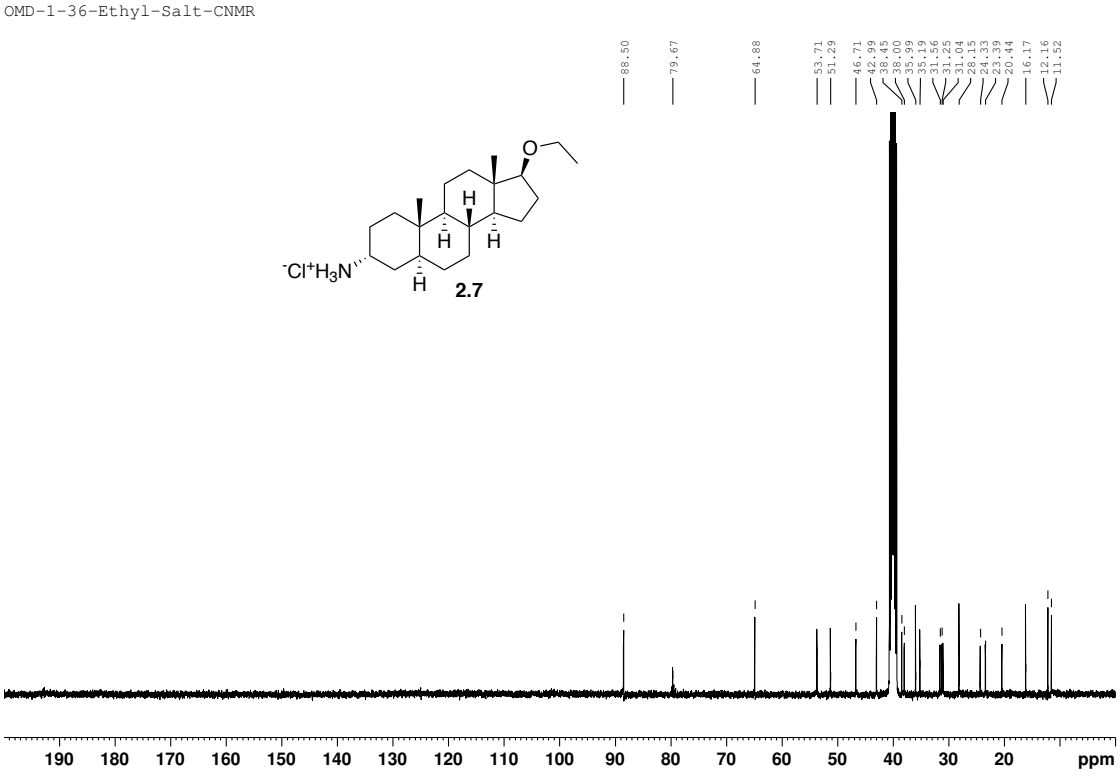
OMD-1-36-Ethyl-Salt-CNMR
88.50
79.67
64.88
53.71
51.29
46.71
42.99
38.45
38.00
36.99
35.19
31.56
31.25
31.04
28.15
24.33
23.39
20.44
16.17
12.16
11.52
O
H
H
H
H
$^{-}Cl^{+}H_3N$
2.7
190
180
170
160
150
140
130
120
110
100
90
80
70
60
50
40
30
20
ppm

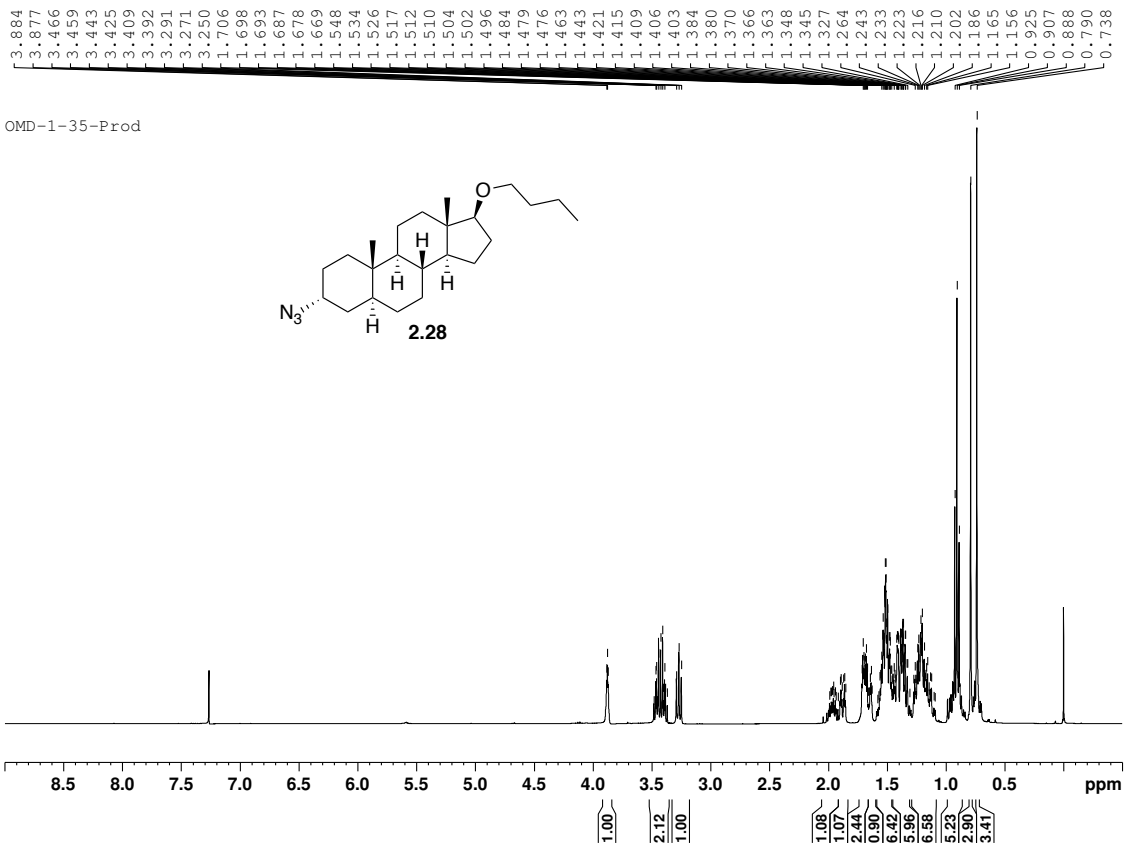
3.884
3.877
3.466
3.459
3.443
3.425
3.409
3.392
3.291
3.271
3.250
1.706
1.698
1.693
1.687
1.678
1.669
1.548
1.534
1.526
1.517
1.512
1.510
1.504
1.502
1.496
1.484
1.479
1.476
1.463
1.443
1.421
1.415
1.409
1.406
1.403
1.384
1.380
1.370
1.366
1.363
1.348
1.345
1.327
1.264
1.243
1.233
1.223
1.216
1.210
1.202
1.186
1.165
1.156
0.925
0.907
0.888
0.790
0.738
OMD-1-35-Prod
O
H
H
H
H
N3
2.28
8.5
8.0
7.5
7.0
6.5
6.0
5.5
5.0
4.5
4.0
3.5
3.0
2.5
2.0
1.5
1.0
0.5
ppm
1.00
2.12
1.00
1.08
1.07
2.44
0.90
6.42
5.96
6.58
5.23
2.90
3.41

OMD-1-35-Prod-CNMR

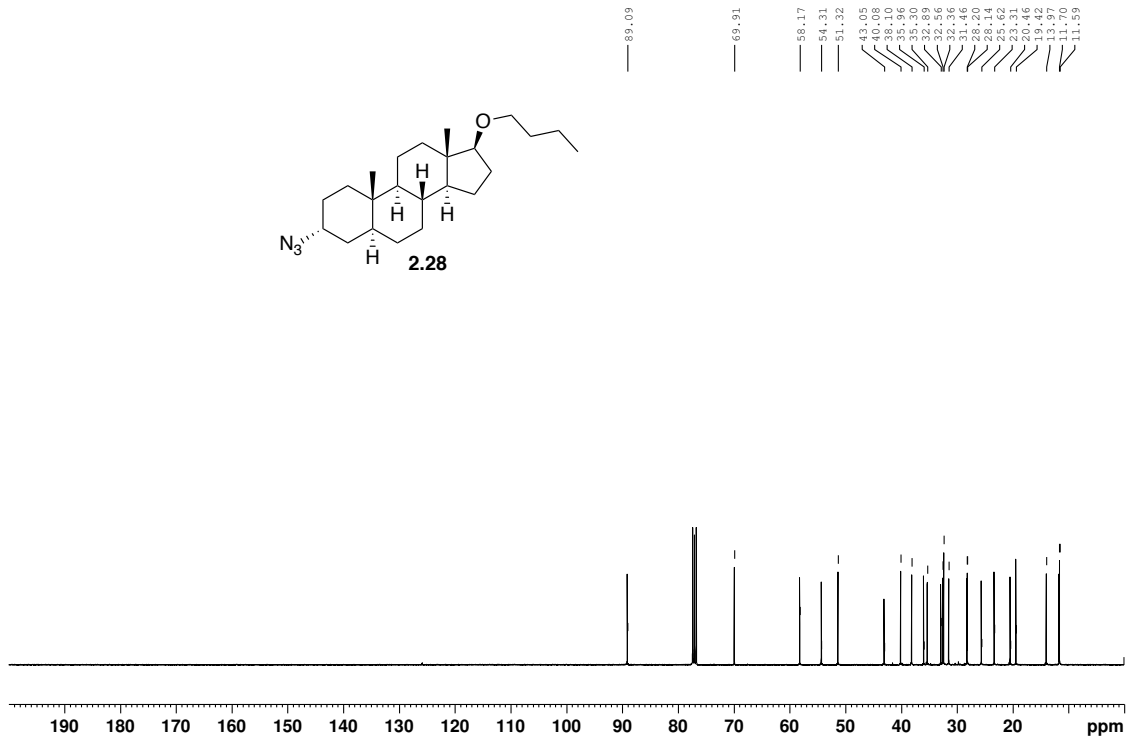

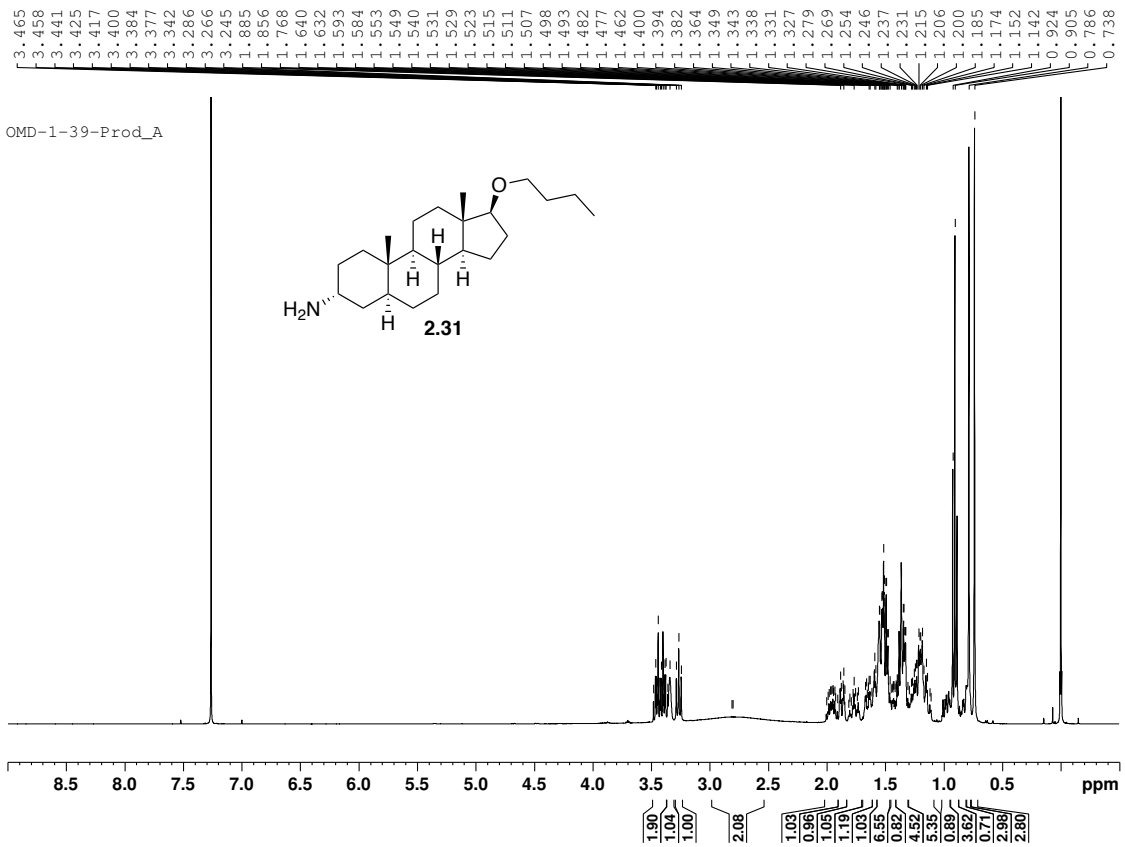
3.465
3.458
3.441
3.425
3.417
3.400
3.384
3.377
3.342
3.286
3.266
3.245
1.885
1.856
1.768
1.640
1.632
1.593
1.584
1.553
1.549
1.540
1.531
1.529
1.523
1.515
1.511
1.507
1.498
1.493
1.482
1.477
1.462
1.400
1.394
1.382
1.364
1.349
1.343
1.338
1.331
1.327
1.279
1.269
1.254
1.246
1.237
1.231
1.215
1.206
1.200
1.185
1.174
1.152
1.142
0.924
0.905
0.786
0.738
OMD-1-39-Prod_A
O
H
H
H
H
H2N
2.31
8.5
8.0
7.5
7.0
6.5
6.0
5.5
5.0
4.5
4.0
3.5
3.0
2.5
2.0
1.5
1.0
0.5
ppm
1.90
1.04
1.00
2.08
1.03
0.96
1.05
1.19
1.03
6.55
0.82
4.52
5.35
0.89
3.62
0.71
2.98
2.80

OMD-1-39-Prod-CNMR

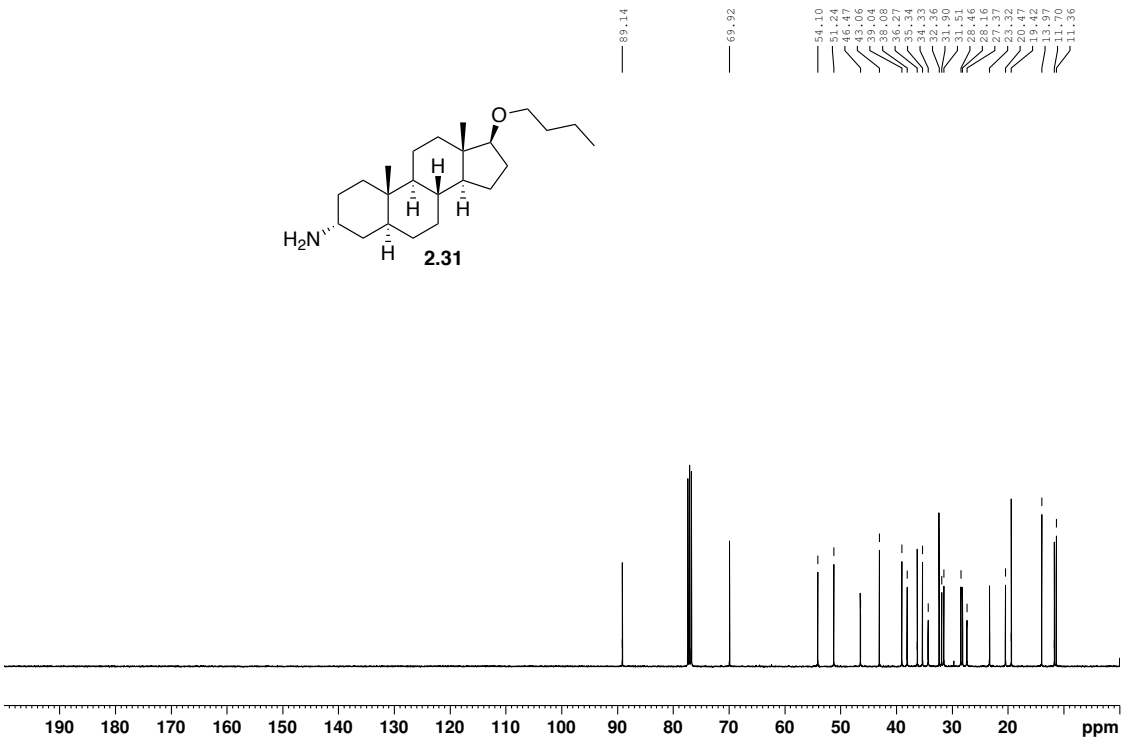

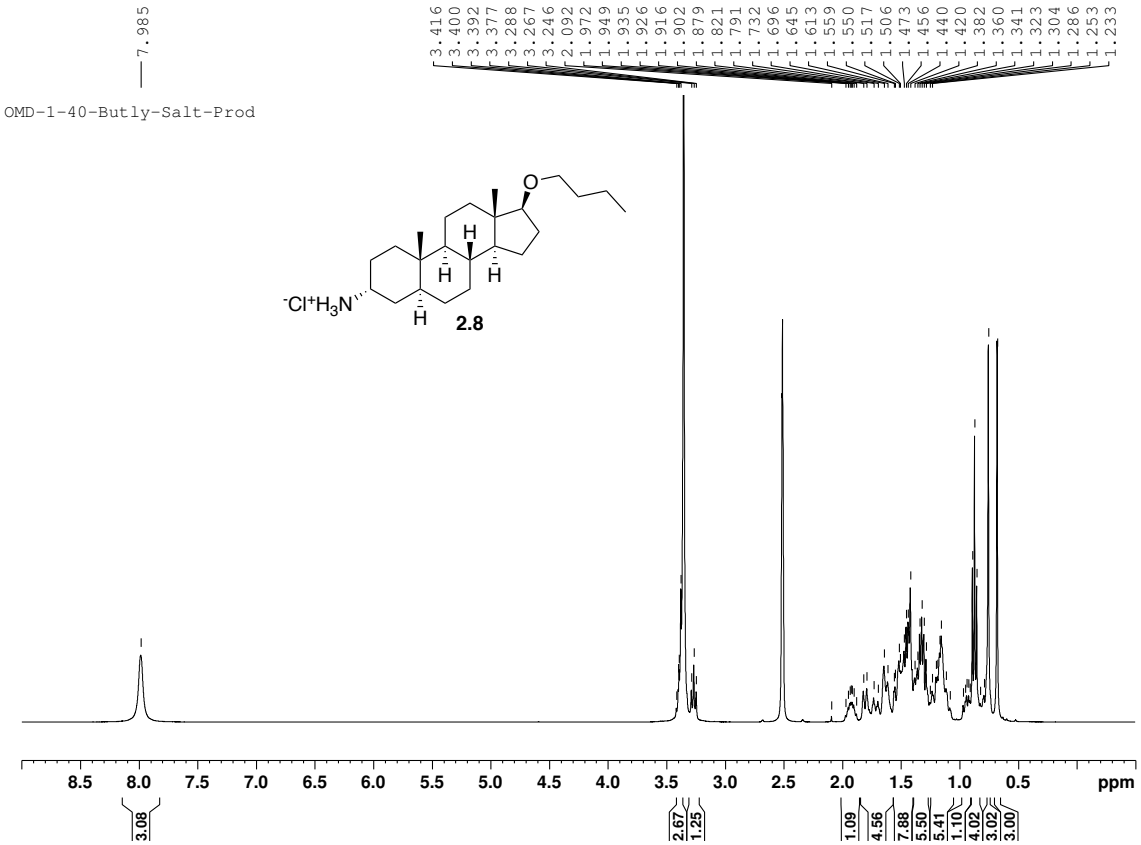
7.985
3.416
3.400
3.392
3.377
3.288
3.267
3.246
2.092
1.972
1.949
1.935
1.926
1.916
1.902
1.879
1.821
1.791
1.732
1.696
1.645
1.613
1.559
1.550
1.517
1.506
1.473
1.456
1.440
1.420
1.382
1.360
1.341
1.323
1.304
1.286
1.253
1.233
OMD-1-40-Butly-Salt-Prod
O
H
H
H
H
-Cl+H3N
2.8
8.5
8.0
7.5
7.0
6.5
6.0
5.5
5.0
4.5
4.0
3.5
3.0
2.5
2.0
1.5
1.0
0.5
ppm
3.08
2.67
1.25
1.09
4.56
7.88
5.50
5.41
1.10
4.02
3.02
3.00

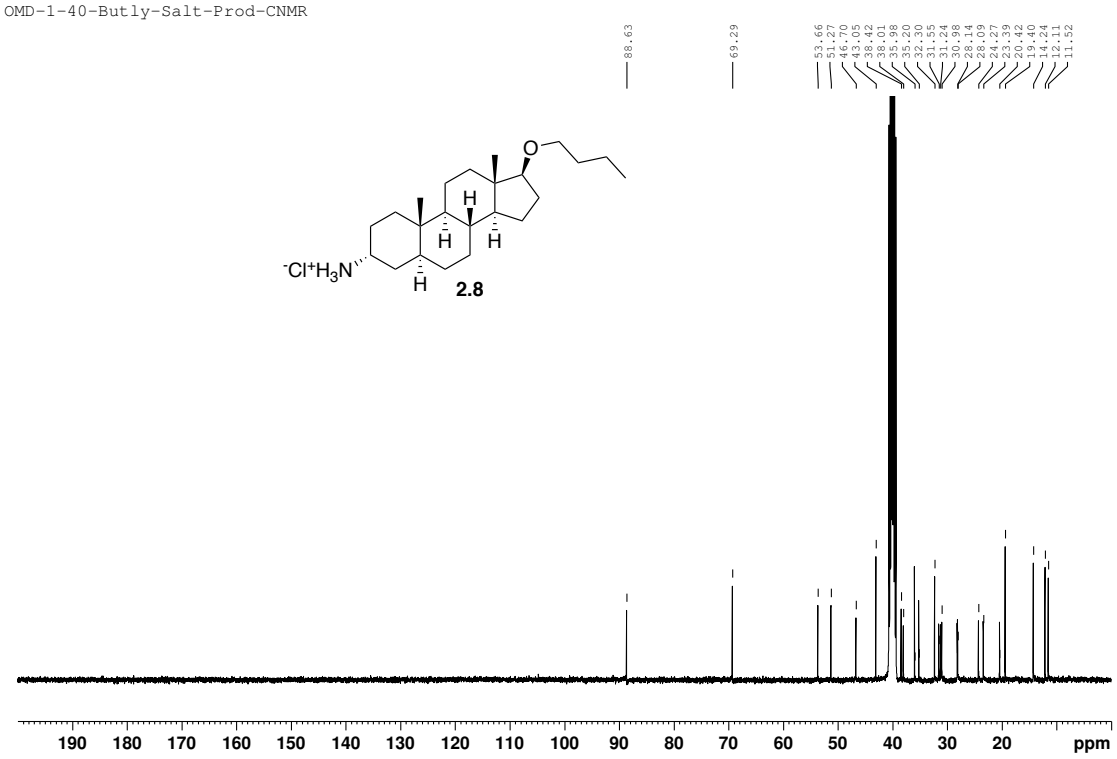
OMD-1-40-Butly-Salt-Prod-CNMR
88.63
69.29
53.66
51.27
46.70
43.05
38.42
38.01
35.98
35.20
32.30
31.55
31.24
30.98
28.14
28.09
24.27
23.39
20.42
19.40
14.24
12.11
11.52
O
H
H
H
H
-Cl+H3N
2.8
190 180 170 160 150 140 130 120 110 100 90 80 70 60 50 40 30 20 ppm

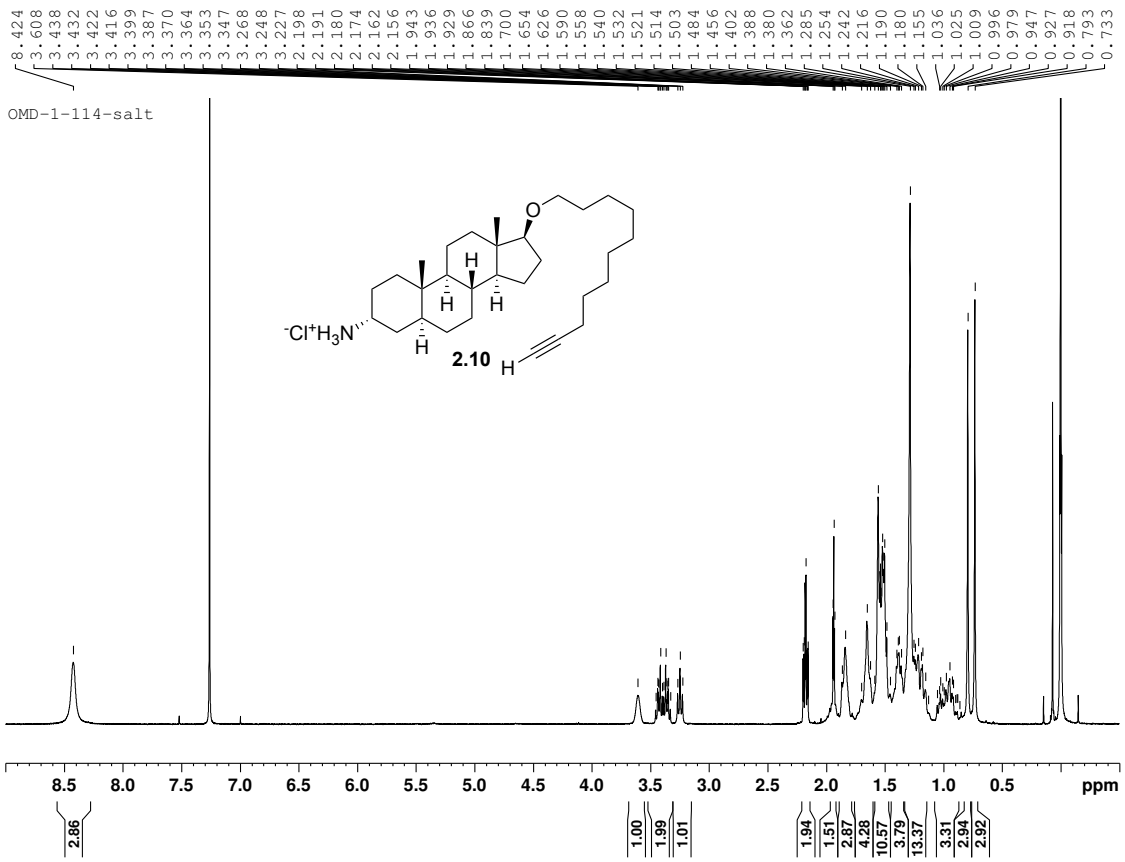
8.424
3.608
3.438
3.432
3.422
3.416
3.399
3.387
3.370
3.364
3.353
3.347
3.268
3.248
3.227
2.198
2.191
2.180
2.174
2.162
2.156
1.943
1.936
1.929
1.866
1.839
1.700
1.654
1.626
1.590
1.558
1.540
1.532
1.521
1.514
1.503
1.484
1.456
1.402
1.388
1.380
1.362
1.285
1.254
1.242
1.216
1.190
1.180
1.155
1.036
1.025
1.009
0.996
0.979
0.947
0.927
0.918
0.793
0.733
OMD-1-114-salt
O
H
H
H
H
-Cl+H3N
2.10
8.5
8.0
7.5
7.0
6.5
6.0
5.5
5.0
4.5
4.0
3.5
3.0
2.5
2.0
1.5
1.0
0.5
ppm
2.86
1.00
1.99
1.01
1.94
1.51
2.87
4.28
10.57
3.79
13.37
3.31
2.94
2.92

OMD-1-114-CNMR

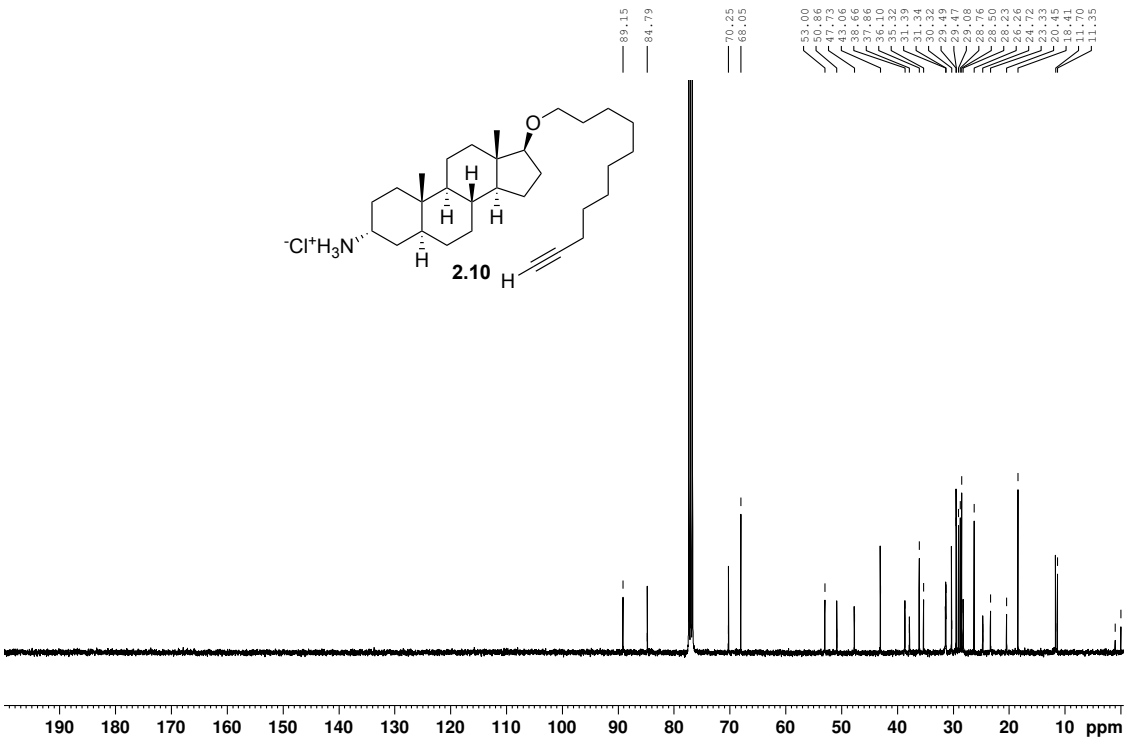

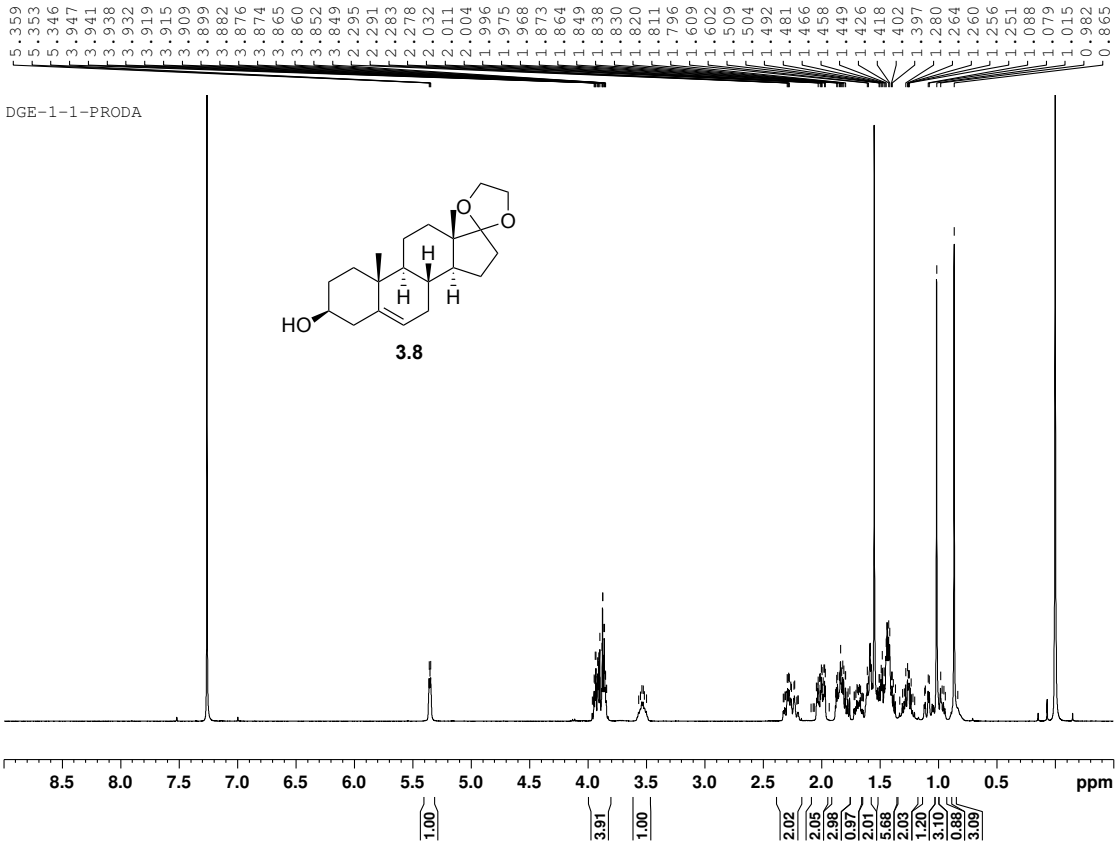
5.359
5.353
5.346
3.947
3.941
3.938
3.932
3.919
3.915
3.909
3.899
3.882
3.876
3.874
3.865
3.860
3.852
3.849
2.295
2.291
2.283
2.278
2.032
2.011
2.004
1.996
1.975
1.968
1.873
1.864
1.849
1.838
1.830
1.820
1.811
1.796
1.609
1.602
1.509
1.504
1.492
1.481
1.466
1.458
1.449
1.426
1.418
1.402
1.397
1.280
1.264
1.260
1.256
1.251
1.088
1.079
1.015
0.982
0.865
DGE-1-1-PRODA
O
O
H
H
H
HO
3.8
8.5
8.0
7.5
7.0
6.5
6.0
5.5
5.0
4.5
4.0
3.5
3.0
2.5
2.0
1.5
1.0
0.5
ppm
1.00
3.91
1.00
2.02
2.05
2.98
0.97
2.01
5.68
2.03
1.20
3.10
0.88
3.09

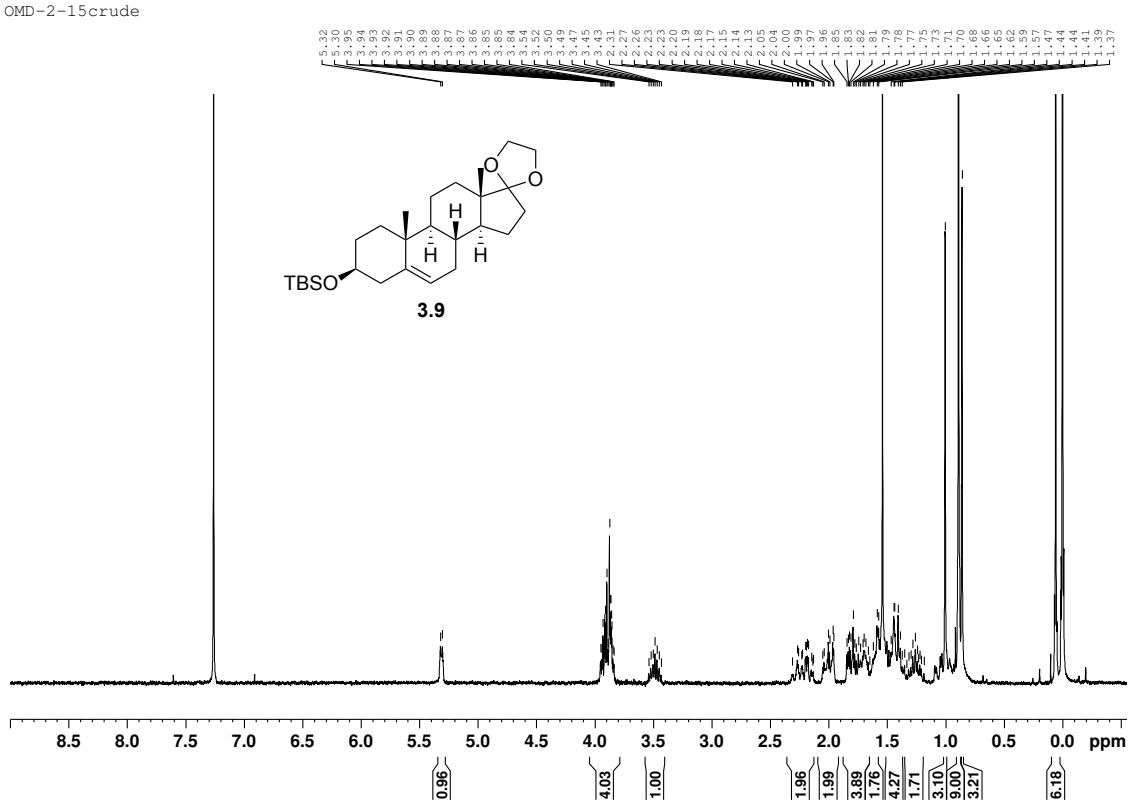
OMD-2-15crude
TBSO
3.9
8.5 8.0 7.5 7.0 6.5 6.0 5.5 5.0 4.5 4.0 3.5 3.0 2.5 2.0 1.5 1.0 0.5 0.0 ppm
0.96
4.03
1.00
1.96
1.99
3.89
1.76
4.27
1.71
3.10
9.00
3.21
6.18

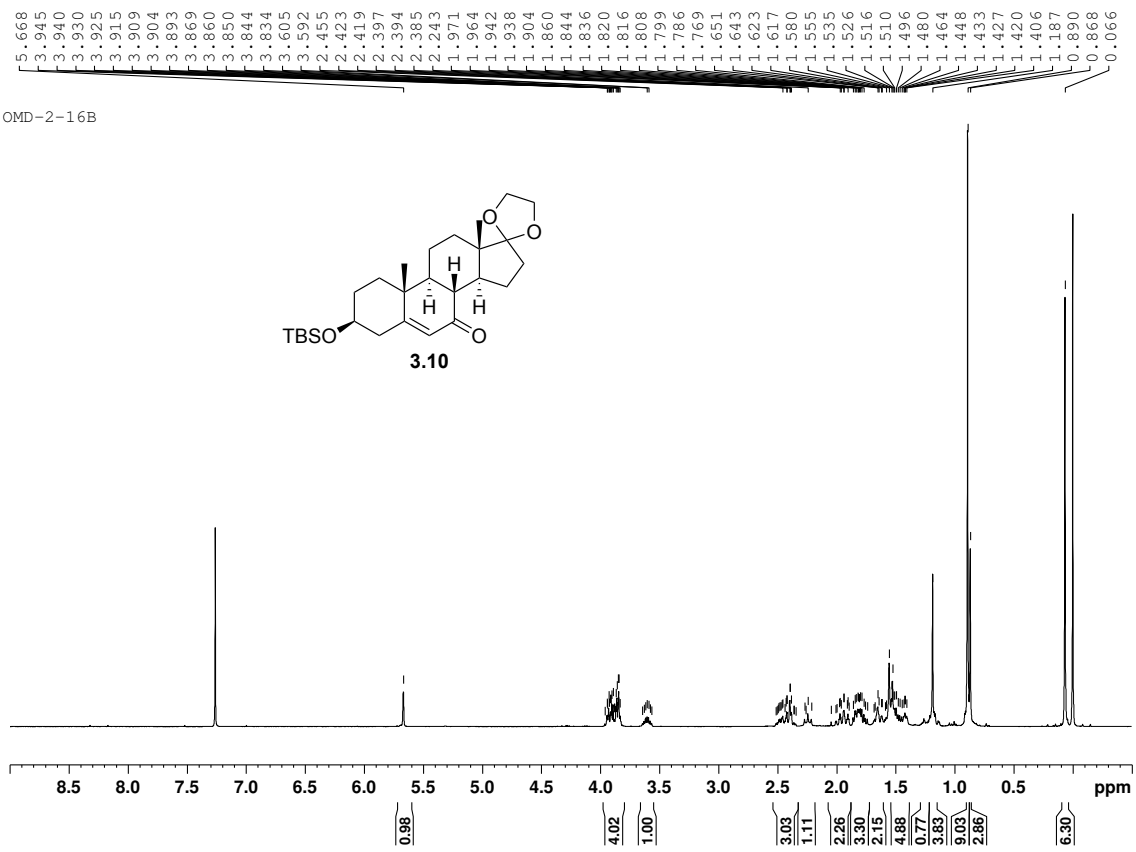
5.668
3.945
3.940
3.930
3.925
3.915
3.909
3.904
3.893
3.869
3.860
3.850
3.844
3.834
3.605
3.592
2.455
2.423
2.419
2.397
2.394
2.385
2.243
1.971
1.964
1.942
1.938
1.904
1.860
1.844
1.836
1.820
1.816
1.808
1.799
1.786
1.769
1.651
1.643
1.623
1.617
1.580
1.555
1.535
1.526
1.516
1.510
1.496
1.480
1.464
1.448
1.433
1.427
1.420
1.406
1.187
0.890
0.868
0.066
OMD-2-16B
O
O
H
H
H
TBSO
O
3.10
8.5
8.0
7.5
7.0
6.5
6.0
5.5
5.0
4.5
4.0
3.5
3.0
2.5
2.0
1.5
1.0
0.5
ppm
0.98
4.02
1.00
3.03
1.11
2.26
3.30
2.15
4.88
0.77
3.83
9.03
2.86
6.30

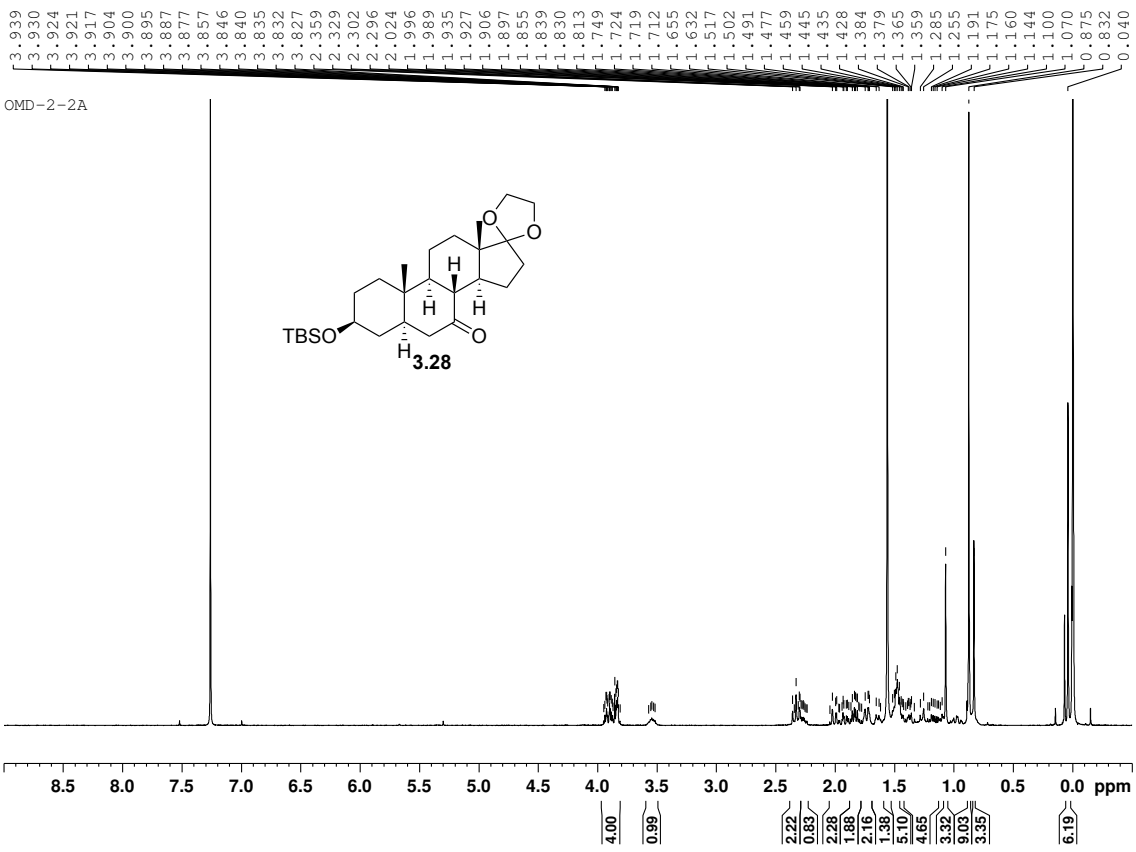
3.939
3.930
3.924
3.921
3.917
3.904
3.900
3.895
3.887
3.877
3.857
3.846
3.840
3.835
3.832
3.827
2.359
2.329
2.302
2.296
2.024
1.996
1.989
1.935
1.927
1.906
1.897
1.855
1.839
1.830
1.813
1.749
1.724
1.719
1.712
1.655
1.632
1.517
1.502
1.491
1.477
1.459
1.445
1.435
1.428
1.384
1.379
1.365
1.359
1.285
1.255
1.191
1.175
1.160
1.144
1.100
1.070
0.875
0.832
0.040
OMD-2-2A
TBSO
O
O
H
H
H
H
O
3.28
8.5
8.0
7.5
7.0
6.5
6.0
5.5
5.0
4.5
4.0
3.5
3.0
2.5
2.0
1.5
1.0
0.5
0.0
ppm
4.00
0.99
2.22
0.83
2.28
1.88
2.16
1.38
5.10
4.65
3.32
9.03
3.35
6.19

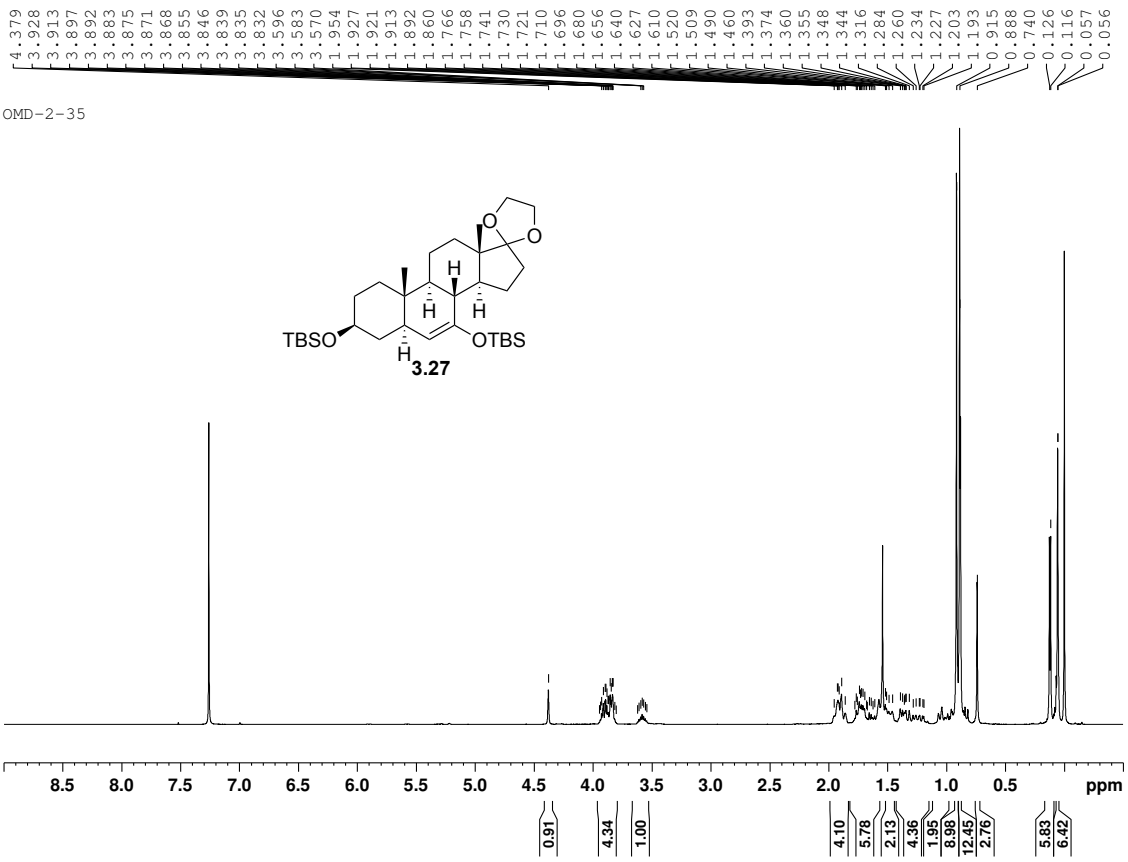
4.379
3.928
3.913
3.897
3.892
3.883
3.875
3.871
3.868
3.855
3.846
3.839
3.835
3.832
3.596
3.583
3.570
1.954
1.927
1.921
1.913
1.892
1.860
1.766
1.758
1.741
1.730
1.721
1.710
1.696
1.680
1.656
1.640
1.627
1.610
1.520
1.509
1.490
1.460
1.393
1.374
1.360
1.355
1.348
1.344
1.316
1.284
1.260
1.234
1.227
1.203
1.193
0.915
0.888
0.740
0.126
0.116
0.057
0.056
OMD-2-35
O
O
H
H
H
H
TBSO
OTBS
3.27
8.5
8.0
7.5
7.0
6.5
6.0
5.5
5.0
4.5
4.0
3.5
3.0
2.5
2.0
1.5
1.0
0.5
ppm
0.91
4.34
1.00
4.10
5.78
2.13
4.36
1.95
8.98
12.45
2.76
5.83
6.42

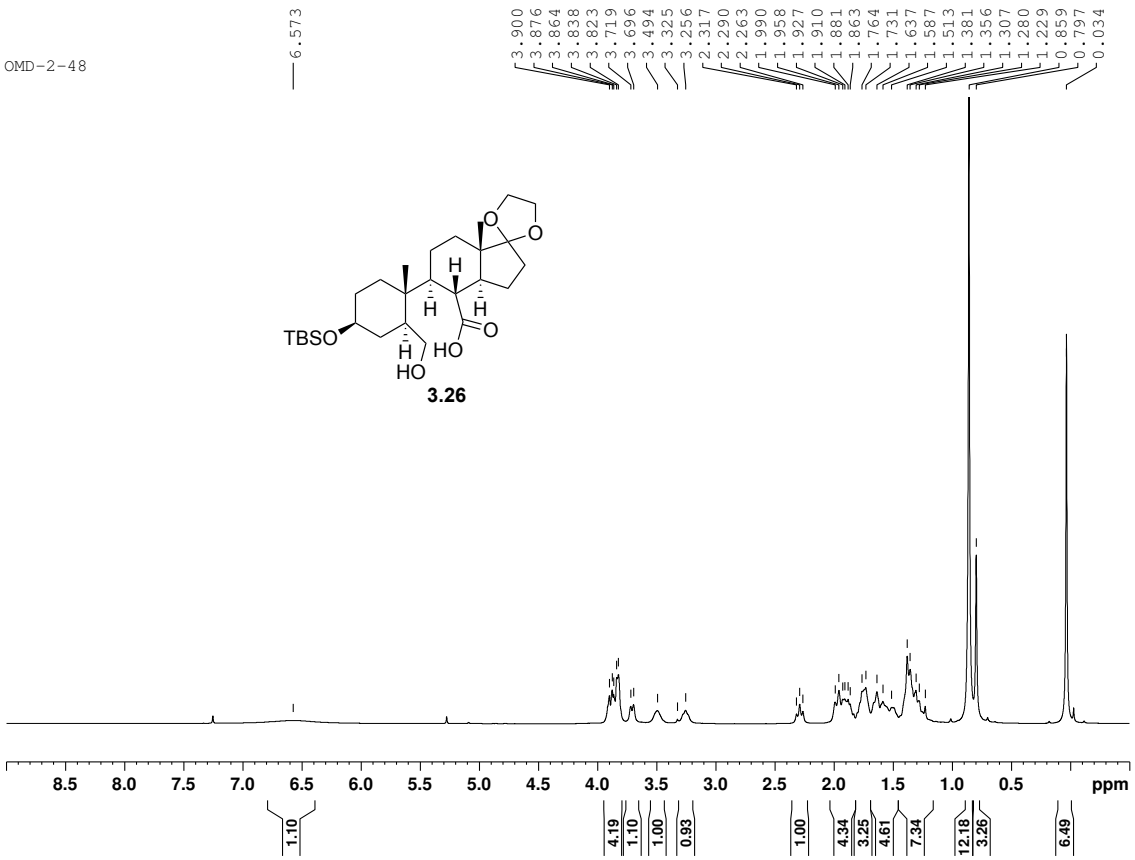
OMD-2-48
6.573
3.900
3.876
3.864
3.838
3.823
3.719
3.696
3.494
3.325
3.256
2.317
2.290
2.263
1.990
1.958
1.927
1.910
1.881
1.863
1.764
1.731
1.637
1.587
1.513
1.381
1.356
1.307
1.280
1.229
0.859
0.797
0.034
TBSO
HO
HO
3.26
8.5
8.0
7.5
7.0
6.5
6.0
5.5
5.0
4.5
4.0
3.5
3.0
2.5
2.0
1.5
1.0
0.5
ppm
1.10
4.19
1.10
1.00
0.93
1.00
4.34
3.25
4.61
7.34
12.18
3.26
6.49

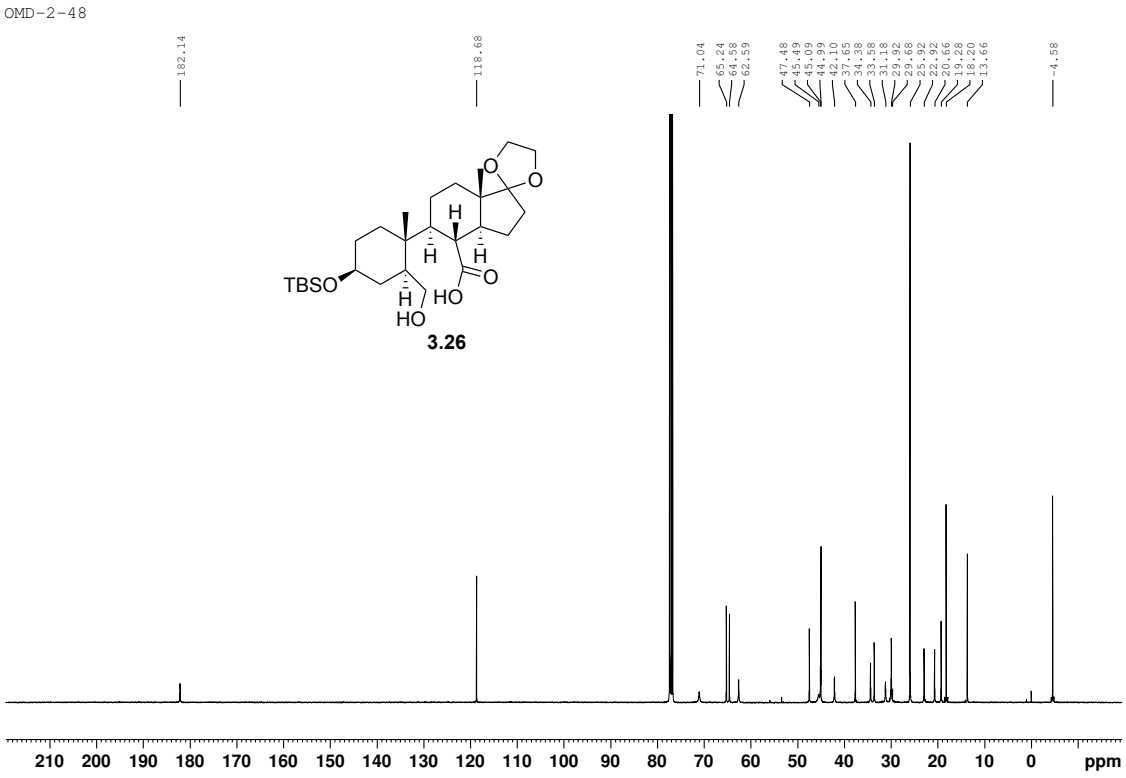
OMD-2-48
182.14
118.68
71.04
65.24
64.58
62.59
47.48
45.49
45.09
44.99
42.10
37.65
34.38
33.58
31.18
29.92
29.68
25.92
22.92
20.66
19.28
18.20
13.66
-4.58
TBSO
HO
HO
3.26
210 200 190 180 170 160 150 140 130 120 110 100 90 80 70 60 50 40 30 20 10 0 ppm

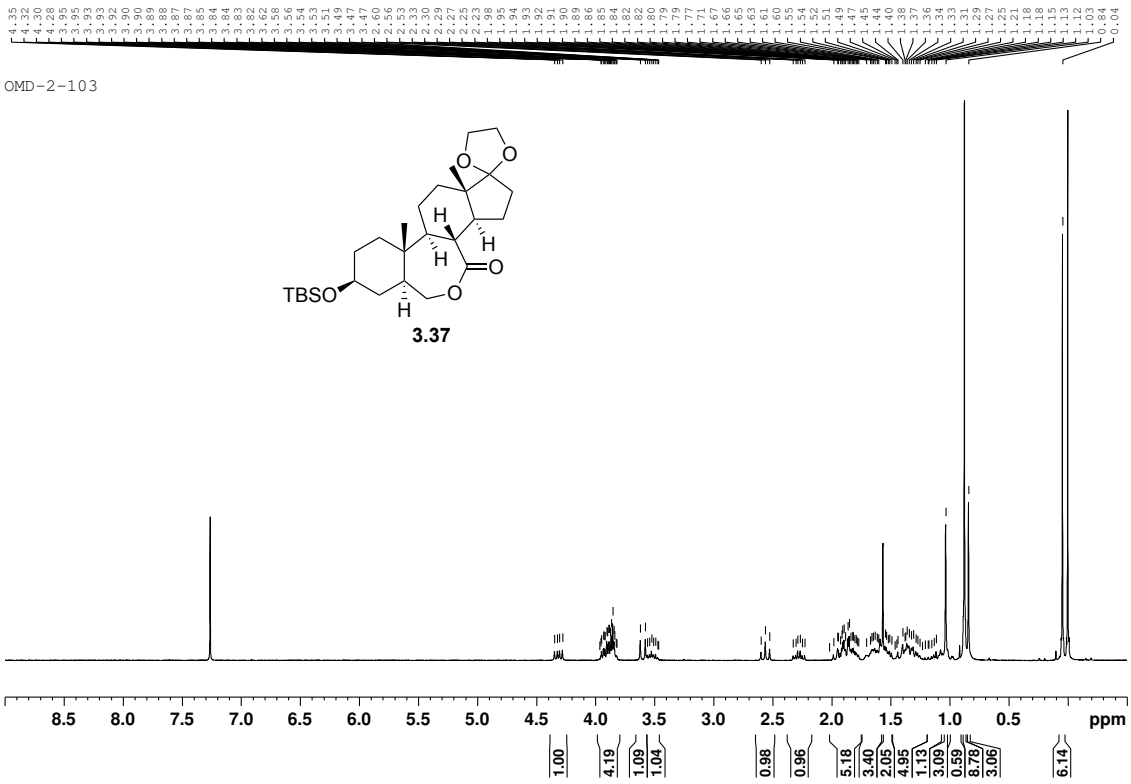
OMD-2-103
TBSO
H
O
3.37
ppm
8.5
8.0
7.5
7.0
6.5
6.0
5.5
5.0
4.5
4.0
3.5
3.0
2.5
2.0
1.5
1.0
0.5
1.00
4.19
1.09
1.04
0.98
0.96
5.18
3.40
2.05
4.95
1.13
3.09
0.59
8.78
3.06
6.14

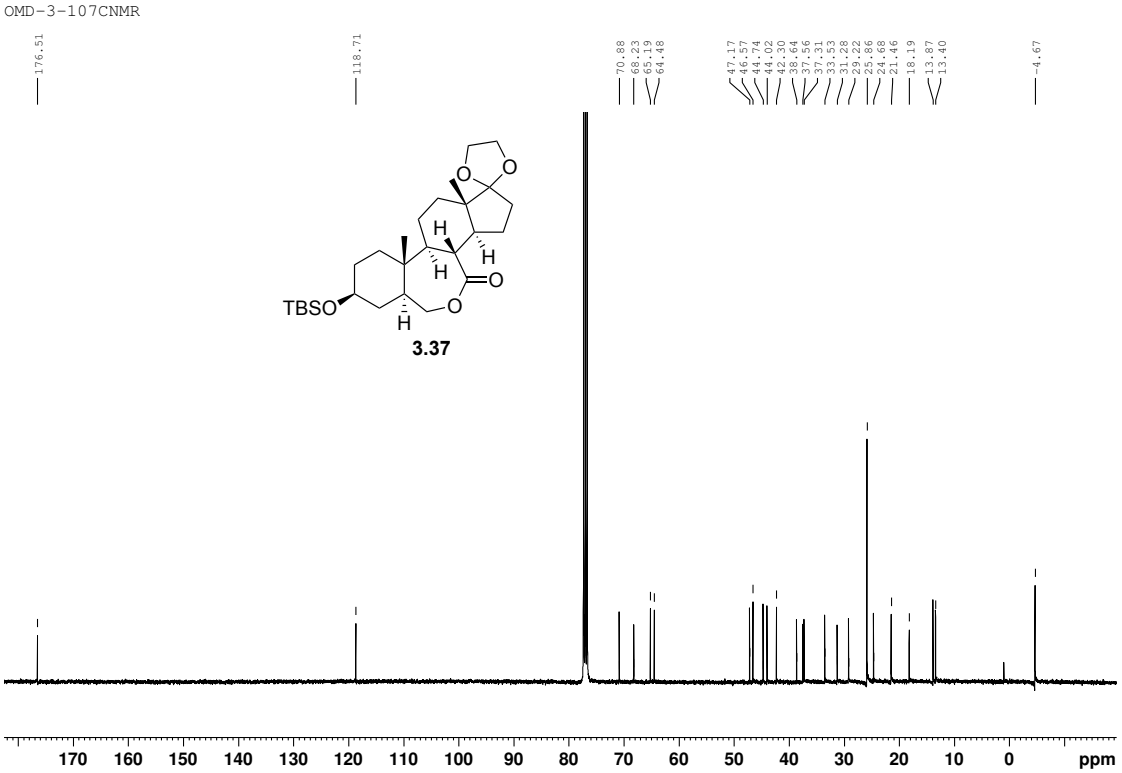
OMD-3-107CNMR
176.51
118.71
70.88
68.23
65.19
64.48
47.17
46.57
44.74
44.02
42.30
38.64
37.56
37.31
33.53
31.28
29.22
25.66
24.68
21.46
18.19
13.87
13.40
-4.67
TBSO
H
H
H
H
O
O
O
O
3.37
170
160
150
140
130
120
110
100
90
80
70
60
50
40
30
20
10
0
ppm

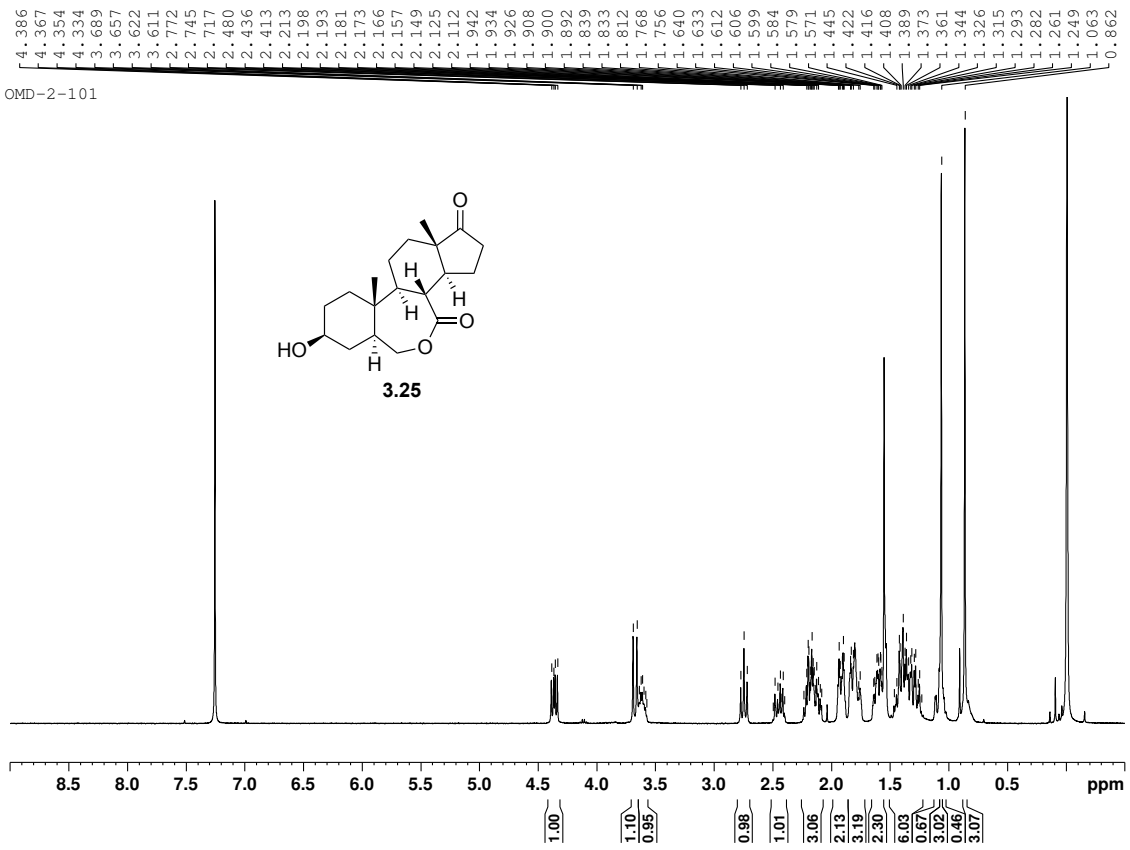
4.386
4.367
4.354
4.334
3.689
3.657
3.622
3.611
2.772
2.745
2.717
2.480
2.436
2.413
2.213
2.198
2.193
2.181
2.173
2.166
2.157
2.149
2.125
2.112
1.942
1.934
1.926
1.908
1.900
1.892
1.839
1.833
1.812
1.768
1.756
1.640
1.633
1.612
1.606
1.599
1.584
1.579
1.571
1.445
1.422
1.416
1.408
1.389
1.373
1.361
1.344
1.326
1.315
1.293
1.282
1.261
1.249
1.063
0.862
OMD-2-101
HO
O
H
H
H
O
O
H
8.5
8.0
7.5
7.0
6.5
6.0
5.5
5.0
4.5
4.0
3.5
3.0
2.5
2.0
1.5
1.0
0.5
ppm
1.00
1.10
0.95
0.98
1.01
3.06
2.13
3.19
2.30
6.03
0.67
3.02
0.46
3.07

3.25

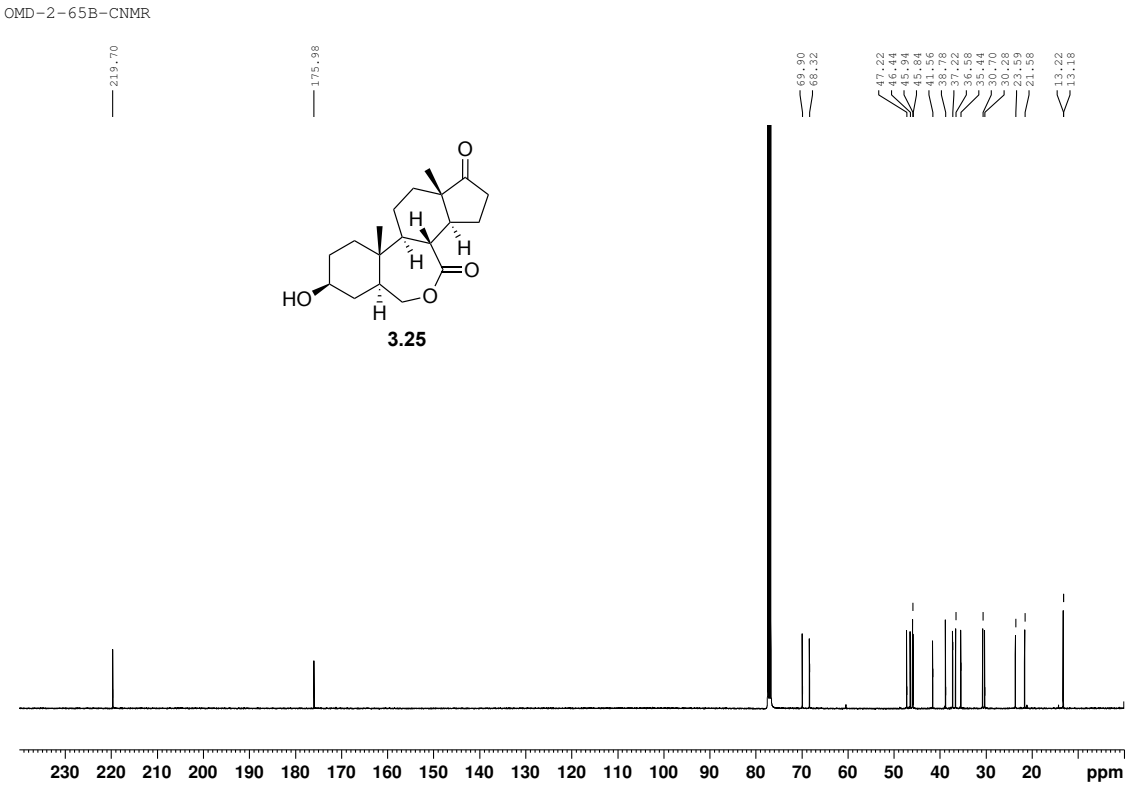
OMD-2-65B-CNMR
219.70
175.98
69.90
68.32
47.22
46.44
45.94
45.84
41.56
38.78
37.22
36.58
35.44
30.70
30.28
23.59
21.58
13.22
13.18
O
H
H
H
HO
O
O
H
3.25
230 220 210 200 190 180 170 160 150 140 130 120 110 100 90 80 70 60 50 40 30 20 ppm

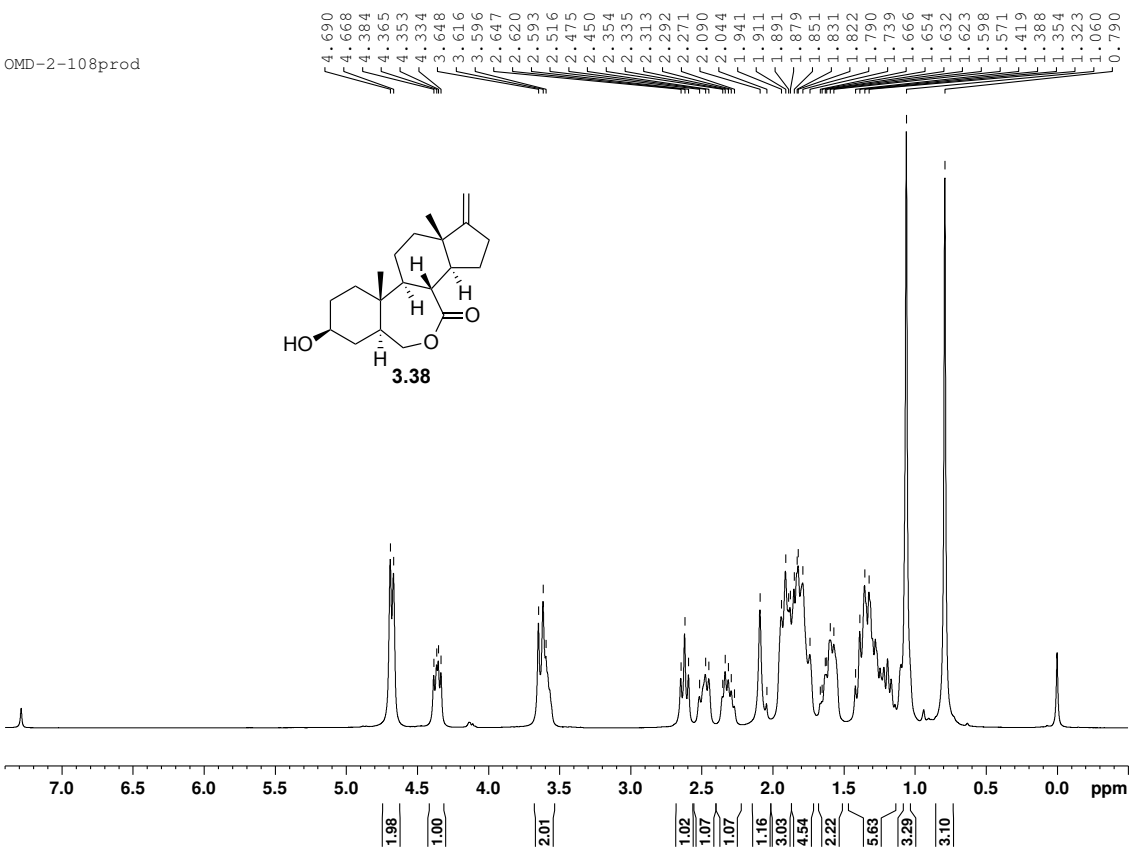
OMD-2-108prod
4.690
4.668
4.384
4.365
4.353
4.334
3.648
3.616
3.596
2.647
2.620
2.593
2.516
2.475
2.450
2.354
2.335
2.313
2.292
2.271
2.090
2.044
1.941
1.911
1.891
1.879
1.851
1.831
1.822
1.790
1.739
1.666
1.654
1.632
1.623
1.598
1.571
1.419
1.388
1.354
1.323
1.060
0.790
HO
O
O
H
H
H
H
3.38
7.0
6.5
6.0
5.5
5.0
4.5
4.0
3.5
3.0
2.5
2.0
1.5
1.0
0.5
0.0
ppm
1.98
1.00
2.01
1.02
1.07
1.07
1.16
3.03
4.54
2.22
5.63
3.29
3.10

OMD-2-108prodCNMR

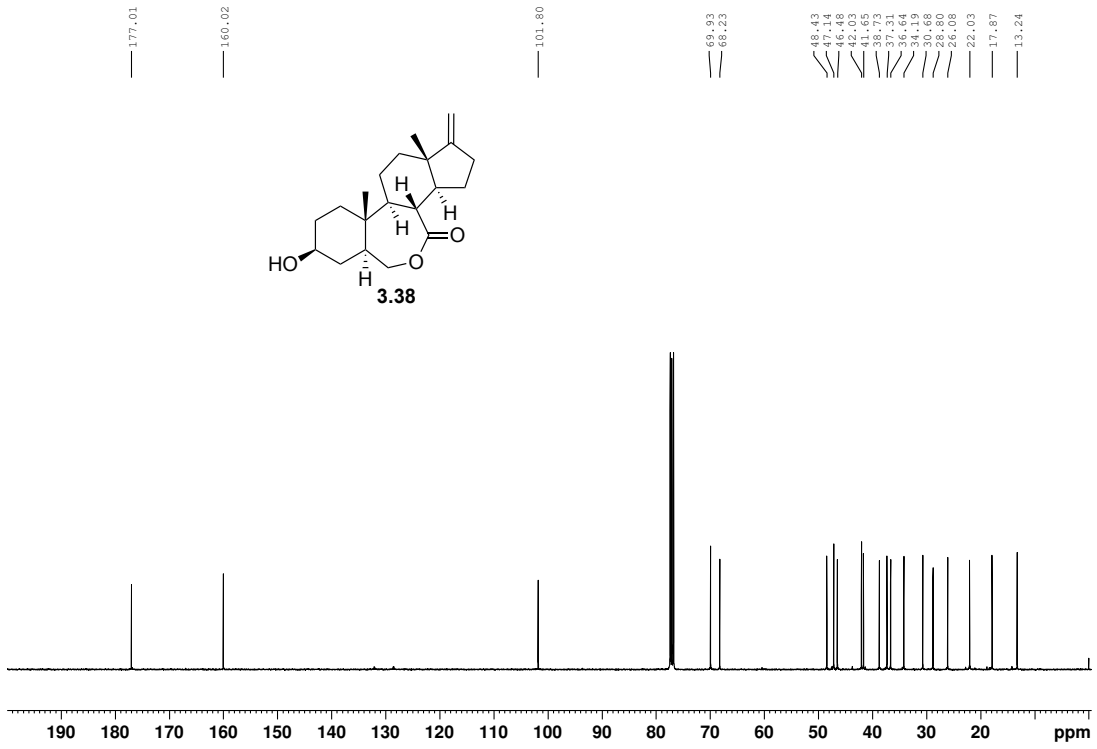

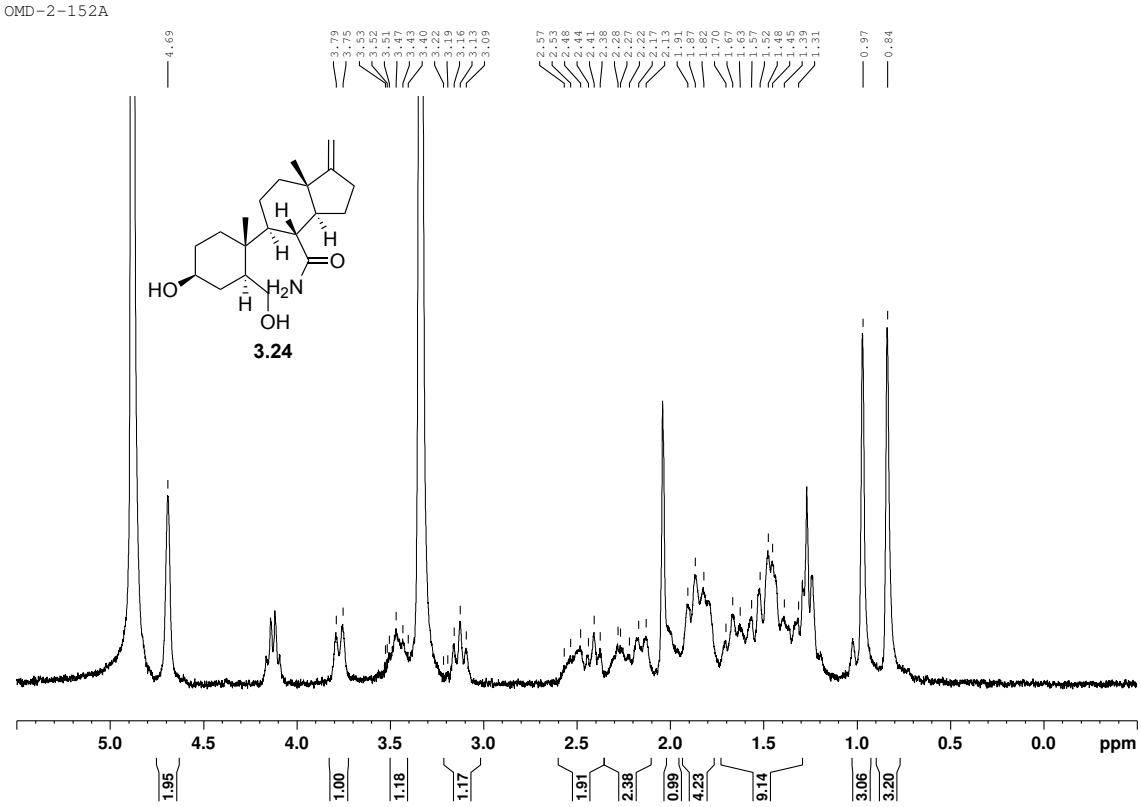
OMD-2-152A
4.69
3.79
3.75
3.53
3.52
3.51
3.47
3.43
3.40
3.22
3.19
3.16
3.13
3.09
2.57
2.53
2.48
2.44
2.41
2.38
2.28
2.27
2.22
2.17
2.13
1.91
1.87
1.82
1.70
1.67
1.63
1.57
1.52
1.48
1.45
1.39
1.31
0.97
0.84
HO
H
H
H
H
O
H2N
OH
3.24
5.0
4.5
4.0
3.5
3.0
2.5
2.0
1.5
1.0
0.5
0.0
ppm
1.95
1.00
1.18
1.17
1.91
2.38
0.99
4.23
9.14
3.06
3.20

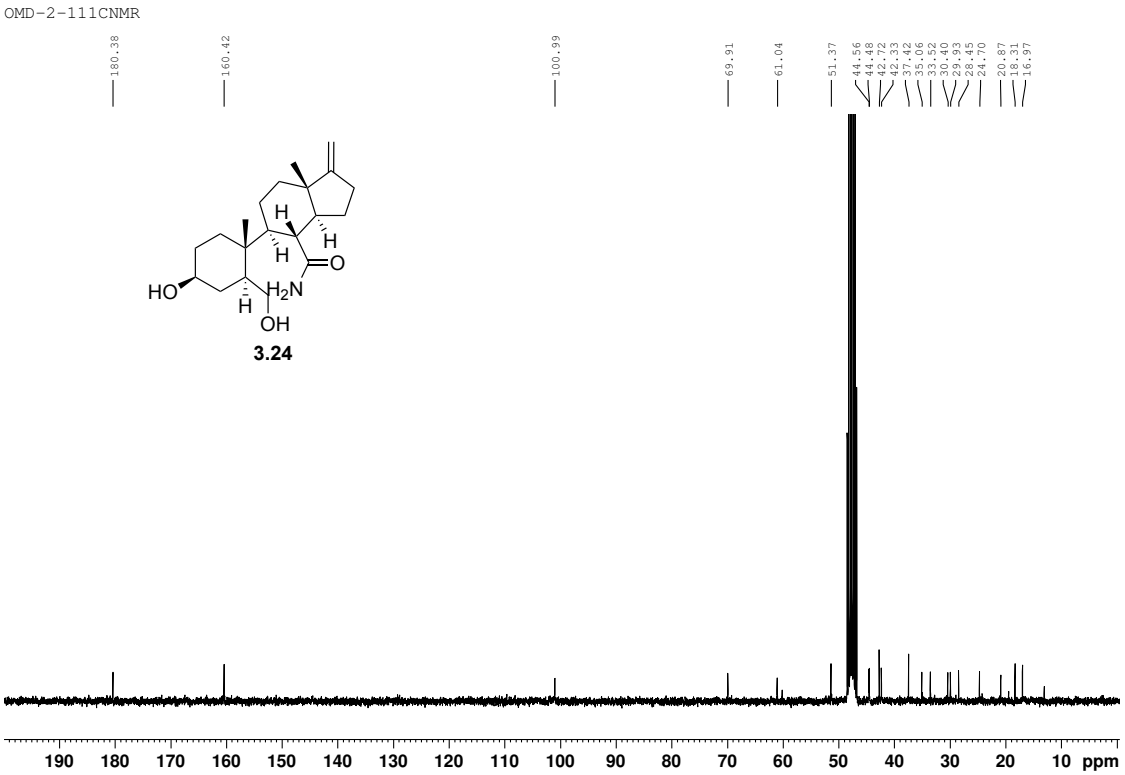
OMD-2-111CNMR
180.38
160.42
100.99
69.91
61.04
51.37
44.56
44.48
42.72
42.33
37.42
35.06
33.52
30.40
29.93
28.45
24.70
20.87
18.31
16.97
H
H
H
O
HO
H
H_2N
OH
190 180 170 160 150 140 130 120 110 100 90 80 70 60 50 40 30 20 10 ppm

3.24

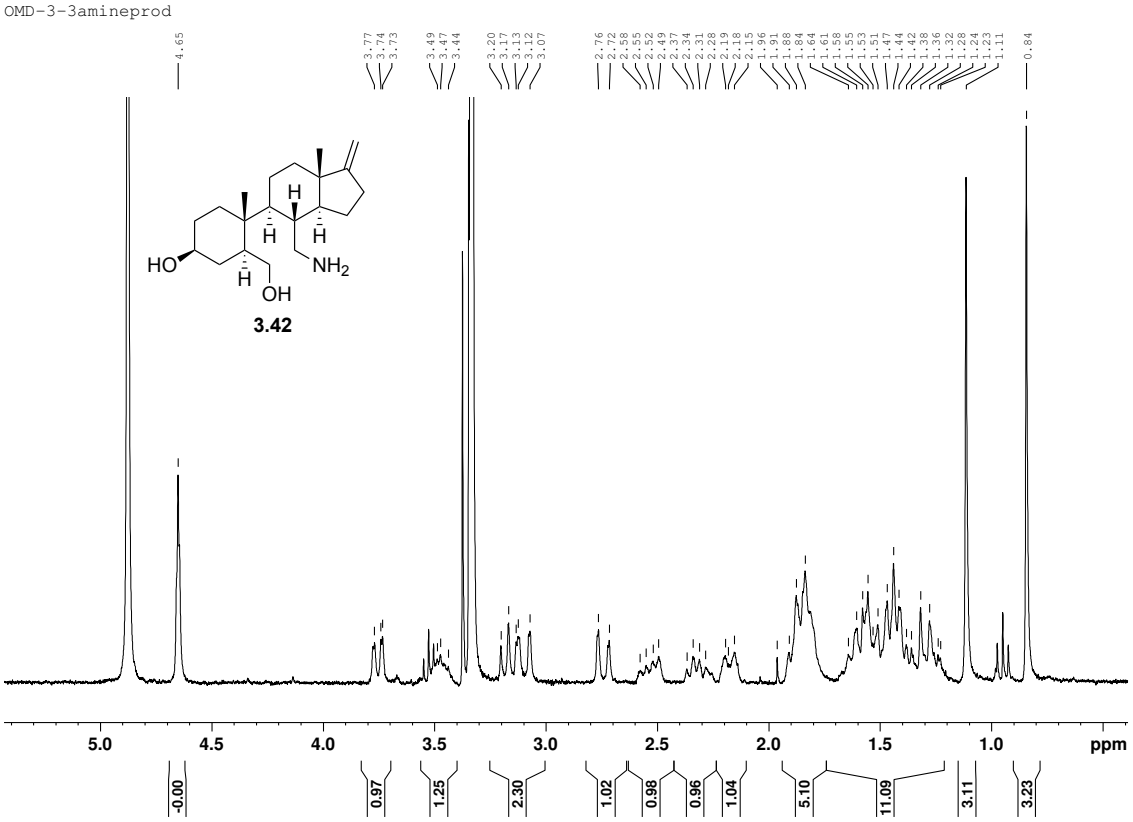
OMD-3-3amineprod
4.65
3.77
3.74
3.73
3.49
3.47
3.44
3.20
3.17
3.13
3.12
3.07
2.76
2.72
2.58
2.55
2.52
2.49
2.37
2.34
2.31
2.28
2.19
2.18
2.15
1.96
1.91
1.88
1.84
1.64
1.61
1.58
1.55
1.53
1.51
1.47
1.44
1.42
1.38
1.36
1.32
1.28
1.24
1.23
1.11
0.84
HO
H
H
H
H
NH2
OH
3.42
5.0
4.5
4.0
3.5
3.0
2.5
2.0
1.5
1.0
ppm
-0.00
0.97
1.25
2.30
1.02
0.98
0.96
1.04
5.10
11.09
3.11
3.23

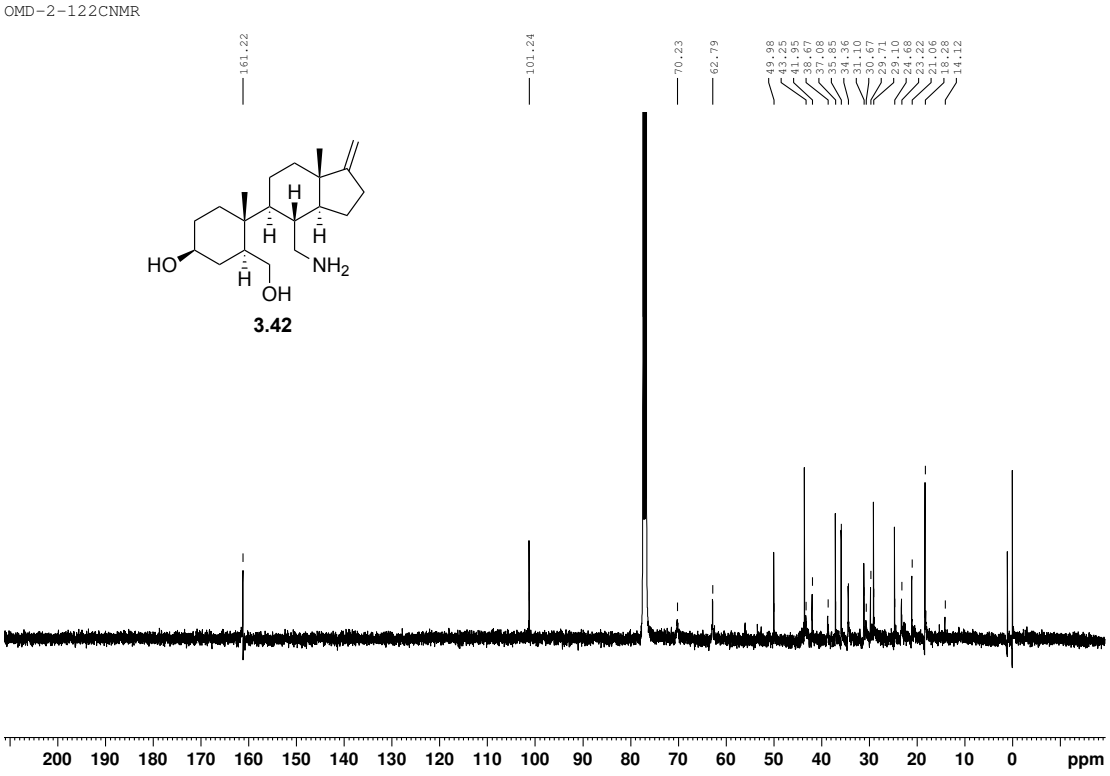
OMD-2-122CNMR
161.22
101.24
70.23
62.79
49.98
43.25
41.95
38.67
37.08
35.85
34.36
31.10
30.67
29.71
29.10
24.68
23.22
21.06
18.28
14.12
HO
H
H
H
H
NH2
OH
3.42
200 190 180 170 160 150 140 130 120 110 100 90 80 70 60 50 40 30 20 10 0 ppm

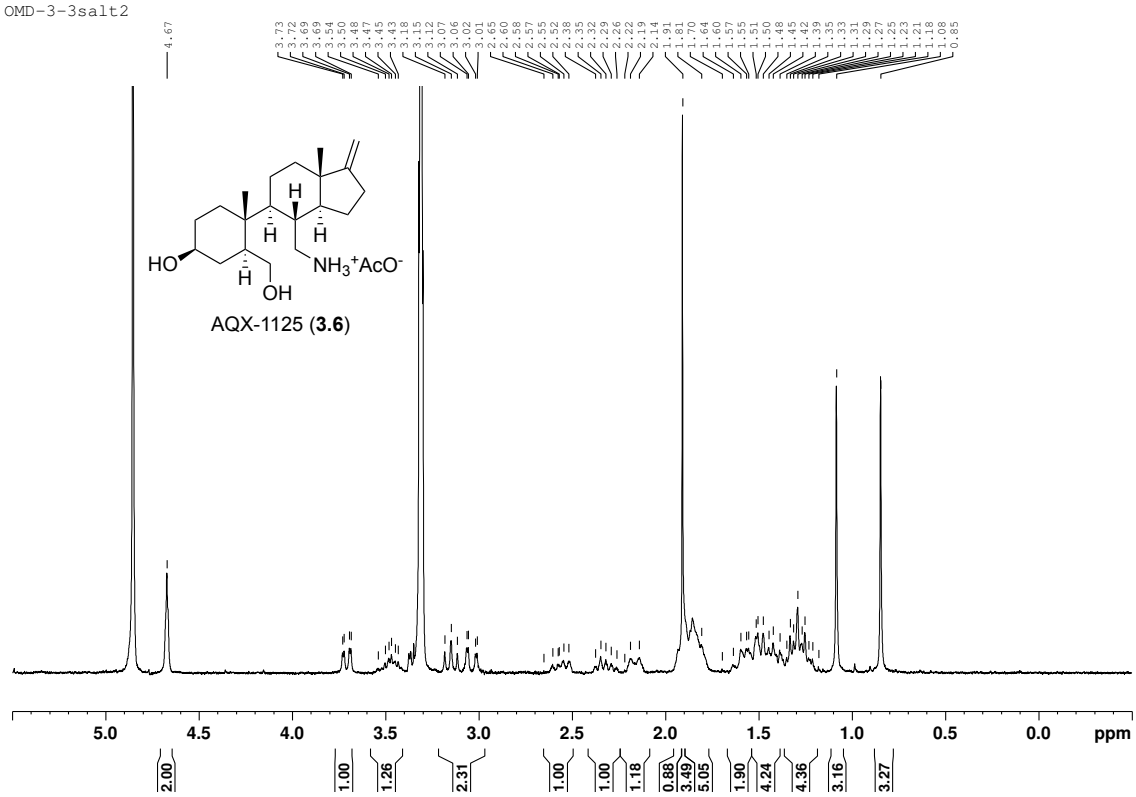
OMD-3-3salt2
AQX-1125 (3.6)
ppm

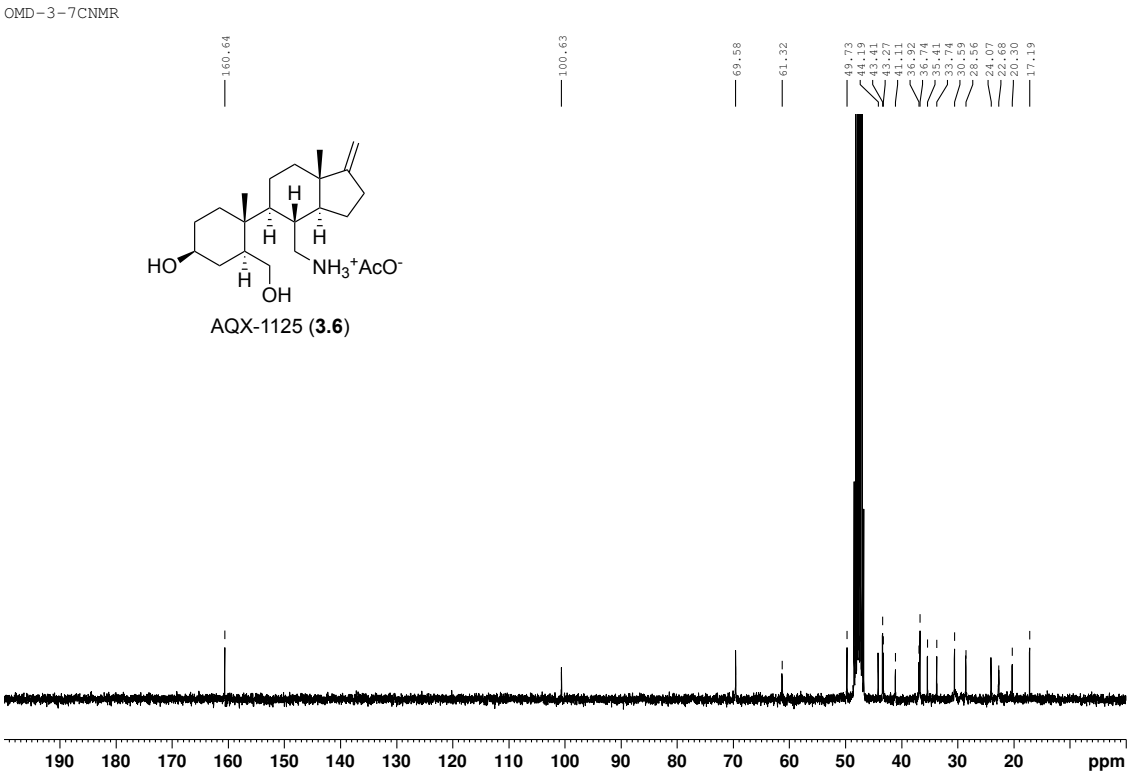
OMD-3-7CNMR
160.64
100.63
69.58
61.32
49.73
44.19
43.41
43.27
41.11
36.92
36.74
35.41
33.74
30.59
28.56
24.07
22.68
20.30
17.19
HO
H
H
H
H
OH
NH3+AcO-
190
180
170
160
150
140
130
120
110
100
90
80
70
60
50
40
30
20
ppm

AQX-1125 (**3.6**)

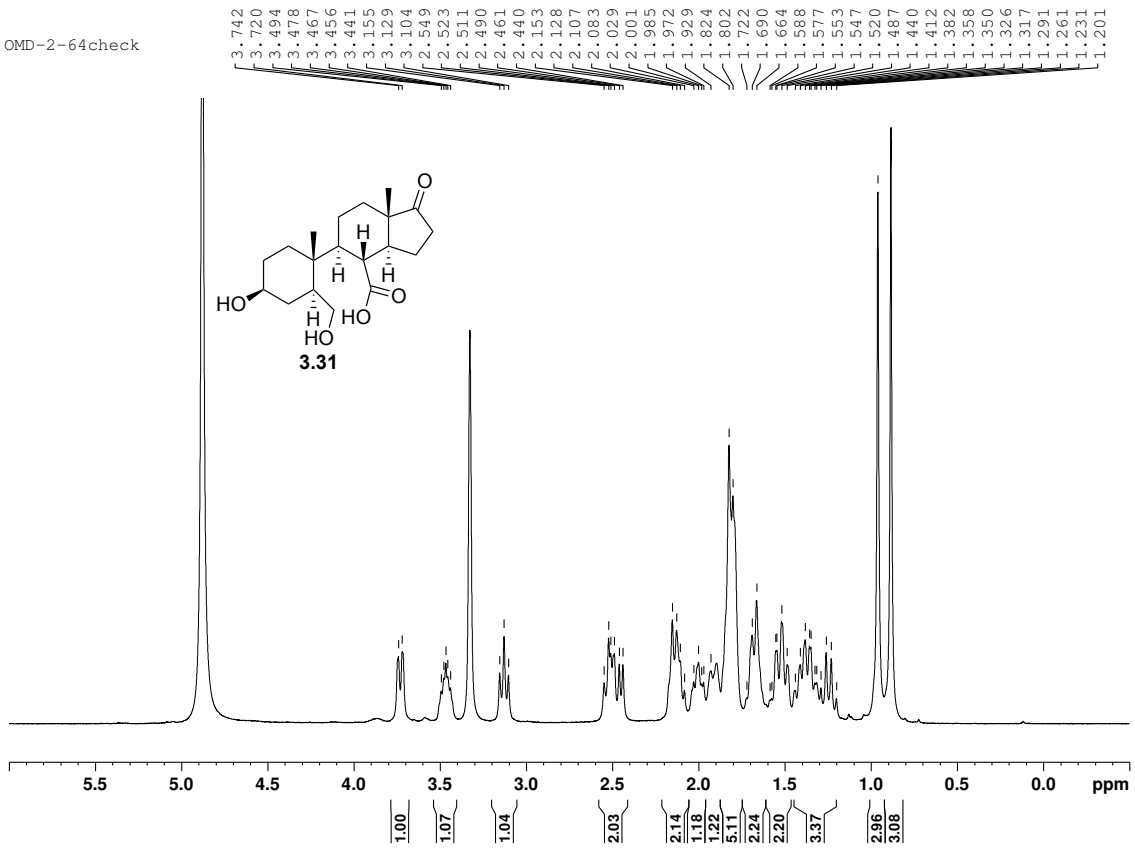
OMD-2-64check
3.742
3.720
3.494
3.478
3.467
3.456
3.441
3.155
3.129
3.104
2.549
2.523
2.511
2.490
2.461
2.440
2.153
2.128
2.107
2.083
2.029
2.001
1.985
1.972
1.929
1.824
1.802
1.722
1.690
1.664
1.588
1.577
1.553
1.547
1.520
1.487
1.440
1.412
1.382
1.358
1.350
1.326
1.317
1.291
1.261
1.231
1.201
O
H
H
H
O
HO
HO
HO
H
3.31
5.5
5.0
4.5
4.0
3.5
3.0
2.5
2.0
1.5
1.0
0.5
0.0
ppm
1.00
1.07
1.04
2.03
2.14
1.18
1.22
5.11
2.24
2.20
3.37
2.96
3.08

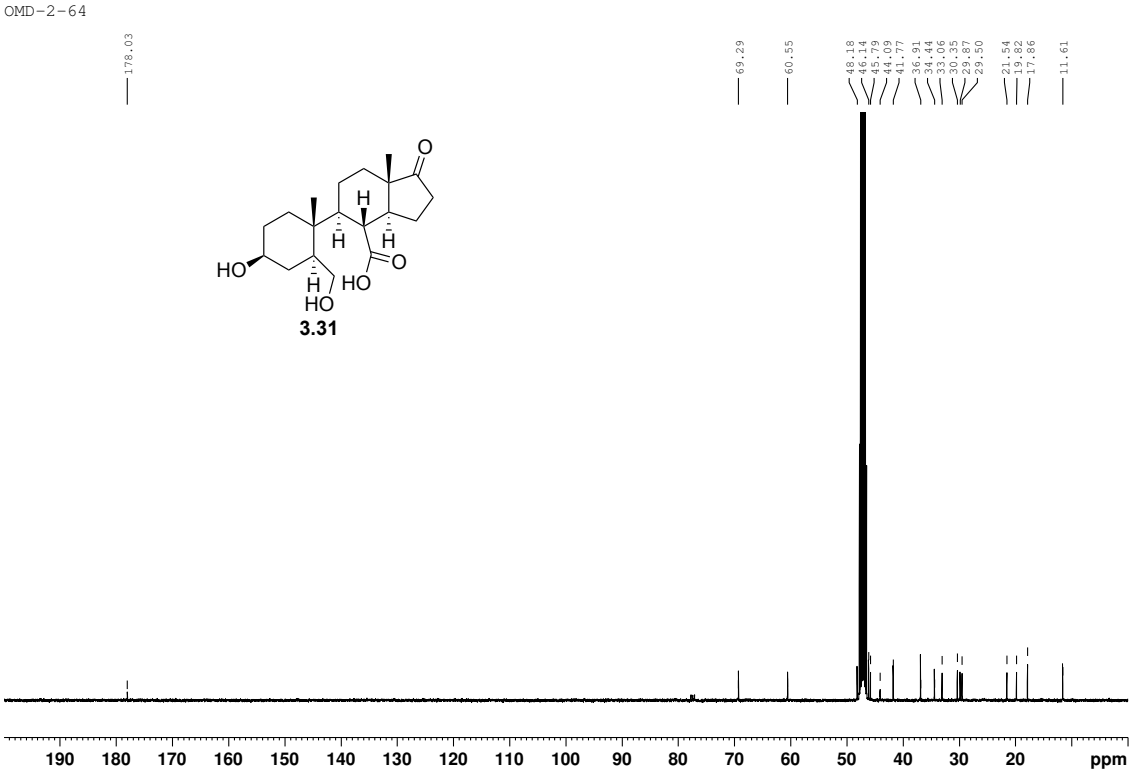
OMD-2-64
178.03
69.29
60.55
48.18
46.14
45.79
44.09
41.77
36.91
34.44
33.06
30.35
30.07
29.50
21.54
19.82
17.86
11.61
HO
HO
HO
H
H
H
H
O
O
190
180
170
160
150
140
130
120
110
100
90
80
70
60
50
40
30
20
ppm

3.31

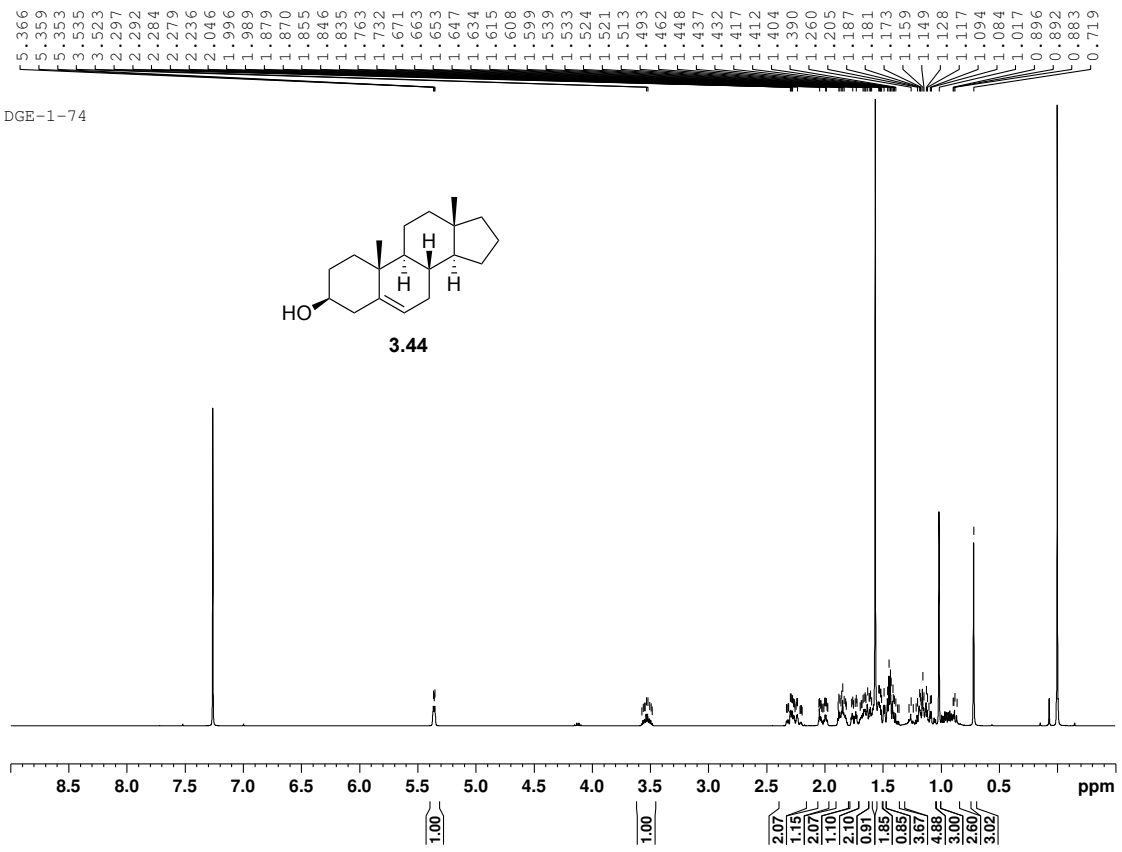
5.366
5.359
5.353
3.535
3.523
2.297
2.292
2.284
2.279
2.236
2.046
1.996
1.989
1.879
1.870
1.855
1.846
1.835
1.763
1.732
1.671
1.663
1.653
1.647
1.634
1.615
1.608
1.599
1.539
1.533
1.524
1.521
1.513
1.493
1.462
1.448
1.437
1.432
1.417
1.412
1.404
1.390
1.260
1.205
1.187
1.181
1.173
1.159
1.149
1.128
1.117
1.094
1.084
1.017
0.896
0.892
0.883
0.719
DGE-1-74
H
H
H
HO
3.44
8.5
8.0
7.5
7.0
6.5
6.0
5.5
5.0
4.5
4.0
3.5
3.0
2.5
2.0
1.5
1.0
0.5
ppm
1.00
1.00
2.07
1.15
2.07
1.10
2.10
0.91
1.85
0.85
3.67
4.88
3.00
2.60
3.02

DGE-1-47 CNMR

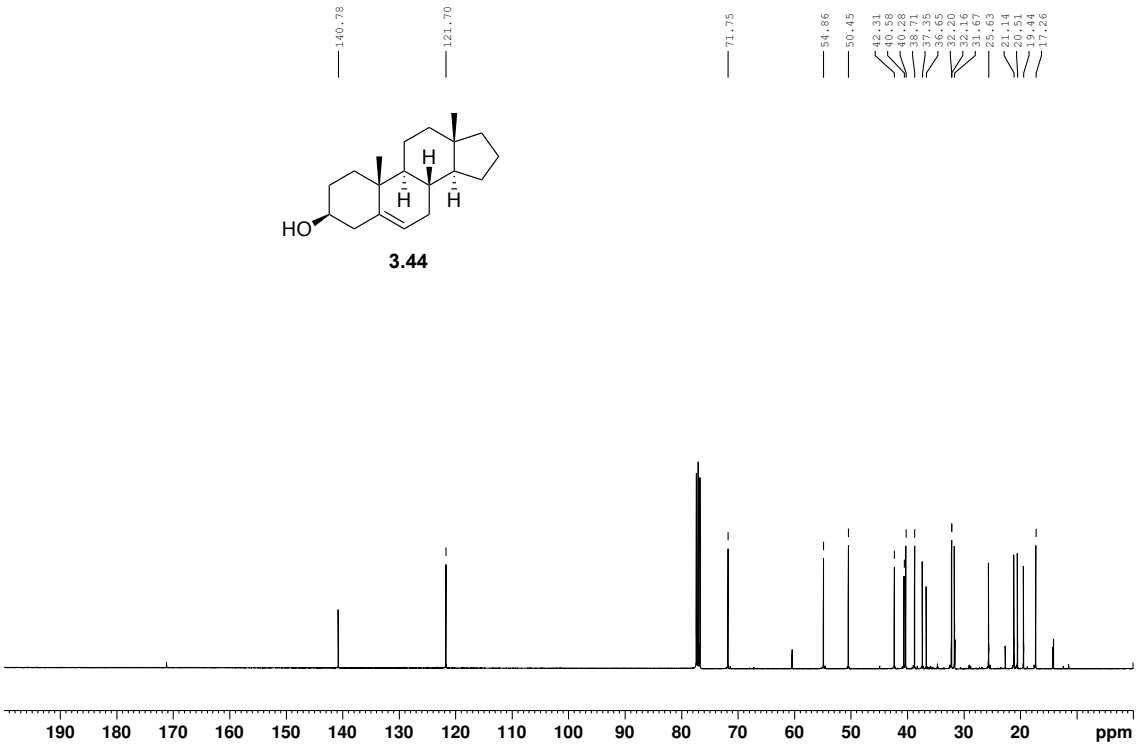
140.78
121.70
71.75
54.86
50.45
42.31
40.58
40.28
38.71
37.35
36.55
35.20
32.16
31.67
25.63
21.14
20.51
19.44
17.26
H
H
H
HO
3.44
190
180
170
160
150
140
130
120
110
100
90
80
70
60
50
40
30
20
ppm

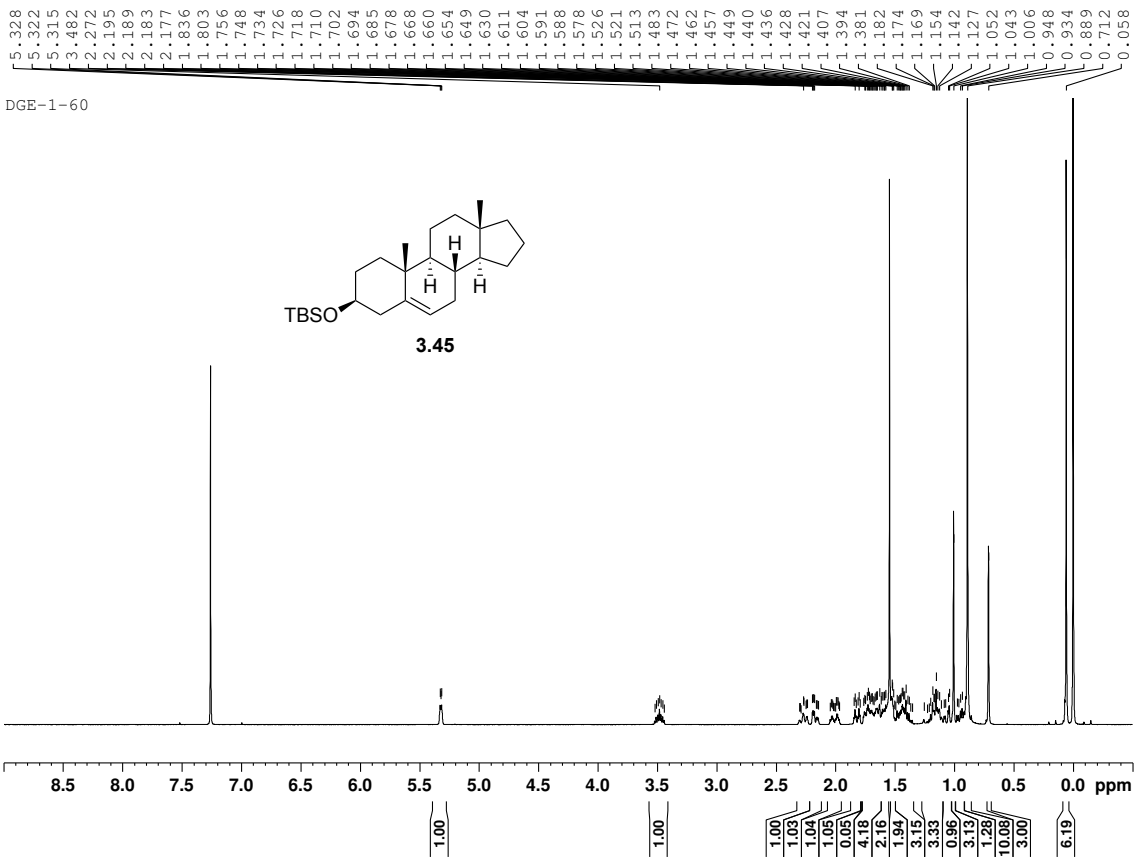
5.328
5.322
5.315
3.482
2.272
2.195
2.189
2.183
2.177
1.836
1.803
1.756
1.748
1.734
1.726
1.718
1.710
1.702
1.694
1.685
1.678
1.668
1.660
1.654
1.649
1.630
1.611
1.604
1.591
1.588
1.578
1.526
1.521
1.513
1.483
1.472
1.462
1.457
1.449
1.440
1.436
1.428
1.421
1.407
1.394
1.381
1.182
1.174
1.169
1.154
1.142
1.127
1.052
1.043
1.006
0.948
0.934
0.889
0.712
0.058
DGE-1-60
H
H
H
TBSO
3.45
8.5
8.0
7.5
7.0
6.5
6.0
5.5
5.0
4.5
4.0
3.5
3.0
2.5
2.0
1.5
1.0
0.5
0.0
ppm
1.00
1.00
1.00
1.03
1.04
1.05
0.05
4.18
2.16
1.94
3.15
3.33
0.96
3.13
1.28
10.08
3.00
6.19

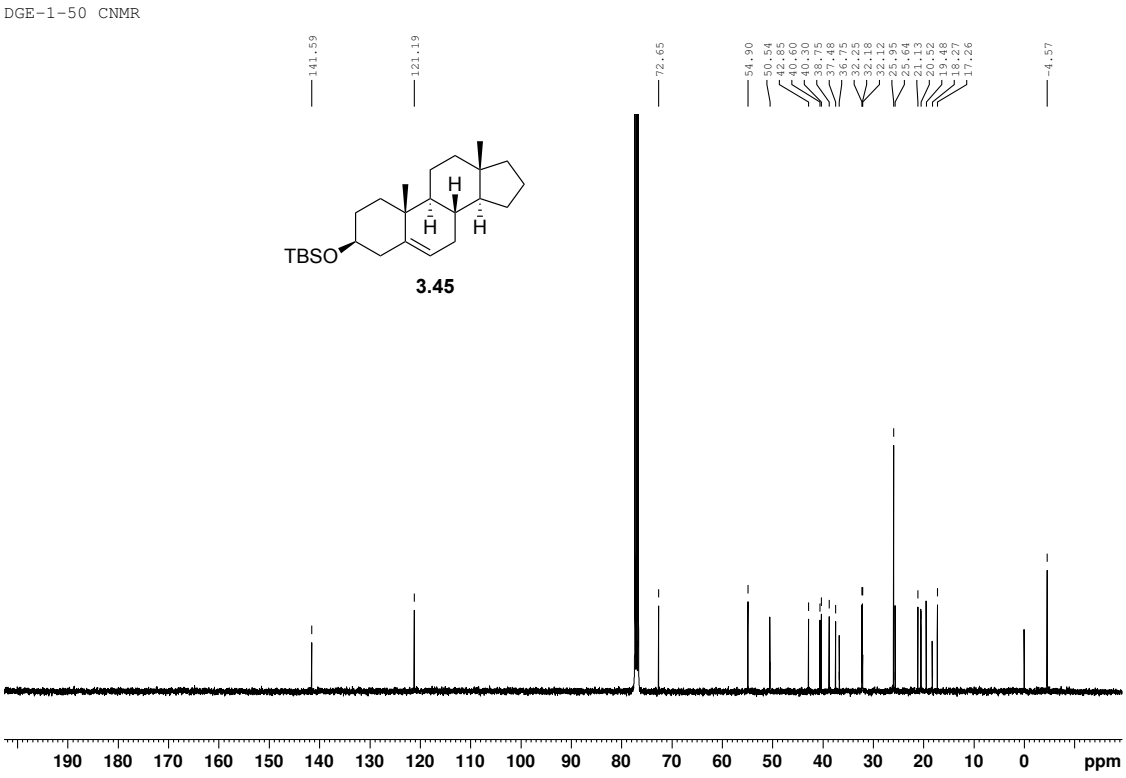
DGE-1-50 CNMR
141.59
121.19
72.65
54.90
50.54
42.85
40.60
40.30
38.75
37.48
36.75
32.25
32.18
32.12
25.95
25.64
21.13
20.52
19.48
18.27
17.26
-4.57
H
H
H
TBSO
3.45
190 180 170 160 150 140 130 120 110 100 90 80 70 60 50 40 30 20 10 0 ppm

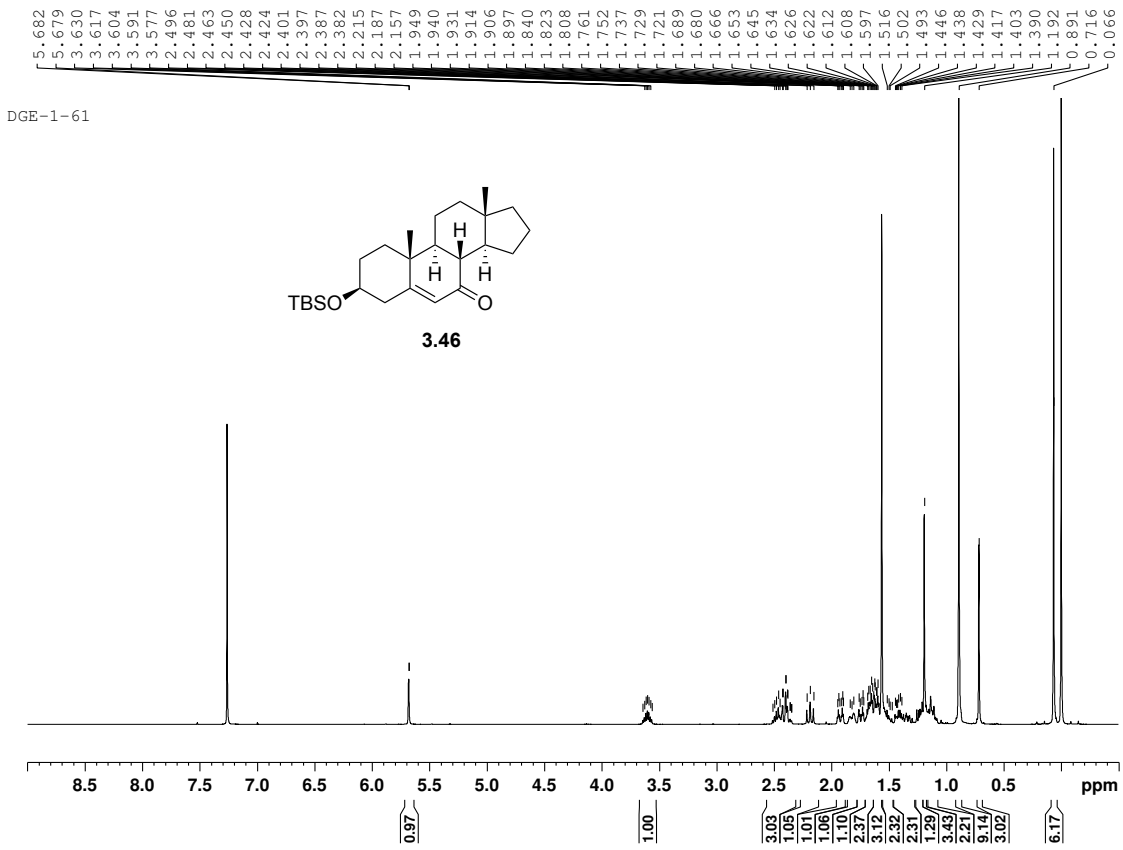
5.682
5.679
5.630
3.617
3.604
3.591
3.577
2.496
2.481
2.463
2.450
2.428
2.424
2.401
2.397
2.387
2.382
2.215
2.187
2.157
1.949
1.940
1.931
1.914
1.906
1.897
1.840
1.823
1.808
1.761
1.752
1.737
1.729
1.721
1.689
1.680
1.666
1.653
1.645
1.634
1.626
1.622
1.612
1.608
1.597
1.516
1.502
1.493
1.446
1.438
1.429
1.417
1.403
1.390
1.192
0.891
0.716
0.066
DGE-1-61
H
H
H
TBSO
O
8.5
8.0
7.5
7.0
6.5
6.0
5.5
5.0
4.5
4.0
3.5
3.0
2.5
2.0
1.5
1.0
0.5
ppm
0.97
1.00
3.03
1.05
1.01
1.06
1.10
2.37
3.12
2.32
2.31
1.29
3.43
2.21
9.14
3.02
6.17

3.46

DGE-1-63 CNMR

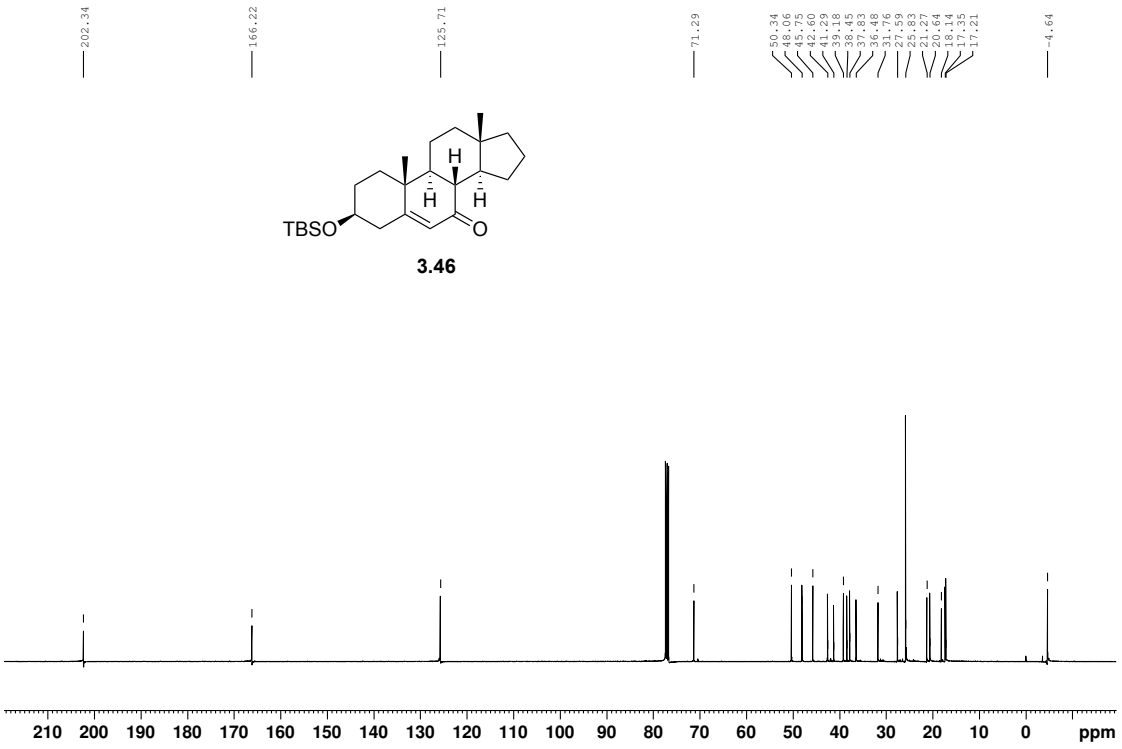

3.46

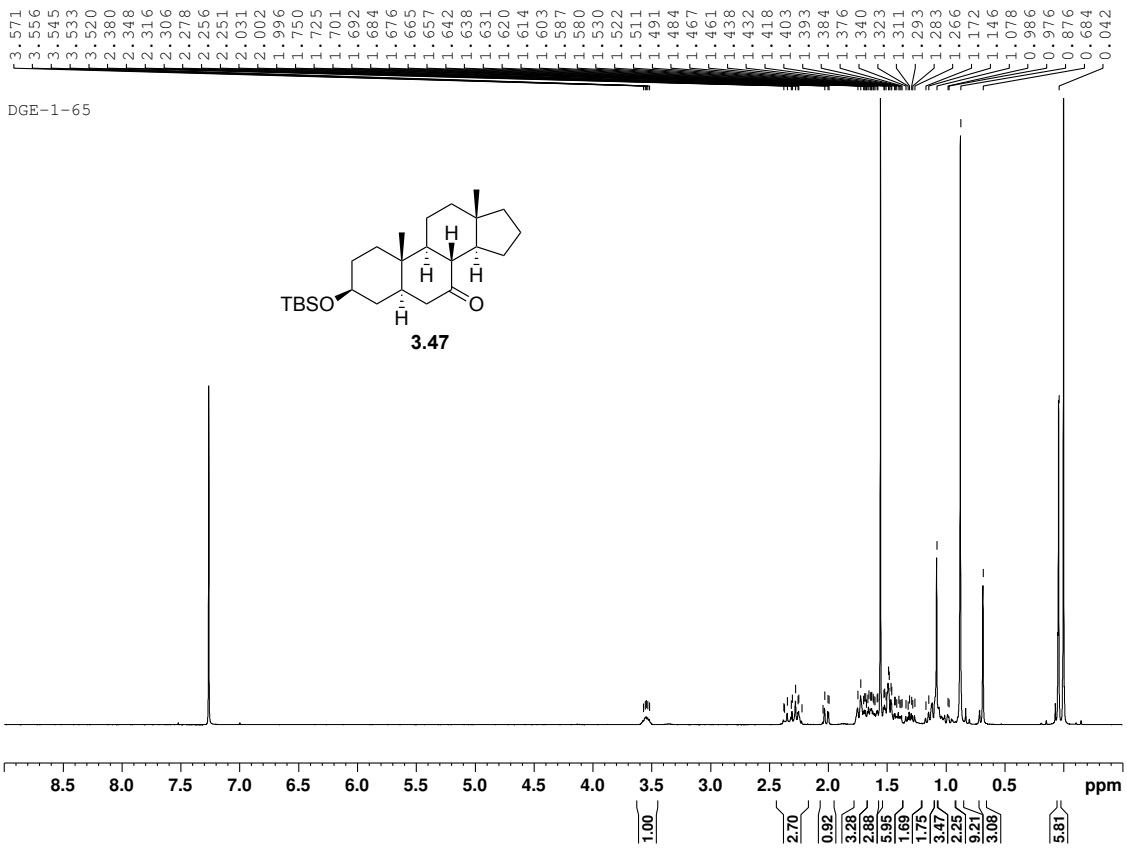
3.571
3.556
3.545
3.533
3.520
2.380
2.348
2.316
2.306
2.278
2.256
2.251
2.031
2.002
1.996
1.750
1.725
1.701
1.692
1.684
1.676
1.665
1.657
1.642
1.638
1.631
1.620
1.614
1.603
1.587
1.580
1.530
1.522
1.511
1.491
1.484
1.467
1.461
1.438
1.432
1.418
1.403
1.393
1.384
1.376
1.340
1.323
1.311
1.293
1.283
1.266
1.172
1.146
1.078
0.986
0.976
0.876
0.684
0.042
DGE-1-65
TBSO
H
H
H
H
O
3.47
8.5
8.0
7.5
7.0
6.5
6.0
5.5
5.0
4.5
4.0
3.5
3.0
2.5
2.0
1.5
1.0
0.5
ppm
1.00
2.70
0.92
3.28
2.88
5.95
1.69
1.75
3.47
2.25
9.21
3.08
5.81

DGE-1-65 CNMR

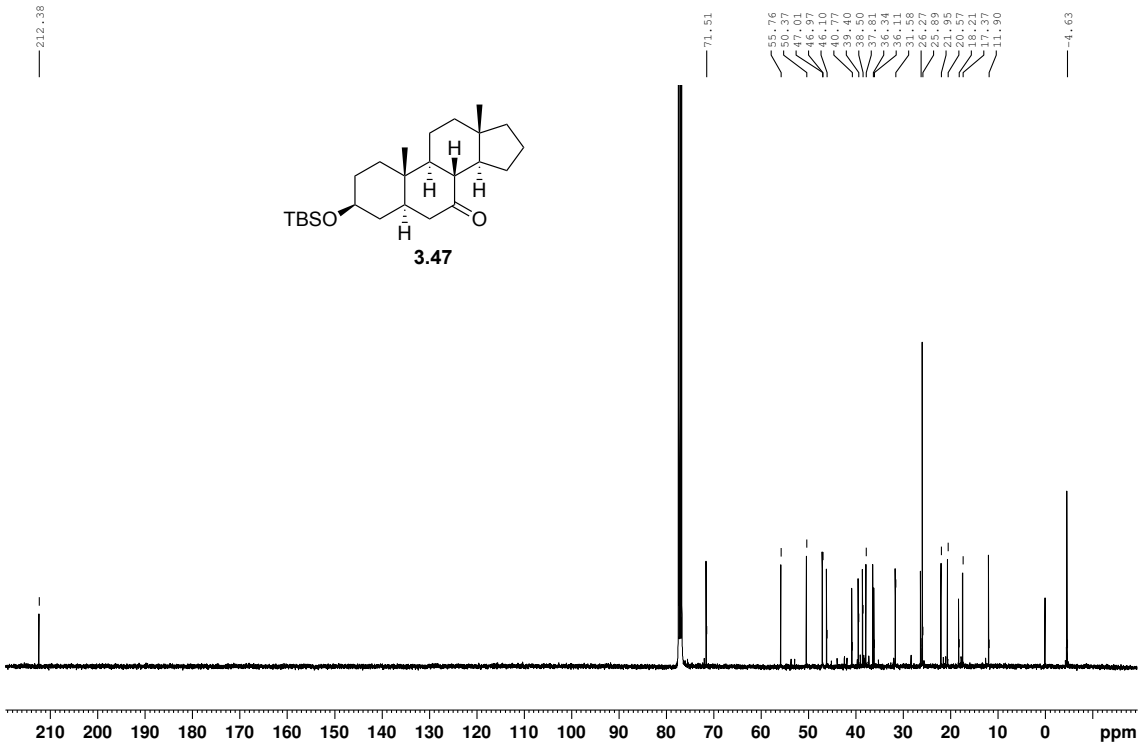
212.38
71.51
55.76
55.37
47.01
46.97
46.10
40.77
39.40
38.50
37.81
36.34
36.11
31.58
26.27
25.89
21.95
20.57
18.21
17.37
11.90
-4.63
TBSO
H
H
H
H
O
3.47
210 200 190 180 170 160 150 140 130 120 110 100 90 80 70 60 50 40 30 20 10 0 ppm

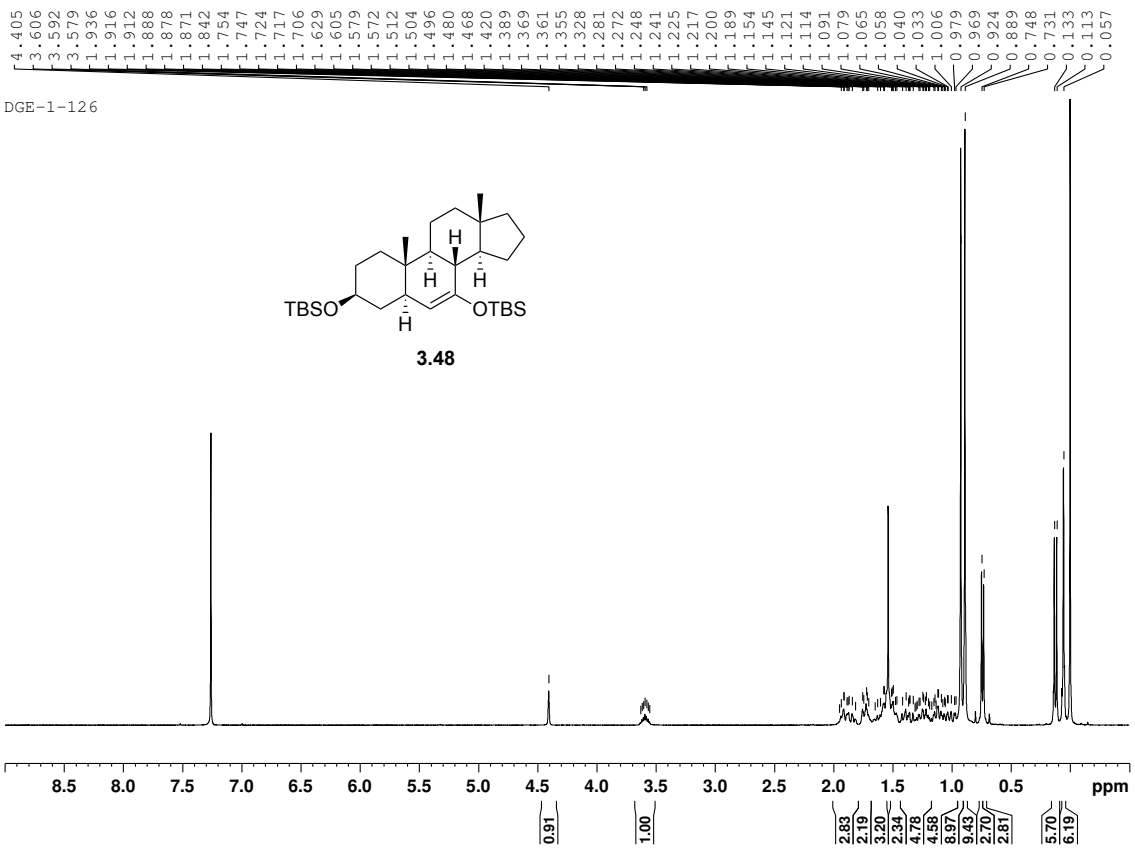
4.405
3.606
3.592
3.579
1.936
1.916
1.912
1.888
1.878
1.871
1.842
1.754
1.747
1.724
1.717
1.706
1.629
1.605
1.579
1.572
1.512
1.504
1.496
1.480
1.468
1.420
1.389
1.369
1.361
1.355
1.328
1.281
1.272
1.248
1.241
1.225
1.217
1.200
1.189
1.154
1.145
1.121
1.114
1.091
1.079
1.065
1.058
1.040
1.033
1.006
0.979
0.969
0.924
0.889
0.748
0.731
0.133
0.113
0.057
DGE-1-126
H
H
H
H
TBSO
OTBS
3.48
8.5
8.0
7.5
7.0
6.5
6.0
5.5
5.0
4.5
4.0
3.5
3.0
2.5
2.0
1.5
1.0
0.5
ppm
0.91
1.00
2.83
2.19
3.20
2.34
4.78
8.97
9.43
2.70
2.81
5.70
6.19

DGE-1-70 CNMR

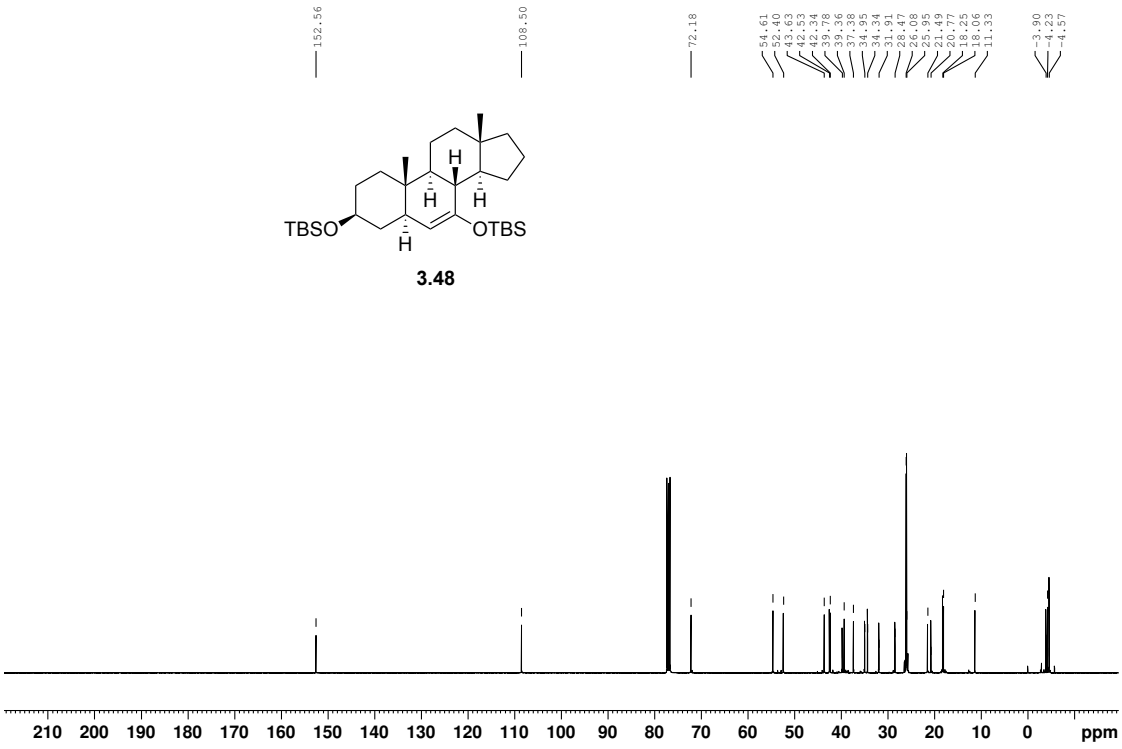

3.48

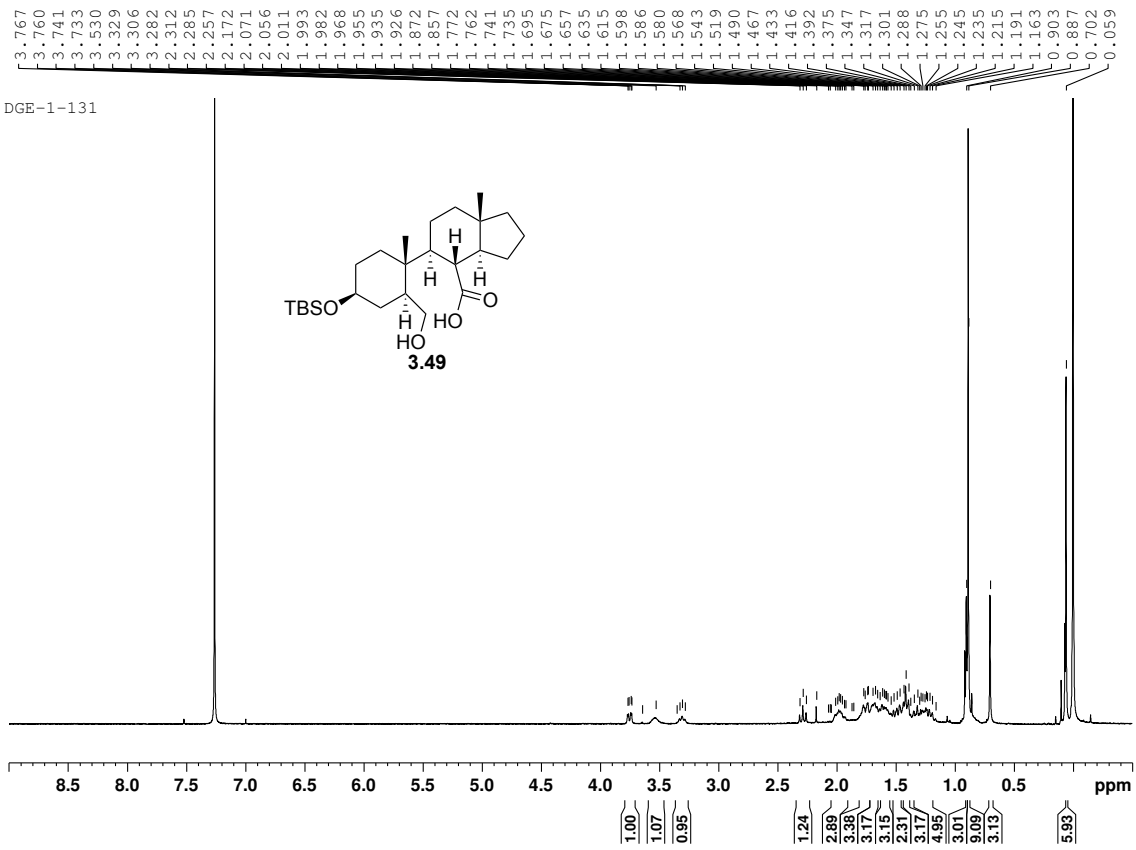
3.767
3.760
3.741
3.733
3.530
3.329
3.306
3.282
2.312
2.285
2.257
2.172
2.071
2.056
2.011
1.993
1.982
1.968
1.955
1.935
1.926
1.872
1.857
1.772
1.762
1.741
1.735
1.695
1.675
1.657
1.635
1.615
1.598
1.586
1.580
1.568
1.543
1.519
1.490
1.467
1.433
1.416
1.392
1.375
1.347
1.317
1.301
1.288
1.275
1.255
1.245
1.235
1.215
1.191
1.163
0.903
0.887
0.702
0.059
DGE-1-131
TBSO
H
H
H
O
H
HO
HO
3.49
8.5
8.0
7.5
7.0
6.5
6.0
5.5
5.0
4.5
4.0
3.5
3.0
2.5
2.0
1.5
1.0
0.5
ppm
1.00
1.07
0.95
1.24
2.89
3.38
3.17
3.15
2.31
3.17
4.95
3.01
9.09
3.13
5.93

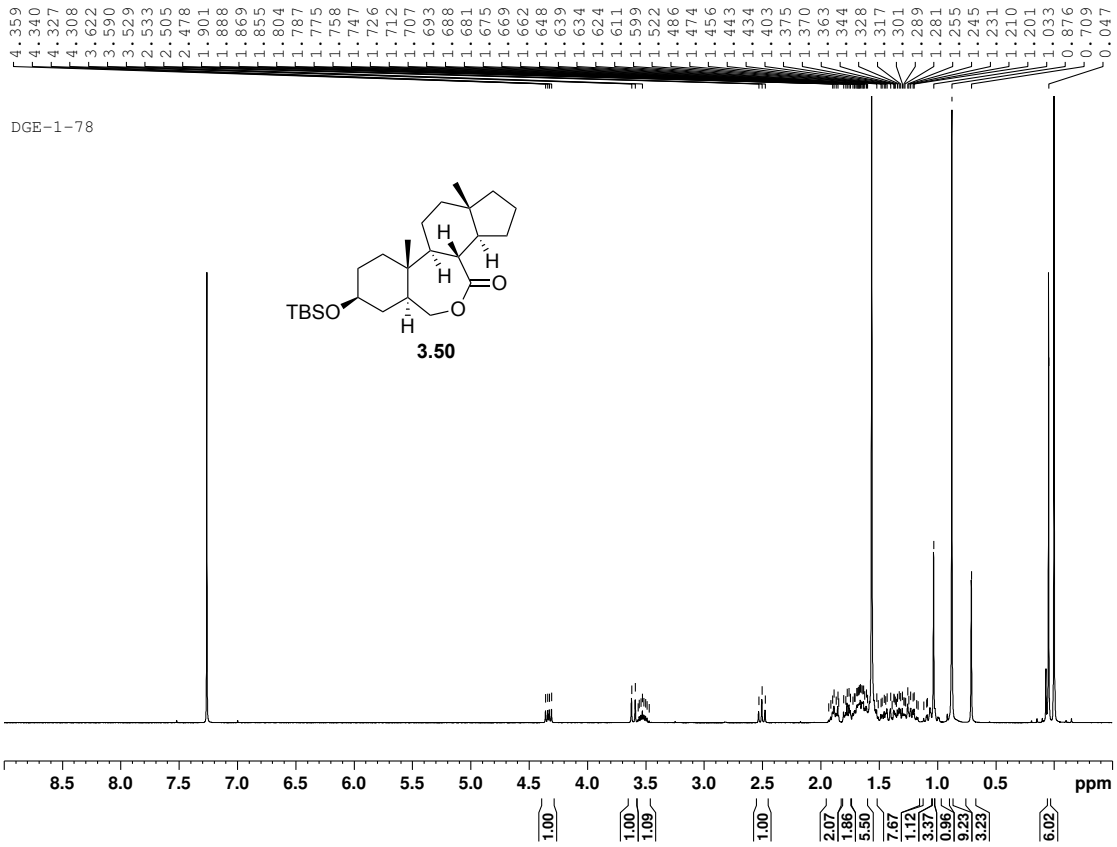
DGE-1-78
TBSO
H
H
H
O
O
H
3.50
ppm

DGE-1-78 CNMR

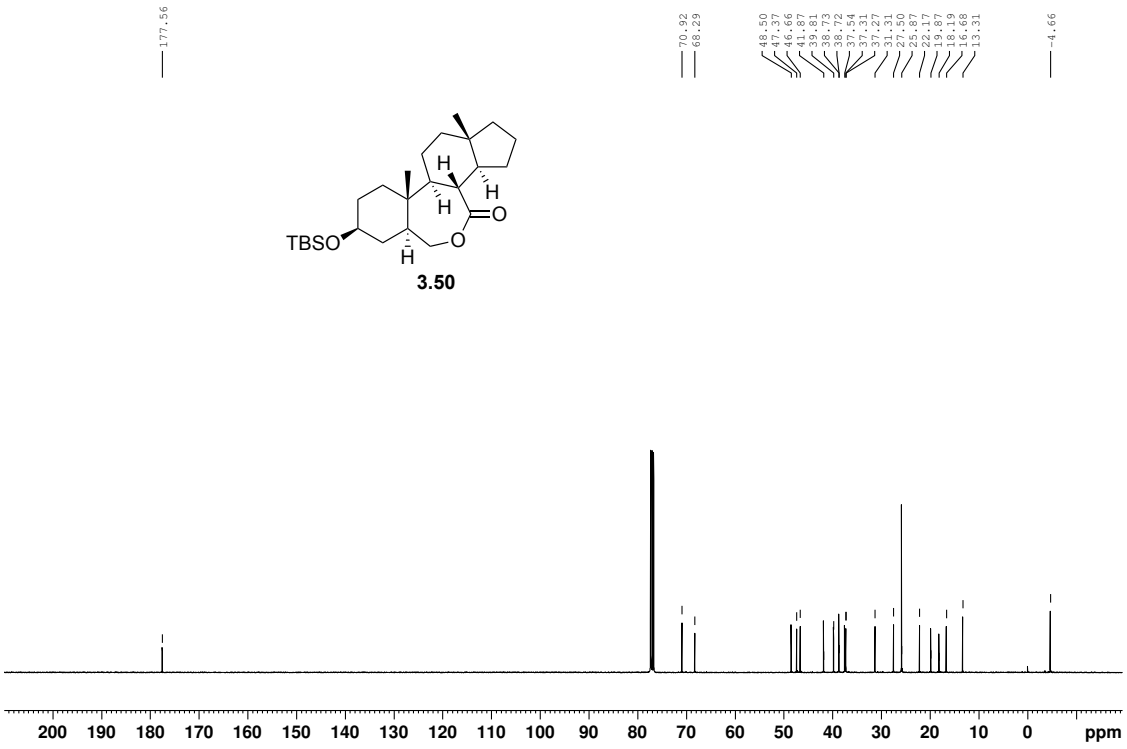

3.50

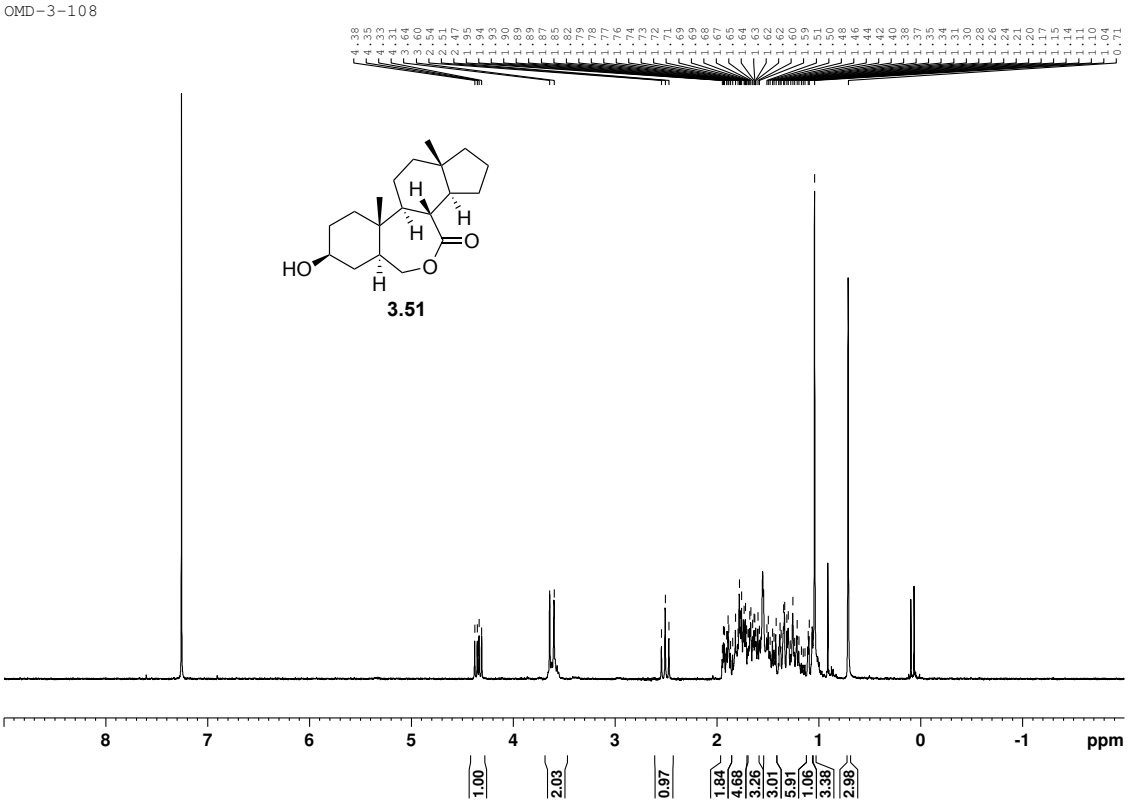
OMD-3-108
HO
O
O
H
H
H
H
3.51
8
7
6
5
4
3
2
1
0
-1
ppm
1.00
2.03
0.97
1.84
4.68
3.26
3.01
5.91
1.06
3.38
2.98

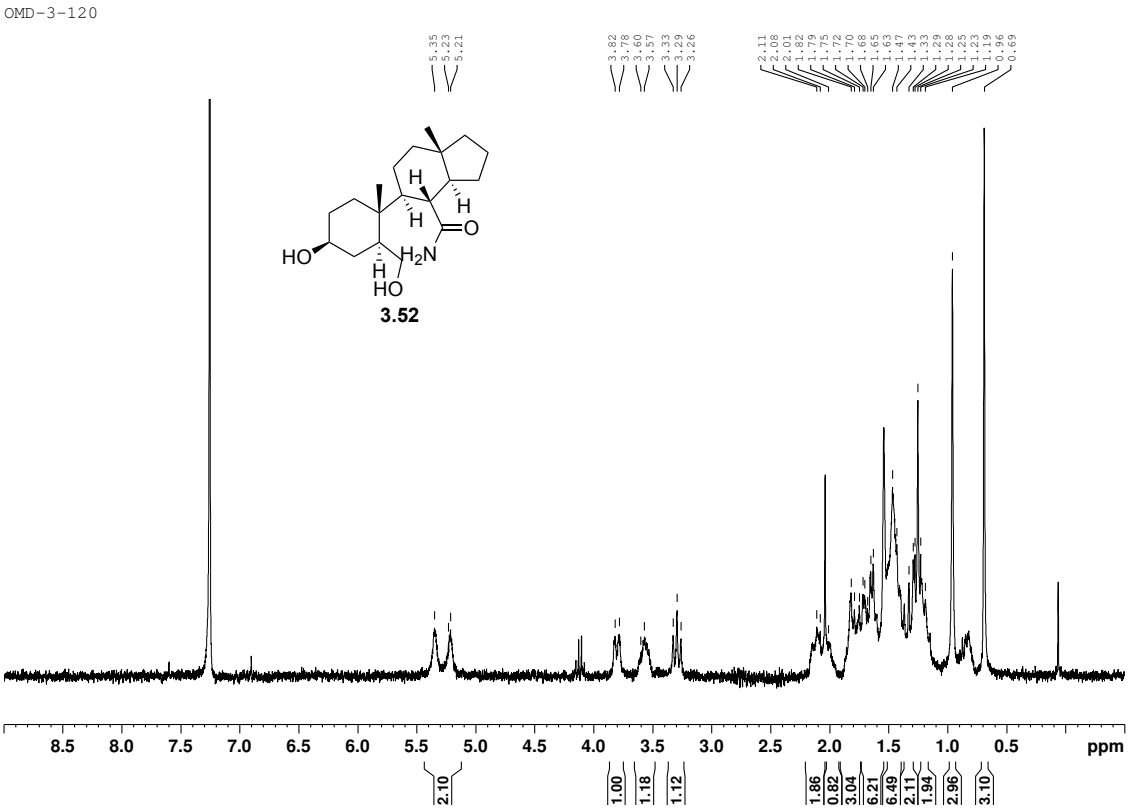
OMD-3-120
5.35
5.23
5.21
3.82
3.78
3.60
3.57
3.33
3.29
3.26
2.11
2.08
2.01
1.82
1.79
1.75
1.72
1.70
1.68
1.65
1.63
1.47
1.43
1.33
1.29
1.28
1.25
1.23
1.19
0.96
0.69
HO
H
H
H
O
H2N
H
HO
3.52
8.5
8.0
7.5
7.0
6.5
6.0
5.5
5.0
4.5
4.0
3.5
3.0
2.5
2.0
1.5
1.0
0.5
ppm
2.10
1.00
1.18
1.12
1.86
0.82
3.04
6.21
6.49
2.11
1.94
2.96
3.10

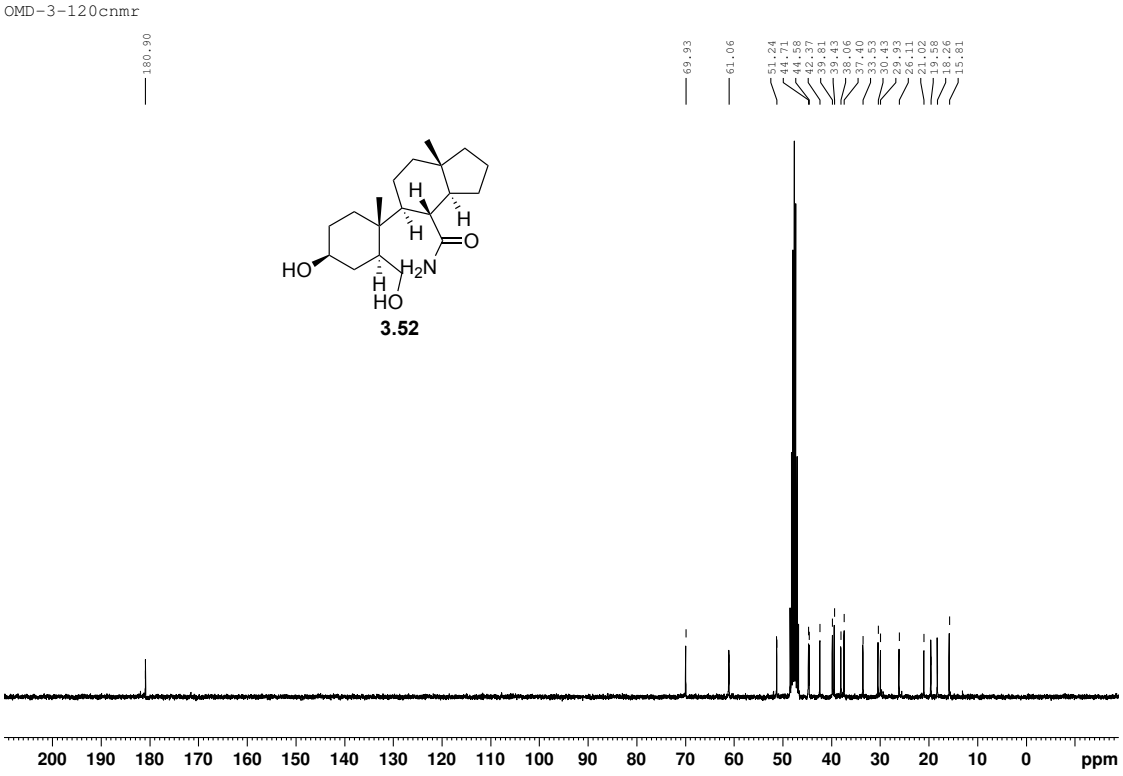
OMD-3-120cnmr
180.90
69.93
61.06
51.24
44.71
44.58
42.37
39.81
39.43
38.06
37.40
33.53
30.43
29.33
26.11
21.02
19.58
18.26
15.81
HO
H
H
H
O
H2N
H
HO
3.52
200 190 180 170 160 150 140 130 120 110 100 90 80 70 60 50 40 30 20 10 0 ppm

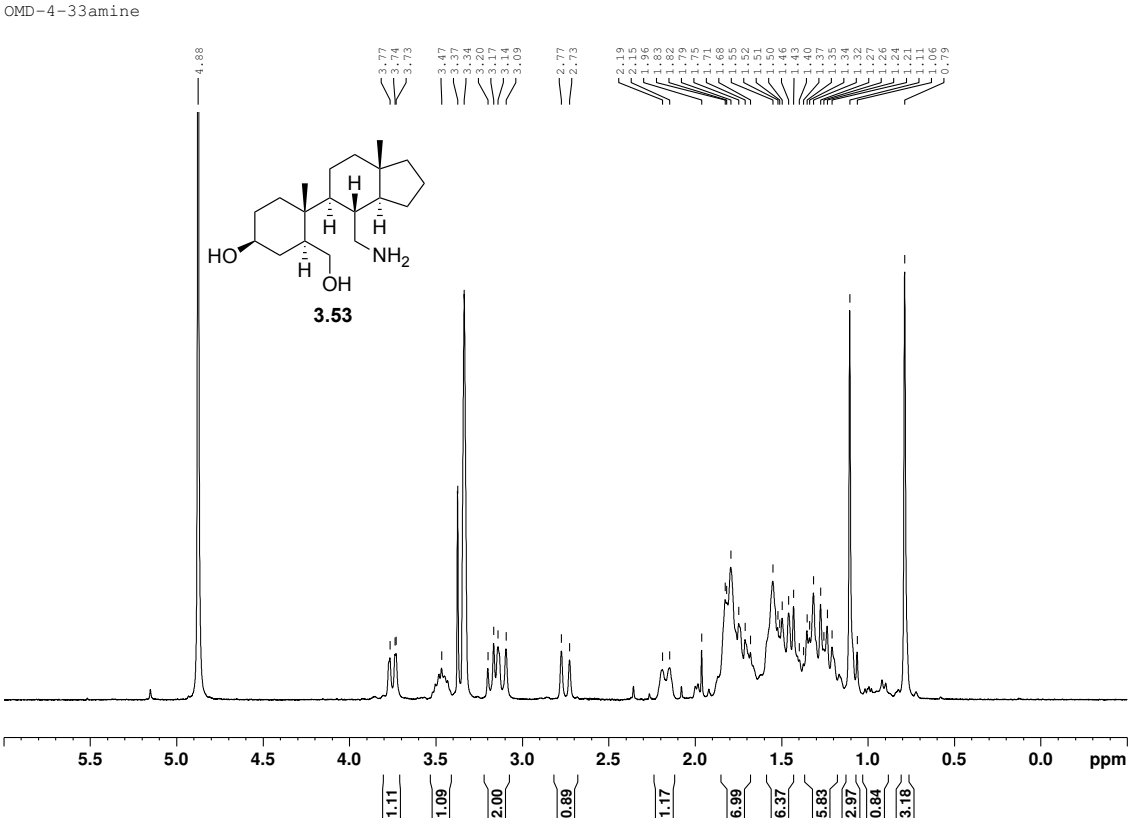
OMD-4-33amine
4.88
3.77
3.74
3.73
3.47
3.37
3.34
3.20
3.17
3.14
3.09
2.77
2.73
2.19
2.15
1.96
1.83
1.82
1.79
1.75
1.71
1.68
1.55
1.52
1.51
1.50
1.46
1.43
1.40
1.37
1.35
1.34
1.32
1.27
1.26
1.24
1.21
1.11
1.06
0.79
HO
H
H
H
NH2
H
OH
3.53
5.5
5.0
4.5
4.0
3.5
3.0
2.5
2.0
1.5
1.0
0.5
0.0
ppm
1.11
1.09
2.00
0.89
1.17
6.99
6.37
5.83
2.97
0.84
3.18

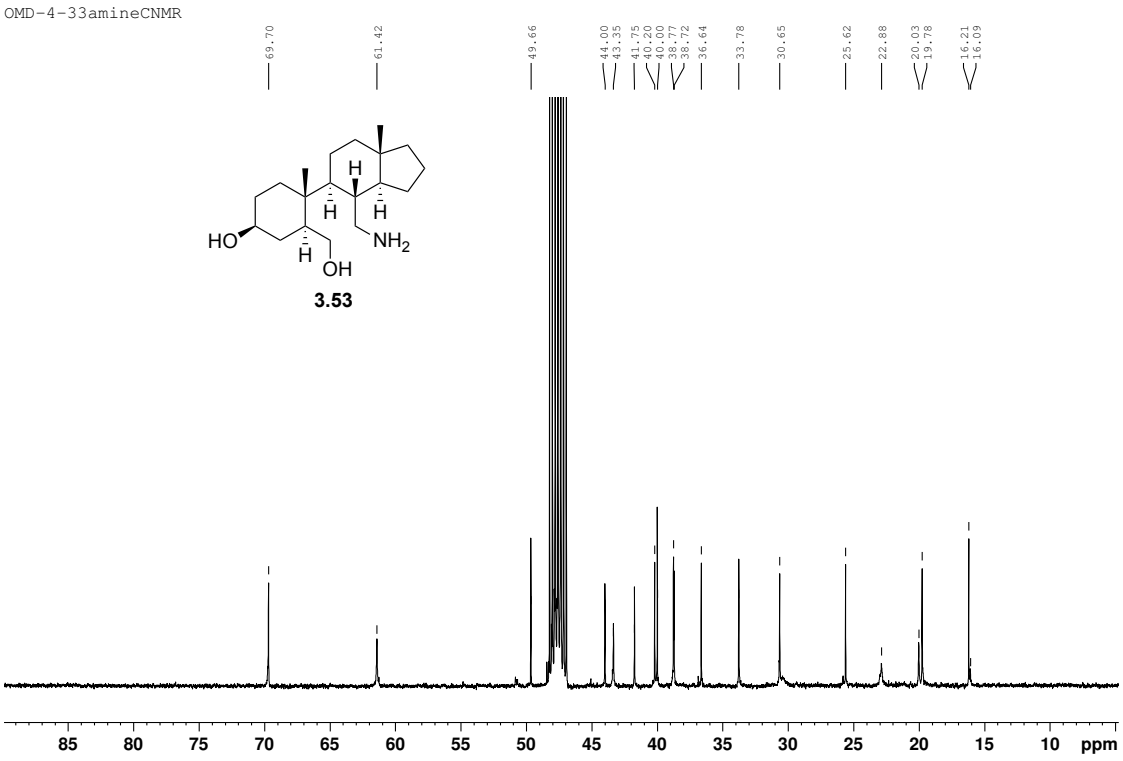
OMD-4-33amineCNMR
69.70
61.42
49.66
44.00
43.35
41.75
40.20
40.00
39.77
38.72
36.64
33.78
30.65
25.62
22.88
20.03
19.78
16.21
16.09
HO
H
H
H
NH2
H
OH
3.53
85
80
75
70
65
60
55
50
45
40
35
30
25
20
15
10
ppm

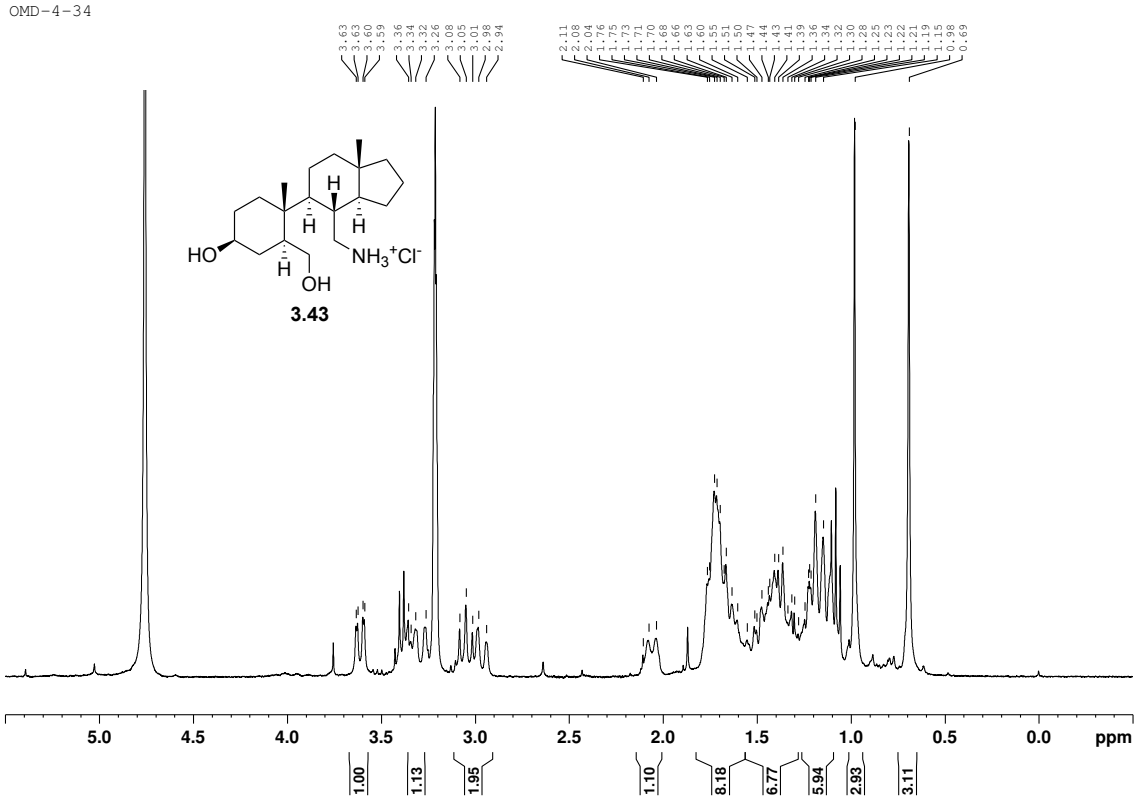
OMD-4-34
3.63
3.62
3.60
3.59
3.36
3.34
3.32
3.26
3.08
3.05
3.01
2.98
2.94
2.11
2.08
2.04
1.76
1.75
1.73
1.71
1.70
1.66
1.63
1.60
1.55
1.51
1.50
1.47
1.44
1.43
1.41
1.39
1.36
1.34
1.32
1.30
1.28
1.25
1.23
1.22
1.21
1.19
1.15
0.98
0.69
HO
H
H
H
H
OH
NH3+Cl-
3.43
5.0
4.5
4.0
3.5
3.0
2.5
2.0
1.5
1.0
0.5
0.0
ppm
1.00
1.13
1.95
1.10
8.18
6.77
5.94
2.93
3.11

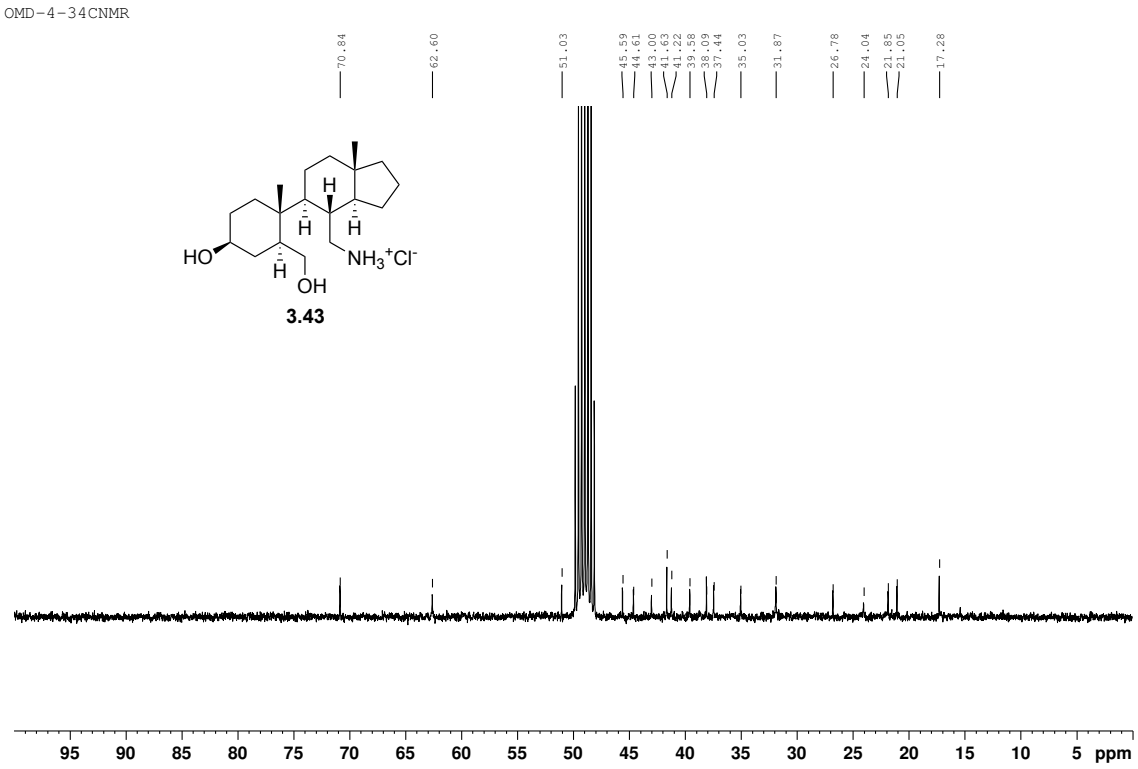
OMD-4-34CNMR
70.84
62.60
51.03
45.59
44.61
43.00
41.63
41.22
39.58
38.09
37.44
35.03
31.87
26.78
24.04
21.85
21.05
17.28
HO
H
H
H
H
OH
NH3+Cl-
3.43
95 90 85 80 75 70 65 60 55 50 45 40 35 30 25 20 15 10 5 ppm

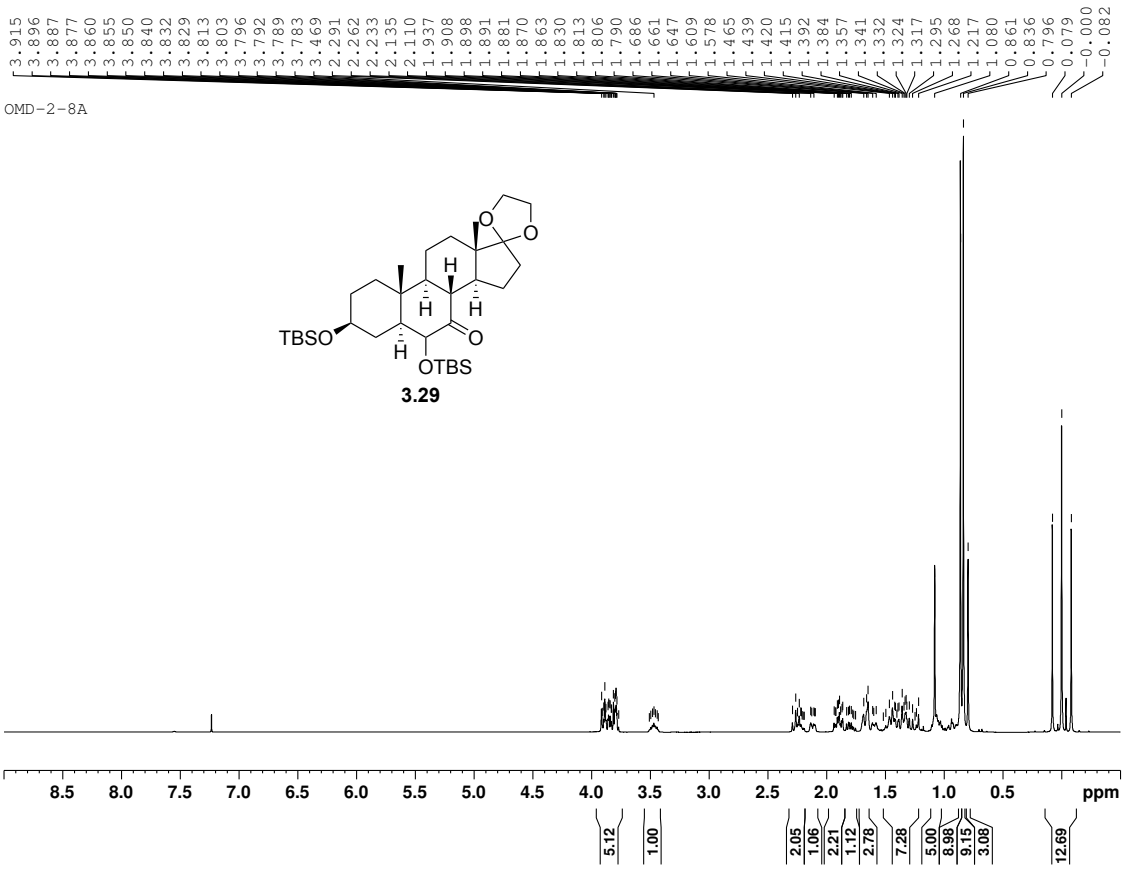
3.915
3.896
3.887
3.877
3.860
3.855
3.850
3.840
3.832
3.829
3.813
3.803
3.796
3.792
3.789
3.783
3.469
2.291
2.262
2.233
2.135
2.110
1.937
1.908
1.898
1.891
1.881
1.870
1.863
1.830
1.813
1.806
1.790
1.686
1.661
1.647
1.609
1.578
1.465
1.439
1.420
1.415
1.392
1.384
1.357
1.341
1.332
1.324
1.317
1.295
1.268
1.217
1.080
0.861
0.836
0.796
0.079
-0.000
-0.082
OMD-2-8A
TBSO
OTBS
3.29
8.5
8.0
7.5
7.0
6.5
6.0
5.5
5.0
4.5
4.0
3.5
3.0
2.5
2.0
1.5
1.0
0.5
ppm
5.12
1.00
2.05
1.06
2.21
1.12
2.78
7.28
5.00
8.98
9.15
3.08
12.69

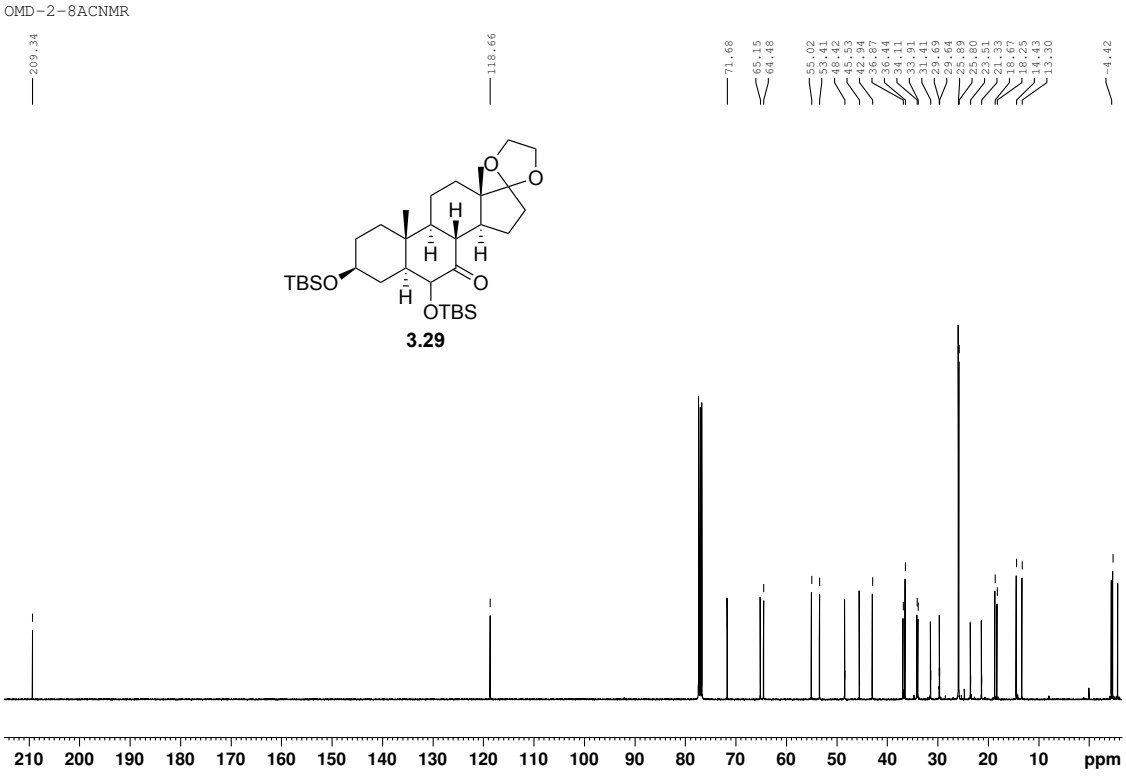
OMD-2-8ACNMR
209.34
118.66
71.68
65.15
64.48
55.02
53.41
48.42
45.53
42.94
36.87
36.44
34.11
33.91
31.41
29.69
29.64
25.89
25.80
23.51
21.33
18.67
18.25
14.43
13.30
-4.42
O
O
H
H
H
TBSO
H
O
OTBS
3.29
210 200 190 180 170 160 150 140 130 120 110 100 90 80 70 60 50 40 30 20 10 ppm

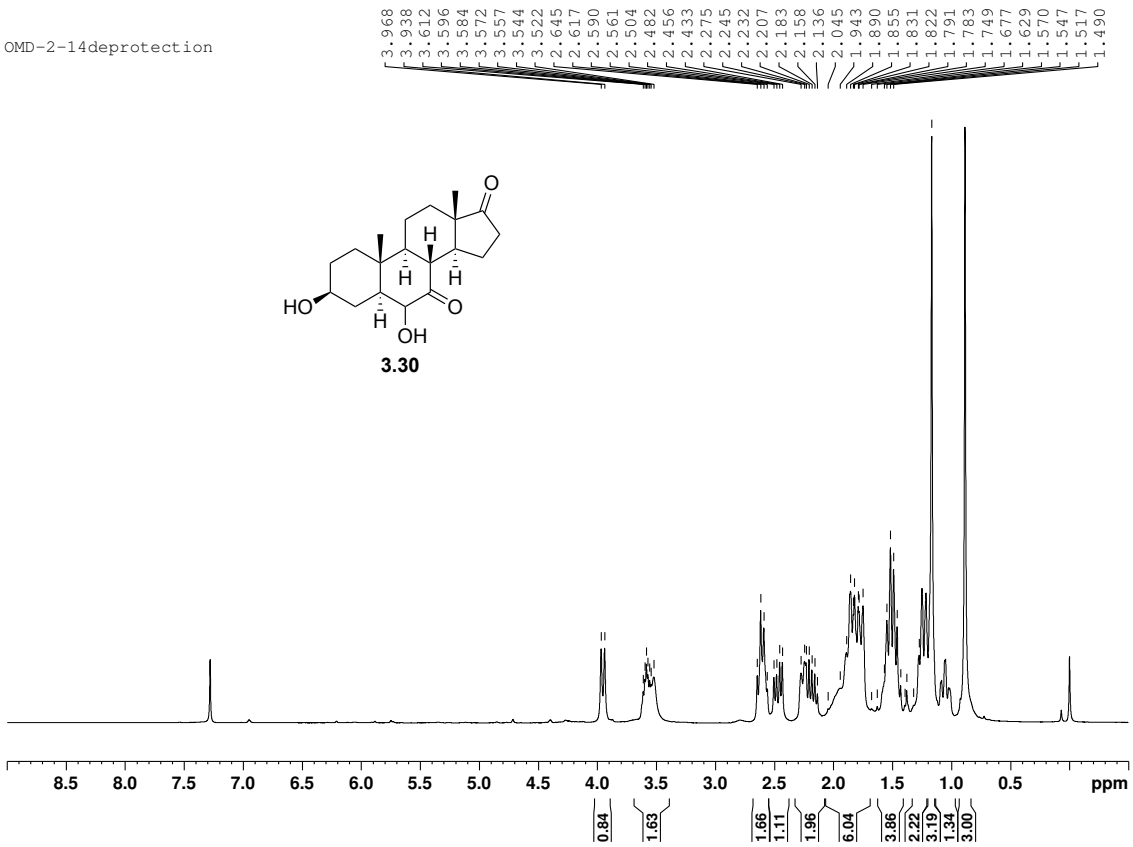
OMD-2-14deprotection
3.968
3.938
3.612
3.596
3.584
3.572
3.557
3.544
3.522
2.645
2.617
2.590
2.561
2.504
2.482
2.456
2.433
2.275
2.245
2.232
2.207
2.183
2.158
2.136
2.045
1.943
1.890
1.855
1.831
1.822
1.791
1.783
1.749
1.677
1.629
1.570
1.547
1.517
1.490
O
H
H
H
HO
O
H
OH
3.30
8.5
8.0
7.5
7.0
6.5
6.0
5.5
5.0
4.5
4.0
3.5
3.0
2.5
2.0
1.5
1.0
0.5
ppm
0.84
1.63
1.66
1.11
1.96
6.04
3.86
2.22
3.19
1.34
3.00

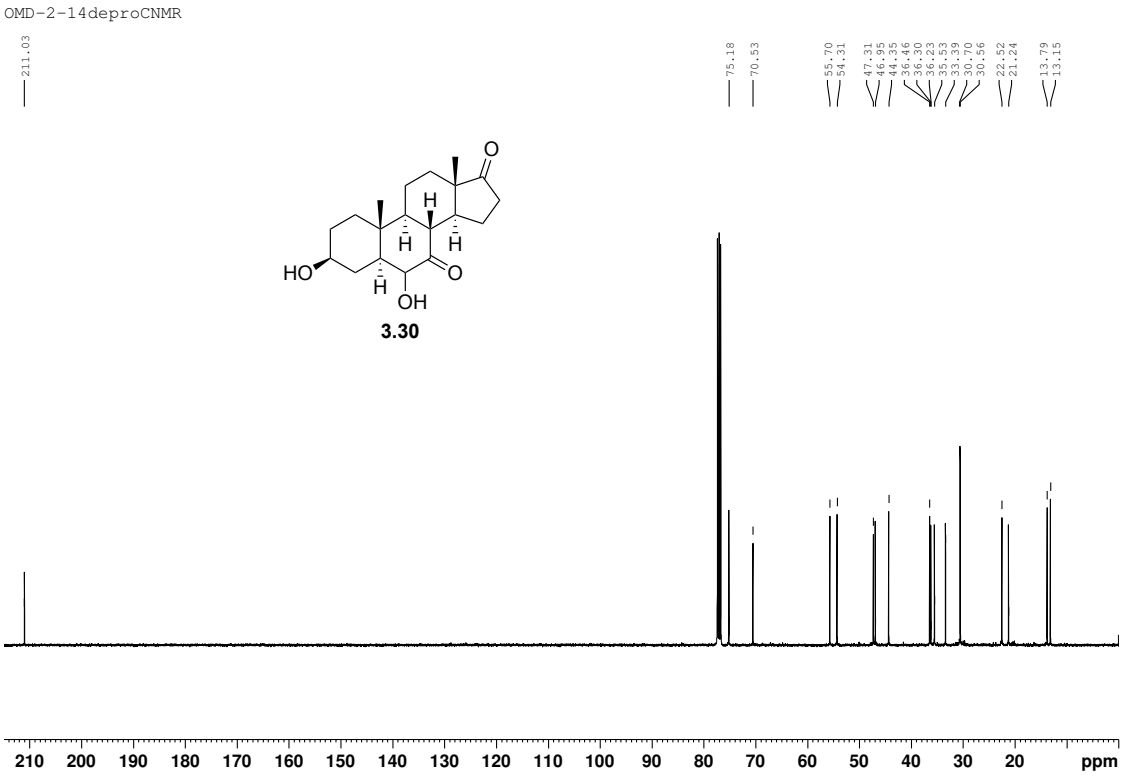
OMD-2-14deproCNMR
211.03
75.18
70.53
55.70
54.31
47.31
46.95
44.35
36.46
36.30
36.23
35.53
33.39
30.70
30.56
22.52
21.24
13.79
13.15
O
H
H
H
HO
O
H
OH
3.30
210 200 190 180 170 160 150 140 130 120 110 100 90 80 70 60 50 40 30 20 ppm

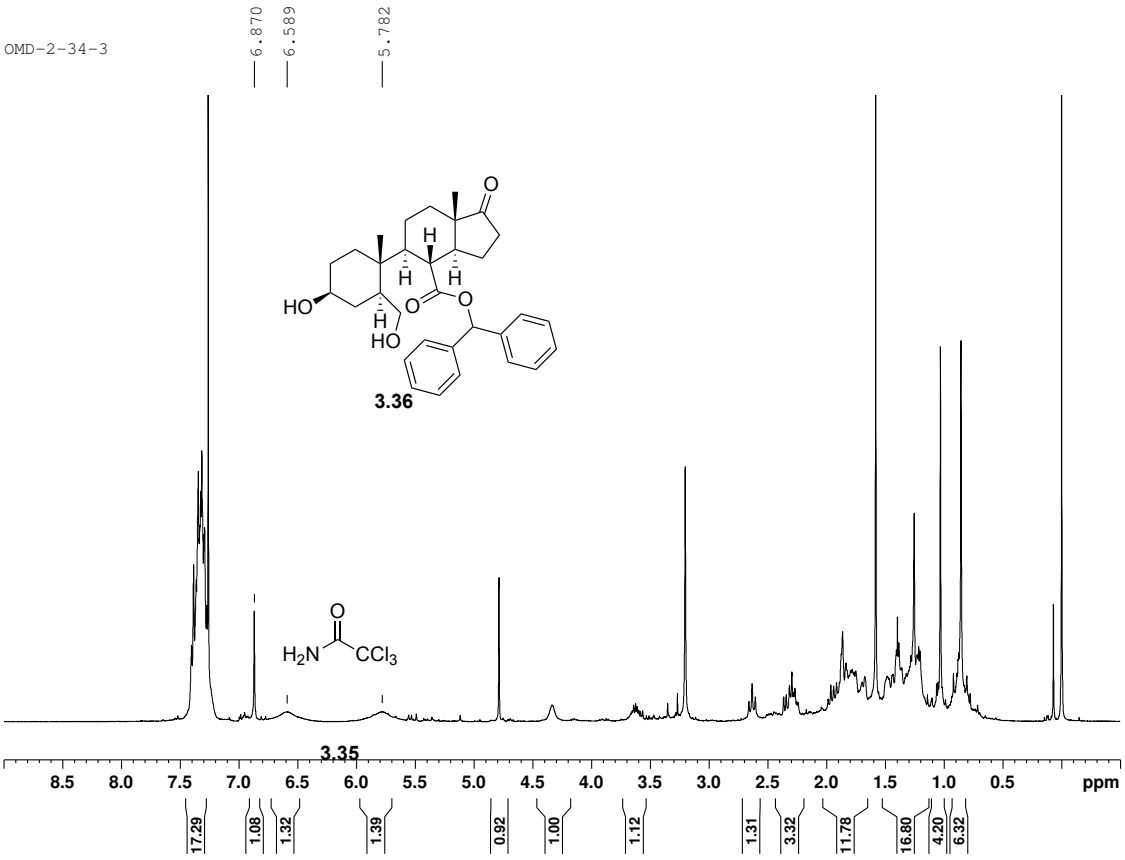
OMD-2-34-3
6.870
6.589
5.782
3.36
3.35
8.5
8.0
7.5
7.0
6.5
6.0
5.5
5.0
4.5
4.0
3.5
3.0
2.5
2.0
1.5
1.0
0.5
ppm
17.29
1.08
1.32
1.39
0.92
1.00
1.12
1.31
3.32
11.78
16.80
4.20
6.32

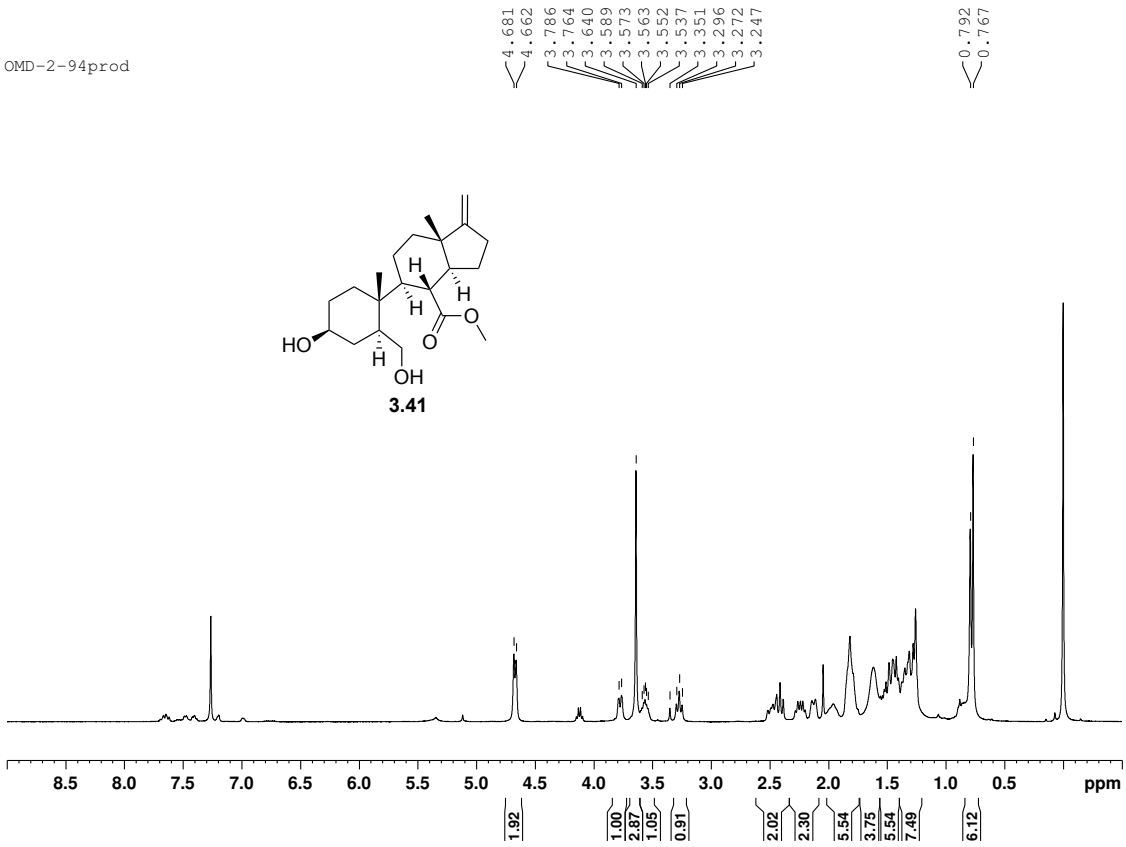
OMD-2-94prod
4.681
4.662
3.786
3.764
3.640
3.589
3.573
3.563
3.552
3.537
3.351
3.296
3.272
3.247
0.792
0.767
HO
H
H
H
O
O
H
OH
3.41
8.5
8.0
7.5
7.0
6.5
6.0
5.5
5.0
4.5
4.0
3.5
3.0
2.5
2.0
1.5
1.0
0.5
ppm
1.92
1.00
2.87
1.05
0.91
2.02
2.30
5.54
3.75
5.54
7.49
6.12

Otto M. Dungan
1108 E Genesee Street, Syracuse, NY 13210

407-590-3704 odungan@syr.edu

EDUCATION

Doctor of Philosophy: Chemistry — Syracuse University, Syracuse, NY 13244
GPA: 3.81 — *August 2014 – August 2019*
Major field of study: Synthetic Organic and Medicinal Chemistry
Advisor: John Chisholm, Ph.D. — Defended: July 2019

Master of Philosophy: Chemistry — Syracuse University, Syracuse, NY 13244
GPA: 3.81 — *August 2014 - 2016*
Advisor: John Chisholm, Ph.D.

Bachelor of Science: Chemistry — Florida State University, Tallahassee, FL, 32306
GPA: 3.43 — *Graduated: May 2014*

TEACHING EXPERIENCE

Graduate Teaching Assistant – Organic Chemistry I and II
Syracuse University, *January 2018 – December 2018*
Graduate Teaching Assistant – Organic Chemistry I and II
Syracuse University, *January 2016 – December 2016*
Lead Graduate Teaching Assistant – Organic Chemistry I Lab
Syracuse University, *August 2015 – December 2015*
Graduate Teaching Assistant – Organic Chemistry I and II Lab
Syracuse University, *August 2014 – May 2015*
Undergraduate Teaching Assistant – General Chemistry I Lab
Florida State University, *January 2014 – May 2014*

RESEARCH EXPERIENCE

Doctoral Research
Syracuse University, *May 2015 – August 2019*

- Organic Synthesis and Medicinal Chemistry
- Synthetic and Structure Activity Relationship Studies of SHIP inhibitors and agonists
- Development of a shorter route to the patented SHIP 1 agonist AQX-1125
- Development and synthesis of the more potent SHIP 1 agonist K204
- Characterization of small organic compounds by NMR, IR, mass spectroscopy, and combustion analysis

PRESENTATIONS

1. "Synthetic studies on the seco-steroidal indene AQX-1125" (O. M. Dungan, B. C. Duffy, D. G. Effiong, W. G. Kerr, J. D. Chisholm) presented by O. Dungan at the Poster Session for the 256th ACS National Meeting, Boston, Massachusetts, 2018.

2. “Synthetic Studies on AQX-1125” (O. M. Dungan, D. G. Effiong, W. G. Kerr, J. D. Chisholm) presented by O. Dungan at the Poster Session for Visiting Students, Department of Chemistry, Syracuse University, Syracuse, New York, March, 2018.

3. “Synthetic Studies on SHIP1 Inhibitors” (K. T. Howard, D. R. Viernes, W. G. Kerr, J. D. Chisholm) presented by O. Dungan at the Poster Session for Visiting Students, Department of Chemistry, Syracuse University, Syracuse, New York, March, 2016.

4. “Tethered Systems for Homogenoeous and Heterogeneous 2:1 Charge-Transfer Complexes,” (J. M. Watts, O. Dungan, E. J. Lavelle, Y. W. Kahok, R. T. Kearney, B. C. Bowden, and E. F. Hilinski) presented by O. Dungan at the Poster Session for Visiting Students, Department of Chemistry and Biochemistry, Florida State University, Tallahassee, Florida, February, 2014.

5. “Tethered Systems for Unsymmetrical 2:1 Electron Donor-Acceptor Complexes,” (J. M. Watts, E. D. Webb, J. B. Mullenix, N. B. Kerckhoff, J. P. Gershenson, O. Dungan, and E. F. Hilinski) presented by O. Dungan at the Poster Session for Visiting Students, Department of Chemistry and Biochemistry, Florida State University, Tallahassee, Florida, February, 2013.

6. “Tethered Systems for Homogenoeous and Heterogeneous 2:1 Charge-Transfer Complexes,” (J. M. Watts, O. Dungan, E. J. Lavelle, Y. W. Kahok, R. T. Kearney, B. C. Bowden, and E. F. Hilinski) presented by O. Dungan at the Poster Session for Visiting Students, Department of Chemistry and Biochemistry, Florida State University, Tallahassee, Florida, March, 2013.

PUBLICATIONS

1. Saz-Leal, P.; Fresno, C. D.; Brandi, P.; Martínez-Cano, S.; Dungan, O. M.; Chisholm, J. D.; Kerr, W. G.; Sancho, D. Targeting SHIP-1 in Myeloid Cells Enchances Trained Immunity and Boosts Response to Infection. *Cell Reports* 2018, *25* (5), 1118–1126.

2. Dungan, O.; Fernandes, S.; Duffy, B. C.; Kerr, W. G.; Chisholm, J. D. "An Improved Synthetic Pathway to the SHIP1 Agonist AQX-1125." *In preparation.*

3. Dungan, O.; Fernandes, S.; Duffy, B. C.; Kerr, W. G.; Chisholm, J. D. "Discovery of a new class of SHIP1 Agonists." *In preparation.*